The development of a novel biosensor for single species detection using environmental DNA

Molly Ann Williams, BSc, MSc

Supervisors: Prof. Anne Parle-McDermott and Prof. Fiona Regan

School of Biotechnology, Dublin City University

A thesis submitted for the degree

of Doctor of Philosophy.

January 2022

I hereby certify that this material, which I now submit for assessment on the programme of study leading to the award of Doctor of Philosophy is entirely my own work, and that I have exercised reasonable care to ensure that the work is original, and does not to the best of my knowledge breach any law of copyright, and has not been taken from the work of others save and to the extent that such work has been cited and acknowledged within the text of my work.

Signed:  (Candidate)

ID No: 17213275

Date: 06/01/2022

"Walking into the future means trusting in yourself even when you can't see around the bend. As long as you're certain this is what you want, all will be well"

– Kerry Maniscalco, Capturing the Devil

"Today is going to be a good day. And here's why; because today, today at least you're you and that's enough."

– Evan Hansen

Acknowledgements

I have to start this section by thanking my supervisors Prof. Anne Parle-McDermott and Prof. Fiona Regan. To Fiona, thank you for taking me on as a Forensic Science Master's student, encouraging me to apply for this PhD and providing all your sensor knowledge throughout the last four years. To Anne, I can't thank you enough for all the support you have given me throughout this project, from the 'EUREKA!' moment in your office to listening to me present the same presentation numerous times. This thesis would not have happened without you and I am unbelievably grateful to have had such a strong mentor to inspire me every day to be better.

Other academic thank yous go to Dr. Elvira de Eyto for all your help with everything regarding the Burrishoole Catchment, from helping sample to sending on relevant data/maps when needed. You are honestly an encyclopaedia of knowledge and were a huge help throughout this PhD project. Also to the DCU technical staff. You are all an absolute pleasure to work with and have had a hugely positive impact on my time at DCU. In addition, I have to thank all of my collaborators: the BEYOND2020 network for brainstorming sessions, Dr. Ciprian Briciu-Burghina, Joyce O'Grady and Sean Power for providing all of your sensor knowledge to this project, answering my countless questions and making SensEDNA happen and also, a huge thanks to Prof. Louis Bernatchez and team for your excitement regarding the CRISPR method and your drive to get the second paper published. Moreover, I want to thank my examiners Dr. Linda Holland and Prof. Mike Kinnison for the exciting discussion about the broader applications of CRISPR to eDNA and the use of LODs/LOQs in eDNA studies. The discussion has made this thesis all the better.

It is well known that a PhD can be quite an isolating experience, but I feel like a complete imposter to this feeling thanks to my fellow postgrad students who got me through this whole thing! I was so lucky to start this PhD at the same time as three other wonderful humans. Niamh, Paola and Darren, we started this together as mere fledglings and I still can't believe we are now the experienced ones. From the bottom of my heart, I could not have done this without you. We didn't always have an easy ride but your friendship

and support was everything and I'm sure it will go on way beyond this PhD! In third year, we were also lucky to add an honouree member to the group. Conor, thank you for providing daily doggos, daily laughter and always cheering me on. The joy (and board of hate) of the Quality Street gang made me happy coming in to DCU every day. You guys are honestly the best.

Outside of the DCU lab, I am very grateful for my support network! Maria, thanks for long pandemic walks, starting pole with me and being roped into watching anything to do with Jonas Brothers and High School Musical. The One Measly Euro gang; Becca, Lauren, Rachel, Liz and Chloe, you girls have known me for a long old time and have always supported my craziness. May our friendship never change. Thanks for believing in me, making time to see me whenever I was home and popping across the water to visit me in Ireland!

My penultimate thanks goes to my wonderfully supportive other half, Aaron. You have pretty much been there since day one and have always been my biggest cheerleader. Listening to my endless rambles about science and lab life, celebrating the highs and comforting me through the lows. This PhD is partly yours.

Finally, the biggest thank you has to go to my loving family. Beccy, Ben, Matt, Katie, Luke, Laura, Rhys, Sujin, Noah, Jacob, Felicity, Jack and Lily; thanks for pretending to care about what I was doing in my PhD and for making me Aunty Molly. You're the best family a girl could ask for. Also thanks to my Nanny, for all of her support throughout my academic career! Thank you to my Dad for being my biggest inspiration. Because of you I wanted to be a doctor, and although I might not be a medical doctor, your encouragement and support throughout my life has meant I will still be Dr. Williams. Also, thanks for reading all my academic work and being proud of all my achievements. Lastly, to my Mum. My best friend and biggest fan. Thank you for always believing in me and reminding me "you are braver than you believe, stronger than you feel and smarter than you think". I will always be grateful for the hours of phone calls we have had, both good and bad and your endless love and support.

This work was funded by the Marine Institute. Burrishoole Ecosystem Observatory Network 2020: BEYOND 2020 PBA/FS/16/02.

Table of Contents

List of Figures

List of Tables

Abbreviations

AuNP	Gold Nanoparticle
ATP	Adenosine triphosphate
BHQ	Black Hole Quencher
Cas	CRISPR associated proteins
cnPCR	Conventional PCR
COI	Cytochrome Oxidase Subunit I
CRISPR	Clustered Regularly Interspaced Short Palindromic Repeats
CRISPR-Dx	CRISPR Diagnostics
crRNA	CRISPR Ribonucleic Acid
CRP	Conjugate Release Pad
C_T	Crossing Threshold
CV	Coefficient of Variation
ddPCR	Droplet Digital PCR
DNA	Deoxyribonucleic Acid
dNTP	Deoxy Nucleotide Phosphate
dsDNA	Double Stranded DNA
DTT	Dithiothreitol
eDNA	Environmental Deoxyribonucleic Acid
EDTA	Ethylenediaminetetraacetic acid
FAM	6-carboxyfluorescein
FB	FAM-Biotin
FQ	Fluorophore-Quencher

FRET	Forster Resonance Energy Transfer
gRNA	Guide Ribonucleic Acid
HCl	Hydrochloric Acid
IPC	Internal Positive Control
IPTG	Isopropyl-beta-D-thiogalactopyranoside
KCl	Potassium Chloride
LAMP	Loop-Mediated Isothermal Amplification
LF	Lateral Flow
LFIA	Lateral Flow ImmunoAssay
LOD	Limit of Detection
LOQ	Limit of Quantification
MCS	Multiple Cloning Site
MgOAc	Magnesium Acetate
MgCl2	Magnesium Chloride
MGB	Minor Grove Binding
mtDNA	Mitochondrial Deoxyribonucleic Acid
NAB	Nucleic Acid Biosensor
NADH	Nicotinamide Adenine Dinucleotide
ND2	NADH Dehydrogenase Subunit 2
ND5	NADH Dehydrogenase Subunit 5
PAM	Protospacer Adjacent Motif
PBS	Phosphate Buffered Saline
PCR	Polymerase Chain Reaction

POC	Point-of-Care
PtNP	Platinum Nanoparticle
qPCR	Quantitative Polymerase Chain Reaction
RNA	Ribonucleic Acid
RNP	Ribonucleoprotein
RPA	Recombinase Polymerase Amplification
RT	Room Temperature
SD	Standard Deviation
sedaDNA	Sedimentary Deoxyribonucleic Acid
SNP	Single Nucleotide Polymorphism
Ssa	*Salmo salar*
ssDNA	Single Stranded DNA
ssDNA-FB	Single Stranded DNA FAM-Biotin Reporter
ssDNA-FQ	Single Stranded DNA Fluorophore Quencher Reporter
Taq	*Thermus aquaticus*
TBE	Tris Borate EDTA
TE	Tris EDTA

Units

%	Percentage
(w/v)	Weight per volume
aM	Attomolar
bp	Base Pair
cm	Centimetre
g	Gram
Hz	Hertz
Km	Kilometre
L	Litre
m	Metre
M	Molar
mg	Microgram
mA	Miliamps
mL	Mililitre
mM	Milimolar
mm	Milimetre
min	Minutes
ng	Nanogram
nM	Nanomolar
nm	Nanometre
°C	Degrees Celsius
pg	Picogram

rpm	Rotations per minute
sec	Seconds
U	Units
µg	Microgram
µL	Microlitre
µM	Micromolar
V	Volt
W	Watt
YBP	Years Before Present

Abstract

The development of a novel biosensor for single species detection using environmental DNA

Molly Ann Williams

Rapid monitoring of aquatic organisms, particularly endangered and invasive species, is essential for preserving the biodiversity in Earth's water. Management and conservation of fish species, such as *Salmo salar, Salmo trutta* and *Salvelinus alpinus*, within these environments requires knowledge of distribution, traditionally gained through visual detection. These methods are expensive, labour intensive and can lead to habitat disruption and harm to the target species. Environmental DNA (eDNA) offers a solution to this, using non-invasive molecular techniques to detect DNA shed into the environment.

Conventional eDNA approaches use PCR-based methodology for single-species detection. In this thesis, a qPCR assay was developed for *S. salar* detection. However, although sensitive and specific, PCR-based methods pose a logistical challenge for on-site monitoring due to the need for high temperatures and thermal cycling. To circumvent this, we developed an isothermal approach that couples Recombinase Polymerase Amplification to CRISPR-Cas12a detection as a route to a cost-effective biosensor device. This system harnesses the collateral cleavage activity of Cas12a, a ribonuclease guided by a specific CRISPR RNA. We show the applicability of this technique to three salmonid species, with the *S. salar* assay compared to qPCR as a detection/non-detection assay in samples from Ireland and Canada.

To facilitate this RPA-CRISPR-Cas assay as an on-site detection tool, the method was adapted for visualisation on a custom portable fluorometer and via lateral flow. Both systems maintain the specificity and sensitivity of the original assay but enable simplified readouts without complex instrumentation. The assays and visualisation methods developed in this thesis were applied to samples from the Burrishoole Catchment, Co. Mayo, demonstrating their applicability to environmental monitoring.

In summary, this thesis provides the first application of CRISPR-Cas diagnostics to eDNA monitoring, and further progresses the field towards field-based applications, by removing the need for complex instrumentation and allowing rapid species detection.

Chapter 1. Introduction

1.1. Overview

The urgency of biodiversity monitoring is at an all-time high due to the increasing threat of climate change to global ecosystems, in particular freshwater (Revenga *et al.*, 2005). Whilst traditional methods such as electrofishing are readily used for this purpose, they are limited by their expense, labour intensity and invasiveness (Snyder, 2003). Molecular methods such as the detection of environmental DNA (eDNA), defined as genetic material shed and excreted by organisms into their environment, offer new opportunities to monitor biodiversity and track endangered or invasive species (Thomsen and Willerslev, 2015). Nevertheless, current eDNA methodologies, relying primarily on PCR-based techniques, are time consuming and limited to laboratory-based settings, thus reducing their applicability in the field. The development of a portable biosensor device could help overcome such limitations. This project aims to develop a biosensor device that utilises the eDNA approach to allow on-site detection of salmonids, but seeks to be adaptable to any target species to further improve molecular monitoring of biodiversity.

1.2. Biodiversity

Biodiversity is broadly described as "the variety and variability among living organisms and the ecological complexes in which they occur" (OTA, 1987). It plays a critical role in human health, wealth and security; providing food, water, energy and medicines, whilst also regulating our climate, water quality and pollution (WWF, 2020).

There are five major threats to global biodiversity: changes in land and sea use (causing habitat loss and degradation), species overexploitation, invasive species and disease, pollution, and climate change (WWF, 2020). The proportional effect of these threats varies based on global region; however it is reported that in each region over 40% of loss is caused by changes in land and sea use, over 17% is caused by species overexploitation and over 10% by invasive species and disease (WWF, 2020). These increasing threats are reflected in the latest WWF Living Planet Index, which shows a

global decline of 68% in monitored vertebrate population sizes since 1970 (Figure 1.1) (WWF, 2020). This major crisis has resulted in international agreements to slow or halt this decline in order to protect our global biodiversity (Alvarado-Quesada and Weikard, 2017).

1.2.1. Freshwater biodiversity

Freshwater ecosystems are home to one third of all vertebrate species (Dudgeon *et al.*, 2006) including fish, amphibians, aquatic reptiles and mammals, yet surface freshwater covers only about 0.8% of the Earth's surface (Gleick, 1998). The high connectivity of these systems means the major threats to global biodiversity (as above) can have a profound effect on species decline and freshwater ecosystem degradation (Revenga *et al.*, 2005). One considerable area of concern for freshwater species is that of widespread invasion of exotic species (Dudgeon *et al.*, 2006). Alongside pollution and disease (Collen *et al.*, 2014), invasive species are easily spread throughout watersheds particularly in regions already modified or degraded by humans (Bunn and Arthington, 2002). The impact of invasive species on native biodiversity (Linders *et al.*, 2019) and subsequently on ecosystem services (Pejchar and Mooney, 2009) is well established with examples including the Crayfish plague in Europe. This arose due to the deliberate introduction of North American Crayfish into European waters, but this species has decimated native populations (Palmer and Menninger, 2013).

Furthermore, the position of freshwater ecosystems within the landscape means they are commonly receivers of waste and pollutants in run off. Unfortunately, unlike marine water which also acts as a receiver, lakes and rivers lack the volume of marine water and thus their capacity to dilute contaminants or mitigate other threats is limited (Dudgeon *et al.*, 2006). The combined influences of these major threats have resulted in a decline of freshwater populations, as reflected in the latest WWF Living Planet Index, which reports an 84% decline in freshwater population sizes (Figure 1.1) (WWF, 2020). This worrying decrease highlights the need to monitor native diversity, invasive species and the extinction risk of species in freshwater ecosystems.

1.2.2. Salmonid species

The Salmonidae family, consisting of three lineages (Coregonminae, Thymallinae and Salmoninae) is one that relies on the freshwater environment. The Salmoninae subfamily consists of three main genera: *Salmo, Oncorhynchus* and *Salvelinus* (Figure 1.2). Many members of this family have a tolerance for fresh and marine water, with both landlocked and anadromous forms found throughout the clean, well-oxygenated, colder waters of the Northern Hemisphere (Royce, 1996). *Salmo salar* (Atlantic salmon), *Salmo trutta* (brown trout) and *Salvelinus alpinus* (Arctic char) are members of the Salmonidae family that are indigenous to Ireland.

1.2.2.1. *Salmo salar*

S. salar is a fish species with landlocked and anadromous forms found throughout its range in the North Atlantic (Chaput, 2012). *S. salar* has huge economic and ecological importance. In Europe, it represents the primary farmed fish in terms of biomass and economic value since aquaculture production was established in the 1960s (Dalvin *et al.*, 2010). In Ireland specifically, *S. salar* has socio-economic value in angling, commercial fishing and aquaculture. In 2006, a combined value of ~€160 million and an estimated total employment effect of 2,000 full-time job equivalents was reported (Whelan *et al.*, 2006). However, there is increasing consumer demand for seafood and in 2018, Ireland's fisheries and aquaculture production valued ~€420 million (OECD, 2021). Despite the economic benefit, this growth in aquaculture threatens wild *S. salar* populations with challenges concerning genetic interactions and disease dynamics (Krkošek *et al.*, 2007). Several studies have examined the genetic interaction between farmed and wild *S. salar* suggesting an overall shift towards lower heterozygosity in selected alleles as a result of interbreeding (McGinnity *et al.*, 2003). This interbreeding between farmed escapees and the wild population could cause changes in fitness and productivity, which would consequently threaten the wild population. Furthermore, large farmed *S. salar* escapees occur frequently in areas of intensive aquaculture, raising concern about their potential invasiveness (Fisher *et al.*, 2014).

Wild *S. salar* is designated a high level of protection under Annex II and Annex V of the European Habitats Directive. As a consequence, both the fish and its environment demands a high degree of assessment and reporting in respect of status (Chaput, 2012). Despite substantial controls on exploitation and increased environmental protection, numbers of wild *S. salar* continue to decline (Friedland *et al.*, 2008). In 2020, the Standing Scientific Committee on Salmon reported that only 45% of Ireland's *S. salar* rivers are meeting biologically based conservation limits, which are defined by the International Council for the Exploration of the Sea (ICES) as the level of stock (number of spawners) that will maximise the long term average maximum sustainable yield (Gargan *et al.*, 2020). Furthermore, marine survival rates in the past 5 years are amongst the lowest recorded since the 1980s (Gargan *et al.*, 2020). This highlights the need to monitor *S. salar* abundance in freshwater rivers to ensure *S. salar* stocks do not fall below ICES conservation limits.

1.2.2.2. *Salmo trutta*

S. trutta also has a freshwater (commonly referred to as brown trout) and anadromous (known as sea trout) form. They play a significant role in the economic and social aspect of recreational fishery in Ireland, as well as contributing to native biodiversity (Loughs Agency, 2021). Due to this association with human interests, *S. trutta* are widely managed, not only to sustain leisure activities but to protect against species decline (Saint-Pé *et al.*, 2019). As part of the European Water Framework Directive requirements, Inland Fisheries Ireland carries out regular fish monitoring programmes to assess the health of Ireland's rivers, lakes and estuaries (Inland Fisheries Ireland, 2019). In a 2019 survey, they reported that *S. trutta* are the most common species found. They were detected in 91% of the rivers and 93.8% of the lakes surveyed (Inland Fisheries Ireland, 2019). Despite this prevalence, stocks continue to decline. This is particularly pertinent to anadromous forms of *S. trutta,* which are suffering from reduced marine survival, due to increased predation and risk of infestation (Jensen *et al.*, 2019) and disruptions to migratory routes caused by anthropogenic barriers and flow modifications (Ferguson *et al.*, 2019). As with *S. salar*, it is also possible that where

domesticated strains of *S. trutta* have been used to sustain wild populations, they are having a negative effect in terms of fitness and genetic diversity (Hansen, 2002; Araki and Schmid, 2010).

S. trutta are also a known invasive species in the Southern Hemisphere (Minett *et al.*, 2021). For example, in New Zealand the extinction of the native grayling, *Prototroctes oxyrhynchus,* has in part been attributed to the introduction of *S. trutta* (McDowall, 2006), which exert strong selection pressure upon native fish due to their predation and competition (Arismendi *et al.*, 2009). In Chile and the Falkland Islands, the areas where *S. trutta* have been introduced show wide spread ecological damage, leading to *S. trutta* being labelled as one of the "100 of the world's worst invasive species" (Lowe *et al.*, 2000). This highlights their need to be monitored both as a native species in the Northern Hemisphere and as an exotic, invasive species in the Southern Hemisphere.

1.2.2.3. Salvelinus alpinus

S. alpinus is a cold water salmonid found throughout the Northern Hemisphere. Whilst often considered an anadromous species, in Ireland, populations have fully adapted to a freshwater life cycle (Mirimin *et al.*, 2020). Due to confinement at the end of the last ice age (Maitland *et al.*, 2007), populations are highly isolated from each other across Ireland and Great Britain, leading to large genetic variation previously recognised as distinct species (Maitland *et al.*, 2007). Unfortunately, this isolation of *S. alpinus* populations makes them highly vulnerable to climatic changes particularly in the southerly part of their distribution (Connor *et al.*, 2019). Anthropogenic pressures such as agricultural intensification (Igoe *et al.*, 2001), eutrophication, acidification, aquaculture and introduction of nonindigenous species are causing a rapid decline in populations with 30% of Irish populations now considered extinct (Mirimin *et al.*, 2020).

In addition, *S. alpinus* are threatened by long term climate warming (Winfield *et al.*, 2010). Due to their reproductive nature, with a low thermal range whilst spawning,

increases in lake temperature can lead to smaller egg sizes, reduced hatch success and smaller emergent larvae (Farmer *et al.*, 2015). These increasing threats make it vital for *S. alpinus* to be monitored and protected, such as dictated in the European Water Framework Directive, to prevent further decline (Mirimin *et al.*, 2020).

Overall, salmonids are of ecological, economic and cultural importance, requiring routine monitoring to help in their conservation. These species are likely to be highly susceptible to the effects of climate change, due to their dependence on cold waters. For example, increasing air temperatures result in increased stream and lake temperatures, which can cause increasing stress and metabolic rates (Williams *et al.*, 2015). Moreover, changes in precipitation and flow regimes can influence spawning activity such as that of autumn-spawning salmonids (Low *et al.*, 2011; Goode *et al.*, 2013). In addition, many existing stressors for salmonids are likely to be heightened by climate change, for instance an increase in invasive species that compete with salmonids (Lawrence *et al.*, 2014). As salmonid habitats are subject to ever-increasing threats, it is vital that conservation efforts are made to prevent further vulnerability.

1.2.3. Approaches and limitations to traditional monitoring of aquatic organisms

Species monitoring has traditionally relied on the sighting and often the capture of organisms of interest. Specifically, the monitoring of fish in aquatic environments can prove challenging and usually requires sighting and collection of organisms. In Ireland for example, *S. salar* is carefully monitored by Inland Fisheries Ireland to evaluate *S. salar* stocks and influence management measures or policies (Gargan *et al.*, 2020). To assess species abundance, the Standard Scientific Committee on Salmon use data from five main methods (Gargan *et al.*, 2020); commercial catch, rod catch, total traps and counters, national coded-wire tagging and electrofishing. The different methods provide information into various aspects of *S. salar* ecology; for example, national coded-wire tag recovery data provides an index of marine survival over a long period of

time whereas electrofishing data provides information on the abundance of juvenile *S. salar* (Gargan *et al.*, 2020).

Traditional monitoring techniques such as those listed above, can be expensive, labour intensive and potentially harmful to the species of interest (Snyder, 2003). Electrofishing uses electric fields in water to capture or control fish (Snyder, 2003) but has been shown to cause spinal injuries and associated haemorrhage (Sharber and Carothers, 1988), which may go undetected unless very severe. Electrofishing can also damage species reproduction, effecting gametes and reducing viability of fertilised eggs (Snyder, 2003). Although a valuable tool in fishery management, the unintended adverse effects of electrofishing can be a significant problem. It is therefore suggested that less harmful alternatives should be sought for species monitoring (Snyder, 2003).

Moreover, traditional methods require taxonomic expertise to accurately identify taxa at different life stages and they can miss rare taxa due to their low capture probabilities (Magnuson *et al.*, 1994). This is highly problematic when monitoring endangered species and invasive species whereby species abundance may be low. As described previously, invasive species are a major recognised threat to biodiversity in aquatic systems (Molnar *et al.*, 2008), but detection of these species using traditional methods may be slow, enabling their establishment prior to detection. This threatens native biodiversity (Mooney and Cleland, 2001) and can cause native species extinction (Gurevitch and Padilla, 2004). To circumvent these limitations, there has been an increase in the use of non-invasive molecular methods for species detection. These methods include the use of environmental DNA (eDNA), which is not only able to detect all life stages without taxonomic expertise (Thomsen and Willerslev, 2015) but has also been shown to improve detection of invasive species (Dejean *et al.*, 2012).

1.3. Environmental DNA (eDNA)

Environmental DNA (eDNA) is genetic material obtained directly from an environmental sample such as water, soil and sediment (Taberlet *et al.*, 2012). The use of eDNA assessment is well established for detecting the presence or absence of rare or invasive species from the organic material they leave behind (Goldberg *et al.*, 2015). An organism provides a rich source of eDNA through the cells and waste they shed and excrete including faeces, mucus, gametes, hair and skin (Thomsen *et al.*, 2012). eDNA has been used to monitor a wide variety of species in a diverse range of environments. This includes: fresh/marine water (Ficetola *et al.*, 2008; Jerde *et al.*, 2011; Thomsen *et al.*, 2012; Sigsgaard *et al.*, 2015; Atkinson *et al.*, 2018; Parsons *et al.*, 2018; Uthicke *et al.*, 2018), sediment and ice cores (Willerslev *et al.*, 2007; Turner *et al.*, 2015), snow terrains (Franklin *et al.*, 2019) and even species drinking sources (Rodgers and Mock, 2015; Williams *et al.*, 2017). To date, most eDNA studies have focused on water samples, with the majority targeting freshwater or marine species (Ficetola *et al.*, 2008; Jerde *et al.*, 2011; Wilcox *et al.*, 2013; Merkes *et al.*, 2014; Jane *et al.*, 2015; Erickson *et al.*, 2016; Ikeda *et al.*, 2016; Baldigo *et al.*, 2017; Lafferty *et al.*, 2018; Xia *et al.*, 2018). However, it has also been used to monitor terrestrial or semi-aquatic species from both lotic (e.g. rivers and streams) (Sales *et al.*, 2020; Broadhurst *et al.*, 2021) and lentic (e.g. ponds and lakes) systems (Ushio *et al.*, 2017; Harper *et al.*, 2019).

1.3.1. Approaches to eDNA monitoring

There are two main approaches to eDNA monitoring: targeting of specific species or detection of multiple species from a single sample, termed eDNA metabarcoding (Deiner *et al.*, 2017) (Figure 1.3). Monitoring of specific species, particularly endangered or invasive species, is vital for conservation purposes. The sensitivity, and importantly specificity, of molecular techniques has enabled the non-invasive monitoring of individual species from a variety of environmental samples (Thomsen and Willerslev, 2015). Due to the low concentration of eDNA, these techniques require specific amplification of target DNA to a detectable limit (Thomsen and Willerslev, 2015). For this reason, quantitative PCR (qPCR) is most commonly used and through robust primer

design, has been shown to enable monitoring of hundreds of target species (Dejean *et al.*, 2012; Laramie *et al.*, 2015; Cai *et al.*, 2017; Carlsson *et al.*, 2017; Beans, 2018; Uthicke *et al.*, 2018; Robinson *et al.*, 2019). Moreover, qPCR has the potential to be adapted for any target of interest (to be discussed further in Chapter 3). Although the gold standard, other nucleic acid amplification techniques also offer potential for use in single species detection (Williams *et al.*, 2019). For example, isothermal amplification techniques such as Recombinase Polymerase Amplification (RPA) and Loop-Mediated Isothermal Amplification (LAMP) have been used for diagnostics in the medical field (Obande and Singh, 2020) highlighting their specificity and sensitivity. These methods rely on enzymatic activity to maintain DNA amplification efficiency without the need for thermal cycling. This is discussed in more depth in Chapter 4.1.2.

On the other hand, eDNA metabarcoding allows identification of multiple species across all taxa from microbes to higher vertebrates (Taberlet *et al.*, 2012). It is thus the main molecular method used to assess biodiversity as it provides a snapshot of numerous taxa from a single sample. This includes the possibility to identify microbes that previously would have required cultivation on an artificial medium or more critically could not be grown outside of their host and hence not amenable to identification using conventional methods (DeLong, 2005).

Metabarcoding is primarily being driven by developments in next generation sequencing technologies (Shokralla *et al.*, 2012). It involves the use of universal primers for PCR amplification of a wide range of species, for example, the MiFish primer set that target a hypervariable region of the 12S rRNA gene and allow detection of a vast array of fish species (Miya *et al.*, 2015). This is followed by next generation sequencing to generate thousands of reads (Ruppert *et al.*, 2019). The sequence data produced can be aligned back to available genomic sequences to enable organism identification. Primers used for eDNA metabarcoding require stringent design to ensure they bind a highly conserved region, with sufficient interspecific variation to allow species identification

(Epp *et al.*, 2012). To remove primer bias, which may lead to preferential amplification of some target species, multiple primer sets may be used (Drummond *et al.*, 2015).

1.3.2. Advantages of eDNA monitoring

The number of studies utilising eDNA is ever expanding due to the advantages it provides over traditional monitoring techniques.

Firstly, using eDNA for species monitoring is a non-invasive technique (Rees *et al.*, 2014; Antognazza *et al.*, 2019; Leempoel *et al.*, 2020), meaning organisms do not have to be caught for their presence to be detected and habitats are virtually untouched by sampling. This is highly beneficial over traditional methods that can cause stress to organisms and can be destructive to habitats. Secondly, eDNA based techniques are relatively inexpensive (Rees *et al.*, 2014; Ficetola *et al.*, 2019) when considering the cost of consumables and personnel. Although eDNA can require high starting expenses due to the costs associated with laboratory set up, developing primers/probes and sample processing (Smart *et al.*, 2016), these expenses do not increase linearly with increased sampling sites and therefore costs may be maximised when carrying out large sampling campaigns (Harper *et al.*, 2018).

Many studies have also found that using eDNA has higher detection probabilities than traditional methods (Renshaw *et al.*, 2015; Wilcox *et al.*, 2016). Although this is dependent on the species of interest and the sampling location (Wilcox *et al.*, 2013), eDNA techniques have been shown to be extremely sensitive and allow detection of species of low abundance which might be missed by traditional methods. This is very important for the detection of small cryptic species (Carvalho *et al.*, 2019), as well as for providing early warning signals of invasive species and monitoring the success of subsequent eradication efforts (Robinson *et al.*, 2019).

Additionally, eDNA allows accurate identification of all life stages with a broad taxonomic breadth (Beng and Corlett, 2020). It enables simultaneous assessment of a wide range of organisms (Sawaya *et al.*, 2019) with individual species discernible between morphologically indistinguishable species (Marshall and Stepien, 2019). Traditional methods of monitoring target species rely on morphological keys for identification. These keys are based on the phenotypic traits of adult organisms. As a result, they can lead to misidentification of eggs and juvenile forms. On the other hand, eDNA allows detection of all life stages of a species from egg to adult and can provide higher taxonomic resolution than traditional methods which may restrict identification to the genus or family level (Caesar *et al.*, 2006). Although eDNA also has limitations (discussed in section 1.3.4), with such benefits over traditional monitoring, eDNA methodologies have already been applied to many scenarios. These include detection of invasive species (Jerde *et al.*, 2011), assessing conservation status in difficult to access habitats (Reinhardt *et al.*, 2019), studying spawning ecology (Bylemans *et al.*, 2017; Antognazza *et al.*, 2019) and monitoring ecosystem health and dynamics (Cordier *et al.*, 2019).

1.3.3. eDNA abundance and persistence

The abundance and persistence of eDNA in aquatic environments is affected by a large number of biotic and abiotic factors (Figure1.4). These influence both the source and sinks of eDNA within a given environment. The primary source of eDNA is thought to be from excretion (Klymus *et al.*, 2015), with invasive carp fed with algae diets shedding one order of magnitude more eDNA than non-fed fish. It has also been shown that the amount of eDNA increases linearly with biomass (Takahara *et al.*, 2012; Klymus *et al.*, 2015) and that although temperature has little effect in controlled conditions, it might influence fish behaviour and thus increase eDNA yield in natural environments (Takahara *et al.*, 2012). This complex interaction between species size, diet, behaviour and eDNA shedding rate makes it difficult to predict the expected abundance of eDNA in an environment, without even considering eDNA persistence (Pilliod *et al.*, 2014).

This persistence has been widely studied (Dejean *et al.*, 2011; Collins *et al.*, 2018) and is affected by three main factors: transportation, sedimentation and degradation (Figure 1.4) (Goldberg *et al.*, 2015). The process of transport of eDNA varies between lentic and lotic systems but is critical when considering sampling design. In lotic systems, detection rates may be high but spatial inference is unknown, with eDNA from macro-organisms having been detected downstream from established populations (Deiner and Altermatt, 2014). However, the consistent relationship between increasing distance from a known population and decreasing eDNA concentration indicates that eDNA is not accumulating downstream and is likely settling or being degraded. Dejean *et al.*, (2011) reported short fragments (<100 bp) of detectable suspended DNA after 25 days at 8-11 °C, or 21 days at 17 °C. However, if eDNA settles it can be adsorbed to soil particles and persist in freshwater systems longer than dissolved or suspended DNA (more than 3 months) (Turner *et al.*, 2015). Disturbance of sediment adsorbed eDNA could lead to false positive indication of species presence and thus sediment should be avoided when collecting water samples for eDNA analysis, particularly if temporal inference is required (Turner *et al.*, 2015). eDNA concentration and detectability can also be influenced by production rate, temperature and light conditions, and time since colonisation or extirpation from a site (Pilliod *et al.*, 2014).

In addition to eDNA removal by transport or settling, eDNA degradation can have a strong influence on concentrations present in a system (Goldberg *et al.*, 2015). The abiotic factors affecting degradation are multifaceted but include exposure to UV-B, high temperature and more acidic conditions (Strickler *et al.*, 2015). Biotic factors, such as the action of bacteria and fungi present in the environment (Dejean *et al.*, 2011), also influence eDNA degradation. This breakdown of eDNA results in short fragments and consequently most eDNA studies favour short amplicons (90-120 base pairs (bp)) (Rees *et al.*, 2014). This increases the chance of target detection even though the DNA may be highly degraded.

The risk of eDNA degradation in the environment also influences the assay target site of choice, with the majority of eDNA studies to date targeting mitochondrial DNA (mtDNA). This is primarily due to its high copy number compared to nuclear DNA (Rees *et al.*, 2014). The nuclear genome of fish tends to be diploid (although variations in ploidy can be seen (Jørgensen *et al.*, 2018)), which limits the number of target sequences present per cell. However, each mitochondria has between 2 and 10 copies of their own genome with hundreds to thousands of mitochondria per cell (Hosgood *et al.*, 2010). Additionally, mtDNA has the ability to resist environmental degradation (Olson *et al.*, 2012) and thus persist in the environment for longer than nuclear DNA. This resistance is thought to be due to the mtDNA being contained within the mitochondrion of the cell and its circular, rather than linear, structure (Foran, 2006). For these reasons, most existing eDNA assays tend to target mtDNA as there is a perceived greater abundance present in the environment.

1.3.4. Limitations of eDNA methods

The complicated relationship between eDNA release, abundance, transport and persistence leads to many of the limitations associated with an eDNA approach for species detection. Perhaps the most pertinent of which is the lack of clarity between eDNA abundance and species biomass; a topic which has been thoroughly reviewed in Rourke *et al.*, (2021). Several studies have shown a positive relationship between eDNA quantities and fish biomass/abundance in controlled experimental systems (Takahara *et al.*, 2012; Pilliod *et al.*, 2013; Klymus *et al.*, 2015; Lacoursière-Roussel *et al.*, 2016). For example, Klymus *et al.*, (2015) found that eDNA shedding rates increased with fish biomass and that fed fish showed an approximately 10-fold increase in shedding rates compared to unfed fish. In addition, Salter *et al.*, (2019) observed significantly positive correlations between Atlantic cod biomass (kg) and eDNA quantities (copies) in oceanic waters. However, these correlations may be strongly altered by varying environmental conditions (Lacoursière-Roussel *et al.*, 2016) which are known to affect eDNA persistence. There is also little known about how mtDNA quantity (the target for most eDNA assays) relates to species biomass. It is known that numbers of mitochondria can

vary between tissue types and species life stages (Fernández-Vizarra *et al.*, 2011) and therefore the particular cellular debris of the target organism would affect how the eDNA quantity can relate back to biomass.

Additionally, the link is complicated by the vast array of ways eDNA can enter an ecosystem. Whilst eDNA shedding rates have been explored (Klymus *et al.*, 2015), these may vary depending on the life stage of the target organism (Thomsen and Willerslev, 2015). There is also little known about alternate routes of eDNA acquisition such as introduction via vectors. These may include wastewater, slime residue and predator faeces (Merkes *et al.*, 2014) and can result in misinterpreted detection of target organisms. These factors should be considered when estimating biomass from eDNA concentration.

Another limitation of using eDNA for species monitoring is that eDNA methods cannot distinguish between living and dead organisms (Darling and Mahon, 2011; Merkes *et al.*, 2014). Decomposing organisms still provide a source of eDNA into an ecosystem, which can be detected for at least one month after deposition (Merkes *et al.*, 2014). However, it has been shown that DNA from dead organisms is found predominately at the bottom of a water column (Kamoroff and Goldberg, 2018), meaning sampling methodology could be adapted to reduce the impact of DNA from dead organisms on presence/absence inference. Another potential avenue of exploration, is using metabarcoding of co-extracted eDNA and eRNA (Pochon *et al.*, 2017). It is suggested that when an Operational Taxonomic Unit (OTU) is only detected in the eDNA portion it is from a dead organism, whilst OTUs found in both the eDNA and eRNA fraction represent living species (Pochon *et al.*, 2017). This area of research is still in its infancy but offers a potential method for clarifying the source of eDNA.

Further limitations relate to using mtDNA as a target site for molecular assays. mtDNA is maternally inherited, meaning assays using such a target can only detect the maternal lineage of organisms including hybrid species (Thomsen and Willerslev, 2015). Interspecific hybridisation events are common in nature but can also be increased in frequency or originated by anthropogenic actions such as habitat modification (Quilodrán *et al.*, 2014). These events have frequently been reported for salmonid species; both between wild type populations (Hórreo *et al.*, 2011) and between wild and farmed escapees (Wringe *et al.*, 2018). Whilst studying mtDNA markers allows identification of possible hybridisation zones, i.e. where two mitochondrial types overlap - a potential contact zone, it fails to identify hybrid individuals (Stewart and Taylor, 2020). In order for hybrid species to be identified, a nuclear target with diagnostic single nucleotide polymorphisms (SNPs) is required (Stewart and Taylor, 2020). Studies have shown that nuclear targets can be used for eDNA detection (Bylemans *et al.*, 2017; Minamoto *et al.*, 2017) and not only facilitate detection of species with a high degree of mitochondrial sequence similarity (Dysthe *et al.*, 2018) but could also enable detection of hybridisation events (Minamoto *et al.*, 2017). Despite this potential, nuclear DNA targets require extensive knowledge of reference sequences of which there is a deficit. This is particularly pertinent for low trophic level taxa such as zooplankton. These organisms make up a large proportion of biodiversity, are highly sensitive to environmental stressors (Chiba *et al.*, 2018) and could provide valuable insight into the state of our environment, yet there is little genomic data available for them.

Unfortunately, the lack of publicly available whole genome sequences extends beyond low trophic level taxa, affecting high resolution detection of many organisms (Ruppert *et al.*, 2019). To date, annotated mitochondrial genome sequences for many fish species are publicly available on databases such as NCBI GenBank and more specific databases like MitoFish (Iwasaki *et al.*, 2013). These favour mitochondrial targeting eDNA assays because there is a distinct lack of nuclear reference data available. For many groups of organisms including viruses and microbial metazoan, there is a total ‘genome deficit’, whereby any sequence data in public databases remains sparse (Creer *et al.*, 2016). This

restricts the use of targeted eDNA analysis and prevents identification of OTUs generated with metabarcoding. Fortunately, with the improvement of genome technologies and the reduction in cost associated with whole genome sequencing, the number of species with sequenced genomes will continue to rise. It is also possible that local reference databases can be curated to account for sequence diversity expected within a region (Stoeckle *et al.*, 2020).

Despite this general genome deficit, the available genomic data for salmonids is relatively good, with specific databases such as SalmoBase (Samy *et al.*, 2017) providing genome sequences for five of the eleven salmonid genera. The complete *S. salar* genome was sequenced by the International Cooperation to Sequence the Atlantic Salmon Genome (Davidson *et al.*, 2010) and provided insights into rediploidisation following a whole genome duplication event ~80 million years ago within the Salmonidae lineage (Lien *et al.*, 2016). In 2018, the Sanger Institute announced they were sequencing 25 genomes representing key areas of biodiversity in Great Britain (Wellcome Sanger Institute), in order to decrease the above mentioned reference genome deficit. These genomes have subsequently been published and included the *S. trutta* genome (Wellcome Sanger Institute, 2019). Access to the whole genome sequence and intraspecific polymorphism data of target species, is vital for designing species specific assays. Prior to sequencing of the *S. salar* genome, only five fish genomes had been sequenced, including fugu, stickleback and zebrafish (Davidson *et al.*, 2010).

Overall, eDNA is effective at detecting presence/absence of organisms in multiple environments with an increasing use in the detection of rare or invasive species (Rees *et al.*, 2014). As highlighted, there are still several limitations with the technique, but eDNA methodologies may improve biodiversity monitoring by providing data on the variety, geographic range (Beans, 2018) and potentially the abundance of species, enabling greater ecosystem protection (Guisan *et al.*, 2013). To enhance rapid species detection, this monitoring should be performed in the field as laboratory processing

times can take days or weeks during which researchers do not know whether the target species' DNA is present or not (Thomas *et al.*, 2019). Although this delay may not be as detrimental for conservation purposes, it limits the range of eDNA applications and could prevent its use in rapid management responses such as of invasive species (Egan *et al.*, 2015) or parasites (Nguyen *et al.*, 2018). Nevertheless, the majority of assays to date rely on laboratory-based techniques and thus there is still progress to be made regarding on-site eDNA monitoring using a biosensor device.

1.4. Biosensors

The development of a biosensor device for single species monitoring can enable eDNA technology to be taken out of the laboratory and into the field. A biosensor is defined by the IUPAC as "a device that uses specific biochemical reactions mediated by isolated enzymes, immunosystems, tissues, organelles or whole cells to detect chemical compounds usually by electrical, thermal or optical signals" (Nagel *et al.*, 1992). The first example of a biosensor, developed in 1962, was used to monitor glucose concentration in blood samples (Clark and Lyons, 1962); however, since then the field has rapidly expanded.

1.4.1. Types of biosensor

There are many types of biosensor which consist of three main components: sensor, transducer and associated electronics (Figure 1.5) (Malhotra *et al.*, 2017); combining biology, chemistry and physics respectively. The sensor consists of a biological element such as enzymes, antibodies or nucleic acids. The transducer is the detection element that transforms the biological interaction to a readable output such as optical or electrochemical. Biosensors can be grouped based on their transduction method or their biological sensing element.

1.4.1.1. Transduction method

There are three main types of transduction element: piezoelectric, electrochemical and optical. Piezoelectric biosensors rely on the ability of a material to produce voltage when mechanically stressed (Pohanka, 2018). Electrochemical sensors use sensing molecules coated onto or bonded to an electrical probe surface. Upon reaction with the desired analyte, a change in electrical signal is produced which is proportional to the concentration of the analyte (Malhotra *et al.*, 2017). The first biosensor developed by Clark and Lyons, (1962) consisted of an enzyme coated oxygen-electrode and would thus be categorised as an electrochemical sensor.

Optical biosensors allow detection of analytes based on absorption, fluorescence or light scattering. They are the most commonly reported class of biosensor due to their ease of detection and ability to produce a signal proportional to the concentration of the measured analyte (Damborský *et al.*, 2016). Optical sensors can be label free, where the signal is generated directly by the interaction of the analyte with the transducer, or label-assisted which involves the addition of an optical label to the assay allowing generation of a signal by a colorimetric, fluorescent or luminescent method (Damborský *et al.*, 2016). Since they are non-electrical, optical sensors are advantageous for *in vivo* applications and can be used for the detection of multiple analytes using different wavelengths including by eye (Malhotra *et al.*, 2017).

1.4.1.2. Biological sensing element

1.4.1.2.1. Enzymes and antibodies

Enzymatic biosensors utilise the specific binding capabilities and catalytic activity of enzymes to detect target analytes. They have several advantages for use on a biosensor; they have highly specific enzyme-substrate interactions, they are able to catalyse a large number of reactions and they are not consumed during the reaction meaning they can be used repetitively (Katchalski-Katzir, 1993). The sensing principle of enzyme based biosensors involves measuring changes such as uptake/release of gases which occur

during the enzymatic reaction (Nguyen *et al.*, 2019). The coupling of enzymatic activity to a biosensor device allows qualitative and quantitative analysis of target analytes, with the main downfall being the potential reduction in signal response and selectivity due to interference caused by chemicals in the sample matrix (Nguyen *et al.*, 2019). Despite this, enzyme-based biosensors have already been commercialised and are used in many industries for portable, highly sensitive analysis of target analytes.

Antibodies are also frequently used as the biological sensing element of biosensors with immunoassays coupled to both optical (Sapsford *et al.*, 2002) and electrochemical (Zhang *et al.*, 2008) transducers. Use of immunoassay-based assays for viral diagnostics has been thoroughly reviewed in Cassedy *et al.*, (2021). Optical immunoassay sensors commonly use the colorimetric lateral flow immunoassay platform (LFIA). For example the home pregnancy test which uses a direct sandwich LFIA to measure human chorionic gonadotropin (hCG) (Butler *et al.*, 2001). This system requires an antibody pair; an antibody to one analyte epitope is labelled with a reporter and a secondary capture antibody to a second epitope of the same analyte is immobilised on the test line of a lateral flow strip (Figure 1.6) (Kozel and Burnham-Marusich, 2017). In direct LFIAs, the presence of the test line indicates a positive result (Koczula and Gallotta, 2016). This simple readout has made LFIAs amenable to the detection of multiple infectious diseases (Kozel and Burnham-Marusich, 2017).

1.4.1.2.2. Nucleic acids

Nucleic acids can also act as the biological sensing element of biosensor devices, for example in DNA hybridisation assays (Wang, 2002). Nucleic acid biosensors (NABs) primarily use DNA or RNA as oligonucleotide probes which rely on complementary base pairing for detection of the target analyte (Bora *et al.*, 2013). Hybridisation occurs between a known DNA sequence which can be immobilised to a solid, and an unknown target counterpart (Zhai *et al.*, 1997). The transducer in NABs is commonly optical such as use of molecular beacons, which are oligonucleotides labelled with a fluorophore and quencher. They enable detection of the target nucleic acid based on a change in

fluorescent signal upon hybridisation (Bora *et al.*, 2013). NABs can also use electrochemical transducers which use DNA immobilised onto an electrode and measure a change in electrical parameters generated by hybridisation of target (Erdem *et al.*, 1999). Nanopore sequencing is a form of electrochemical sensing which decodes the specific DNA or RNA sequence by monitoring changes to an electrical current as nucleic acids are passed through a protein nanopore (Bayley, 2015). It has been used for low-cost eDNA metabarcoding of white sharks in the open ocean (Truelove *et al.*, 2019) and for long read detection of North Sea fish (Doorenspleet *et al.*, 2021). Hybridisation based NABs have been used for clinical diagnostics (Bora *et al.*, 2013) and environmental pollution monitoring (Palchetti and Mascini, 2008). However, in several circumstances the starting concentration of target DNA may be insufficient and thus there is still a drive to integrate sample preparation with amplification and detection in a cost effective, robust manner (Niemz *et al.*, 2011).

Pre-amplification of DNA, due to the low abundance, is traditionally done using PCR. Although hugely influential in life sciences, conventional PCR (cnPCR) has several disadvantages for amplification including high usage of biological reagents such as *Taq* polymerase and dNTPs, multiple tube manipulation, potential for sample contamination, potentially long reaction times and a large thermal mass resulting in slow ramping rates. Miniaturisation of PCR can overcome some of these limitations by reducing consumption of biological agents, decreasing fabrication costs and time for amplification and increasing portability of the device (Zhang *et al.*, 2006). These benefits have led to a drive to adapt PCR based detection platforms to biosensor devices (Auroux *et al.*, 2004).

Several methods have been adapted to allow for miniaturisation of PCR by taking advantage of rapid heat transfer due to large surface-to-volume ratio in microfluidic systems. One of the main ways to achieve thermal cycling on a device is using thermoelectric techniques. These involve putting heating elements directly into contact with the microfluidic device and originally used stationary chambers containing the

reaction (Northrup *et al.*, 1993). However, due to the slow ramping rates of the heating elements, these stationary devices were not ideal for PCR on a miniaturised scale. Consequently, continuous flow PCR devices were developed whereby the sample is moved between heating elements at fixed temperatures (Kopp *et al.*, 1998). Major drawbacks of these systems include: the fixed number of cycles, the distinctive parabolic flow profile leading to uneven distribution of temperature across the mixture (Auroux *et al.*, 2004), the increased risk of sample contamination due to adsorption of PCR mixture components to the channel surface (Erill *et al.*, 2003) and the different flow rates between the centre and the areas closest to the channel surface (Giuffrida and Spoto, 2017).

Droplet digital PCR technology (described in Chapter 3) addresses some of these issues with miniaturisation by allowing uniformity of temperature across the sample and has thus been incorporated into continuous flow microfluidic devices (Mohr *et al.*, 2007). Within each droplet, an individual reaction is carried out reducing the risk of contamination between samples due to physical isolation. The lower thermal mass of oil, in comparison to water, means the oil takes less time to reach the required temperature than the external heaters allowing uniformity across each droplet (Mohr *et al.*, 2007). Although droplet technology overcomes some of the limitations associated with miniaturised PCR devices, development of isothermal systems would remove the difficulties with thermal cycling all together. Whilst PCR-based methodologies are still commonly used in laboratory-based settings, applications of isothermal techniques are surging due to their applicability in low resource settings and relatively robust nature (Cassedy *et al.*, 2021). These methods of amplification (as discussed further in Chapter 4.1.2) may advance the applicability of NABs and have already been adapted to microfluidic biosensor devices (Zanoli and Spoto, 2013). These devices often require no fluid movement, making them easily adaptable as battery based portable systems with a much lower energy requirement than thermal cyclic devices (Asiello and Baeumner, 2011).

Of particular interest for low cost isothermal sensing, are lateral flow nucleic acid tests due to their rapidity, ease of implementation and low equipment requirement (Zheng *et al.*, 2021). There are two main types of nucleic acid based lateral flow tests; Nucleic Acid Lateral Flow (NALF) and Nucleic Acid Lateral Flow ImmunoAssay (NALFIA) platforms (Jauset-Rubio *et al.*, 2016). NALF platforms use primers with modified carbon chains to directly detect target DNA via hybridisation of amplified products to reporter and capture probes (Jauset-Rubio *et al.*, 2016; Javani *et al.*, 2017). NALFIA platforms also use modified primers, with forward and reverse primers typically tagged with biotin and another antigen with high antibody affinity (such as FAM) (Liu *et al.*, 2018; Pecchia and Da Lio, 2018; Zheng *et al.*, 2021). These sensing platforms are typically combined with isothermal amplification methods and have successfully been used in several fields such as veterinary (El-Tholoth *et al.*, 2019) and agriculture (Zhao *et al.*, 2019).

1.4.2. Applications of biosensors

Biosensors have been designed for use in many fields including the food industry (Scognamiglio *et al.*, 2014), water quality monitoring (Hossain and Mansour, 2019), plant biology (Okumoto, 2012) and extensively in the medical field (Dineva *et al.*, 2005; Lee *et al.*, 2010; Yoo and Lee, 2010; Jarvis *et al.*, 2011; Wand *et al.*, 2018). For example, the presence of *Escherichia coli* in food/drinking water is a major concern as it acts as a bioindicator of faecal contamination. This threat has resulted in an expansion of research in to the development of rapid and reliable methods for direct detection of *E. coli* (Ercole *et al.*, 2003; Arora *et al.*, 2011; Heery *et al.*, 2016).

1.4.2.1. Point-of-Care diagnostics

The medical field is driving the development of biosensors due to the requirement for point-of-care (POC) diagnostics particularly in low resource settings. Such advances can and should be adapted by other fields such as environmental monitoring. Since the development of the first biosensor used for the detection of blood-glucose levels during cardiovascular surgery (Clark and Lyons, 1962), biosensors for blood-glucose monitoring

have significantly improved. They now account for approximately 85% of the world market for biosensors (Newman and Turner, 2005) and are predominantly used in the management of diabetes (Yoo and Lee, 2010). The majority of these biosensors are enzymatic amperometric devices meaning they measure a change in electrical current based on interactions of glucose with an enzyme, commonly glucose oxidase (Yoo and Lee, 2010).

In addition, medical biosensors have been developed for rapid detection of pathogens and disease biomarkers (Vashist, 2017). These sensors are designed to improve the monitoring and management of patient's health, with a particular drive towards low cost resource settings whereby the inability to rapidly diagnose numerous diseases leads to an increased number of deaths (Sharma *et al.*, 2015). Biosensors for this application have been developed using both antibodies and nucleic acid sensing elements. Many of the existing POC immunoassays, such as tests for early diagnosis of cryptococcal meningitis (Jarvis *et al.*, 2011), use the LFIA platform (Kozel and Burnham-Marusich, 2017). These platforms are well suited for developing countries due to their increased stability for long periods of time, precise performance, ease of shipping and storage (i.e. no refrigeration) and their ability to be interpreted by minimally trained users (Sharma *et al.*, 2015). In spite of these advantages, LFIAs are limited by their accuracy and low sensitivity (Sharma *et al.*, 2015).

Nucleic acid biosensors allow sequence specific detection of infectious agents at a sensitivity greater than that of antigen detection (Dineva *et al.*, 2005). As discussed previously, these have also been adapted to a lateral flow platform. For example, Lee *et al.*, (2010) developed an NALFA for detection of human immunodeficiency virus type 1 using isothermal amplification, named SAMBA. Detection was achieved by sandwich nucleic acid hybridisation (Nicholls and Malcolm, 1989), with two target specific oligonucleotide probes, one for capture and one for detection (Dineva *et al.*, 2005). More recently, molecular methods such as isothermal amplification and CRISPR-Cas detection have been applied to POC testing (discussed further in Chapter 4) (van Dongen

et al., 2020). With the rapid increase in the number of POC devices for different infectious agents, it is important that criteria be followed when developing such diagnostic devices. The World Health Organisation (WHO) state that POC testing should follow the ASSURED guidelines (Affordable, Sensitive, Specific, User-friendly, Robust and rapid, Equipment-free, Deliverable to all people who need the test) (Kosack *et al.*, 2017). Whilst this has been suggested for disease diagnostics, the guidelines are also applicable to other fields, such as environmental monitoring, whereby testing may be performed in the field by individuals with minimal training.

1.4.2.2. Environmental monitoring

Despite the major biosensor drive being for POC diagnostics, considerable developments have also been made for environmental monitoring. Enzymes, antibodies and nucleic acids have all been used as the recognition element for biosensor monitoring various environmental pollutants including pesticides (Zhang *et al.*, 2014), pathogens (Briciu-Burghina *et al.*, 2019) and toxins (Maguire *et al.*, 2018). A thorough review by Justino *et al.*, (2017) concluded that electrochemical and enzymatic biosensors are most commonly used for environmental monitoring of such pollutants due to their simplicity, specificity and cost-effectiveness. However, nucleic acid aptamers have also been readily exploited for a range of targets from small molecules to bacteria cells (McKeague *et al.*, 2015). These are well-suited for environmental monitoring because they are chemically stable, easily modified and relatively easy to synthesise (McConnell *et al.*, 2020).

Biosensor monitoring of eDNA offers its own unique challenges due to the low copy number of target sequences and the potential interference from non-target sequences. With an increasing demand for on-site devices in this field, it is surprising that the number of published studies are limited. Of the research moving towards on-site monitoring, qPCR detection has led the way, specifically using the commercially available Biomeme^{TM} system (Sepulveda *et al.*, 2018; Thomas *et al.*, 2019; Skinner *et al.*, 2020). This system combines a quick “dirty” sample preparation column with a handheld

thermal cycler connected to a phone, for POC qPCR monitoring (Nguyen *et al.*, 2018). Although it offers potential for eDNA monitoring, the Biomeme^{TM} system (discussed further in Chapter 3.4) is expensive and has lower detection probabilities than laboratory-based methods (Sepulveda *et al.*, 2018) and thus there is room to progress alternative methods.

Overall, despite the potential of bio-receptors to be adapted to sensor devices, there are still major challenges associated with on-site environmental monitoring such as the complexity of the sample matrix, the need for sample preparation, the low concentration of targets and the lack of laboratory-based conveniences such as electricity (McConnell *et al.*, 2020). In addition, although widely exploited for pathogen detection in the medical industry, food industry and environment, there is a need for adapting biosensor devices for biodiversity management and conservation purposes. This will remove the need for invasive techniques that may be detrimental to the target species and their habitats, whilst providing rapid, on-site monitoring.

1.5. Aims and Objectives

The overall aim of this research project is to progress single species detection using environmental DNA, towards a novel biosensor platform. The vision of the project for on-site monitoring involves development of a system in which a single sensor can be used at multiple sites with minimal sample handling, whilst maintaining the high levels of sensitivity and target specificity seen with laboratory-based monitoring. The device should have the minimum number of steps required, run at low temperatures and ideally use an optical transducer. The project focuses on the detection of salmonid species within freshwater ecosystems, with a particular interest in species monitoring of the Burrishoole Catchment, Co. Mayo, Ireland. The project has three main aims:

1) Development of a biological assay for single species detection using eDNA.
2) Adaptation of this assay to a biosensor device suitable for on-site monitoring.
3) Field validation of the developed methodology for salmonid monitoring.

The above aims will be met by achieving the following objectives:

1) Development of a *S. salar* specific qPCR assay for validation of eDNA extraction techniques and comparison to developed methodologies (Chapter 3).
2) Development of isothermal assays targeting *S. salar, S. trutta* and *S. alpinus* (Chapter 4).
3) Validation of the isothermal *S. salar* assay against an independent dataset – samples collected and analysed by collaborators in eastern Canada (Chapter 4).
4) Exploration of two biosensing platforms: a colorimetric lateral flow approach and a handheld fluorometer approach (Chapter 5).
5) Application of developed methodologies to environmental samples collected from the Burrishoole Catchment, Co. Mayo, Ireland (Chapter 6).

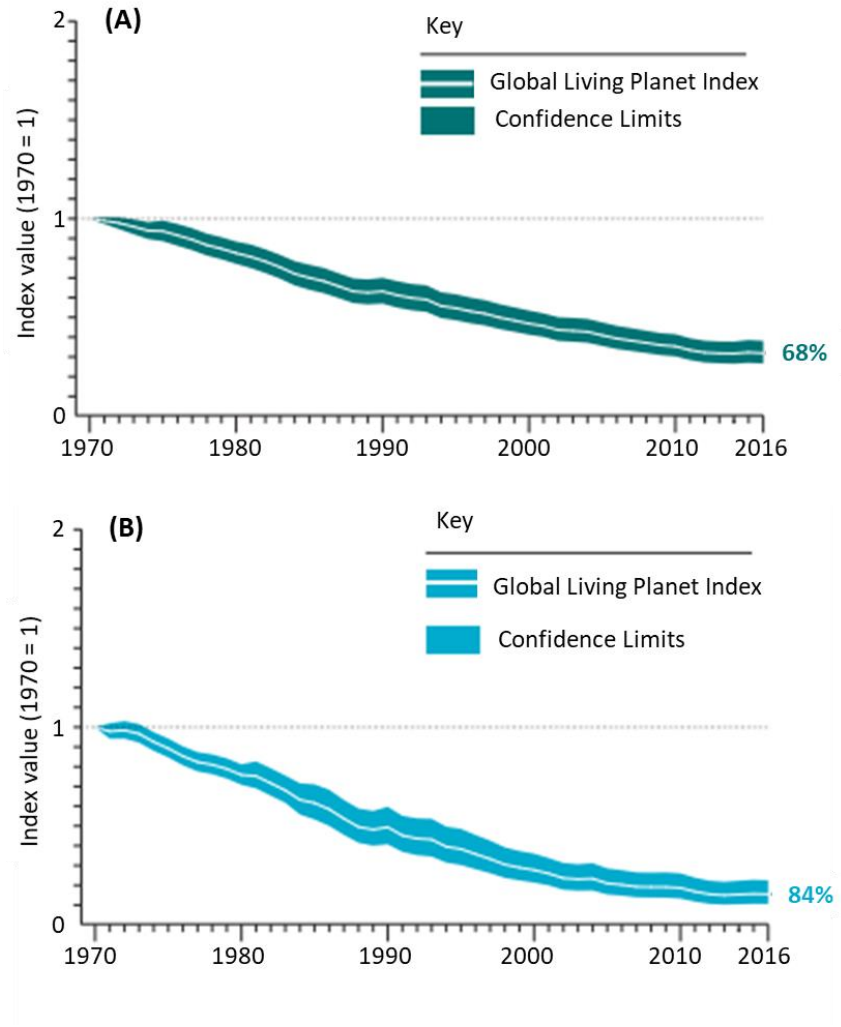

Figure 1.1 World Wildlife Fund Living Planet Index from 1970 to 2016. The white line shows the index values and the shaded areas represent the statistical certainty surrounding the trend. (A) Global Living Planet Index showing average decline of 68% (range -73% to -62%). (B) Freshwater Living Planet Index showing average decline of 84% (range -89% to -77%). Taken from WWF (2020).

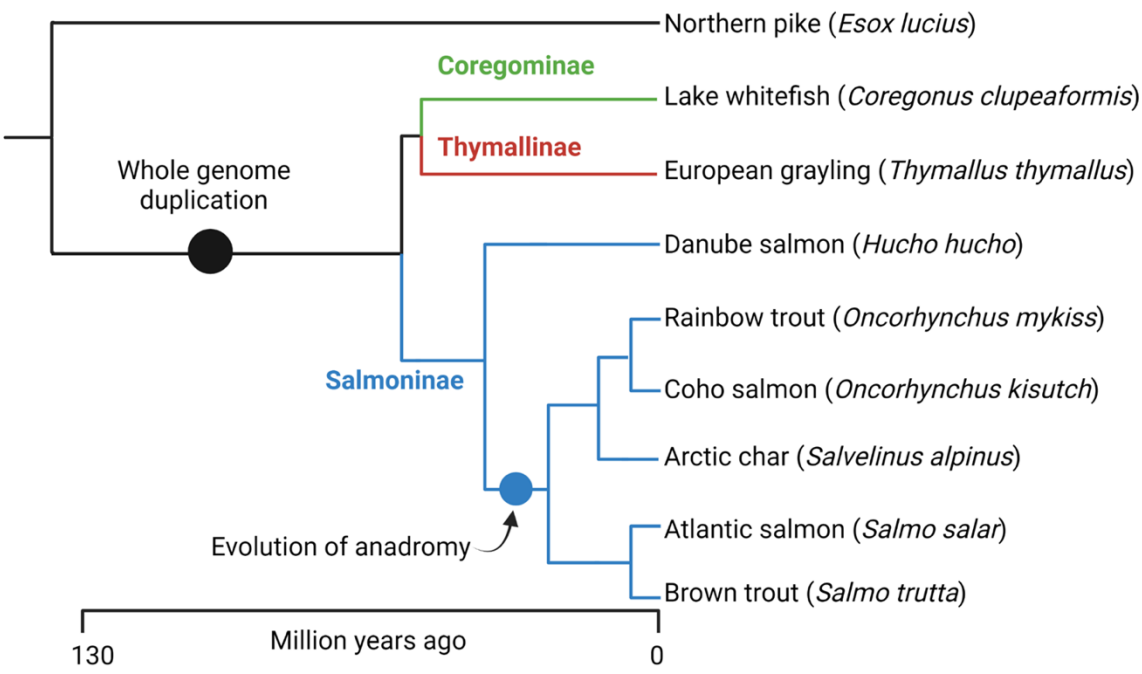

Figure 1.2 Phylogenetic tree of major Salmonidae lineage showing a whole genome duplication event in this family approximately 80 million years ago. Salmonidae subfamilies are shown: Salmoninae (salmon, trout and char), Coregominae (whitefishes) and Thymallinae (graylings). Adapted from Macqueen *et al.*, (2017).

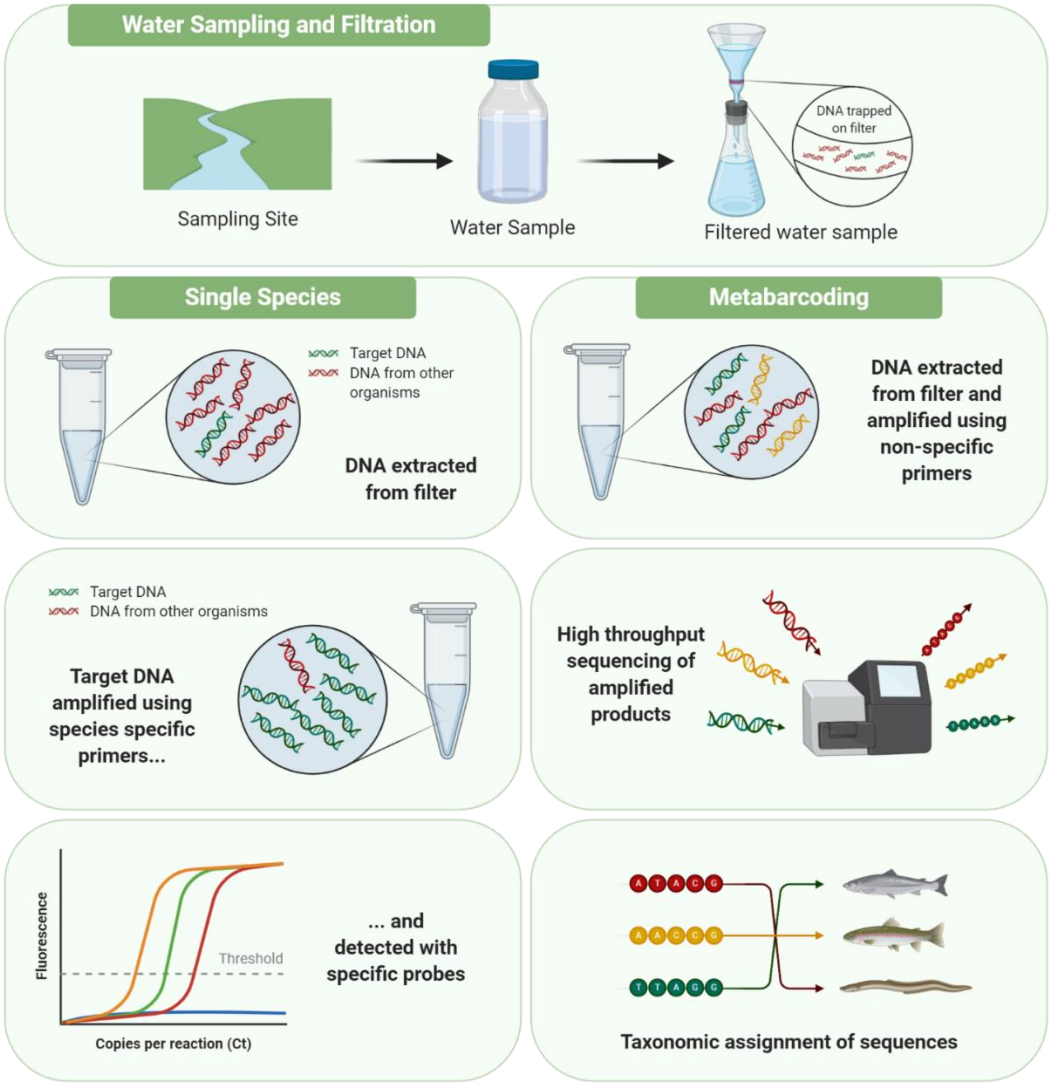

Figure 1.3 Simplified schematic of the two main approaches to eDNA monitoring from water. Initial processing of samples is the same for both methods of analysis with water samples collected filtered and eDNA extracted (note: there are large variations in this exact process but a simplified version is presented for ease of understanding). Single species analysis is commonly carried out using a targeted qPCR approach with sequence specific primers and probes used to amplify and detect the target organism only. The metabarcoding approach uses universal primers to amplify a wide-range of species. This is followed by high throughput next generation sequencing and bioinformatics taxonomic assignment. The metabarcoding approach is used to monitor multiple species simultaneously.

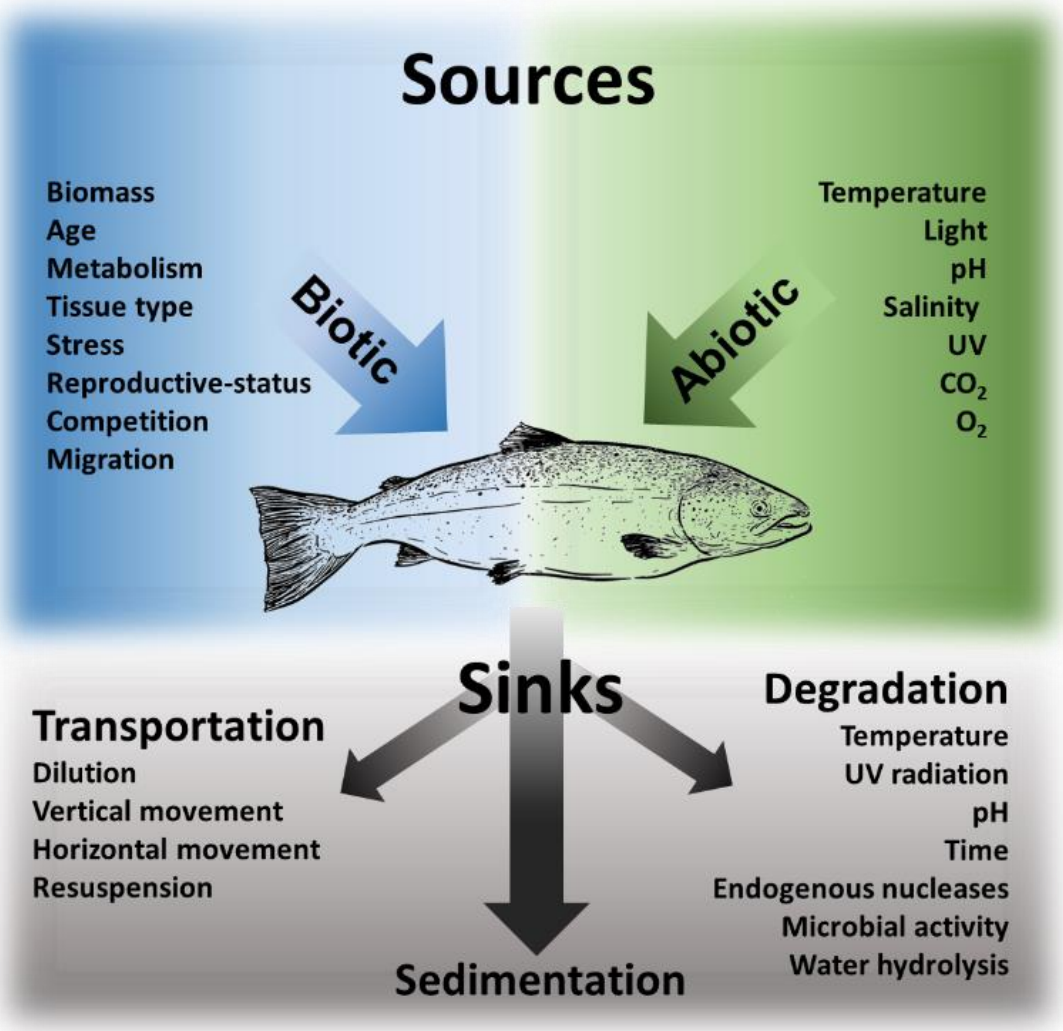

Figure 1.4 The factors influencing eDNA abundance and persistence in the environment. This includes the effect of various biotic and abiotic factors on the source of eDNA and potential DNA sinks through transportation, degradation and sedimentation. Adapted from Stewart, (2019).

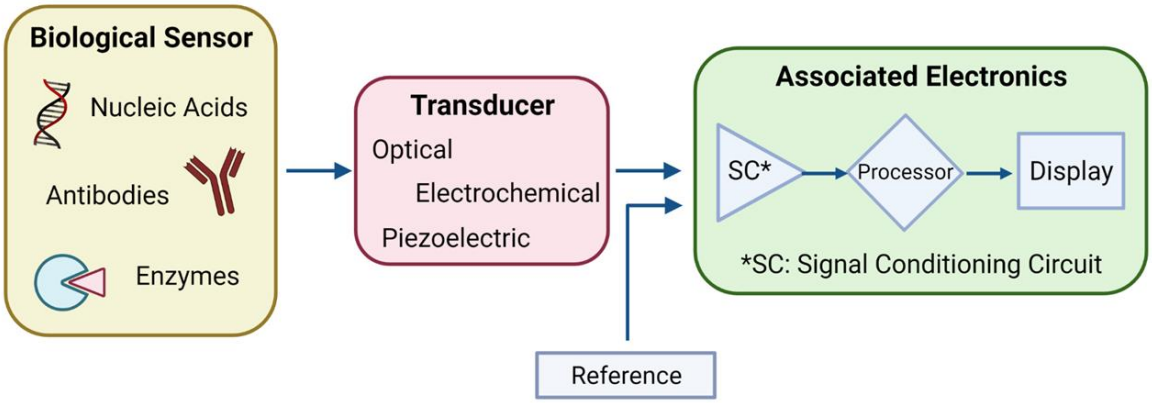

Figure 1.5 The main components of a biosensor including a biological sensing element, transducer and associated electronics. Adapted from Malhotra *et al.*, (2017).

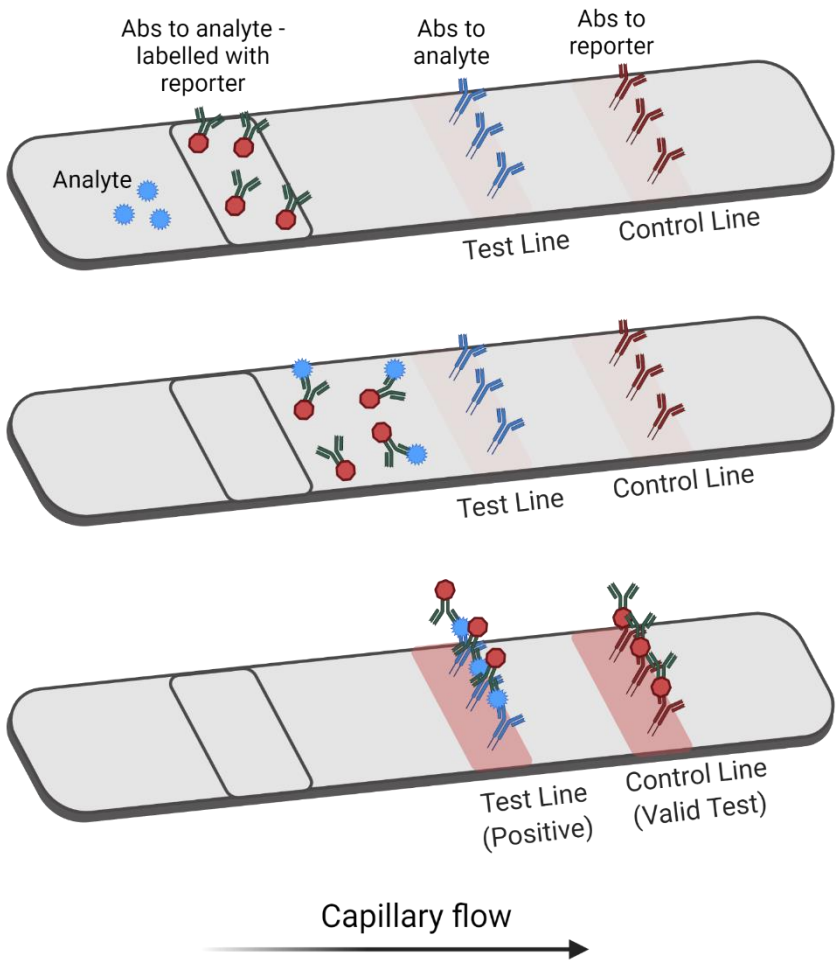

Figure 1.6 Mechanism of a Lateral Flow Immunoassay platform. An antibody (Abs) pair is required for this sandwich immunoassay; one antibody to one epitope of the analyte is labelled with a reporter, a secondary capture antibody to a different epitope of the same analyte is immobilised to the platform (test line). The control line consists of an antibody to the reporter and ensures the test is valid. Adapted from Lee *et al.*, (2013).

Chapter 2. General materials and methods

2.1. Reagents

Bioline: Isolate II Plasmid Mini Kit #bio-52056

Fisher Scientific: Ethanol, absolute 99% #E/0600DF/17

IDT: Alt-R® Acidaminococcus sp. BV3L6 (A.s) Cas12a nuclease #1081068; Custom ssDNA-FQ Reporter; Custom ssDNA-FB Reporter

Invitrogen: OneShot Top 10 chemically competent *Escherichia coli* cells #C404003; PBS #14200-067; pUC19 DNA #C404003; Qubit™ dsDNA HS Assay Kit #Q32851

Lennox: Industrial Methylated Spirit (IMS) 99% #CRTSI0330716

Merck Millipore: Sterivex 0.22 µm polyethersulfone membrane filter unit #SVGPL10RC

New England Biolabs: 1 kb DNA ladder #N0468S; 100 bp DNA ladder #N0467S; CutSmart Buffer #B7204S; *Dpn*I 20 U/µL #ROI76S; *Kpn*I 10 U/µL #R0142S; NEBuffer 1.1 #B7201S; Purple loading dye #B7024S; Q5 High Fidelity Polymerase 2U/µL #M0491S; Q5 Reaction Buffer #M0491S

Qiagen: DNeasy Blood and Tissue Kit #69506; DNeasy PowerSoil Pro Kit #47014

Roche: Ampicillin #835269; LightCycler480 Probes Master #04707494001

Sigma-Aldrich: 10x Reaction Buffer #D4545; Agarose #A9539; Boric acid #B6768; Bovine Serum Albumin (BSA) #A2153; dATP #D4788; dCTP #D4913; dGTP #D5038; dTTP #T9656; DTT #D0632; EDTA #E9884; Ethidium Bromide #E1510; Glycerol #G5516; Heparin #H3149; LB Broth #L3022; LB Broth with Agar #L2897; Molecular Biology Grade $MgCl_2$ #D4545; Magnesium Chloride #M8266; Orange G #O3756; Potassium Chloride #P9541; SDS #L3771; Sodium Acetate #S2889; Sodium Chloride #S7653; Sodium Hydroxide #221465; *Taq* DNA Polymerase 5 U/µL #D4545; Tris Base #T6066; Tris HCl #T5941; Molecular Biology Grade Water #W4502

ThermoFisher Scientific: O'RangeRuler 10 bp DNA ladder #SM1313

TwistDx: Milenia HybriDetect 1 #MILENIA01; TwistAmp Basic Kit #TABAS03KIT

Whatman: Nitrocellulose Membrane Filters (diam. 47 mm, pore size 0.45 µm) #WHA10401170

All primers were synthesised commercially by Sigma. All gRNAs were synthesised commercially by IDT.

2.2. Solutions

Agarose Gel (1% w/v): 1 g of agarose per 100 mL of 1x Tris-Borate-EDTA (TBE) buffer.

Ampicillin (100 mg/mL): 1 g ampicillin in 10 mL Molecular Biology Grade water. Filter sterilised through 0.22 µm syringe filter.

Binding Buffer for CRISPR-Cas Detection (1x): 20 mM Tris-HCl, pH 7.5, 100 mM KCl, 5 mM $MgCl_2$, 1 mM DTT, 5% glycerol, 50 µg/mL heparin.

LB Agar: 35 g of LB agar per L of distilled water.

LB Broth: 20 g of LB broth per L of distilled water.

Longmire's Solution: 100 mL of 1 M Tris-HCl, pH 8.0, 200 mL of 0.5 M EDTA, pH 8.0, 2 mL of 5 M NaCl, and 25 mL of 20% SDS made up to 1 L in distilled water.

NEBuffer 2.1 (1x): 50 mM NaCl, 10 mM Tris-HCl, 10 mM $MgCl_2$ and 100 µg/mL BSA (pH 7.9)

Sodium Acetate Solution (3 M): 12.3 g Sodium Acetate per 50 mL distilled water (pH 5.2)

Sodium Hydroxide Solution (0.33 M): 2.65 g Sodium Hydroxide per 200 mL distilled water

TBE Buffer (10x): 0.89 M Tris Base, 0.89 M Boric acid, 20 mM EDTA, distilled water.

TE Buffer (1x): 10 mM Tris Base (pH 7.5), 0.5 M EDTA (pH 8), distilled water.

Tris-EDTA Buffer (1x): 10 mM Tris-HCl, 1 mM EDTA, distilled water (pH 6.7)

Tris-HCl Solution (1 M): 31.52 g Tris-HCl per 200 mL distilled water (pH 6.7)

2.3. Methods

2.3.1. Contamination prevention

All pre-amplification work with eDNA was carried out in a dedicated DNA clean room. eDNA extractions from water and sediment samples were spatially separated from pre-amplification set up steps. All sampling and filtration equipment was either newly sterile or soaked in a 20% bleach bath overnight and cleaned with 70% IMS prior to use. DNA extractions from tissue samples and post-amplification steps were carried out in a separate laboratory.

2.3.2. Gel electrophoresis

Agarose gels were made by boiling 1%, 2% or 4% (w/v) agarose in 1x TBE. Liquid solutions were cooled and mixed with Ethidium Bromide to a final concentration of 0.1 µg/mL before pouring into the mould. The electrophoresis buffer was also 1x TBE. Amplified product was mixed with either 5x Orange G loading dye or 6x Purple Loading dye (depending on the product size) and electrophoresised at 80 V for approximately 60 min. Gels were visualised using a DNR MiniBIS Pro Bio-Imaging system.

2.3.3. Sanger sequencing

DNA samples (including PCR products and recombinant plasmid clones) were Sanger sequenced by Source Biosciences (IRL).

2.3.4. DNA extraction from fish tissue

DNA was extracted from *S. salar, S. trutta* and *S. alpinus* tissue samples using the Qiagen DNeasy Blood and Tissue Kit. Extraction followed manufacturer's instructions but with a final elution step in 50 µL Buffer AE. To confirm species identity, the mitochondrial DNA Cytochrome Oxidase subunit I (*COI*) region was amplified and confirmed following Sanger sequencing using previously published generic fish primers, Fish F1 (5'-

TCAACCAACCACAAAGACATTGGCAC-3') and Fish R1 (5'-TAGACTTCTGGGTGGCCAAAGAATCA-3') and conditions (Ward *et al.*, 2005).

2.3.5. Field sampling and eDNA extraction from freshwater samples

2.3.5.1. Burren, Dalligan and Delour Rivers, Ireland (Chapter 4)

Water sampling and eDNA extraction of these rivers was carried out by Dr. Jens Carlsson's laboratory, University College Dublin, as reported in Atkinson *et al.*, (2018).

2.3.5.2. Srahrevagh River, Co. Mayo, Ireland (Chapter 4)

Environmental water samples were collected from Srahrevagh River, Co. Mayo, Ireland in sterilised 1 L Nalgene bottles. Samples were collected mid-stream from the surface of the river by directly dunking the sterile bottles. Samples were subsequently separated and 550 mL (Turner *et al.*, 2014) per replicate was vacuum filtered through a 47 mm cellulose nitrate filter (0.45 µm). One negative control consisting of distilled water was also filtered for each sampling session. Filters were cut in two and stored at -20 °C prior to extraction. Environmental DNA was extracted from half the filter using the Qiagen DNeasy Blood and Tissue Kit with some modifications based on Renshaw *et al.*, (2015). Filters were cut into small pieces using a sterile scalpel, immersed in 567 µL Buffer ATL and 37.8 mAU Proteinase K and incubated in a water bath for 60 min at 65 °C. Following incubation, 630 µL Buffer AL and 630 µL absolute ethanol were added, the filter was removed and three centrifugation steps, at 6,000 x *g*, were required to load the samples into the DNeasy Mini Spin Column. The remainder of the protocol followed manufacturers protocol but with a final elution step in 50 µL Buffer AE. Extracted DNA was quantified using a Qubit® Fluorometer (#Q32857, Thermo Fisher Scientific) with the dsDNA high sensitivity assay kit and stored at -20 °C prior to analysis.

2.3.5.3. Miramichi and Jacques Cartier Watersheds, Canada (Chapter 4)

Note: Field sampling and eDNA extraction for eastern Canada sites were carried out externally (see Williams *et al.*, (2021)), but RPA-CRISPR-Cas and comparative data analysis was carried out by Molly Ann Williams.

Water samples were collected from the Miramichi Watershed following a protocol established by Carim *et al.*, (2016). At each site, 3.5 L of water was pumped through a pre-packaged filter (cellulose nitrate membrane filters: Whatman - 47 mm diameter/0.45 µm), housed within a Nalgene 145-2020 analytical test filter funnel - 250 mL capacity, using a peristaltic pump. Sample filters were then stored at -20 °C at the University of New Brunswick, until they were shipped to University Laval for extraction.

Water samples from the Jacques-Cartier Watershed were collected by the team from the Ministry of Forests, Wildlife and Parks (MFFP). At each site, 250 mL of water was filtered on-site using a 0.7-µm glass microfiber filter (Whatman GF/F, 25 mm) and a 60 mL syringe. All filters were preserved in 2 mL microtubes containing 700 µl of Longmire's solution and then frozen at −20°C until extraction (detailed in Leduc *et al.*, (2019).

DNA from both watersheds was extracted following the protocol developed by Goldberg *et al.*, (2011). Briefly, each filter was divided in half and extracted using the Qiagen DNeasy Blood and Tissue Kit. No negative field controls were performed during sampling. To account for this, several “negative stations” were selected with known absence of *S. salar* (i.e., sites located upstream of a waterfall and *S. salar* absence confirmed by electrofishing). Separate negative controls were included during eDNA extraction and both detection protocols to account for any contamination at these stages.

2.3.5.4. Burrishoole Catchment, Ireland (Chapter 6)

Water samples from the Burrishoole Catchment were sampled and extracted based on protocols established by Spens *et al.*, (2017). At each site, two samples of 250 mL were collected and syringe filtered on-site using a sterile Sterivex 0.22 µm polyethersulfone membrane filter unit (Merck Millipore) and 60 mL luer lock syringes. Samples were taken by directly filing a sterilised 250 mL Nalgene bottle from surface water, mid-stream for river samples and at the shore for lake samples. Filters were preserved in ~2 mL Longmire's solution, sealed at both ends and transported back to Dublin City University for eDNA extraction. Three negative field controls were taken in total, consisting of distilled water filtered in the field at sites one, six and thirteen. Negative controls were treated identically to field samples.

DNA was extracted from the Sterivex filters using the Qiagen DNeasy Blood and Tissue Kit following a modified protocol. Longmire's solution was transferred to a 2 mL Eppendorf tube and centrifuged at 17,000 x *g* for 30 min. The liquid was discarded and the pellet was left to dry. Simultaneously, the caps were removed from the Sterviex filter unit and the filter was left to dry for 30 min. Lysis mixture (9:1 ratio of ATL buffer and Proteinase K) was added directly to the Sterivex filter unit and the pellet, 800 µL and 200 µL, respectively. Both were sealed and incubated at 56 °C overnight in a rotating incubator. Following incubation, liquid was removed from the Sterivex filter unit. Buffer AL and ice-cold 100% ethanol was added to both samples (liquid from Sterivex and lysed pellet from Longmire's solution) in equal volumes, vortexed and transferred to a DNeasy Mini Spin Column via centrifugation at 6,000 *x g*. Subsequent steps followed manufacturers protocols with DNA eluted in 100 µL Buffer AE. Extracted DNA was quantified using a Qubit® Fluorometer (#Q32857, Thermo Fisher Scientific) with the dsDNA high sensitivity assay kit (Appendix A) and stored at -20 °C prior to analysis.

2.3.6. Sediment core sampling (Chapter 6)

The sediment coring operation was carried out as part of the SEQUESTER and BEYOND2020 projects by Aaron Potito, Karen Molloy, Carlos Chique and Catherine Dalton. An 8 m long sediment core was extracted towards the southern end of Lough Feeagh (N 53.55., 54.70; E 9.34., 33.07*) at a water depth of 25 m, using a Usinger piston corer (Spencer *et al.*, 2019). The top 6.4 m consisted of lake sediment and the remaining 1.6 m was composed of glacial clay. Following extraction, the core segments were stored in the cold room at the Palaeoenvironmental Research Unit, NUI-Galway. Radiocarbon dating of the core was used to estimate the age of subsamples from six depths. These dates were then converted to calibrated years before present (YBP) using the default calibration curve of IntCal20 and OxCal (ver 4.4) (Ramsey, 2009; Reimer *et al.*, 2020).

2.3.6.1. Core subsampling for eDNA analysis

Subsampling for eDNA was carried out by Ryan Smazal in October 2020 at Dundalk Institute of Technology (DkIT). In total, 13 samples were taken at depths of 0 cm, 5 cm, 10 cm, 15 cm, 25 cm, 50 cm, 75 cm, 100 cm, 200 cm, 305 cm, 400 cm, 500 cm, and 600 cm. A clean scalpel was used to cut the tops off 14 plastic syringes, which were subsequently washed in tap water and air-dried. The syringes were then placed into a 6% bleach solution for one minute and rinsed in a beaker containing de-ionised water. Falcon tubes followed the same general process. Once the syringes and tubes were dry, they were placed into a plastic bag and stored before usage. The pre-cleaned syringes were used to take 3 cm^3 of sediment which were then placed into the corresponding Falcon tube. Gloves were changed between each sample to reduce contamination. Samples were wrapped in tin foil and placed into a plastic bag for storage at -80 °C prior to transport to DCU in February 2021. At DCU, samples were stored at -20 °C prior to extraction.

2.3.7. DNA extraction from sediment

DNA was extracted from core sediment samples following the protocol developed by Sakata *et al.*, (2020). This protocol combines an alkaline lysis with ethanol precipitation and a sediment DNA extraction kit (Qiagen, DNeasy PowerSoil Pro Kit). Briefly, 6 mL of 0.33 M sodium hydroxide solution and 3 mL of Tris-EDTA buffer was added to 3 g of sediment sample, vortexed and incubated at 94 °C for 50 min. The sample was subsequently cooled to RT, centrifuged at 3,000 *xg* for 1 min and 7.5 mL of supernatant was transferred to a new tube and neutralised with 7.5 mL 1 M Tris-HCl (pH 6.7). Next, 1.5 mL of 3 M sodium acetate solution and 30 mL absolute ethanol was added to the mixture and incubated at – 20 °C for 60 min. Samples were then centrifuged at 3,000 *xg* for 30 min, the supernatant was discarded and the pellet was transferred to the PowerBead tube of the PowerSoil Pro Kit. The remainder of the protocol followed manufacturer's protocol. Extracted DNA was quantified using a Qubit® Fluorometer (#Q32857, Thermo Fisher Scientific) with the dsDNA high sensitivity assay kit (Appendix U) and stored at -20 °C prior to analysis.

2.3.8. Bioinformatics resources

2.3.8.1. BLAST – Basic Local Algorithm Search Tool (NCBI)

The Basic Local Alignment Search Tool (BLAST) finds regions of similarity between sequences. The program compares nucleotide sequences to sequence databases (particularly GenBank Release 229.0) and calculates the statistical significance of matches. BLAST 2.8.0 was used to check species specificity of designed primers and probes. (https://blast.ncbi.nlm.nih.gov/Blast.cgi)

2.3.8.2. dbSNP Build 151 (NCBI)

The Single Nucleotide Polymorphism Database (dbSNP) is a public-domain archive for polymorphism including SNPs, deletion insertion polymorphisms and short tandem repeats of multiple species. The database was used to assess *S. salar* polymorphisms in assay targeting regions. (https://www.ncbi.nlm.nih.gov/snp/)

2.3.8.3. ClustalW algorithm (Geneious 11.1.5, Biomatters Ltd)

ClustalW is an algorithm used for multiple sequence alignment of DNA. It was used to align sequences from closely related species to select a targeting region of assays. (https://www.geneious.com/)

2.3.8.4. BioRender

BioRender is a scientific design program used to make the schematics throughout this thesis. (https://biorender.com/)

2.3.8.5. GelQuant.NET Software (version 1.7.8, BioChem Lab Solutions)

GelQuant.NET software was used to determine absolute band intensity of the test line in lateral flow studies. Values produced are arbitrary but allow qualitative comparison of band intensities. (http://biochemlabsolutions.com/GelQuantNET.html)

2.3.8.6. IDT PrimerQuest Tool (version 2.2.3)

Used to design hydrolysis probe for qPCR assays. (https://eu.idtdna.com/primerquest/home/index)

Chapter 3. Validation of environmental DNA extraction and assay protocols through the development of a *Salmo salar* qPCR assay.

3.1. Introduction

3.1.1. Overview

Molecular methods using environmental DNA offer new opportunities to monitor biodiversity and track endangered and invasive species. PCR-based methods are easily adaptable for detection of species of low abundance in the environment (Robinson *et al.*, 2019) and allow detection of organisms missed by traditional methods. Using qPCR detection of target species from eDNA enables high specificity and sensitivity whilst allowing non-invasive environmental monitoring. In this chapter, a specific qPCR assay for the detection of *S. salar* from eDNA is developed. The mitochondrial gene Cytochrome Oxidase subunit I (*COI*) is selected as the target of the assay. This gene is considered the barcode of life (Hebert *et al.*, 2003) with sequence divergence enabling the discrimination of closely related species in most animal phyla. The development of a conventional eDNA detection method allows verification of the eDNA workflow, including water sampling, contamination prevention, eDNA extraction and molecular detection, whilst simultaneously highlighting the utility of the eDNA approach for *S. salar.* As the gold standard technique for eDNA assays, it can also be used for subsequent validation of new technologies to be developed throughout this project.

3.1.2. Molecular methods for eDNA detection

PCR-based methods are the most commonly used for single species eDNA detection. These techniques allow selective amplification of target DNA which is often low in abundance in environmental samples (Robinson *et al.*, 2019). Over time, there has been a transition from conventional PCR (cnPCR) (Dejean *et al.*, 2011; Thomsen, Kielgast, Lars Lønsmann Iversen, *et al.*, 2012) to quantitative PCR (qPCR) (Wilcox *et al.*, 2013; Boothroyd *et al.*, 2016; Carlsson *et al.*, 2017; Gargan *et al.*, 2017; Atkinson *et al.*, 2018; Rusch *et al.*, 2018) and droplet digital PCR (ddPCR) (Baker *et al.*, 2018; Uthicke *et al.*, 2018). This is primarily due to the increased need for highly sensitive and specific assays.

3.1.2.1. Conventional PCR (cnPCR)

Conventional PCR or end-point PCR refers to PCR amplification using a thermal cycler with product visualisation via gel electrophoresis (Figure 3.1). This method was first applied to eDNA (Ficetola *et al.*, 2008) due to its ability to increase the quantity of target DNA in a sample to a visible amount. It has primarily been used for single species detection from lotic systems (Jerde *et al.*, 2011; Deiner and Altermatt, 2014) and is solely used to verify presence/absence of a species (Dejean *et al.*, 2012; Davy *et al.*, 2015). As with all PCR-based assays, cnPCR requires careful design of highly specific primers and optimisation of conditions to maximise detection, to prevent cross reactivity and reduce the risk of false positives. It is the least sensitive of the PCR-based methods and has been shown to have a higher limit of detection (LOD) and lower detection rate in-field samples than quantitative PCR methods (Nathan *et al.*, 2014; Xia *et al.*, 2018).

In the literature, there is a disparity in the specific details of PCR methodology, preventing direct comparison of results such as LOD and reaction efficiencies. There is large variation in the volume (and thus concentration) of eDNA used, from 1-3 µL (Dejean *et al.*, 2012; Xia *et al.*, 2018), the number of PCR cycles, from 30-55 cycles (Dejean *et al.*, 2012; Hempel *et al.*, 2020) and the number of replicates, from 3-8 (Jerde *et al.*, 2011; Dejean *et al.*, 2012; Deiner and Altermatt, 2014). This makes designing new detection assays based on the literature challenging. To compensate for reduced sensitivity compared to the other PCR-based methodologies, it is recommended that the number of PCR replicates be increased (Davy *et al.*, 2015). It is important however to account for a potential increase in false positives and therefore, most studies send a subset of positive samples for Sanger DNA sequencing in order to validate the successful detection of target species (Deiner and Altermatt, 2014; Janosik and Johnston, 2015). Overall, cnPCR has a definite place in eDNA studies, particularly if surveys require low cost, qualitative assessment of highly abundant species. It however, does not offer quantitative measurements and lacks the sensitivity for organisms of low abundance in the environment.

3.1.2.2. Quantitative PCR (qPCR)

qPCR has been adapted for single species detection from a wide range of aquatic (Goldberg *et al.*, 2013; Wilcox *et al.*, 2013; Lugg *et al.*, 2018; O'Sullivan *et al.*, 2020) and terrestrial organisms (Franklin *et al.*, 2019). Unlike cnPCR, qPCR collects data during the exponential phase of amplification (Figure 3.2) allowing an assessment of reaction efficiency before depletion of reagents begins (Kubista *et al.*, 2006). This enables quantification of starting DNA concentration as fluorescence is directly proportional to the amount of product during this phase (Kubista *et al.*, 2006). qPCR is a well-established technique throughout Molecular Biology and robust guidelines, known as the MIQE guidelines (Bustin *et al.*, 2009) have been developed to ensure the integrity of the literature and consistency between laboratories. The quantitative element, on top of the increased speed, sensitivity and reproducibility (Yang and Rothman, 2004), has led to qPCR being the favoured method for eDNA studies.

Probe-based qPCR offers increased species specificity over cnPCR, due to 5'-3' exonuclease cleavage of a fluorescently labelled, sequence specific molecular probe by the DNA polymerase. Such assays are commonly referred to as "TaqMan® assays" or "5' nuclease assays" and often use hydrolysis probes. These probes consist of a short DNA fragment, complementary to the target, labelled with a reporter dye on one end and a quencher molecule on the other. The quencher absorbs reporter fluorescence when the probe is intact *via* fluorescent resonance energy transfer (FRET). During each PCR cycle, the 5'-3' nuclease activity of the DNA polymerase cleaves the probe during target elongation (Holland *et al.*, 1991). This cleavage separates the quencher and results in an amplification-dependent increase in fluorescence (Figure 3.2). TaqMan® MGB probes are a specific type of hydrolysis probe commonly used in eDNA assays (Herrero *et al.*, 2010; Carlsson *et al.*, 2017; Atkinson *et al.*, 2018). They have the advantage of having a 3' modification allowing the formation of extremely stable duplexes with the target strand and allowing construction of short probes highly sensitive to nucleotide differences (Kutyavin *et al.*, 2000).

qPCR can also involve other types of fluorescence measurement such as the use of intercalating dyes like SybrGreen. This non-sequence specific method of detection works due to the intensity of fluorescence increasing when the SybrGreen dye binds to the minor groove of double stranded DNA (dsDNA). As more dsDNA is produced during the PCR process, more dye binds to the DNA and the fluorescence increases. Although SybrGreen lacks the specificity of hydrolysis probes, it provides a cheaper method of detection and has been shown to allow reliable detection (Davy *et al.*, 2015). It has also been shown to reduce the susceptibility of qPCR to inhibitors often present in the environment (Mauvisseau *et al.*, 2018). Considerations should be made to assess this benefit with the increased risk of false positive results due to the removal of a sequence dependent element (Harper *et al.*, 2018).

In addition to increasing specificity, the move to qPCR allows an increase in sensitivity and thus raises the probability of detecting organisms of low abundance (Piggott, 2016). This improved sensitivity has enhanced monitoring of invasive species and measuring the decline in species following eradication events (Robinson *et al.*, 2019). Furthermore, the mechanism of qPCR allows reactions to be multiplexed enabling detection of multiple species from the same sample, simultaneously (Tsuji *et al.*, 2018; Hulley *et al.*, 2019).

Due to the benefits of qPCR, there was an influx of studies answering previously unknown questions regarding the interaction of eDNA as a molecule and the ecology of an organism. Researchers have used the quantitative aspect of qPCR to establish the link between eDNA abundance and biomass (Takahara *et al.*, 2012), the quantity of eDNA during spawning (Erickson *et al.*, 2016; Bylemans *et al.*, 2017) and the effect of species distance from sampling location on eDNA concentration (Jane *et al.*, 2015; Wood *et al.*, 2020). These questions remain to be fully answered due to current limitations with eDNA assays as discussed in Chapter 1.3.4.

3.1.2.3. Droplet digital PCR (ddPCR)

Droplet digital PCR is the most recent PCR-based technique to be applied to eDNA studies and is currently the most quantitative molecular method available (Hindson *et al.*, 2013). Compared to qPCR, it offers superior quantification of DNA samples by splitting molecules into individual droplets and reactions (Figure 3.3). This means that rather than requiring a standard curve, as in qPCR, ddPCR offers absolute quantification directly from the sample (Hindson *et al.*, 2013). Several studies have compared single species detection using both qPCR and ddPCR and show that ddPCR has greater sensitivity (Doi *et al.*, 2015) with reduced variability at low concentrations (Nathan *et al.*, 2014). The nature of partitioning the sample into droplets also reduces the effect of PCR inhibitors on the reaction (Capo *et al.*, 2019). This could be favourable when working with eDNA samples with high levels of inhibition such as those with a high organic matter content (McKee *et al.*, 2015).

Despite its promise, ddPCR still has limited use in the eDNA community. Assays are easily adapted from a qPCR platform as the molecular mechanism and assay design are the same, however use is likely stunted by the expense, reportedly two times higher than qPCR (Yang *et al.*, 2014) and limited availability of equipment.

3.1.3. Species specific assay design

Regardless of the selected PCR-based methodology, eDNA studies require robust assay design to reduce the risk of false positive detection. It is vital that sequence specificity is checked against closely related, sympatric taxa throughout the design process (Wilcox *et al.*, 2013). This may be limited by insufficient reference sequences and polymorphism data for a given species (as discussed in Chapter 1.3.4).

Ideally, assays should be designed to contain a high number of base pair differences in all sequence dependent elements such as primers and, if applicable, probes.

Mismatches in primer binding regions reduce the affinity of the primers for non-target DNA and consequently reduce amplification of non-target DNA. On the other hand, mismatches in the probe-binding region reduce affinity of the probe for non-targets, ergo reducing or eliminating fluorescence from non-target species. Wilcox *et al.*, (2013) found that assay specificity was most influenced by nucleotide mismatches in the primers rather than the probe, resulting in reduced or no amplification of non-target sequences. The location of mismatches within primers is also important, with previous literature showing that mismatches near the 3' end of the primer have a much larger impact on specificity than mismatches at the 5' end (Whiley and Sloots, 2005). Although qPCR generally increases specificity compared to cnPCR, previous studies have shown that measurable signals can be produced with a mismatch of up to five base pairs (Herrero *et al.*, 2010). This increases the risk of false positives, especially when the eDNA sample may have much greater quantities of closely related DNA sequences than the target species sequence itself.

3.1.4. Aims and Objectives

The central aim of this chapter is to develop a specific probe-based qPCR assay for the detection of *S. salar* from environmental samples as a means to verify the eDNA protocols, such as extraction and contamination prevention, newly adapted in the Molecular Genetics Lab. To do this, the following objectives will be performed:

1) Selection of a *S. salar* mitochondrial target site with sufficient base pair mismatches with closely related species.
2) Development of a cnPCR assay with agarose gel visualisation.
3) Adaption to a qPCR assay.
4) Assessment of assay sensitivity and specificity using DNA extracts from fish tissue.
5) Validation on a small number of eDNA samples and consideration of future adaption to a biosensor device.

3.2. Methods

3.2.1. Target site selection

In order to select a target site for the PCR assay, mitochondrial *COI* sequences of 10 fish species present in the Burrishoole catchment (Appendix B) were obtained from GenBank Release 229.0 (NCBI) and aligned using a ClustalW alignment algorithm (Geneious 11.1.5, Biomatters Ltd). This region is considered the barcode of life and is popularly used for species detection in the literature (Hebert *et al.*, 2003).

The resulting alignment was visually scanned to design primers specific to *S. salar* (forward primer SsaCOI470_F: 5'-CCAGCTATCTCTCAGTATCAAACC-3' and reverse primer SsaCOI470_R: 5'-AGTATGGTAATGCCTGCTGCT-3'). The total amplicon length, including primers, was 107 bp for the assay termed SsaCOI470. The small amplicon size conforms to literature recommendations (Rees *et al.*, 2014) for eDNA analysis (as discussed in Chapter 1). A specific hydrolysis probe complementary to the amplicon sequence was designed using IDT Primer Quest Tool (SsaCOI470 Probe: 5'-/6-FAM/TTGAGCTGTATTAGTCACTGCCGTCC/BHQ-1/-3'). The melting temperature of the hydrolysis probe was greater than that of the primers to ensure strong binding and generation of fluorescent signal prior to displacement by the polymerase, as recommended by IDT (Prediger, 2013). The fluorophore reporter (FAM) and quencher (BHQ) molecules were based on the Universal Probe Library (Roche). Selected primer and probe sequences were subject to a BLASTn 2.8.0 search (NCBI) to ensure *S. salar* specificity.

3.2.2. cnPCR conditions

The designed SsaCOI470 assay was optimised using cnPCR before being adapted for qPCR. PCR reaction mixes consisted of the following (total volume of 25 µL): 10x Buffer, 1.25 mM $MgCl_2$, 200 µM dNTPS, 0.24 µM forward and reverse primers, 0.75 U *Taq* DNA Polymerase and 2.8 ng/µL to 2.8 x 10^{-4} ng/µL of template DNA. Thermal cycling was

carried out using a GeneAmp® PCR system 9700 (Applied Biosystems) with the following conditions: 95 °C for 2 min followed by 30 cycles of 94 °C for 30 sec, annealing at 57 °C for 30 sec and extension at 72 °C for 30 sec. A final extension step was carried out at 72 °C for 10 min. PCR products were visualised by gel electrophoresis using a 4% (w/v) agarose gel. An O'RangeRuler 10 bp DNA ladder was used for size comparison.

3.2.3. qPCR reaction conditions

The qPCR reaction was conducted in a final reaction volume of 20 µL, comprising 10 µL LightCycler480 Probes Master, 0.5 µM custom forward and reverse primers, 0.1 µM SsaCOI470 probe, DNA sample (tissue extraction [2.5 – 7.9 x 10^{-7} ng/µL] or water extraction [1 – 20 ng/µL]) and molecular grade water. Pre-cycling conditions of 95 °C for 5 min were used, followed by 45 cycles of 94 °C for 30 sec, 57 °C for 30 sec and 72 °C for 30 sec and a final 10 sec cooling step at 40 °C. qPCR runs were carried out on a LightCycler 480 system (Roche) with fluorescence acquisition (λex = 485 nm, λem = 535 nm) following each 72 °C elongation step.

DNA extracted from tissue of a single farmed *S. salar* (quantified with Nanodrop-1000 spectrophotometer) was used to generate the standard curve using a six-point 1 in 10 serial dilution series (Appendix C). DNA concentrations for the serial dilution ranged from 2.536 to 2.536 x 10^{-5} ng/µL. A calibrator sample was run across the two plates and the same standard curve was used for calculating DNA concentrations from water samples. All samples were run in triplicate. Each plate contained three non-template controls to ensure that no contamination occurred during preparation of the qPCR plate.

The LOD and limit of quantification (LOQ) of the assay were calculated based on Forootan *et al.*, (2017). These refer to the minimum amount of target that can be detected and quantified with a given assay. Each parameter is vital for diagnostic assays,

as non-detection from samples may not mean absence of target, merely concentrations below the detection limits.

The LOD is stated as "the measured concentration that produces at least 95% positive replicates" and was calculated by plotting the fraction of positive replicates (where n=7) against the concentration of each dilution. An approximation of LOD was made by fitting a line at y = 95 with data points above this deemed detectable. The LOQ was calculated based on the mean and standard deviation (SD) of C_T values for replicates at each concentration. The coefficient of variation (CV) was calculated using:

$$\mathrm{CV} = 100 \text{ x } \frac{SD}{Mean} \quad (1)$$

Plotting percentage CV against concentration allowed for estimation of LOQ based on a threshold line at y = 35. Data points below this were deemed quantifiable. This threshold can vary depending on sample complexity, but a CV ≤ 35% was suggested by TATAA Biocenter (Forootan *et al.*, 2017).

To calculate the LOD and LOQ of the SsaCOI470 qPCR assay, a dilution series was set up (six-point 1 in 10 serial dilution series followed by five-point 1 in 2 serial dilution). Concentrations ranged from 2.536 to 7.925 x 10^{-7} ng/µL. Three negative controls (no DNA template added) were added to the 96-well plate to ensure no contamination and seven replicates of each dilution were used. The second derivative maximum method was used to calculate crossing point PCR cycle (C_T) values, whereby the C_T of a sample is identified "as the point where the sample's fluorescence curve turns sharply upward" (Roche Diagnostics GmbH, 2008).

3.2.4. qPCR assay specificity

Assessment of assay specificity requires testing the designed assay on DNA extracted from close relatives/species present in the same habitat. To do this, DNA extracted from

tissue of a single *S. trutta* (1.45 - 0.0145 ng/µL) and *S. alpinus* (1.25 – 0.0125 ng/µL) individual was run using the optimised qPCR conditions stated previously. A positive control, consisting of 1.15 ng/µl *S. salar* DNA and a negative control were also included. All samples and controls were run in triplicate.

3.3. Results

3.3.1. DNA target site selection

Target site selection is vital in developing an assay that is highly specific to the organism of interest. As highlighted by Wilcox *et al.*, (2013), robust primer design is required to differentiate sympatric taxa and reduce false positives/negatives when using PCR assays for environmental samples. To generate an assay highly specific to *S. salar,* a multiple alignment of the *COI* region of the mitochondrial genome for species present in the Burrishoole catchment (Appendix B) was visually scanned for suitable regions of high sequence variation but suitable for primer design. The design focused on differences between the *S. salar* and *S. trutta* sequences. *S. trutta* is the most closely related to the target species in the Burrishoole catchment and thus most likely to be the source of false positive results. The region selected (Figure 3.4) had a total of six mismatches in the primer regions and four mismatches in the probe binding site between *S. salar* and *S. trutta*.

3.3.2. cnPCR enables *S. salar* detection but lacks sensitivity required for eDNA studies.

Initially the primers were optimised using a cnPCR assay to enable thermal cycling temperatures and reagent concentrations to be optimised prior to adaptation to a qPCR assay. The sensitivity of the end-point assay was tested using a five-point 1:10 dilution series with visualisation revealing the target band (107 bp amplicon) in all but the lowest concentration (Figure 3.5). This suggests an end-point sensitivity down to a DNA concentration of 2.8×10^{-3} ng/µL when using whole *S. salar* tissue extraction.

3.3.3. SsaCOI470 qPCR increases assay sensitivity down to a concentration of 10^{-4} ng/µL

To enhance the specificity and sensitivity of the assay, it was adapted to a qPCR assay. As discussed previously (Chapter 3.1.2), this is preferred for eDNA detection which may consist of low levels of target DNA beyond the limits of the developed cnPCR assay. The standard curve was made using a 1:10 dilution series of DNA extracted from *S. salar* tissue. This was due to the increased standard deviation with lower DNA concentrations. It was generated using the second derivative maximum method and has a calculated efficiency of 99.5% (Appendix C). This is between the optimal efficiency of 90-100%, however does not consider potential PCR inhibitors present in environmental samples.

3.3.3.1. LOD and LOQ of SsaCOI470 qPCR assay

In clinical settings, it is vital to investigate the limits of a qPCR assay to ensure that a 'negative' result is not merely outside the range of detection of the assay. These metrics refer to a single technical replicate and can be used to assess the sensitivity of different biosensing platforms, but should be interpreted with caution when translating to eDNA samples. To calculate the LOD and LOQ, seven replicates of a dilution series of commercially available *S. salar* were used. Amplification of standards was successful and no amplification was observed in the negative controls (samples with no DNA template added). Samples deemed "negative" were set to a value of zero for the purpose of LOQ calculation.

From visual inspection, the LOD, working at 95% confidence, was approximated as 2.536 x 10^{-5} ng/µL with the subsequent dilution having less than 95% successful replicates (Figure 3.6a). This is likely higher than the theoretical limit of the assay due to noise contributed by sampling and extraction (Forootan *et al.*, 2017).

The LOQ is determined by calculating standard deviations of the replicate samples at different concentrations. For qPCR data this should be calculated in the logarithmic scale so that data is normally distributed (Forootan *et al.*, 2017) and expressed as a percentage of the mean or coefficient of variation (CV). The LOQ was also estimated to be 2.536 x 10^{-5} ng/µL with the subsequent dilution having a CV value greater than the recommended threshold of 35% (Figure 3.6b). The LOQ is expected to be greater than the LOD, however the precision of the calculated limits is restricted due to the number of replicates (n = 7) used. The limits of this assay are only estimates used as a first-cut assessment of whether an assay lacks sensitivity comparable to eDNA concentrations. The precision of LOD and LOQ estimates is influenced by the number of replicates performed, with Forootan *et al.,* (2017) recommending at least 20 replicates at each concentration. By increasing the number of replicates, the standard deviation and consequently the LOD and LOQ, become more precise.

3.3.4. SsaCOI470 qPCR assay lacks total specificity with high concentrations of non-target DNA

The developed SsaCOI470 assay lacks total specificity when using high concentrations of non-target DNA extracted from tissue of closely related species (described in Chapter 2) (Figure 3.7). Compared to the detection of *S. salar* at the same concentration (~1 ng/µl), the C_T values for *S. trutta* are much higher, 22.24 ± 0.026 and 35.75 ± 0.38, respectively (Table 3.1). Decreasing the concentration of *S. trutta* DNA, resulted in C_T values that are above the C_T cut-off point of 37, based on the calculated LOD. This cut-off thus protects from bias towards false positive detection due to *S. trutta* presence. No detection of *S. alpinus* was observed at all concentrations.

3.3.5. SsaCOI470 qPCR successfully detects *S. salar* in eDNA samples from the Burrishoole Catchment

The designed assay was successful in detecting *S. salar* from an eDNA sample (Table 3.2) with known *S. salar* presence. The C_T range of the standard curve was between 20.3 and

37.1 (Appendix C). The lowest detected eDNA concentration within this range was 0.297 pg/µL, at an average C_T value of 35.8 (over three technical replicates, standard deviation 0.0957 pg/µL). No amplification occurred in the negative controls (no DNA template added) nor the negative field control. The results of the eDNA analysis mirrored what was observed in the electrofishing surveys (Appendix D), with *S. salar* only detected in downstream samples below the migration barrier (Table 3.2). Of note, *S. trutta* has known presence in both sampling sites and thus an absence of detection upstream in the Srahrevagh indicates the qPCR assay is not detecting *S. trutta* in eDNA samples. This proof of concept sampling highlights the use of eDNA as a non-invasive method of species detection.

3.4. Discussion

The aim of this chapter was to develop a specific and sensitive qPCR-based method for the detection of *S. salar* from eDNA as a means to verify assay design approach and validate the eDNA extraction protocol. This is the most commonly used laboratory-based technique for eDNA analysis and has been adapted to biosensor devices for use in other fields (Zhang and Xing, 2007). The developed qPCR assay highlights the utility of eDNA as a non-invasive method for detection of *S. salar.*

The SsaCOI470 assay successfully detects *S. salar* in environmental samples with presence confirmed by electrofishing (Appendix D). This demonstrates the applicability of the assay for eDNA detection and shows sufficient sensitivity for intended use. The calculated limits of the assay, although require additional replicates to improve precision, are comparable to that in the literature. Xia *et al.,* (2018) report an LOD of 1 x 10^{-7} and LOQ of 1 x 10^{-4} for their assay detecting golden mussels. Although the LOD appears to be two magnitudes lower than the developed SsaCOI470 assay, it is not based on the 95% confidence interval and merely indicates one successful detection (out of five) at this concentration (of note, there was no successful detection at 1 x 10^{-6}). Compared to the Atkinson *et al.,* (2018) *S. salar* qPCR assay, the dynamic range of the

standard curve was similar and C_T values for eDNA samples were comparable, further suggesting the applicability of the developed assay.

In addition to high sensitivity, the developed assay is also specific for the *S. salar COI* gene at DNA concentrations expected in the environment. High specificity is of extreme importance for eDNA assays due to the presence of closely related species in the same environment, which could lead to cross amplification and generation of false positives or negatives. These errors could be disastrous if they lead to an overestimation of endangered species or missed detection of potentially harmful invasive species (Wilcox *et al.*, 2013). In order to ensure target specificity, the SsaCOI470 assay was robustly designed with three targeting sequences checked *in silico* and further tested on DNA extracted from tissue of closely related species to confirm specificity. *In silico* analysis showed four sequence mismatches in the forward primer, four in the probe binding region and two sequence mismatches in the reverse primer between *S. salar* and *S. trutta* (Figure 3.4). Despite this, non-specific detection of *S. trutta* DNA extracted from tissue was seen at DNA concentrations of ~1 ng/µl (Figure 3.7 and Table 3.1). To increase the specificity it would be preferable for sequence mismatches to be in the 3' end of the primers (Wilcox *et al.*, 2013) and for hydrolysis probes to have as many mismatches as possible, reportedly TaqMan® probes can tolerate up to five mismatches (Yao *et al.*, 2006). Further optimisation such as primer concentrations and annealing temperature could also enhance the specificity (Zhao *et al.*, 2021) of the assay. When the *S. trutta* DNA concentration was reduced (~0.1 ng/µL and 0.01 ng/µL), amplification was deemed above the cut-off threshold of 37 C_T (Table 3.1), thus considered a PCR artefact and eliminated from the analysis. This qPCR threshold value was selected based on the mean C_T value of the DNA concentration calculated as the LOD. It is also worth noting, that there was no detection in eDNA samples taken upstream of the Srahrevagh river obstacle, where *S. salar* is known to be absent but *S. trutta* is present, suggesting that at DNA concentrations present in the environment, non-specific detection is not seen.

The use of single species eDNA assays for management purposes requires extensive specificity testing to ensure the robustness of the assay and strengthen the certainty of detection. This has been highlighted by Natural England and the eDNA monitoring program of the Great Crested Newt (Biggs J *et al.*, 2014), which uses primers and probes that have undergone stringent testing prior to use commercially. If this level of stringency were required for *S. salar* monitoring, the SsaCOI470 assay would be redesigned or further optimised to ensure no cross reactivity with co-habiting species. The exact species examined for specificity, would be dependent on the monitoring location.

Careful design is essential for any qPCR assay, assuring that a positive signal is due to target species presence and not the presence of any closely related species. On the other hand, it is important to note that a lack of detection may simply mean that an organism is at too low an abundance to be detected i.e. the eDNA concentration is below the LOD. It is therefore more appropriate to deem these samples as having a "low probability of occurrence" rather than merely "present" or "absent" (Baldigo *et al.*, 2017).

A key requirement of the developed assay is its adaptability as a bio-receptor on a biosensor device to enable on-site eDNA monitoring. With an increasing demand for in-field devices, it is surprising that the number of published studies are limited. However, of the research moving towards on-site monitoring, qPCR detection has led the way, specifically using the commercially available Biomeme^{TM} system (Sepulveda *et al.*, 2018; Thomas *et al.*, 2019; Skinner *et al.*, 2020). This system combines a quick "dirty" sample preparation column with a handheld thermal cycler connected to a phone, for POC qPCR monitoring (Nguyen *et al.*, 2018) . It has successfully been used for striped bass (*Morone saxatilis*) detection from mesocosms (Skinner *et al.*, 2020) and New Zealand mudsnails (*Potamopyrgus antipodarum*) and northern pike (*Exoc lucius*) from freshwater samples (Sepulveda *et al.*, 2018; Thomas *et al.*, 2019). These assays showed simple adaptation of existing qPCR assays, but the Biomeme^{TM} system had lower detection probabilities

and greater influence from inhibitors than laboratory-based approaches (Sepulveda *et al.*, 2018). The reduction in detection probabilities could be problematic when monitoring target species of low abundance, meaning future devices should aim to have increased sensitivity. Conversely, one advantage of the Biomeme™ platform is the inclusion of an internal positive control (IPC) to approximate the level of PCR inhibition in a sample. This control step is particularly important in areas of high turbidity where PCR inhibitors are known to be high (Williams *et al.*, 2017). Presence of such inhibitors can lead to an increase in false negative detection, specifically if few replicates are run as is common when using the Biomeme™ system (Skinner *et al.*, 2020).

The Biomeme™ qPCR system highlights the potential for on-site presence/absence studies using PCR-based methodology. However, further development is required to overcome the lower detection probabilities and decreased precision and accuracy of these systems in order for them to be used reliably for routine monitoring. In-field devices must include multiple PCR replicates in order to maintain the robust requirements of eDNA assays. Whilst this limitation can be somewhat overcome by increasing the number of field samples, without technical replicates, particularly for low copy number samples, results would have to be interpreted with caution (Goldberg *et al.*, 2016).

Non-commercial platforms have shown more difficulty with adapting PCR technology to biosensor devices. As discussed in Chapter 1.4.1.2.2, difficulties arise due to the high temperatures required to denature the DNA, which may not be compatible with conventional materials used for sensors and with achieving an even distribution of temperature across samples whilst thermal cycling. The use of droplet technology has allowed these problems to be somewhat overcome, nevertheless new challenges are introduced due to the potential differences in liquid properties between the two phases. These challenges have resulted in a drive towards developing isothermal methods, which circumvent these difficulties by incubating samples at a single temperature.

To conclude, the developed qPCR assay for detection of *S. salar* DNA from environmental samples demonstrates the potential of eDNA as a non-invasive, cost effective method of species monitoring. The assay shows adequate sensitivity for eDNA analysis, with successful detection of *S. salar* presence in Burrishoole samples previously confirmed by electrofishing. It also validates the eDNA workflow set up at DCU, with no contamination seen at any stage of the process. However, despite the success of qPCR for *S. salar* monitoring, the high temperatures required and thermal cyclic nature of the technique pose problems when it comes to adapting the eDNA detection assay to a biosensor device.

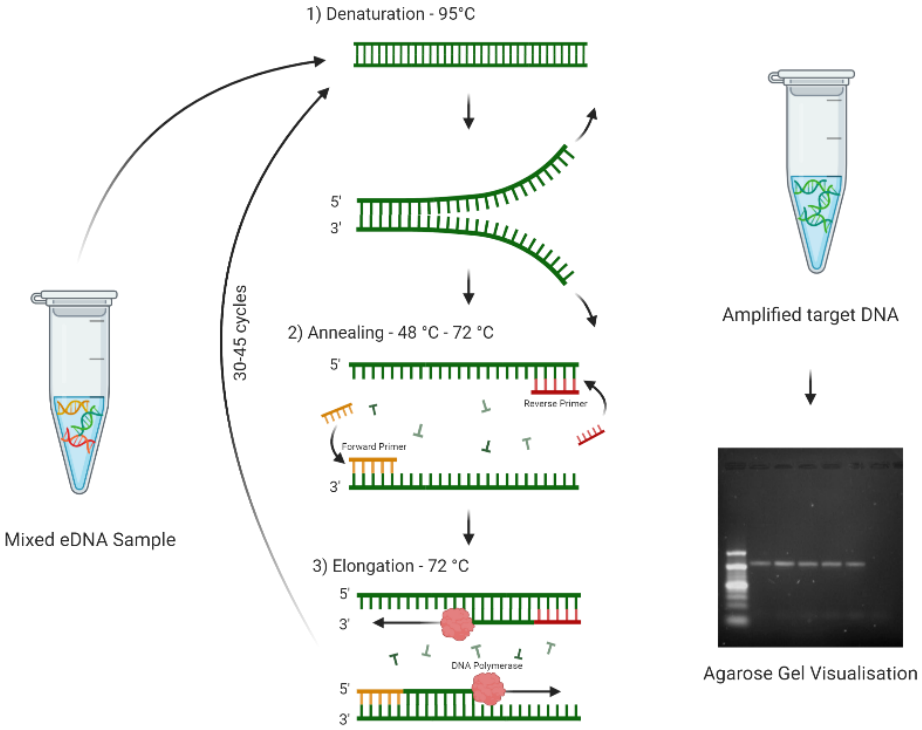

Figure 3.1 Molecular process of conventional Polymerase Chain Reaction (cnPCR). The reaction is heated to 95 °C to denature the dsDNA, then cooled to between 48 and 72 °C to allow annealing of target specific primers and finally heated to 72 °C to allow DNA polymerase elongation of targets. This is repeated in cycles to allow exponential amplification of the target, followed by amplicon visualisation via gel electrophoresis.

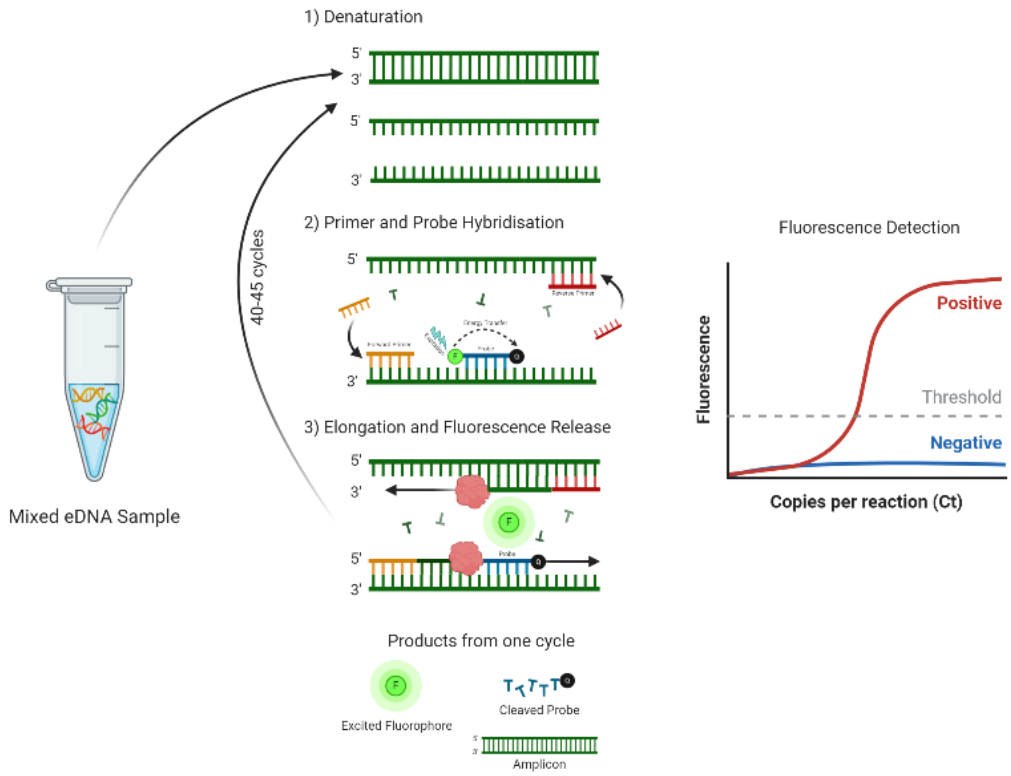

Figure 3.2 Quantitative PCR (qPCR) with fluorescence detection using a hydrolysis probe. The target amplification takes place as with cnPCR; cycles of denaturing, annealing and elongating. The hydrolysis probe binds during the annealing step and is cleaved during target elongation. This releases the 5' fluorophore, previously quenched via FRET, enabling fluorescence detection during the exponential phase of amplification.

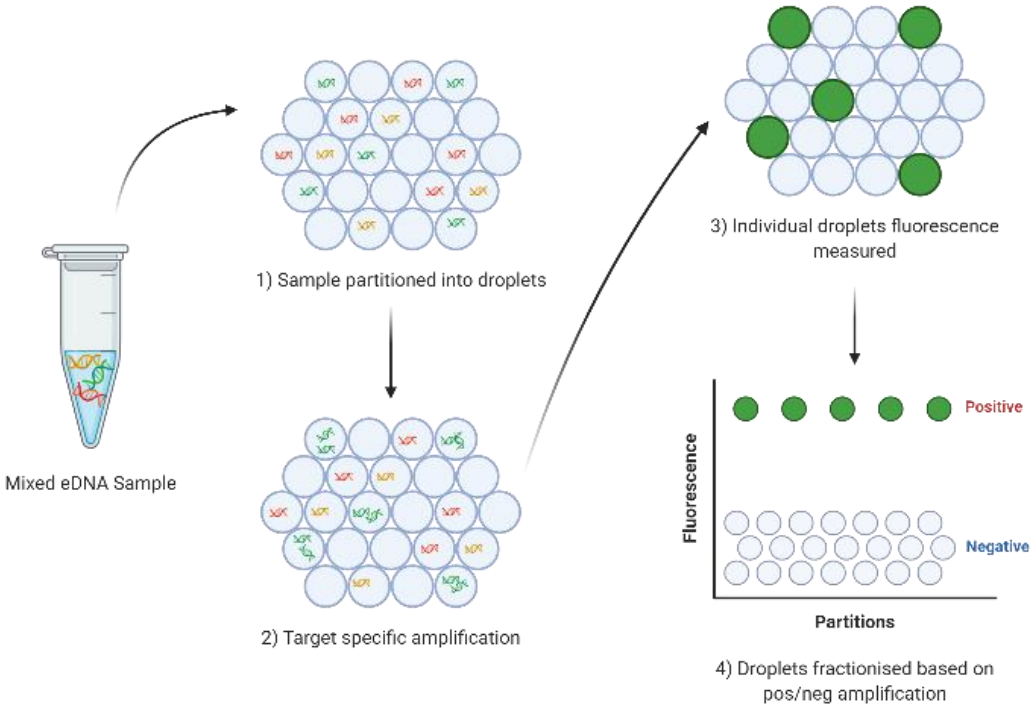

Figure 3.3 Droplet digital PCR (ddPCR) schematic. DNA molecules are split into individual droplets with target specific PCR occurring in each droplet. Following PCR, fluorescence is measured in each individual droplet, which are then fractionised based on the positive or negative amplification of the target DNA. This data is then analysed using Poisson statistics to allow absolute quantification of the original sample.

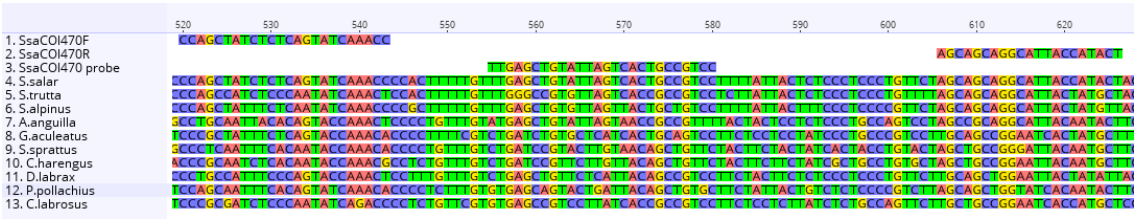

Figure 3.4 Multiple alignment of *COI* sequences of species present in the Burrishoole Catchment for qPCR assay design including target species *S. salar*, closely related species *S. trutta* and *S. alpinus* and SsaCOI470 primers and probe.

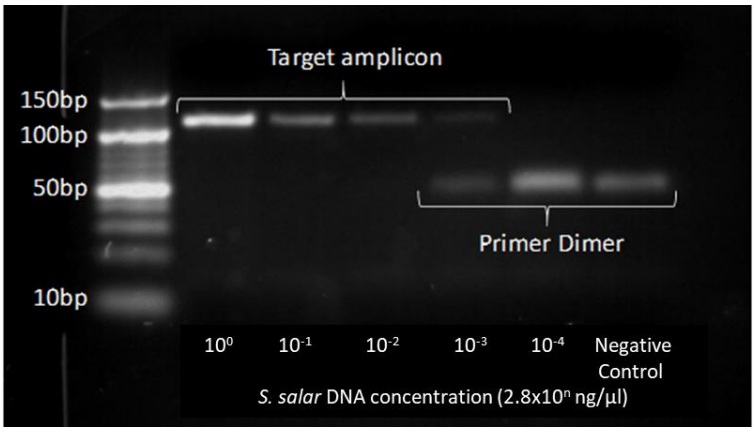

Figure 3.5 Sensitivity of SsaCOI470 cnPCR assay. PCR product of *S. salar* 1:10 dilution series generated using optimised SsaCOI470 PCR conditions and visualised on a 4% (w/v) agarose gel. LOD of cnPCR assay approximates 2.8 x 10^{-3} ng/µL with no amplicon seen at concentrations lower than this. Primer dimer band observed in the negative control and samples with low concentrations of target DNA. Negative control has no DNA template added.

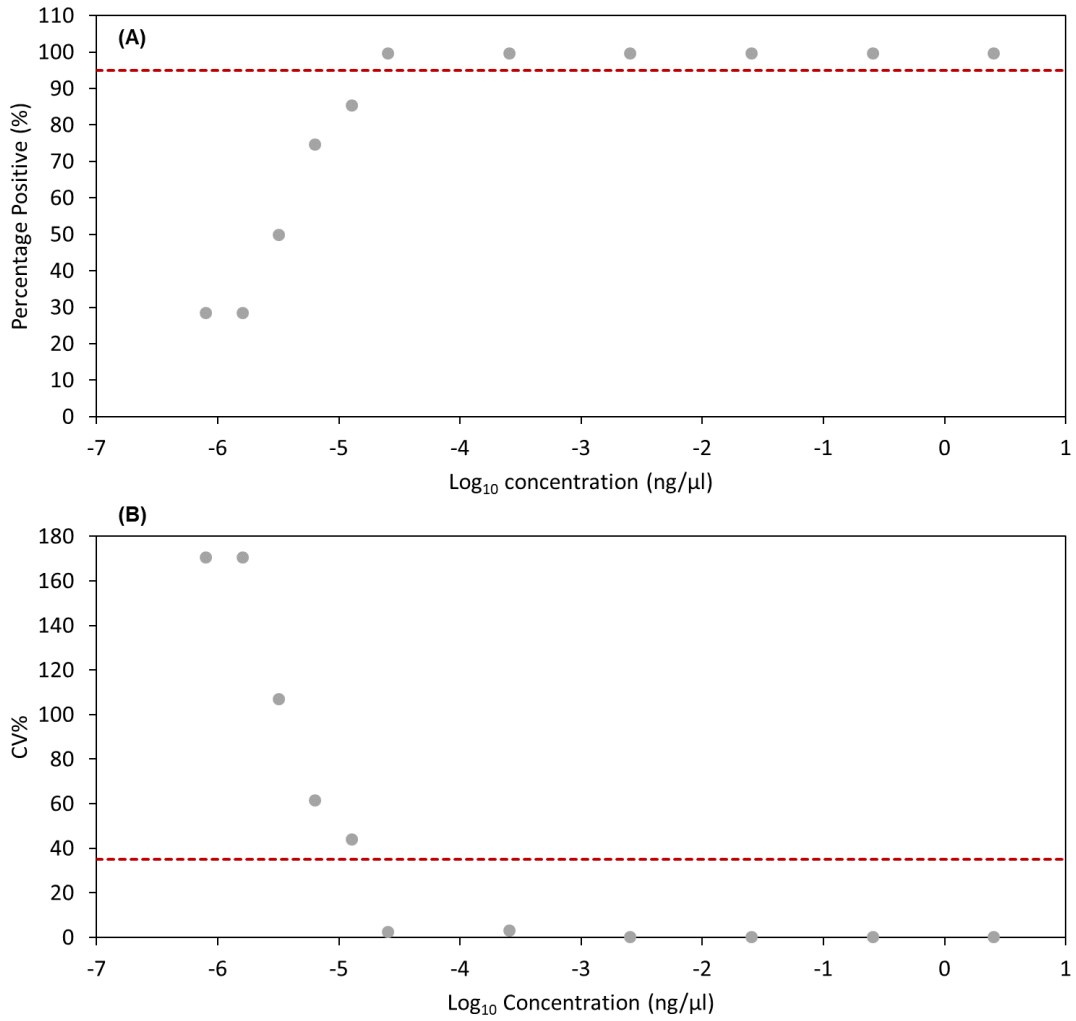

Figure 3.6 Detection and quantification limits of SsaCOI470 qPCR assay. (A) LOD. Percentage of positive replicates (where n = 7) against log concentration of DNA dilution. Percentage positive refers to successful detection of target DNA calculated using the second derivative maximum method. LOD defined as the concentration that produces at least 95% positive replicates. The red dotted line indicates this 95% cut off. SsaCOI470 LOD approximated as 2.536 x 10^{-5} ng/µL. (B) LOQ defined as lowest concentration with a coefficient of variation (CV%) less than 35. CV = 100 x Standard Deviation/Mean based on C_T values of replicates, where n = 7. The red dotted line indicates this 35% cut off. SsaCOI470 LOQ is estimated as 2.536 x 10^{-5} ng/µL.

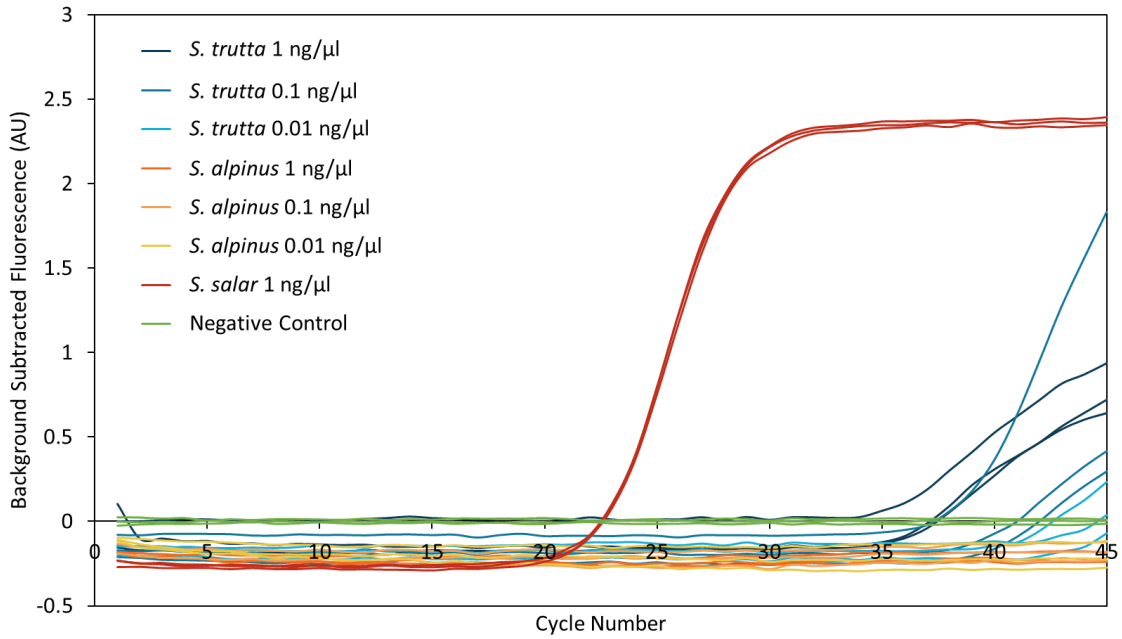

Figure 3.7 Specificity of SsaCOI470 qPCR assay. A three-step 1 in 10 dilution series of *S. trutta* and *S. alpinus* DNA extracts were used to check specificity of SsaCOI470 qPCR assay. *S. salar* DNA at 1 ng/µL was used as a positive control. The negative control contained no template DNA. All samples were run in triplicate.

Table 3.1 C_T values from SsaCOI470 qPCR specificity assessment.

Sample	DNA concentration (ng/µl)	Average C_T† (n=3 technical replicates)	No. of positive replicates (/3)
S. trutta	1	35.75 ± 0.38	2
	0.1	39.53 ± 0.51‡	0
	0.01	40 ± 0‡	0
S. alpinus	1	Undetermined	0
	0.1	Undetermined	0
	0.01	Undetermined	0
S. salar	1	22.24 ± 0.026	3
Negative	-	Undetermined	0

†Crossing point PCR cycle (C_T) value is the cycle at which fluorescence passes a threshold calculated using the second derivative maximum method. Average C_T values (± standard deviation) are given (average over three technical replicates).

‡Detection deemed negative as C_T value of all replicates is greater than the C_T cut-off threshold of 37.

Table 3.2 C_T values and eDNA concentrations from Burrishoole Catchment Samples.

River	Location[+]	*S. salar* present	Site Replicate	Average C_T[‡] (n=3 technical replicates)	DNA concentration[§] (ng/L)
Srahrevagh	Downstream	Yes	1	34.97±0.56	0.395
			2	35.82±0.45	0.216
			3	35.33±0.25	0.294
				35.37±0.53	**0.302±0.09**
Srahrevagh	Upstream	No	1	Undetermined	Undetermined
			2	Undetermined	Undetermined
			3	Undetermined	Undetermined

[+]The Srahrevagh River has a barrier that has the potential to prevent migration of *S. salar.* Location refers to whether sampling was upstream or downstream of this barrier.

[‡]Crossing point PCR cycle (C_T) value is the cycle at which fluorescence passes a threshold calculated using the second derivative maximum method. C_T values and eDNA concentrations (average over three technical replicates) for *S. salar* at each sampling site.

[§]eDNA concentration in original field sample back-calculated from absolute DNA concentration from qPCR. Average concentrations (± standard deviation) are given at each location.

Chapter 4. The application of RPA-CRISPR-Cas to salmonid monitoring from environmental DNA

4.1. Introduction

4.1.1. Overview

Conventional methods for eDNA detection pose a logistical challenge for on-site monitoring and adaptation to biosensor devices, due to the need for high temperatures and thermal cycling. Isothermal amplification methods have evolved as an alternative to PCR, enabling nucleic acid amplification at a constant temperature (Bodulev and Sakharov, 2020). These methods can be coupled to fluorescence-based detection methods to enable highly sensitive and specific analysis of target sequences (Li *et al.*, 2018; Kaminski *et al.*, 2021).

In this chapter, an alternative molecular eDNA approach, coupling isothermal RPA to a CRISPR-Cas12a detection system, is developed. Three salmonid species are targeted, *S. salar, S. trutta* and *S. alpinus,* due to their ecological, economic and cultural importance in Ireland (as discussed in Chapter 1.1.2). The developed assays enable detection of these species at a single temperature of 37 °C. This switch from thermal cycling to isothermal detection enhances the potential for adaptation to a biosensor device. The CRISPR-Cas system, more commonly known for its role in genome editing, enables highly specific sequence recognition (Kaminski *et al.*, 2021), which can be adapted to detect any species from eDNA samples from a variety of sources. This improves the ability to differentiate closely related species and enhances the capabilities of eDNA as a tool for biodiversity monitoring.

4.1.2. Isothermal amplification

Conventional methods of eDNA detection require the use of PCR based amplification techniques (as discussed in Chapter 3). However, although suitable for laboratory-based experiments, these techniques pose multiple challenges regarding adaptation to a biosensor device, primarily due to the high temperatures and requirement of thermal cycling. Isothermal methods of amplification have been developed to overcome such necessities. Temperatures are kept constant and different molecular mechanisms are

used to maintain the DNA amplification efficiency. Many different isothermal methods have been developed for nucleic acid amplification (Gill and Ghaemi, 2008) such as RPA (Piepenburg *et al.*, 2006), transcription mediated amplification (TMA) (Gonzales and McDonough, 1998), strand displacement amplification (SDA) (Walker *et al.*, 1992), rolling circle amplification (RCA) (Lizardi *et al.*, 1998) and LAMP (Notomi *et al.*, 2000).

Loop-Mediated Isothermal Amplification was first described by Notomi *et al.,* (2000). It typically uses a *Bacillus stearothermophilus (Bst)* DNA polymerase, which displays strand displacement activity whilst elongating the target sequence, and user-designed primers that recognise six distinct sequences allowing high levels of target specificity. The use of a *Bst* DNA polymerase allows the whole process to occur at a single temperature between 60 °C and 65 °C. In addition to being highly specific, LAMP has the benefit of being readily adaptable to visualisation with the naked eye. For example, incorporation of magnesium pyrophosphate causes increased turbidity as a by-product of DNA amplification (Mori *et al.*, 2001). Additionally, dyes such as SYBR green can be added to the amplified product, producing a visible colour change (Njiru *et al.*, 2008). LAMP has previously been used for macro-invertebrate eDNA detection, with Williams *et al.,* (2017) showing the applicability to *Dreissena* sp. detection in the Great Lakes. It is therefore surprising that this methodology has not been applied more readily in the eDNA community, given its easy read-out and high specificity. This is likely due to the complexity of assay design, with six primers required, and lower sensitivity compared to qPCR (Martzy *et al.*, 2017).

Another popular isothermal method is RPA. This was developed by Piepenburg *et al.,* (2006) and has been commercialised by TwistDx. Unlike LAMP, RPA relies on only two sequence specific primers which form complexes with a recombinase protein uvsX from T4-like bacteriophages, in the presence of ATP and a crowding agent (high molecular weight polyethylene glycol) (Lobato and O'Sullivan, 2018). This complex seeks and promotes strand invasion at a site complementary to the primer, with the displaced strand stabilised by single stranded binding proteins (Figure 4.1). The recombinase then

disassembles and a strand displacing DNA polymerase elongates the primer in the presence of dNTPs (Lobato and O'Sullivan, 2018), achieving the exponential amplification we see with PCR. Due to the displacement activity of the recombinase and polymerase enzymes, thermal cycling is not required to denature the double stranded target DNA meaning the whole process occurs between 37-42 °C (Piepenburg *et al.*, 2006).

RPA has successfully been used for detection of harmful algae (Toldrà *et al.*, 2019) and parasites from water and soil (Wu *et al.*, 2017), but is yet to be fully explored for eDNA monitoring of vertebrates. This might be due to its reduced specificity, with up to nine mismatches tolerated in primer binding regions (Li *et al.,* 2019). As with qPCR (and discussed in Chapter 3.1.3), the exact location of mismatches influences primer specificity, with 5' mismatches tolerated more than 3' mismatches (Daher *et al.*, 2015). Whilst designing RPA assays, it is thus recommended that a primer screen is performed to select optimal primer pairs (Li *et al.,* 2019).

Despite limitations, the simplicity of RPA makes it the ideal amplification method for an eDNA biosensor device. It is simple to design, two sequence specific primers only, occurs at low temperatures and achieves exponential amplification within 20 min (Lobato and O'Sullivan, 2018). It is also possible to couple RPA with fluorescence-based detection, which can compensate for the lack of specificity seen with RPA primers alone (Kaminski *et al.*, 2021). Fluorescence RPA detection is enabled through incorporation of an exo probe (Li *et al.*, 2018) for real-time RPA or through coupling with a secondary technique such as CRISPR-Cas diagnostics (Kaminski *et al.*, 2021).

4.1.3. CRISPR-Cas detection

Clustered Regularly InterSpaced Palindromic Repeats (CRISPR) play an important role in the adaptive immunity of bacteria and archaea (Horvath and Barrangou, 2010). These genetic loci consist of CRISPR arrays containing bacterial repeat sequences interspersed with short regions of genetic material taken up from invasive elements (protospacers) and CRISPR-Associated (Cas) nuclease genes (Figure 4.2) (Horvath and Barrangou, 2010). The CRISPR-Cas systems are classified based on the structure of the Cas genes (Adli, 2018) with mediation as an adaptive immune response varying depending on the exact CRISPR system. Commonly, the CRISPR-Cas systems act in a three step process: adaptation, expression and interference (Makarova *et al.*, 2011). The CRISPR locus is expressed producing guide RNA molecules that form ribonucleoprotein (RNP) complexes with Cas nucleases. These guide RNA molecules are complementary to the invasive genome (Sontheimer and Marraffini, 2010). Upon recognition of a target molecule, the foreign DNA or RNA is cleaved within the proto-spacer sequence, disabling the invasive element (Garneau *et al.*, 2010).

Evolving knowledge of the specificity of CRISPR-Cas systems, resulted in its application as a tool for genome editing (Jinek *et al.*, 2012). However, since then the adaptation of CRISPR-Cas to a range of applications has expanded, driven by the identification and further characterisation of Cas nucleases and equivalent endonuclease enzymes to perform functions which go beyond genome editing (Barrangou and Doudna, 2016). This expansion has included the field of CRISPR diagnostics (CRISPR-Dx), which uses various Cas nucleases, including Cas9 (Pardee *et al.*, 2016), Cas12a (Chen *et al.*, 2018), Cas13 (Gootenberg *et al.*, 2017) and Cas14 (Harrington *et al.*, 2018) for detection of both RNA and DNA. By coupling amplification methods to CRISPR-Cas detection systems, SHERLOCK (Gootenberg *et al.*, 2017), HOLMES (Li *et al.*, 2018) and DETECTR (Chen *et al.*, 2018) enable nucleic acid detection with attomolar sensitivity for clinical applications. Although in its infancy, the field continues to grow with commercial companies such as SHERLOCK Biosciences and Mammoth Biosciences adapting a CRISRP-Dx approach to

pathogen detection, most recently of SARS-CoV-2 (Broughton *et al.*, 2020; Joung *et al.*, 2020).

The DNA endonuclease-targeted CRISPR trans reporter, DETECTR, system specifically couples RPA to Cas12a detection (Chen *et al.*, 2018) for DNA detection. Cas12a (previously Cpf1) is a single RNA guided ribonuclease that functions similarly to the original genome editing Cas9 enzyme, in that it binds a guide RNA that directs it to a specific sequence of DNA in order to catalyse a double stranded break. The guide RNA (gRNA) consists of a single crRNA region which is complementary to the target DNA (Fonfara *et al.*, 2016) and a scaffold region which interacts with the nuclease (Yamano *et al.*, 2016). The Cas12a nuclease requires a T-rich Protospacer Adjacent Motif (PAM) site (Zetsche *et al.*, 2015) succeeding the gRNA target site in order to bind and cleave the target sequence.

The specific gRNA sequence recognition and double-stranded break activity of Cas12a, makes it ideal for genome editing, however it has an additional functionality, which enables its use for nucleic acid detection. Once bound to its target sequence, Cas12a gains an indiscriminate single stranded DNase activity that can be exploited for diagnostics (Chen *et al.*, 2018). The collateral cleavage activity can be exploited for target detection through incorporation of a single stranded DNA fluorophore quencher (ssDNA-FQ) molecule with fluorescence only released upon cleavage by the Cas12a-gRNA-target site complex (Chen *et al.*, 2018). The presence of the fluorescent signal thus indicates the existence of target in the sample.

Similarly, the Specific High-Sensitivity Enzymatic Reporter UnLOCKing, more commonly termed SHERLOCK, methodology developed by Gootenberg *et al.*, (2017) is a Cas-based system which enables sensitive and specific detection of both RNA and DNA targets. Unlike DETECTR, SHERLOCK utilises a Cas13a (previously C2c2) class II type VI nuclease

that is guided to complementary protospacers by a single crRNA (Abudayyeh *et al.*, 2016). Upon target recognition, Cas13a also engages in non-targeted "collateral cleavage" of nearby nucleic acid (Abudayyeh *et al.*, 2016) enabling its use in a detection system. Although Cas13 is an RNA targeting CRISPR enzyme (Abudayyeh *et al.*, 2016), the SHERLOCK methodology can also be applied to DNA targets, through the incorporation of a T7 RNA polymerase transcription step following isothermal amplification (Gootenberg *et al.*, 2017). Both SHERLOCK and DETECTR have proven to be a valid approach for the detection of clinical pathogens (Mustafa and Makhawi, 2021), but have not yet been considered for eDNA, despite offering the sensitivity, specificity and assay simplicity required for the detection of specific species from eDNA samples.

4.1.4. Aims and Objectives

The aim of this chapter is to adapt the DETECTR methodology combining RPA with CRISPR-Cas12a detection to salmonid species, in order to assess its applicability for nucleic acid monitoring from environmental samples (Figure 4.3). To achieve this aim, a number of objectives were proposed:

1) Selection of mitochondrial target sites in *S. salar, S. trutta* and *S. alpinus* with sufficient base pair mismatches with closely related species.
2) Development of RPA and CRISPR-Cas assays for the three salmonid species.
3) Assessment of Cas12a alone and coupled to RPA for detection of *S. salar* and *S. trutta* recombinant plasmid clones.
4) Assessment of assay specificity and sensitivity on DNA extracted from tissue.
5) Exploration of various RPA-CRISPR-Cas data analysis approaches for eDNA monitoring.
6) Validation of *S. salar* targeting assay on Irish freshwater samples.
7) Optimisation of reagent concentrations including RNP and ssDNA-FQ reporter.
8) Comparison of RPA-CRISPR-Cas and qPCR for monitoring of *S. salar* in freshwater samples from eastern Canada.

4.2. Methods

4.2.1. Target site selection

To select the target site for *S. salar, S. trutta* and *S. alpinus* assays, mitochondrial sequences of all three species were obtained from GenBank Release 229.0 (NCBI) (Appendix B). A multiple sequence alignment of the entire mtDNA sequences was performed using the ClustalW alignment algorithm (Geneious 11.1.5). The alignments were scanned to find regions containing the A.s.Cas12a PAM site (5'-TTTV-3') and with sufficient interspecies sequence mismatches, upstream and downstream of the PAM site, for gRNA binding and RPA primer targeting. For all assays, selected sequences were subject to a BLAST 2.8.0 search (NCBI) to ensure they were species specific.

4.2.1.1. *Salmo salar*

4.2.1.1.1. Version 1 - ND2

The multiple alignment was visually scanned for regions whereby *S. salar* and *S. trutta* both contained the A.s.Cas12a 5'-TTTV-3' PAM site (Zetsche *et al.*, 2015) but had multiple base pair mismatches in the areas adjacent to this for gRNA and RPA primer binding. The region selected resides within the mitochondrial NADH dehydrogenase subunit 2 gene (ND2). Selected RPA primers were as follows: *S. salar* forward primer 5'-CTGACGCCTCAACTTCACCCTCATTACCCTCCCTC-3' and reverse primer 5'-ACGTGGTCACAGCTGGAGTGAGGGGTTGCAAGCCT-3', *S. trutta* forward primer 5'-CTGACGCCTCAACTTCACCTTCATTACCCTCCCCC-3' and reverse primer 3'-TTGCGGTTACAGCCGGAGTGAGGGGTTGCAGGCCT-3'. Custom Alt-R® CRISPR-Cas12a gRNAs containing the custom crRNAs targeting *S. salar* (5'-GAUCAUUACUAUUUUAGCCCU-3') and *S. trutta* (5'-AAUCGUUACUAUCUUGGCCCU-3') were synthesised commercially by IDT.

4.2.1.1.2. Version 2 - ND5

The alignment was visually scanned for regions whereby only *S. salar* contains the A.s.Cas12a 5'-TTTV-3' PAM site (Zetsche *et al.*, 2015). Areas adjacent to appropriate PAM sites were scanned to ensure greatest number of base pair mismatches between the *S. salar* sequence and the sequences of closest relation (*S. trutta* and *S. alpinus*). The final target site selected resides within the NADH dehydrogenase subunit 5 gene (ND5). Intraspecific polymorphisms were assessed using single nucleotide polymorphism (SNP) data obtained from dbSNP Build 151 (NCBI). Species specific RPA primers, targeting *S. salar* were designed to amplify a 120 bp amplicon (forward primer: 5'-GTTATTAATCCCATCAAACGACTAGCTTGAGG-3' and reverse primer: 5'-GGCTAATTTTAATGGGAGGGGTATGGTTATGATAG-3'). A custom Alt-R® CRISPR-Cas12a gRNA (IDT) was designed with a crRNA specifically targeting *S. salar* (5'-UACCCUCCAAAACCCCUAUC-3').

4.2.1.2. *Salmo trutta*

The alignment was visually scanned for regions whereby only *S. trutta* contains the A.s.Cas12a 5'-TTTV-3' PAM site (Zetsche *et al.*, 2015). The final target for the specific assay resides in the ND5 region. Specific RPA primers (forward primer: 5'-GAGCCTACTCCCTCTTTTTATTTTTCTGGACCAA -3' and reverse primer: 5'-CATACAGGGCAATTGGGGTAAAAATGATAGAG -3') were used to amplify a 148 bp amplicon. A custom Alt-R® CRISPR-Cas12a gRNA (IDT) was designed with a crRNA specifically targeting *S. trutta* (5'- GACAUCAACCUUAGCUUUAAAUUC -3').

4.2.1.3. *Salvelinus alpinus*

The alignment was visually scanned for regions whereby only *S. alpinus* contains the A.s.Cas12a 5'-TTTV-3' PAM site (Zetsche *et al.*, 2015). The final target for the specific assay resides in the ND2 region. Specific RPA primers (forward primer: 5'-TCCTTAGCCTTTTCCTGTACATCATCATAAC -3' and reverse primer: 5'-TAGTGGGGCGAGAGCAGGGGATTTAGTTCAGG -3') were used to amplify a 125 bp

amplicon. A custom Alt-R® CRISPR-Cas12a gRNA (IDT) was designed with a crRNA specifically targeting *S. alpinus* (5'- ACUAUCAACACUCUAGCAACUUCC -3'). Note: Design was carried out by Silke Caestecker under the supervision of Molly Ann Williams.

4.2.2. Recombinant DNA cloning of salmonid sequences

Recombinant DNA clones were generated using Fast Cloning as in Li *et al.,* (2011). Clones targeting two different subunits of the mitochondrial NADH dehydrogenase gene were generated using two different strategies based on the insert length. For all clones, empty pUC19 vectors containing an ampicillin marker for selection were used. *S. salar* and *S. trutta* sequences were inserted into the pUC19 vector (Appendix E), replacing the multiple cloning site (Appendix F). Recombinant clones were used for optimisation of the *S. salar* targeting assay only.

4.2.2.1. ND2 insert for *S. salar* targeting assay Version 1

A 103 bp sequence from the mitochondrial ND2 gene of *S. salar* and *S. trutta* was inserted into pUC19 vectors using two primers containing the insert sequence (Figure 4.4) (Appendix G). For the *S. trutta* insert, the PCR reaction mix was as follows (50 µL total volume); 5x Q5 reaction buffer, 200 µM dNTPs, 0.5 µM forward and reverse primer (containing new sequence), 1 U Q5 high fidelity polymerase and 1 pg/µL pUC19 template. For the *S. salar* insert, conditions were as above but the pUC19 template DNA was increased to 3.35 ng/µL. Thermal cycling was carried out using a GeneAmp® PCR system 9700 (Applied Biosystems) with the following conditions for both inserts: 98 °C for 3 min, followed by 18 cycles of 98 °C for 30 sec, 52 °C for 30 sec, 72 °C for 150 sec and a final hold of 72 °C for 5 min. Target amplification was confirmed by gel electrophoresis using a 1% (w/v) agarose gel (Appendix H).

PCR product was digested using *Dpn*I to remove any original plasmid as follows; 20 U *Dpn*I, 5 µL CutSmart Buffer and 40 µL PCR product, made up to 50 µL reaction in

molecular grade water. The mix was incubated at 37 °C for 90 min and then heat inactivated at 80 °C for 20 min.

4.2.2.2. ND5 insert for *S. salar* targeting assay Version 2

Due to increased insert length, generation of plasmids containing a 205 bp and 225 bp sequence from the mitochondrial ND5 gene of *S. salar* and *S. trutta,* respectively, required two separate amplification steps; one of the pUC19 vector and one of the target sequence (Figure 4.5). pUC19 empty vectors were first linearised using a *Kpn*I digest as follows; 10 U *Kpn*I, 6 ng/µL template DNA and 5 µL NEBuffer 1.1 made up to 50 µL in molecular grade water and incubated at 37 °C for 1 h. PCR primers were designed and optimised for each target: the pUC19 vector and ND5 gene of *S. salar* and *S. trutta* (Appendix I). Custom primers for salmonid species contained flanking regions that overlapped the pUC19 vector sequence (Appendix I). PCR reaction mixes (50 µL total volume) were the same for each PCR amplification as follows; 5x Q5 Reaction Buffer, 200 µM dNTPS, 0.5 µM forward and reverse primers, 1 U Q5 high fidelity polymerase and varying concentrations of template DNA.

Thermal cycling conditions varied for each amplicon. pUC19; 98°C for 3 min, followed by 18 cycles of 98 °C for 30 sec, 61 °C for 30 sec, 72 °C for 90 sec and a final hold of 72 °C for 5 min. Target amplification was confirmed by gel electrophoresis using a 1% (w/v) agarose gel (Appendix J). A 1 kb DNA ladder was used for size comparison. *S. salar* insert; 98°C for 3 min, followed by 18 cycles of 98 °C for 10 sec, 63 °C for 30 sec, 72 °C for 30 sec and a final hold of 72 °C for 5 min. *S. trutta* insert; 98 °C for 3 min, followed by 18 cycles of 98 °C for 10 sec, 62 °C for 30 sec, 72 °C for 30 sec and a final hold of 72 °C for 5 min. All thermal cycling was carried out using a GeneAmp® PCR system 9700 (Applied Biosystems). For both salmonid amplicons, target amplification was confirmed by gel electrophoresis using a 2% (w/v) agarose gel (Appendix J). A 100 bp DNA ladder was used for size comparison.

PCR products were mixed in varying ratios based on size of band on agarose gel. *S. salar*: pUC19 3:1 and *S. trutta*: pUC19 1:1 and digested using *Dpn*I to remove original plasmid as follows; 20 U *Dpn*I, 5 µL CutSmart Buffer and 40 µL of the above ratios of DNA template, made up to 50 µL reaction in water. Samples were incubated at 37 °C for 90 min and heat inactivated at 80 °C for 20 min.

4.2.2.3. Transformation of recombinant clone PCR products

Following the *Dpn*I digest of all recombinant clones, they were then transformed into OneShot® Top 10 chemically competent *E. coli* cells using the transformation protocol, briefly as follows: 50 µL of One Shot cells per transformation were thawed on ice, 2 µL *Dpn*I digested PCR product was added and incubated on ice for 30 min. The cells were then heat shocked at 42 °C for exactly 30 sec and 250 µL of LB broth, pre-warmed to 37 °C, was added. The vial was then shaken horizontally at 37 °C for 60 min at 225 rpm in an Innova 43 (New Brunswick Scientific) shaking incubator. Cells were then spread on LB agar plates containing 100 µg/mL ampicillin and incubated at 37 °C overnight. Single colonies were transferred to 3 mL LB broth containing 100 µg/mL ampicillin and incubated at 37 °C overnight at 225 rpm in a shaking incubator.

4.2.2.4. Plasmid DNA preparation

Plasmid DNA was isolated from the liquid culture following the protocol from Isolate II Plasmid Mini Kit with some modifications. Liquid culture in LB broth was centrifuged at 5,000 x *g* for 5 min to pellet the cells. The supernatant was removed. Next, 250 µL of resuspension buffer P1 was added followed by 250 µL lysis buffer P2 and incubated at RT for 5 min. Then 300 µL neutralisation buffer P3 was added to the sample, mixed by inversion and centrifuged at 11,000 x *g* for 5 min. Clarified supernatant was transferred to mini spin column and centrifuged at 11,000 x *g* for 1 min. The sample was then washed using 500 µL wash buffer PW1 and 600 µL wash buffer PW2 with centrifugation at 11,000 x *g* for 1 min between washes. Residual ethanol was removed via

centrifugation at 11, 000 x *g* for 2 min and the sample was eluted in 50 µL elution buffer P following incubation at RT for 1 min and centrifugation at 11,000 x *g* for 1 min.

Purified plasmid DNA was subject to a *Kpn*I digest and visualised on a 1% (w/v) agarose gel (Appendix K). Presumptive successful colonies (indicated by an uncut plasmid) were confirmed by Sanger cycle sequencing (Source Biosciences) (Appendix K) using a custom primer, FastCloneCheck_F (Appendix I).

4.2.3. RPA-CRISPR-Cas12a detection

4.2.3.1. Recombinase polymerase amplification

RPA products were generated using the TwistAmp Basic kit (Twist Dx), following the manufacturers protocol. Briefly, 50 µL reactions containing; 0.48 µM forward and reverse primer, 1x rehydration buffer, 14 mM MgOAc, various concentrations of DNA and one RPA reaction pellet were incubated at 37 °C for 20 min. Manual mixing was carried out after 4 min incubation to prevent local depletion of substrates. During primer optimisation, reactions were cleaned up by heating to 65 °C for 10 min (Londoño *et al.*, 2016) and visualised on a 2% w/v agarose gel stained with ethidium bromide.

4.2.3.2. CRISPR-Cas12a detection

Lyophilised gRNAs were re-suspended in TE buffer upon arrival. Experiments utilised recombinant *Acidaminococcus sp BV3L6* Cas12a nuclease synthesised commercially by IDT. Alt-R® A.s.Cas12a - gRNA complexes were preassembled following the IDT recommended protocol. Briefly, 5 µL reactions were made by incubating 2.52 µM A.s.Cas12a, 3.2 µM species specific gRNA and PBS at RT for 20 min. Complexes were diluted in a solution containing buffer, custom ssDNA-FQ reporter (5'-/56-FAM/TTATT/3IABkFQ/-3') and target DNA. The exact conditions varied across experiments as summarised in Table 4.1. Reactions (20 µL, 96-well plate format) were

incubated in a LightCycler 480 (Roche) for between 30 and 120 min at 37°C with fluorescence measurements taken every 30 sec (λex = 485 nm, λem = 535 nm).

4.2.3.3. Combined assay

The final assay combines the RPA and CRISPR-Cas12a detection protocols with 2 µL of RPA amplified product added to 18 µL CRISPR-Cas12a reaction mix (as above). To account for inter-plate variation due to the volume of samples analysed in the eastern Canada study (Chapter 4.3.4), fluorescence values were normalised against the mean fluorescence value of the positive control run in triplicate on each plate. This consisted of 0.04 ng/µL *S. salar* tissue extracted DNA.

4.2.4. Optimisation of RPA-CRISPR-Cas12a assay

4.2.4.1. RNP concentration

The concentration of the RNP was optimised by varying the concentration of *S. salar* specific gRNA and Cas12a nuclease used in the CRISPR-Cas detection step of the combined RPA-CRISPR-Cas assay. The Cas12a nuclease and gRNA were preassembled at RT for 20 min in PBS. Following preassembly, the RNP was diluted in 1x binding buffer and 50 nM ssDNA-FQ reporter to 25 nM:31.25 nM, 50 nM:62.5 nM, 75 nM:93.75 nM and 100 nM:125 nM, Cas12a:gRNA respectively. The volume of water in the final 20 µL reaction was adjusted accordingly. RPA product made from 0.5 ng/µL *S. salar* tissue was used throughout. Reactions (20 µL, 96-well plate format) were incubated in a LightCycler 480 (Roche) for 120 min at 37°C with fluorescence measurements taken every 30 sec (λex = 485 nm, λem = 535 nm).

4.2.4.2. Fluorophore-quencher reporter concentration

Optimisation of the ssDNA-FQ reporter molecule was carried out using the combined RPA-CRISPR-Cas12a methodology with 1x binding buffer, 50:62.5 nM Cas12a:gRNA,

various concentrations of ssDNA-FQ reporter ranging from 40 nM to 100 nM and RPA product made from 0.5 ng/µL *S. salar* tissue. Reactions (20 µL, 96-well plate format) were incubated in a LightCycler 480 (Roche) for 120 min at 37°C with fluorescence measurements taken every 30 sec (ƛex = 485 nm, ƛem = 535 nm).

4.2.4.3. RNP preassembly

The necessity for RNP preassembly was tested through removal of this step. Reactions were made up (final volume 20 µL) containing the following final concentrations: 1x binding buffer, 50.64 nM Cas12a, 65 nM gRNA, 100 nM ssDNA-FQ reporter and varying concentrations of RPA product (made using 0.5 – 0.005 ng/µL *S. salar* tissue DNA extract). Reactions (20 µL, 96-well plate format) were incubated in a LightCycler 480 (Roche) for 120 min at 37°C with fluorescence measurements taken every 30 sec (ƛex = 485 nm, ƛem = 535 nm).

4.2.4.4. Assay specificity and sensitivity

The specificity of the developed *S. trutta* and *S. alpinus* assays was tested *in vitro* using 0.5 ng/µL *S. salar,* 12.8 ng/µL *S. trutta* and 1 ng/µL *S. alpinus* DNA extracted from tissue. DNA concentrations were selected based on gel band intensity from Fish PCR (described in 2.3.4). This step was carried out during the RPA primer screen to ensure selected primers enabled species-specific detection. The sensitivity of each assay, with single RPA replicates, was determined using a 1 in 10 dilution series of DNA extracted from tissue. The concentrations ranged from 4 ng/µL – 0.004 pg/µL for *S. salar,* 1.28 ng/µL – 0.01 pg/µL for *S. trutta* and 1.1 ng/µL – 0.01 pg/µL for *S. alpinus.*

Specificity of the *S. salar* RPA-CRISPR-Cas12a assay was tested *in vitro* following primer selection. The optimised combined approach (1x NEBuffer 2.1, 50:62.5 nM Cas12a:gRNA and 100 nM ssDNA-FQ reporter) was used with 560 – 5.6 pg/µL *S. trutta* and 480 – 0.48

pg/µL *S. alpinus* DNA extracted from tissue. A positive control consisting of 460 pg/µL *S. salar* DNA was used.

For both specificity and sensitivity experiments, reactions (20 µL, 96-well plate format) were incubated in a LightCycler 480 (Roche) for 30 or 120 min at 37°C with fluorescence measurements taken every 30 sec (λex = 485 nm, λem = 535 nm).

4.2.4.5. *S. salar* assay LOD

To calculate the LOD of the *S. salar* assay, the two-step RPA-CRISPR-Cas approach was used with the CRISPR binding buffer replaced with NEBuffer 2.1 (as optimised in Chapter 6). Briefly, RPA was carried out as above and CRISPR-Cas detection consisted of a 20 µL reaction containing; 50 nM:62.5 nM Cas12a:gRNA, 100 nM FQ-Reporter, 1x NEBuffer 2.1, 2 µL RPA product and molecular grade water. Reactions (20 µL, 96-well plate format) were incubated in a LightCycler 480 (Roche) for 120 min at 37°C with fluorescence measurements taken every 30 sec (λex = 485 nm, λem = 535 nm).

Seven RPA replicates of a 1 in 10 dilution series of DNA extracted from tissue were performed, followed by triplicate CRISPR-Cas analysis. RPA replicates 1-4 were run on one qPCR plate with a delay between plate loading and fluorescence measurement. RPA replicates 5-7 had an immediate start (transferred directly to the LightCycler 480). DNA concentrations ranged from 4.6 ng/µL to 0.004 pg/µL and four negative RPA controls were used. As for the qPCR assay (Chapter 3), the LOD is stated as "the measured concentration that produces at least 95% positive replicates" and was calculated by plotting the fraction of positive samples against the concentration of each sample. An approximation of LOD was made by fitting a line at y = 95 with data points above this deemed detectable.

4.2.5. Study sites

Water samples were taken from four Irish rivers as a proof of concept for *S. salar* monitoring using RPA-CRISPR-Cas. Single samples were collected from the Burren, Delour and Dalligan and two samples from the Srahrevagh, one taken upstream and one downstream of a physical barrier that blocks *S. salar* migration. The Canadian study involved sampling of sixteen sites along the Jacques Cartier River and its tributaries in Quebec, Canada in September 2017. In November 2018, sixty-three sites were sampled throughout the Miramichi watershed, New Brunswick, Canada (Figure 4.6).

4.2.6. *S. salar* qPCR assay for analysis of eastern Canada samples

The qPCR assay used on samples from eastern Canada was developed as in Hernandez *et al.*, (2020) and carried out by Cecilia Hernandez. Briefly, primers and a probe were developed to target the *COI* of *S. salar.* The specific assay resulted in a 205 bp amplicon and had the following sequences; forward primer 5'- CCCCCGAATGAATAACATAAGTTTT-3', reverse primer 5'-AATGGCCCCCAGAATTGAA-3' and probe 5'-CTAGCAGGTAATCTTGC-3'.

4.2.7. Presence/absence criteria for eastern Canada study

The following criteria were used to determine if a given field sample is either positive or negative for species specific eDNA. The qPCR assay used criteria of 1 out of 6 technical replicates showing positive amplification at a C_T value less than 39. A selection of replicates were sent for Sanger sequencing to confirm amplifications were target species. The RPA-CRISPR-Cas assay uses two criteria for presence determination: relaxed and stringent criteria. For two-step RPA-CRISPR-Cas reactions, each assay consists of three RPA replicates, with each RPA replicate repeated three times for CRISPR-Cas detection (CRISPR replicate). Both relaxed and stringent presence/absence criteria require CRISPR replicates to have a standard deviation <0.5 to be accepted. If the standard deviation of the three CRISPR replicates was >0.5, the RPA replicate was discarded. The stringent criterion requires 2+ out of 3 RPA replicates to show positive

detection of *S. salar*, whereas the relaxed criterion assumes 1 out of 3 positive RPA replicates infers *S. salar* presence in the field sample.

4.2.8. Statistical analysis

Statistical analysis was carried out using R studio and Microsoft Excel. An R script was written to manipulate the data and calculate background-corrected fluorescence values. These were calculated by subtracting mean fluorescence values obtained from reactions carried out in the absence of RPA product. The mean and standard deviation of sample fluorescence values were then calculated using the "matrixStats" package in R. The proof of concept study calculated a threshold value for fluorescence as three standard deviations above background fluorescence, obtained from reactions carried out in the absence of target DNA (n = 3). In the eastern Canada study, a threshold value for fluorescence was calculated as ten standard deviations above background fluorescence. Background noise may be present in the sample due to incomplete quenching of the fluorescent reporter. Only fluorescence values greater than this threshold value are considered as positive detection of target.

Comparison of methodology for eastern Canada samples was blinded, with RPA-CRISPR-Cas analysis carried out independently of qPCR analysis. To compare the methods, a Chi-squared test was performed for each of the study sites separately (Miramichi and Jacques-Cartier). In order to carry out this test, all data was made binomial with one positive replicate considered as *S. salar* presence for both methodologies.

4.2.9. Reanalysis of *S. salar* sensitivity and specificity data to assess fluorescence by fold-change

S. salar sensitivity (4.2.4.5) and specificity (4.2.4.4) data sets were reanalysed using fold-change. This analysis was used to show a change in fluorescence between the original output value (measured at 30 sec) and final value (measured at 30 min) following incubation. This was performed using the following equation:

$$\frac{(Fluorescence\ @\ 30\ min) - (Fluorescence\ @\ 30\ sec)}{(Fluorescence\ @\ 30\ sec)} \quad (2)$$

A fold-change threshold value of one was used, indicating a doubling of fluorescence over time. Only fold-change values greater than this threshold were considered as positive detection of target.

4.3. Results

S. salar often co-occur in waters with the closely related *S. trutta* (Macqueen *et al.*, 2017) and *S. alpinus,* so highly specific assays are required for accurate detection from eDNA samples collected from natural aquatic environments. The assays designed target the mitochondrial DNA due to its high copy number compared to nuclear DNA (Rees *et al.*, 2014) as well as its ability to resist degradation in the environment (Foran, 2006) (Chapter 1).

4.3.1. *S. salar* version 1 – assay targeting NADH dehydrogenase subunit 2

4.3.1.1. CRISPR-Cas12a version 1 can distinguish between recombinant *S. salar* and *S. trutta* ND2 sequences.

A 21 bp target sequence in the ND2 mitochondrial gene was selected, to test whether a custom Cas12a-gRNA RNP could distinguish between recombinant versions of *S. salar* and *S. trutta.* The gRNA targeting sequence was located next to a 5'-TTTC-3' PAM site present in the sequence of both species, conforming to the consensus A.s.Cas12a 5'-TTTV-3' PAM site (Zetsche *et al.*, 2015). The subsequent 21 bp sequence consisted of four base pair mismatches between *S. salar* and *S. trutta* (Figure 4.7a). Recombinant clones containing the inserted sequence were incubated with the custom RNP and 50 nM ssDNA-FQ reporter. Only upon target recognition and subsequent collateral cleavage by Cas12a nuclease should the reporter produce a signal. Cleavage of the ssDNA-FQ reporter only occurred when the RNP, with custom gRNA, was exposed to the complementary recombinant target sequence. In the absence of the target (i.e. the *S.*

salar gRNA and the *S. trutta* recombinant plasmid) no fluorescence was detected (Figure 4.7b). Specific detection of recombinant target above background levels was detected down to a plasmid DNA concentration of 10^{-13} M (Figure 4.7b).

4.3.1.2. CRISPR-Cas12a version 1 coupled with RPA reaches attomolar sensitivity.

Detection of eDNA samples requires increased assay sensitivity due to the low abundance of target DNA present in the samples. As previously reported (Gootenberg *et al.*, 2017; Chen *et al.*, 2018), incorporation of a pre-amplification step can increase the sensitivity by several orders of magnitude. Addition of RPA removes the need for thermal cycling, instead using enzymatic activity to amplify small amplicons (<1.5 kb) at a single, low temperature (Piepenburg *et al.*, 2006). *S. salar* specific primers for RPA were designed with two mismatches in the forward primer and six mismatches in the reverse primer between *S. salar* and *S. trutta* (Figure 4.8a). The specific RPA reaction was coupled with the *S. salar* specific CRISPR-Cas12a detection assay. This additional pre-amplification step was tested on the *S. salar* recombinant DNA plasmids and showed an increase in sensitivity down to attomolar range (10^{-18} M) (Figure 4.8b).

4.3.1.3. RPA-CRISPR-Cas12a version 1 enables target sequence detection in whole genome complexity but PAM site presence in closely related species reduces specificity.

A more complex genomic context was required to further test the specificity and sensitivity of the developed RPA-CRISPR-Cas assay, i.e. the entire *S. salar* and *S. trutta* genome rather than a simple recombinant plasmid. Using DNA extracted from tissue of commercially available *S. salar* and rod-caught *S. trutta,* it is shown that the assay can detect down to a concentration of 2 pg/µL in whole genomic *S. salar* (Figure 4.9). However, when introducing this genetic complexity, specificity is reduced as fluorescence detection is seen with high concentrations (5.75 ng/µL) of *S. trutta* DNA (Figure 4.9). This highlights the need for stringent assay design, as although the designed

gRNA sequence is species specific *in silico,* when testing on tissue extracts, presence of the PAM site in both species may lead to false recognition of target and thus false negative results.

4.3.2. *S. salar* version 2 - assay targeting NADH dehydrogenase subunit 5

In order to improve specificity and sensitivity, the assay was redesigned. Upon visual assessment of the multiple alignment of *S. salar, S. trutta* and *S. alpinus* mtDNA sequences, a new 20 bp target sequence was selected, residing in the mitochondrial ND5 gene. This sequence was located next to a 5'-TTTC-3' PAM site present only in the *S. salar* sequence. The 20 bp crRNA sequence consisted of two mismatches between the conserved *S. salar* and *S. trutta* (Figure 4.10a). Recombinant clones of both species, containing the inserted sequence were incubated with an RNP targeting the *S. salar* fragment and 50 nM ssDNA-FQ reporter. Cleavage of the ssDNA-FQ reporter only occurred when the RNP was exposed to the recombinant *S. salar* and not the *S. trutta* DNA (Figure 4.10b). Detection of *S. salar* recombinant plasmid above background levels, without pre-amplification, was detected down to a DNA concentration of $\geq 10^{-15}$ M (Figure 4.10b).

4.3.2.1. CRISPR-Cas12a version 2 coupled with RPA reaches zeptomolar sensitivity for its target sequence.

CRISPR-Cas12a detection was coupled to isothermal amplification to increase the sensitivity of the assay, as required for environmental samples. *S. salar* specific primers were designed to target the ND5 gene and coupled with the *S. salar* specific CRISPR-Cas12a detection assay. When tested on recombinant DNA plasmids, an increased sensitivity was seen from the femtomolar (10^{-15} M) to the zeptomolar (10^{-21} M) range (Figure 4.10c).

4.3.2.2. Sensitivity of CRISPR-Cas12a version 2 is maintained in the context of whole *S. salar* genome complexity.

A more complex genomic context was used to further test the specificity and sensitivity of the newly designed assay. As previously, the assay was tested on DNA extracted from tissue of commercially available *S. salar* and wild *S. trutta.* The developed assay detects down to a concentration of 0.04 pg/µL in whole genomic *S. salar* (Figure 4.11) and shows no detection of *S. trutta.*

4.3.2.3. RPA-CRISPR-Cas12a version 2 can distinguish *S. salar* presence or absence from Irish freshwater eDNA samples confirmed by qPCR and electrofishing.

The final test of the proof of concept assay was to assess if it would work on eDNA samples acquired in the field that may contain amplification inhibitors and consist of a substantial proportion of degraded DNA (Taberlet *et al.*, 2012). eDNA samples extracted from four freshwater rivers across Ireland were used (Chapter 2). Extracts had known presence or absence of *S. salar* confirmed previously using electrofishing surveys (Appendix L) and qPCR (Chapter 3 and Appendix M). Within a 150 min timeframe *S. salar* eDNA was successfully detected using RPA-CRISPR-Cas12a from water samples with known presence of *S. salar* (Figure 4.12). Importantly, no fluorescence signal was seen in the Dalligan or Upstream Srahrevagh River samples where *S. salar* was confirmed absent but known to contain *S. trutta* (Atkinson *et al.*, 2018). Version 2 of the *S. salar* RPA-CRISPR-Cas12a assay was used for all subsequent experimentation.

4.3.3. Optimisation of RPA-CRISPR-Cas12a *S. salar* version 2 assay

4.3.3.1. RNP concentration has minimal effect on fluorescence output

Optimisation of the Cas12a and gRNA concentrations in the RNP using between 25:31.25 nM and 100:125 nM (Cas12:gRNA) showed little variation in fluorescence output (Figure 4.13). Although there is an increase between the lowest and highest concentrations, this is not substantial enough to outweigh the increase in cost associated with higher enzyme and RNA concentrations. It was therefore decided, that the original ratio of 50:62.5 nM Cas12a:gRNA (as described in Chen *et al.*, (2018)) would be used going forward.

4.3.3.2. Fluorescence output has a linear relationship with fluorophore-quencher reporter concentration.

Optimisation of the ssDNA-FQ reporter concentration using varying concentrations from 40 nM to 100 nM, showed a non-proportional linear relationship with fluorescence increasing with ssDNA-FQ concentration (Figure 4.14b). The fluorescence measurements time course (Figure 4.14a) suggests that whilst using current concentrations of other reagents, the ssDNA-FQ reporter is the rate-limiting step. This is apparent due to the clear plateau in fluorescence at all reporter concentrations. Based on the signal amplification and thus the increased difference from background noise, a concentration of 100 nM was selected for further studies.

4.3.3.3. RNP preassembly speeds up fluorescence acquisition compared to separate addition of Cas12a and gRNA to the reaction.

Addition of the Cas12a nuclease and gRNA directly into the reaction, without an RNP preassembly step, delays fluorescence acquisition (Figure 4.15a). The same concentration of Cas12a and gRNA was used for either an RNP preassembly step, whereby Cas12a and gRNA are incubated in PBS for 20 min prior to use, or direct addition into the CRISPR-Cas12a reaction. When visualised, there is a lag in fluorescence measurements at all three *S. salar* tissue concentrations when preassembly is not performed. Although the final fluorescence measurement, at 120 min, is not greatly decreased (Figure 4.15b), this lag restricts shortening of the incubation time which is

preferred for an on-site device. RNP preassembly was therefore continued in future work.

4.3.3.4. LOD calculated across seven amplification replicates estimated as 0.0046 pg/µL.

A confidence interval of 95% was used to determine the assay LOD across seven replicates. The redesigned assay, using NEBuffer 2.1 (as optimised in Chapter 5.3.1.1), preassembled RNP with 50:62.5 nM Cas12a:gRNA and 100 nM ssDNA-FQ reporter, detected the target sequence down to a DNA concentration of 0.046 pg/µL after both 120 min (Figure 4.16a) and 30 min incubation (Figure 4.16b). At both time points, two of the seven replicates positively detected *S. salar* at 0.0046 pg/µL, a percent positive below the threshold of 95% (Figure 4.16c). Using optimised conditions, there is little difference between end-point fluorescence values at 120 min (Figure 4.16a) and 30 min (Figure 4.16b) meaning incubation times were reduced to 30 min for future work. All four negative controls showed no positive detection.

4.3.3.5. Specificity maintained using optimised RPA-CRISPR-Cas12a *S. salar* assay conditions

A more thorough assessment of *in vivo* specificity with tissue extracts from *S. trutta* and *S. alpinus* was performed using optimised conditions. No detection of *S. alpinus* was seen at any of the DNA concentrations used but *S. trutta* was detected above the threshold at 560 pg/µL and 5.6 pg/µL (Figure 4.17b). The time course profile of the *S. trutta* detection (Figure 4.17a) shows a minimal increase in fluorescence compared to the positive *S. salar* control.

4.3.4. RPA-CRISPR-Cas *S. salar* version 2 assay shows no statistical difference to qPCR for presence/absence detection in eastern Canada.

Note: Results from eastern Canada sites were generated from a collaboration with Louis Bernatchez (University Laval). Field sampling and qPCR analysis was carried out externally (see Williams *et al.*, (2021)), but RPA-CRISPR-Cas and comparative data analysis was carried out by Molly Ann Williams.

In general, six replicates were performed for qPCR analysis and only three replicates for RPA-CRISPR-Cas analysis. An equal number of replicates were not performed across the two methodologies due to insufficient DNA yields. All field, extraction and amplification negative controls showed no positive detection. This indicates the absence of contamination at any stage of the eDNA workflow and thus we can assume that positive detection of *S. salar* comes from the environmental sample.

4.3.4.1. Miramichi Watershed

In the Miramichi Watershed, of the 63 sites sampled 42 sites showed positive detection for *S. salar* using qPCR and 35 sites were positive using RPA-CRISPR-Cas (Figure 4.18). Using the qPCR method, C_T values for positive detection ranged from 24.2±0.08 to 38.3±0.5 (Appendix N). The number of positive replicates ranged from 3 out of 6, in 2 sites, to 6 out of 6, in 39 sites (Appendix N). To confirm species specificity of amplicons, 19% of positive detections were analysed using Sanger sequencing and confirmed as *S. salar* (Appendix O). Using the RPA-CRISPR-Cas methodology, only four sites were deemed positive using the relaxed criteria of 1 out of 3 positive replicates. The other 31 sites were positive based on the stringent criteria having 2 or 3 positive replicates (Appendix N and P). When comparing the results directly, only 11.1% of sites were incongruous. At these sites, RPA-CRISPR-Cas failed to detect where qPCR reported *S. salar* presence.

The chi-square test of independence, $\chi 2$ (1, N = 63) = 1.636, p = 0.2008, showed there was no statistical difference, given p>0.05, between the methodologies for *S. salar* positive detection when using a binomial approach.

4.3.4.2. Jacques Cartier Watershed

In the Jacques Cartier Watershed, of the 16 sites sampled nine sites showed positive detection for *S. salar* using qPCR and eleven sites were positive using RPA-CRISPR-Cas (Figure 4.19). Using the qPCR method, C_T values for positive detection ranged from 35.3±0.8 to 37.9 (Appendix Q). The number of positive replicates ranged from 1 out of 6, in one site, to 6 out of 6, in five sites (Appendix Q). To confirm species specificity of amplicons, 100% of positive detections were analysed using Sanger sequencing and all confirmed as *S. salar* (Appendix R). Using the RPA-CRISPR-Cas methodology, only three sites were deemed positive using the relaxed criteria of 1 out of 3 positive replicates. The other eight sites were positive based on the stringent criteria; 2 or 3 positive replicates (Appendix S). When comparing the presence/absence data directly, 25% of sites had differing results.

The chi-square test of independence, $\chi 2$ (1, N = 16) = 0.533, p = 0.4652, showed there was no statistical difference, given p>0.05, between the methodologies for *S. salar* positive detection when using a binomial approach.

4.3.5. RPA-CRISPR-Cas *S. trutta* assay is specific and sensitive in a whole genomic context.

The chosen target site for the *S. trutta* specific assay consisted of ten base pair mismatches with *S. salar* and twelve base pair mismatches with *S. alpinus* in the RPA primers and three mismatches in the gRNA binding region with both *S. salar* and *S. alpinus* (Figure 4.20a). Fluorescence detection could be seen down to 1.28 pg/µl in

whole genomic *S. trutta.* Importantly, in the absence of target DNA (i.e. *S. salar* or *S. alpinus* tissue extract) no fluorescence detection was seen (Figure 4.20b).

4.3.6. RPA-CRISPR-Cas *S. alpinus* assay is specific and sensitive in a whole genomic context.

The chosen target site for the *S. alpinus* specific assay consisted of ten base pair mismatches in the RPA primers with both *S. salar* and *S. trutta*, and five mismatches with *S. salar* and six mismatches with *S. trutta* in the gRNA binding region (Figure 4.21a). Fluorescence detection could be seen down to 1.1 pg/µl in whole genomic *S. alpinus.* Importantly, in the absence of target DNA (i.e. *S. salar* or *S. trutta* tissue extract) no fluorescence detection was seen (Figure 4.21b).

4.3.7. Reanalysis of *S. salar* sensitivity and specificity data to assess fluorescence fold-change as an alternative data analysis method

The *S. salar* LOD dataset (Figure 4.16), consisting of seven RPA replicates of six DNA dilutions ranging from 460 pg/µL to 0.0046 pg/µL, was reanalysed to assess fluorescence fold-change. Positive detections from RPA replicates 1 to 4 showed fold-change values between 0.4 and 2 (Figure 4.22a) due to high starting fluorescence values (Appendix T). Positive detections from RPA replicates 5 to 7, had fold-change values between 3 and 8 (Figure 4.22b). Reanalysis of *S. salar* specificity data (Figure 4.17) indicated no detection of *S. trutta* or *S. alpinus* above the fold-change threshold of one, at any of the three DNA concentrations used (Figure 4.23).

4.4. Discussion

CRISPR-Cas diagnostics, combining nucleic acid amplification with CRISPR-Cas detection, offer new ways to sensitively and specifically monitor molecular targets at home, at POC and in the field (Kaminski *et al.*, 2021). Although to date this has primarily been used for

medical diagnostics, such as for infectious and non-infectious diseases (Jolany vangah *et al.*, 2020), it also has potential for use in environmental monitoring. This chapter highlights the utility of RPA-CRISPR-Cas12a technology as a tool for single-species eDNA detection of three salmonid species, *S. salar, S. trutta* and *S. alpinus.* These species are relevant for eDNA monitoring due to their presence in the Burrishoole Catchment, Co. Mayo, Ireland and global ecological and economic importance (as highlighted in Chapter 1.2.2). Additionally, this chapter emphasises the careful design and optimisation of RPA-CRISPR-Cas technology needed to distinguish closely related species and makes some suggestions regarding data analysis and threshold criteria suitable for eDNA monitoring.

4.4.1. RPA-CRISPR-Cas assay design

Initial design of the *S. salar* targeting assay (Figure 4.7-4.9) highlighted several critical factors that should be considered in assay design. Cas12a nuclease activity is dependent on recognition of a T-rich PAM site succeeding the gRNA binding region (Chen *et al.*, 2018). The exact PAM sequence required is dependent on which species the Cas nuclease is derived from, for example, *Fn*Cpf1 from *Francisella novicida* favours a 5'-TTN-3' PAM whereas *As*Cpf1 (as used in this study) from *Acidaminococcus* favours a 5'-TTTV-3' PAM site (Zetsche *et al.*, 2015). It is therefore crucial that the exact Cas12a nuclease used is selected prior to assay design.

Additionally, as with any sequence dependent assay, stringent design is required to ensure sufficient mismatches between target and non-target species. Tolerance of mismatches in RPA primer binding regions, reduces amplification specificity (J. Li, Macdonald and Von Stetten, 2019), however this can be recovered with sufficient mismatches in the gRNA targeting region. Complementarity between the target and a 'seed' sequence in the gRNA strongly influences target specificity (Swarts *et al.*, 2017). A 'seed' sequence of 3-8 nucleotides at the PAM-proximal side of the protospacer has been reported for Cas12a (Zetsche *et al.*, 2015; Fonfara *et al.*, 2016). It has been observed that Cas12a is highly sensitive to mismatches in these nucleotides and also, to a lesser extent, mismatches around the cleavage site (nucleotides 1-4 on the PAM-distal

site) (Fonfara *et al.*, 2016). Despite this, mismatches in the gRNA binding region can be tolerated with Murugan *et al.*, (2020) reporting tolerance of up to four base pair mismatches in this region. In version 1 of the *S. salar* targeting assay, four base pair mismatches were present in the gRNA binding region (Figure 4.7), yet non-specific detection of *S. trutta* was observed (Figure 4.9). This suggests that a combination of PAM site presence and insufficient gRNA mismatches enabled Cas12a cleavage and therefore it is advised that the PAM site should be absent from the target region of closely related or co-habiting species, to reduce the possibility of non-specific recognition.

Conversely, a low level of non-specific detection was also seen in version 2 of the *S. salar* targeting assay when using background subtracted fluorescence analysis (Figure 4.17), despite lacking the PAM site. This is potentially due to relaxed PAM site recognition, whereby Cas12a nucleases recognise C-containing regions, such as CTTV and TCTV, as suboptimal PAMs (Yamano *et al.*, 2017). It is also possible that there were insufficient gRNA mismatches, particularly in the seed region (Figure 4.10a). Moreover, base pair differences between *S. salar* and *S. trutta* in the 3' region of the gRNA, might be removed during RPA amplification of the non-target organism. If non-specific binding of the *S. salar* reverse primer to the *S. trutta* sequence is occurring and successfully being amplified, this could introduce the correct base pairs into the *S. trutta* amplicon as the reverse primer overlaps with the 3' end of the gRNA targeting region. The limitations of this assay could likely be overcome by redesigning the target region ensuring maximum mismatches in the seed region and non-overlapping sequence specific elements. Of note, both the *S. trutta* (Figure 4.20) and *S. alpinus* (Figure 4.21) assays showed high levels of specificity.

4.4.2. Calculating method limits to estimate sensitivity

To compare assay sensitivities, LODs can be calculated using DNA templates such as gBlocks, plasmid DNA constructs or tissue extracts. Klymus *et al.*, (2020) called for establishment of standardised reporting of LODs in the eDNA community, due to the

variety of definitions used in the early eDNA literature. Calculating the LOD of the *S. salar* RPA-CRISPR-Cas method used the same definition and same number of replicates as for qPCR (Chapter 3): "the measured concentration that produces at least 95% positive replicates" (Forootan *et al.*, 2017). The *S. salar* RPA-CRISPR-Cas LOD of 0.046 pg/µL (Figure 4.16) is comparable to the *S. salar* qPCR LOD of 0.025 pg/µL (Figure 3.6). This limit was calculated using DNA extracted from *S. salar* tissue, offering whole genome complexity. However, in the literature the DNA template of choice varies (Eichmiller *et al.*, 2014; Klymus *et al.*, 2020; Langlois *et al.*, 2020), with synthetic double stranded DNA templates (gBlocks) often preferred (Klymus *et al.*, 2020; Langlois *et al.*, 2020). These templates allow for a more accurate assessment of template concentration by removing the variability of the proportion of mitochondrial to nuclear DNA, which makes it difficult to estimate template concentration in DNA preparations from tissue (Langlois *et al.*, 2020). However, it should be noted that use of synthetic templates does not fully reflect the sensitivity of the assay when used for analysis of complex matrices such as eDNA samples. Of note, LODs were not calculated for the *S. trutta* and *S. alpinus* assays although a triplicate DNA dilution series was performed for each to estimate sensitivity (Figure 4.20 and 4.21).

4.4.3. Criteria to assess presence/absence of field replicates

In addition to calculating the LOD (and quantification if applicable) of assays, it is vital that criteria are outlined regarding the number of positive technical replicates required in order for a species to be deemed present in a sample. This is of particular importance when assessing invasive species, given the potential of false negatives (Furlan *et al.*, 2016). Direction must be taken from other fields that are using diagnostic assays of low copy number DNA. For example, when concentrations of DNA are very low (<100 copies), discrepancies between qPCR replicates are expected (Ellison *et al.*, 2006). In clinical diagnostics, one positive qPCR replicate is sufficient to determine whether cancer cells are still present in a patient after remission (van der Velden *et al.*, 2007); however, others suggest there needs to be consistency between replicates to accept as positive (Bustin and Mueller, 2005). This lack of consensus is also apparent in the eDNA

space (Giguet-Covex *et al.*, 2014; Willerslev *et al.*, 2014; Ficetola *et al.*, 2015). The risk of taxa being present at low densities means some accept a single positive qPCR replicate (O'Sullivan *et al.*, 2020). Although Goldberg *et al.*, (2016) suggest that results of this variety, which cannot be replicated, should be interpreted with caution. For this reason, two criteria were developed for the RPA-CRISPR-Cas assay when assessing the eastern Canada data. The stringent criterion requires at least 2 out of 3 positive RPA replicates, whereas the relaxed criterion only uses 1 out of 3 positive RPA replicates to deduce species presence in the field replicate. Whilst analysis using the relaxed criterion is less reliable for inferring species presence and should be interpreted with caution, this could be an artefact of the heterogeneous distribution of eDNA (Goldberg *et al.*, 2016). Therefore, if all controls behave as expected, species presence should be assumed. In practice, the exact research question being asked, the ecological impact of the study and the overall strength of evidence, will affect the exact criterion used.

When using both methodologies, with these established criteria and background subtracted fluorescence, for analysis of eastern Canada samples, 86.1% of the data reported the same result, with no statistical difference in the number of positives in each method. Nevertheless, several locations showed discrepancies possibly due to the subsampling effect. Furlan *et al.*, (2016) discussed the importance of considering eDNA distribution within a water body, sample and subsample when designing eDNA studies. It is possible that the discordant results seen in this study are due to detection failure caused by a lack of target molecules in some replicates. Ideally, the number of field samples and number of technical replicates should be increased to strengthen the outcome of the eDNA analysis (Jerde, 2019). Unfortunately, this is not always possible due to the yield of eDNA extracted from each sample as well as time and monetary constraints. In the eastern Canada study, quantities of eDNA were insufficient to perform more than three RPA-CRISPR-Cas replicates.

4.4.4. Data analysis of RPA-CRISPR-Cas diagnostics

Compared to qPCR, the development of CRISPR-Cas-DX is in its infancy, with the field rapidly expanding. The current format is a qualitative method of detection, only suitable for yes/no diagnostics. Overtime, it is likely that a more quantitative aspect of CRISPR-Cas assays will develop as the enzyme kinetics of the various Cas nucleases are more fully explored (Cofsky *et al.*, 2020). The existing methodology, as described in this chapter, is an end-point detection assay, whereby the target region is fully amplified and then detected. This design means that, unlike in qPCR, fluorescence is not monitored during sigmoidal amplification and consequently the data handling differs. However, as with qPCR it is vital that we set a threshold limit above which signal is deemed positive. In clinical qPCR-based diagnostics, this cut-off is based on the C_T value established during LOD studies (Caraguel *et al.*, 2011; Elfving *et al.*, 2014; Tom and Mina, 2020) and is accepted as best practice based on the MIQE guidelines. Direction may be taken from these guidelines but cannot be applied directly to eDNA applications whereby multiple field samples and technical replicates are used to increase power of results.

To date RPA-CRISPR-Cas diagnostics have no set cut-off thresholds and often no threshold is reported in the literature. Originally a value of 3 x greater than the standard deviation of background fluorescence (no RPA product added) was used as the threshold (as in Figure 4.12), however for the eastern Canada samples (Figure 4.18 and 4.19), it was decided that this should be increased to 10 x the standard deviation. This threshold was raised to increase the chance of a positive signal being outside the background noise present in fluorescence-based assays and reduce false positive results. However, due to the type of assay, these background measurements were taken from individual samples on the same plate rather than the starting fluorescence of each well, as would be done for qPCR. This meant that although some samples may have shown no change in fluorescence across the time course, if the initial fluorescence was higher than the background wells, the samples would appear positive. To circumvent this, a decision was made to reanalyse the *S. salar* sensitivity and specificity samples

using fold-change analysis. This analysis, also used in the literature (Nguyen *et al.*, 2020), means that fluorescence values at 30 min are compared to the starting fluorescence, at 30 sec, only in the individual well and show whether fluorescence is increasing regardless of the background fluorescence noise of a sample. Between replicate standard deviations are still accounted for by removing samples with standard deviations greater than 0.5 prior to fold-change analysis.

A benchtop fold-change threshold of one indicates a doubling of fluorescence across the time course. This value takes into consideration the fold-change seen at the LOD (Figure 4.22) whilst accounting for reduced assay efficiency in environmental samples compared to control DNA. However, when assessing the expected fold-change of samples based on the LOD data (Figure 4.22) some potential pitfalls became apparent. Due to the efficient nature of Cas12a target recognition and collateral cleavage, fluorescence acquisition may begin prior to plate loading into the LightCycler 480 (Appendix T). If this occurs, the fold-change value may not pass the threshold because the starting fluorescence, as measured by the instrument, is already much higher than the true background fluorescence. This is the case in replicates 1 to 4 of the *S. salar* LOD study, which show fold-change values less than 1 in many positive samples (Figure 4.22). To overcome this, it is imperative that samples are prepped on ice and transferred to the LightCycler 480 rapidly. It is also crucial that raw time course datasets are analysed alongside fold-change data to ensure no premature collateral cleavage has occurred. These steps were taken when analysing environmental samples in Chapter 6.

Moreover, using fold-change analysis changed the perceived *S. salar* assay specificity (Figure 4.23). Whilst background subtracted analysis and a standard deviation threshold approach, showed non-target positive detection of *S. trutta,* the fold-change values for these samples were less than the threshold of one, thus deeming the samples as negative. Traditionally data analysis is decided prior to experimentation, however, the early stage of the CRISPR-Cas diagnostics field means analysis has not yet been standardised and thus optimisation of data analysis is required.

4.4.5. Potential use of RPA-CRISPR-Cas for eDNA analysis

Overall, the data produced in this chapter highlights the potential of RPA-CRISPR-Cas detection to add to the current monitoring toolbox with some potential benefits not yet explored. It is possible that RPA-CRISPR-Cas assays could be used where qPCR assays are unable to be designed, such as when two closely related species are found in sympatry. Li *et al.*, (2018) show that HOLMES (PCR coupled to Cas12a detection) can discriminate single-base differences using short crRNA guide sequences (16-17 nucleotides). The HOLMES method, enables PAM independent sequence recognition by incorporating the necessary PAM site during PCR amplification (Li *et al.*, 2018). This meant that single nucleotide polymorphisms (SNPs) could be designed to fall in the 5' seed region of the gRNA binding sequence resulting in a clear fluorescence difference and successful genotyping of multiple SNP loci relating to human health. Although this method used PCR to introduce PAM sites, an upgraded method, named HOLMESv2, was developed to show that PAM independent SNP recognition was possible using an isothermal approach (Li *et al.*, 2019). HOLMESv2 uses LAMP and a Cas12b nuclease to distinguish SNP containing DNA targets. It is thus likely, that with stringent assay design, the RPA-CRISPR-Cas12a methodology could be modified to enable separation of previously indistinguishable species, potentially in a PAM independent manner. This would be of huge importance in cases where invasive species coexist with closely related rare endemic species (Fukumoto *et al.*, 2015) and cannot be distinguished using qPCR.

Furthermore, the different DNA amplification chemistry used in the RPA-CRISPR-Cas method, may mean it works where qPCR does not (Kersting *et al.*, 2014). The matrix of eDNA samples can be very complex (Chapter 1), meaning DNA amplification inhibitors could be highly abundant. When comparing PCR and RPA methodologies for detection from blood, Kersting *et al.*, (2014) showed that RPA out-performed PCR in the presence of many inhibitors such as those common with eDNA extraction procedures. Whilst this was not investigated during this study, it is possible that when water contaminants are high and inhibitory to qPCR, they will not inhibit RPA-CRISPR-Cas based assays. It is also worth noting, that although the developed assay utilised RPA for target amplification,

any pre-amplification method could be coupled to CRISPR-Cas12a detection as displayed in the literature (Li *et al.*, 2018; Broughton *et al.*, 2020; Guo *et al.*, 2020). RPA was specifically selected for this assay due to its low temperature isothermal nature and ease of primer design. However, the possibility of adding other pre-amplification methods removes the limitations that one particular method might have, which is not only advantageous when combating sample inhibitors but also increases the likelihood of finding an assay that suits the ecological question to be answered.

To conclude, this work demonstrates the applicability of RPA-CRISPR-Cas technology to single-species detection. The development of three distinct assays and the successful detection of *S. salar* in Irish and Canadian freshwater samples shows the promise for using RPA-CRISPR-Cas12a as an eDNA detection technique. Through rigorous design of three species specific sequences (forward and reverse RPA primers and a gRNA), the assay may be applied to any target organism to monitor species distribution in the environment.

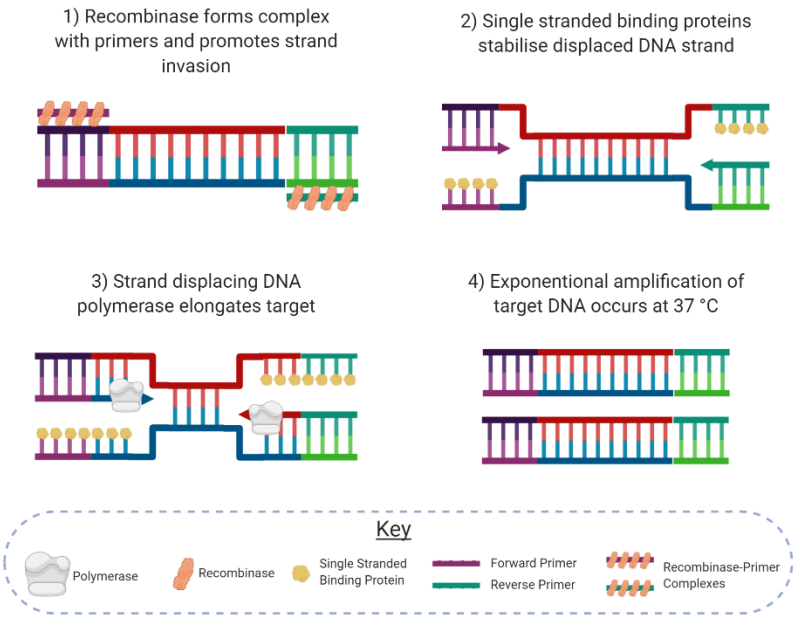

Figure 4.1 Schematic of RPA. Recombinase proteins form complexes with each primer complementary to target DNA, which scan DNA for homologous sequences. Upon recognition of complementary DNA, the primers are inserted by the strand-displacement activity of the recombinase. Single stranded binding proteins stabilise the displaced DNA strand. The recombinase protein disassembles allowing a strand displacing DNA polymerase to bind the 3' end of the primers and elongate the primer. Cyclic repetition of this process enables exponential amplification of target DNA. Adapted from Lobato and O'Sullivan, (2018).

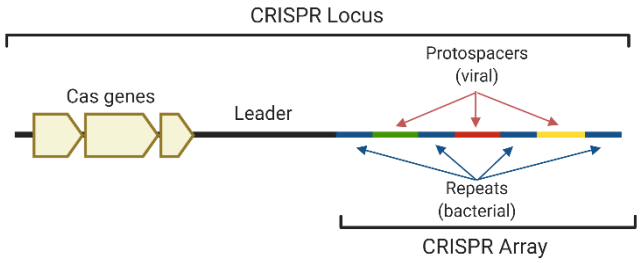

Figure 4.2 CRISPR Locus. A Clustered Regularly InterSpaced Palindromic Repeat (CRISPR) locus found in the genome of bacteria. This consists of the CRISPR array containing viral protospacers interspersed with bacterial repeat sequences and upstream CRISPR-associated (Cas) nuclease genes. Adapted from Barman *et al.*, (2019).

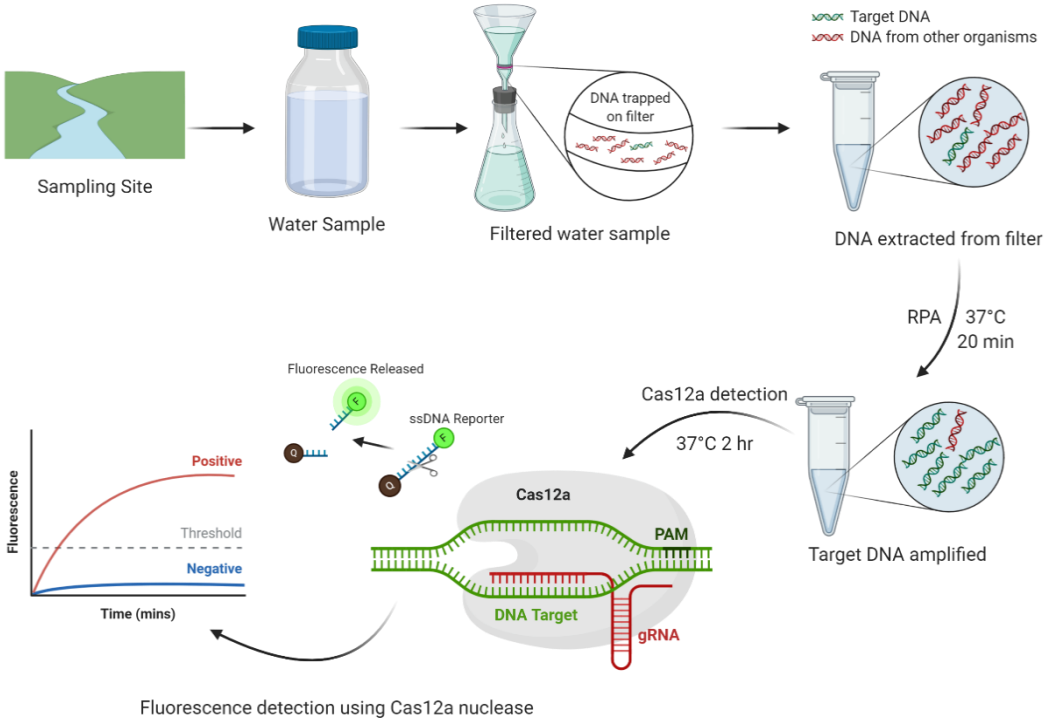

Figure 4.3 Overview of RPA-CRISPR-Cas12a detection for eDNA analysis. Water samples are collected and filtered before DNA extraction. Target DNA is amplified using isothermal RPA prior to CRISPR-Cas12a mediated fluorescence detection of target using an ssDNA-FQ Reporter. PAM, Protospacer Adjacent Motif; F, fluorophore; Q, quencher

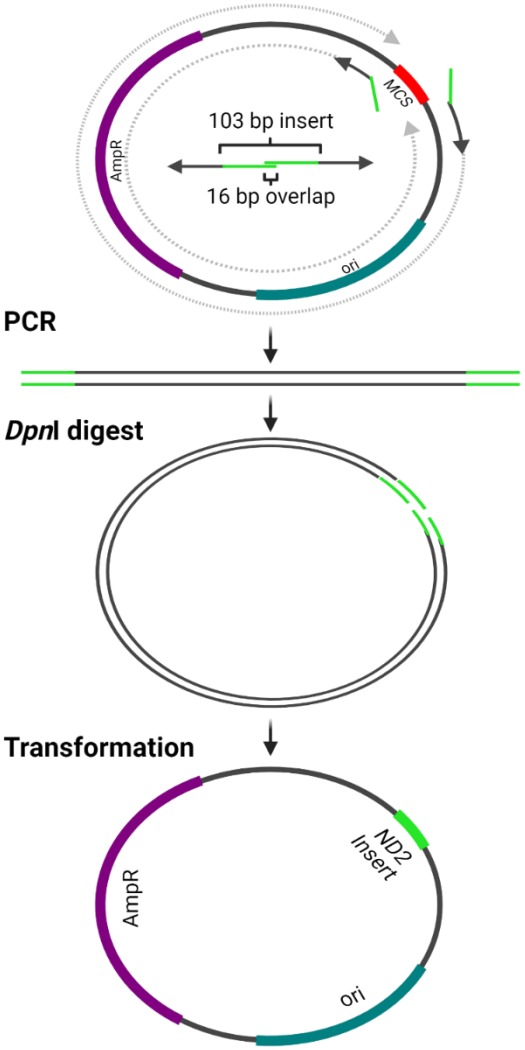

Figure 4.4 Fast Cloning of NADH dehydrogenase subunit 2 (ND2) using single primers targeting pUC19 plasmid with 'tail' regions containing the insert sequence. The forward primer starts immediately downstream of the Multiple Cloning Site (MCS) and has a tail with the 3' part of the ND2 insert whilst the reverse primer starts immediately upstream of the MCS and has a tail with the 5' part of the ND2 insert. Primers have a 16 bp overlap for insertion of the 103 bp sequence. PCR amplification is followed by *Dpn*I digestion and transformation into competent cells. Adapted from Li *et al.*, (2011).

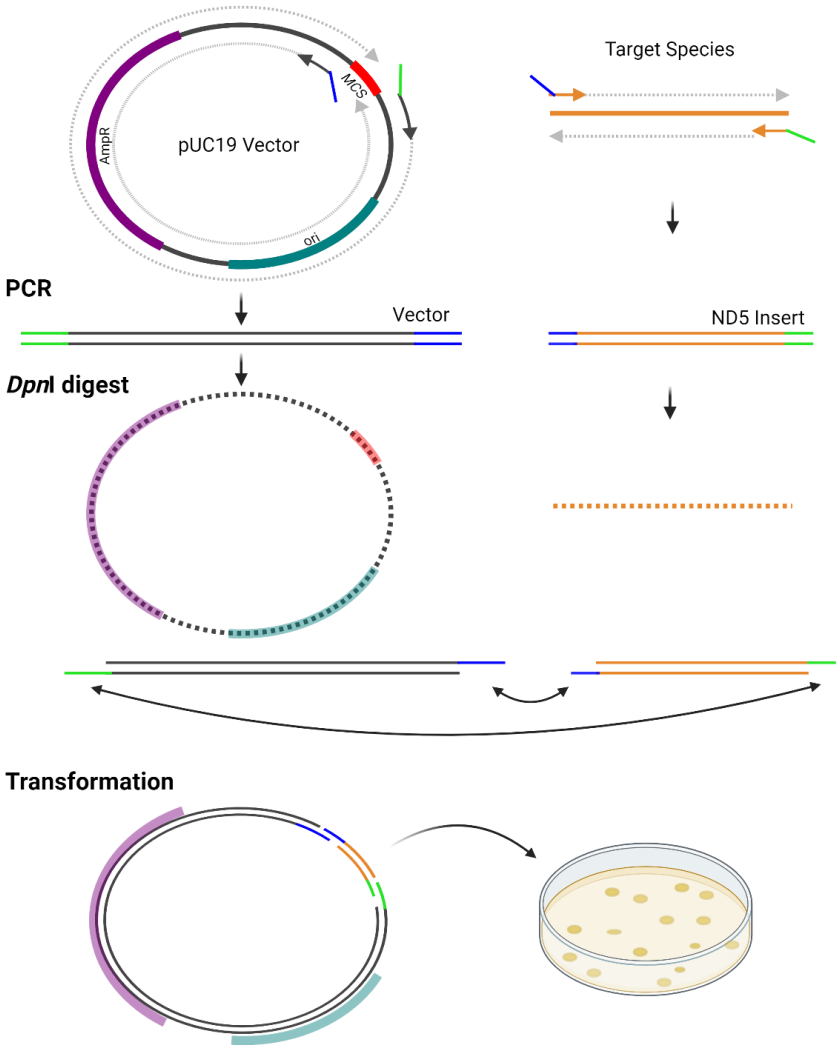

Figure 4.5 Fast Cloning of the NADH dehydrogenase subunit 5 (ND5) using two PCR amplification steps: one for pUC19 vector and one for the target sequence. PCR amplification of the vector and insert sequence are carried out separately with the primer pair for insert amplification containing 16 bp tails which overlap with the PCR-amplified vector ends. Following amplification, PCR products are subject to a *Dpn*I digestion whereby sticky ends for the overlapped regions of the vector and insert are created, allowing the formation of a circular construct (the exact mechanism is unknown). Products are then transformed into competent cells. Adapted from Li *et al.*, (2011).

Table 4.1 Specific CRISPR-Cas12a detection conditions

Figure	Species (Version)	Buffer	FQ Reporter (nM)	Incubation Time (mins)	Data Analysis	Threshold
4.7	*S. salar* (V1)	Binding Buffer	50	120	Background subtraction	N/A
4.8		Binding Buffer	50	120	Background subtraction	3x StDev
4.9		Binding Buffer	50	120	Background subtraction	3x StDev
4.10	*S. salar* (V2)	Binding Buffer	50	120	Background subtraction	3x StDev
4.11		Binding Buffer	50	120	Background subtraction	3x StDev
4.12		Binding Buffer	50	120	Background subtraction	3x StDev
4.13		Binding Buffer	50	120	Background subtraction	N/A
4.14		Binding Buffer	40-100	120	Background subtraction	N/A
4.15		Binding Buffer	100	120	Background subtraction	N/A
4.16		NEBuffer 2.1	100	30 + 120	Background subtraction	10x StDev
4.17		NEBuffer 2.1	100	30	Background subtraction	10x StDev
4.18 and 4.19		Binding Buffer	50	120	Background subtraction	10x StDev
4.22		NEBuffer 2.1	100	30	Fold Change	N/A
4.23		NEBuffer 2.1	100	30	Fold Change	Fold Change = 1
4.20	*S. trutta*	Binding Buffer	100	120	Background subtraction	3x StDev
4.21	*S. alpinus*	Binding Buffer	100	120	Background subtraction	3x StDev

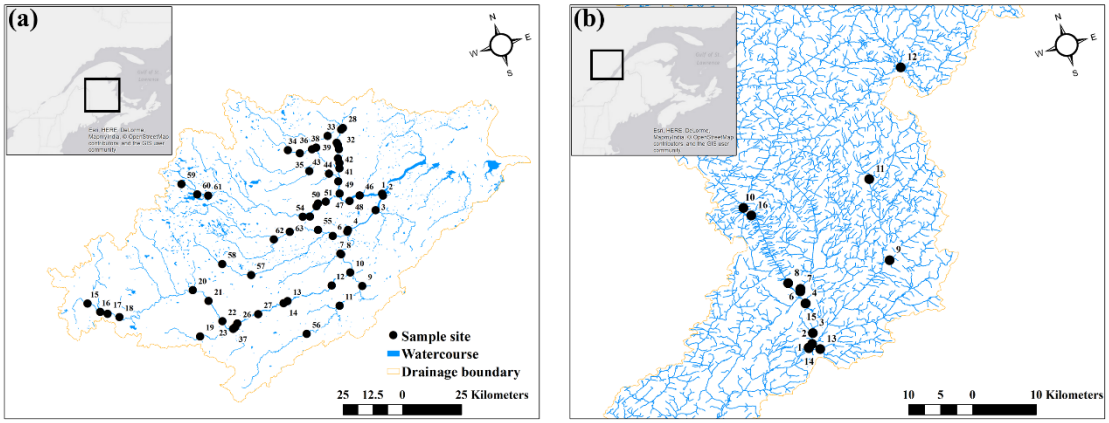

Figure 4.6 Location of sampling sites in eastern Canada. (a) Miramichi Watershed, New Brunswick. (b) Jacques-Cartier Watershed, Quebec.

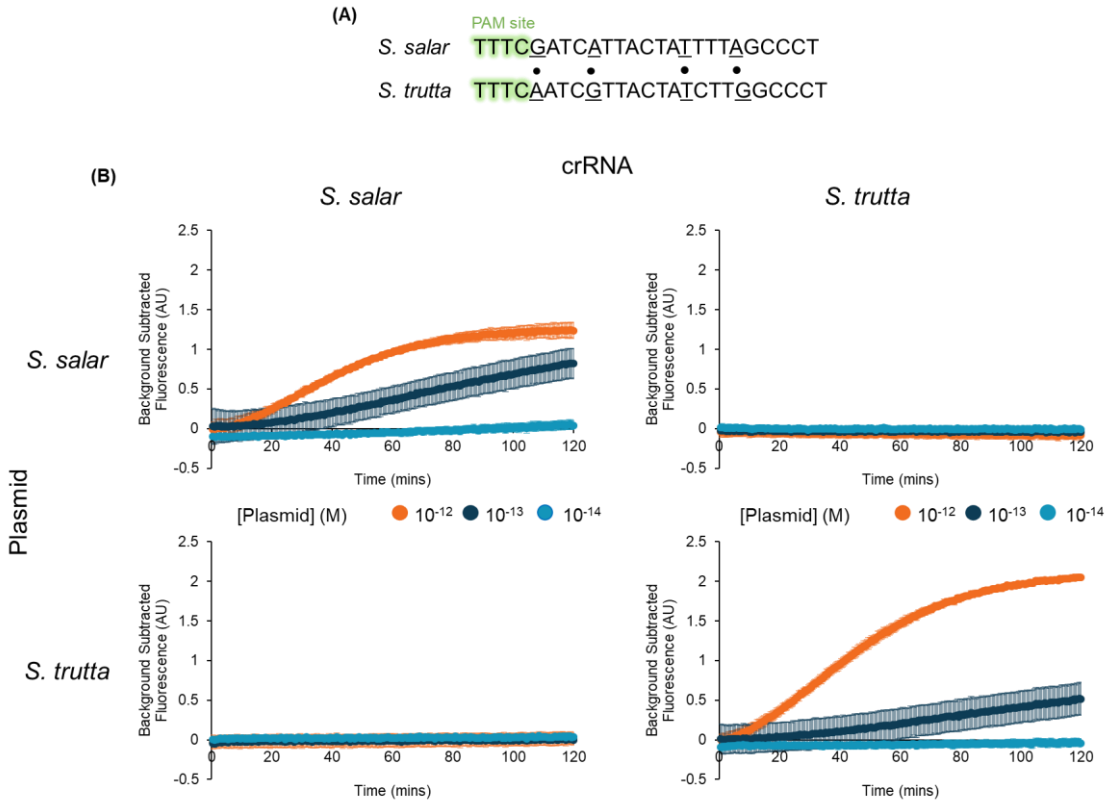

Figure 4.7 Distinguishing *S. salar* and *S. trutta* ND2 recombinant sequences using a Cas12a nuclease. (A) Alignment of gRNA targeting site in *S. salar* and *S. trutta* showing PAM sequence and base pair differences. (B) Background subtracted fluorescence time courses of Cas12a preassembled with gRNA's targeting *S. salar* and *S. trutta* in the presence of recombinant plasmids containing a *S. salar* or *S. trutta* DNA insert and 50 nM ssDNA-FQ reporter. Fluorescence measurements were taken every 30 sec for 120 min at 37 °C (λex = 485 nm, λem = 535 nm). Error bars are mean ± standard deviation, where n = 3. Fluorescence detection is only seen when the gRNA complements the target sequence (i.e *S. salar* gRNA in presence of *S. salar* recombinant plasmid). No fluorescence detection is observed when the gRNA does not complement the target sequence.

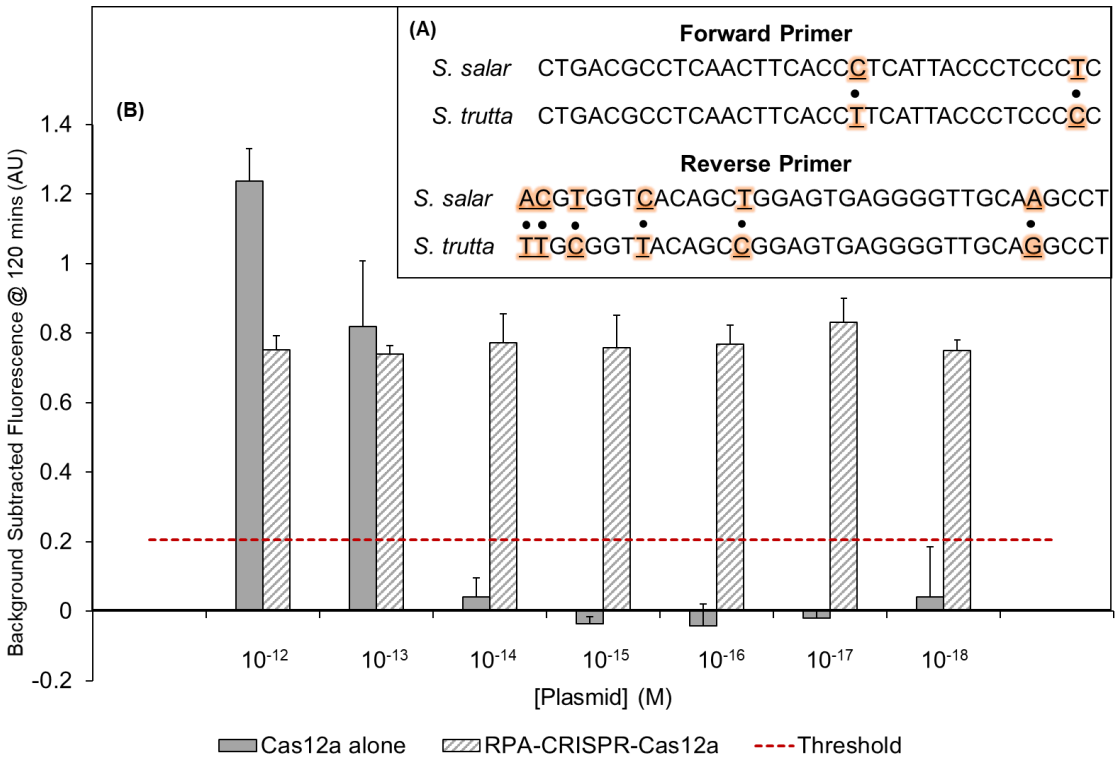

Figure 4.8 Sensitivity of *S. salar* specific CRISPR-Cas12a version 1 using ND2 recombinant plasmids. (A) Alignment of *S. salar* RPA primers showing base pair differences with *S. trutta*. (B) Dilution series of *S. salar* ND2 recombinant plasmid DNA detected with *S. salar* targeting CRISPR-Cas12a alone (without pre-amplification of target DNA) and with RPA-CRISPR-Cas12a. Background subtracted fluorescence reported after 120 min incubation at 37 °C (ƛex = 485 nm, ƛem = 535 nm). Error bars are mean ± standard deviation, where n = 3. Threshold value is 3 x standard deviation of background fluorescence (samples with no DNA template added). Alone, CRISPR-Cas12a shows detection above background at 10^{-13} M while coupling CRISPR-Cas12a to RPA achieved attomolar sensitivity, detecting down to 10^{-18} M.

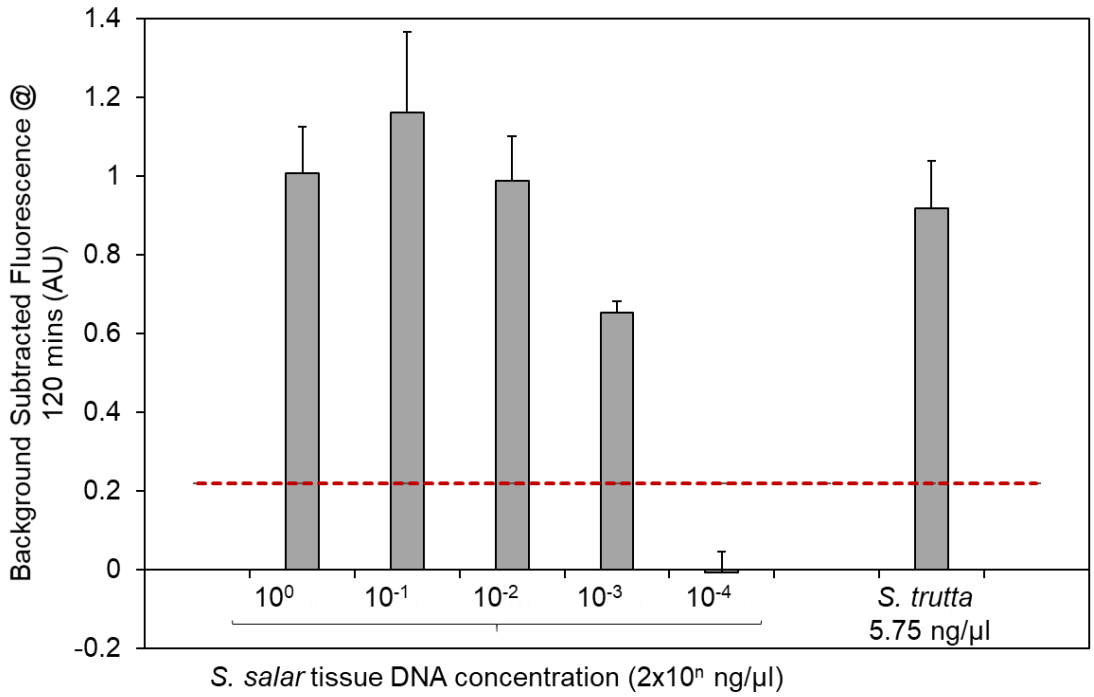

Figure 4.9 Sensitivity and specificity of *S. salar* targeting RPA-CRISPR-Cas12a version 1 assay in whole genomic context. RPA coupled to CRISPR-Cas12a detection was applied to a dilution series of DNA extracted from *S. salar* tissue (2 – 2 x 10^{-4} ng/µL) and DNA extracted from *S. trutta* tissue (5.75 ng/µL). Background subtracted fluorescence reported after 120 min incubation at 37 °C (ƛex = 485 nm, ƛem = 535 nm). Error bars are mean ± standard deviation, where n = 3. Threshold value is 3 x standard deviation of background fluorescence (samples with no DNA template added). DNA from *S. salar* tissue extract detected down to a concentration of 2 pg/µL, however non-specific detection of *S. trutta* DNA also seen.

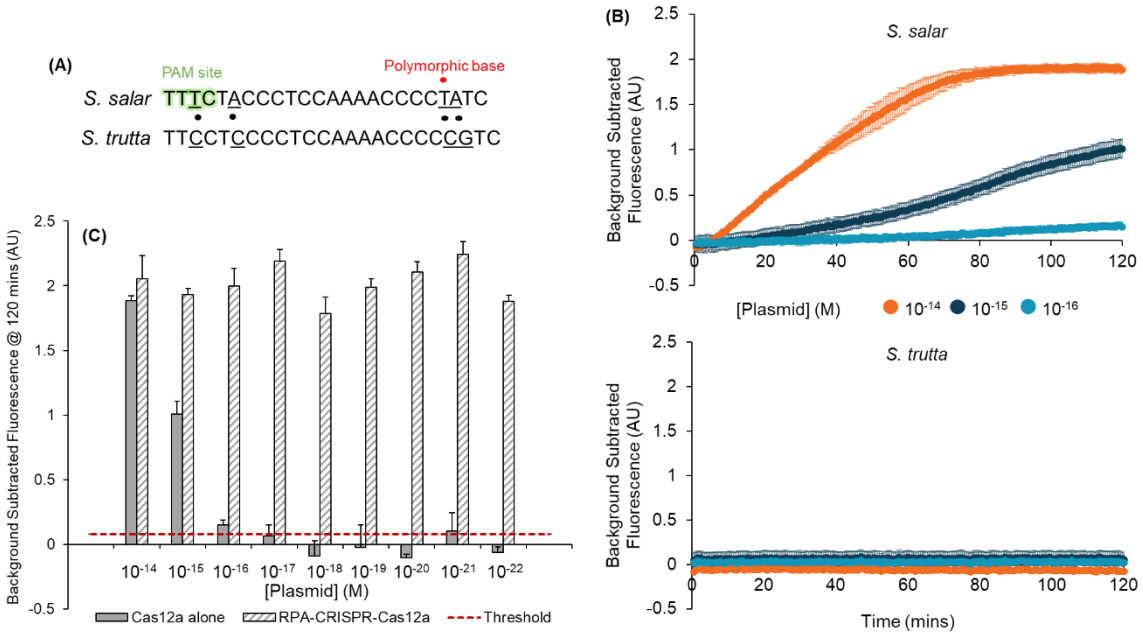

Figure 4.10 Distinguishing *S. salar* and *S. trutta* ND5 recombinant sequences using CRISPR-Cas12a. (A) Alignment of gRNA targeting site in *S. salar* and *S. trutta* showing PAM sequence presence only in *S. salar* sequence, base pair differences and polymorphic bases. (B) Background subtracted fluorescence time course of Cas12a preassembled with a gRNA targeting *S. salar* in the presence of a recombinant plasmid containing a *S. salar* or *S. trutta* ND5 DNA insert and 50 nM ssDNA-FQ reporter. Fluorescence measurements were taken every 30 sec for 120 min at 37°C (λex = 485 nm, λem = 535 nm). Error bars are mean ± standard deviation, where n = 3. Successful detection only seen when gRNA is complementary to target sequence. (C) Dilution series of *S. salar* recombinant plasmid detected with *S. salar* targeting CRISPR-Cas12a alone (without pre-amplification of target DNA) and with RPA-CRISPR-Cas12a. Background subtracted fluorescence reported after 120 min incubation at 37 °C. Error bars are mean ± standard deviation, where n = 3. Threshold value is 3 x standard deviation of background fluorescence (samples with no DNA template added). Alone, Cas12a shows detection above background at 10^{-15} M while coupling CRISPR-Cas12a to RPA achieved zeptomolar sensitivity, detecting down to 10^{-22} M.

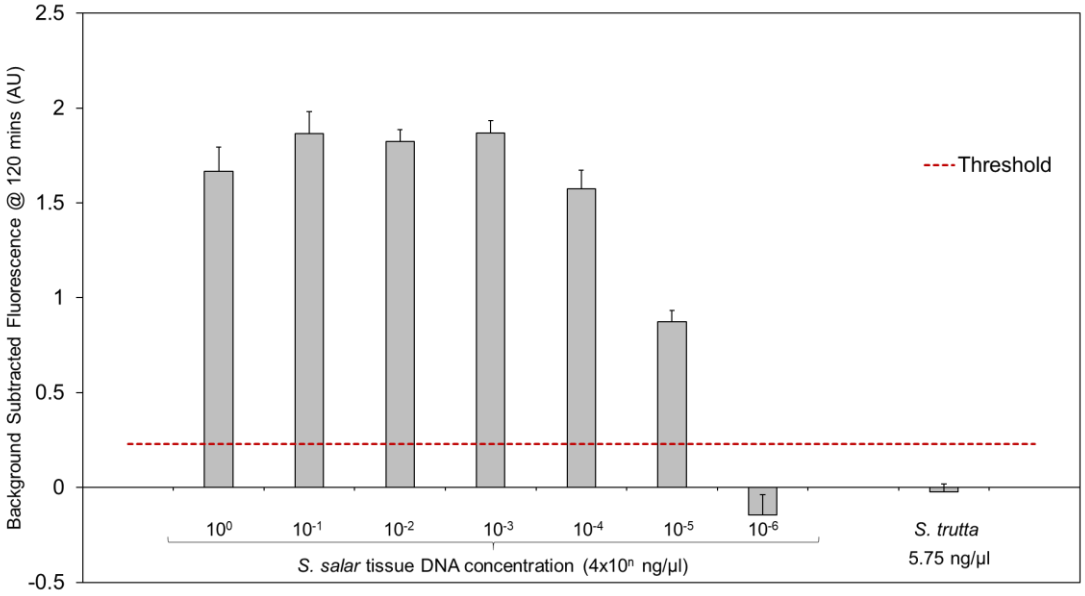

Figure 4.11 Sensitivity and specificity of *S. salar* targeting RPA-CRISPR-Cas12a version 2 assay in whole genomic context. Dilution series of DNA extracted from *S. salar* tissue (4 - 4 x 10^{-6} ng/µL) and DNA extracted from *S. trutta* tissue (5.75 ng/µL). Background subtracted fluorescence reported after 120 min incubation at 37 °C (ƛex = 485 nm, ƛem = 535 nm). Error bars are mean ± standard deviation, where n = 3. Threshold value is 3 x standard deviation of background fluorescence (samples with no DNA template added). *S. salar* was successfully detected down to a concentration of 0.04 pg/µL and no detection of *S. trutta* was observed.

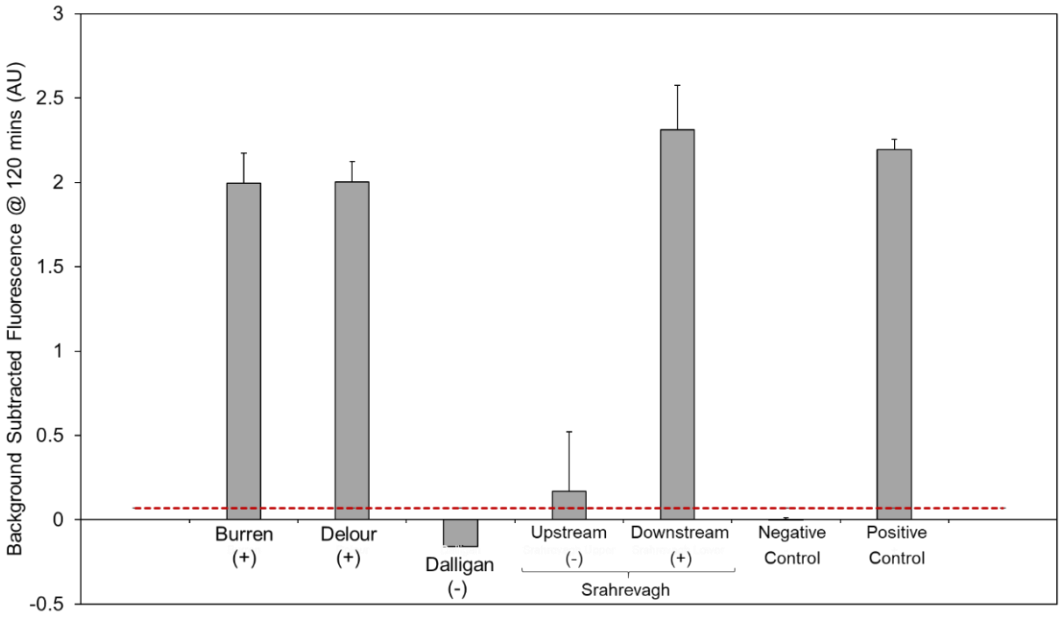

Figure 4.12 Field validation of *S. salar* specific RPA-CRISPR-Cas12a version 2 from Irish freshwater samples. Background subtracted fluorescence reported after 120 min incubation at 37 °C (λex = 485 nm, λem = 535 nm). Error bars are mean ± standard deviation, where n = 3. Threshold value is 3 x standard deviation of background fluorescence (samples with no DNA template added). Positive control: *S. salar* DNA from tissue extract. Negative control: no DNA template added. (+) *S. salar* confirmed present by electrofishing surveys and qPCR. (-) *S. salar* confirmed absent by electrofishing and qPCR. *S. salar* was detected in the Burren, Delour and downstream Srahrevagh samples, but was not detected in the Dalligan and upstream Srahrevagh samples using RPA-CRISPR-Cas12a approach. Note: *S. trutta* was present in all samples but not detected.

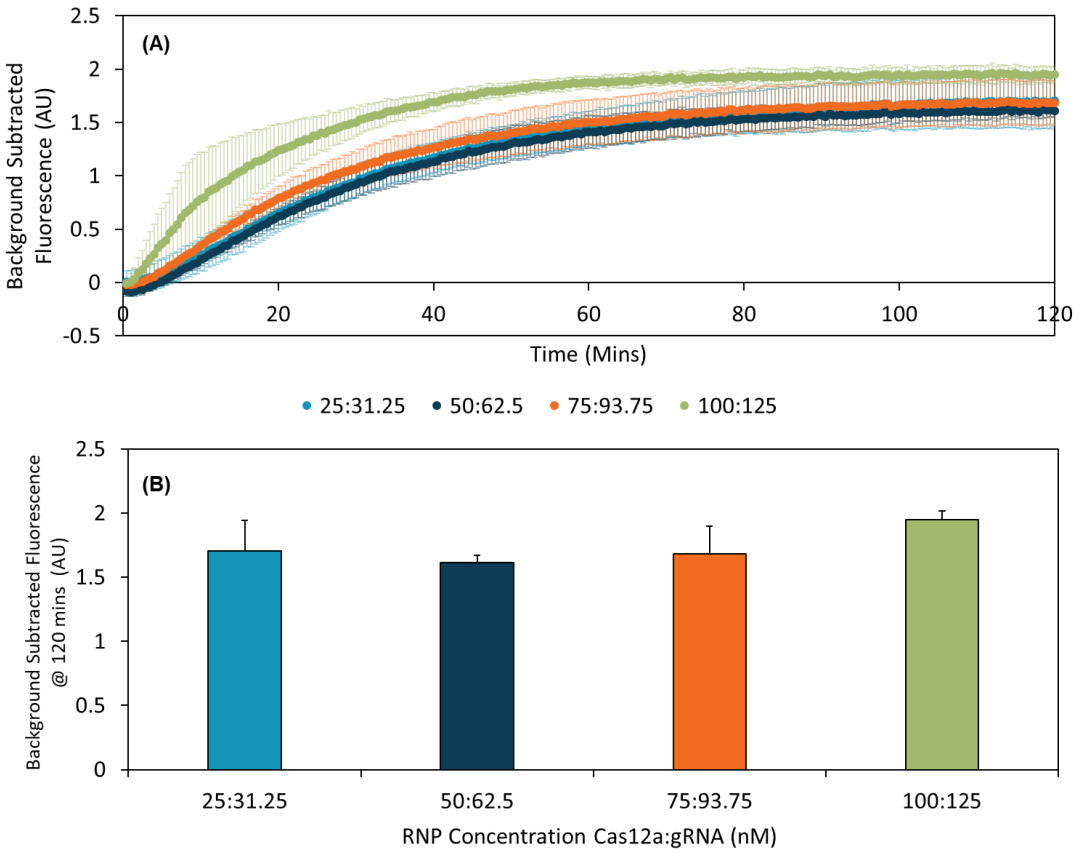

Figure 4.13 Optimisation of Cas12a and gRNA concentration in RNP. Varying concentrations of Cas12a:gRNA (nM) were tested on the CRISPR-Cas stage of the two-step RPA-CRISPR-Cas *S. salar* assay. RPA product using 0.5 ng/µL *S. salar* DNA isolated from tissue was used in all reactions. Error bars are mean ± standard deviation, where n = 3. (A) Time course of background subtracted fluorescence measured every 30 sec for 120 min at 37 °C (λex = 485 nm, λem = 535 nm). (B) Background subtracted fluorescence reported after 120 min incubation at 37 °C. No major difference between concentrations is observed and thus a concentration of 50:62.5 nM Cas12a:gRNA was used for future experiments.

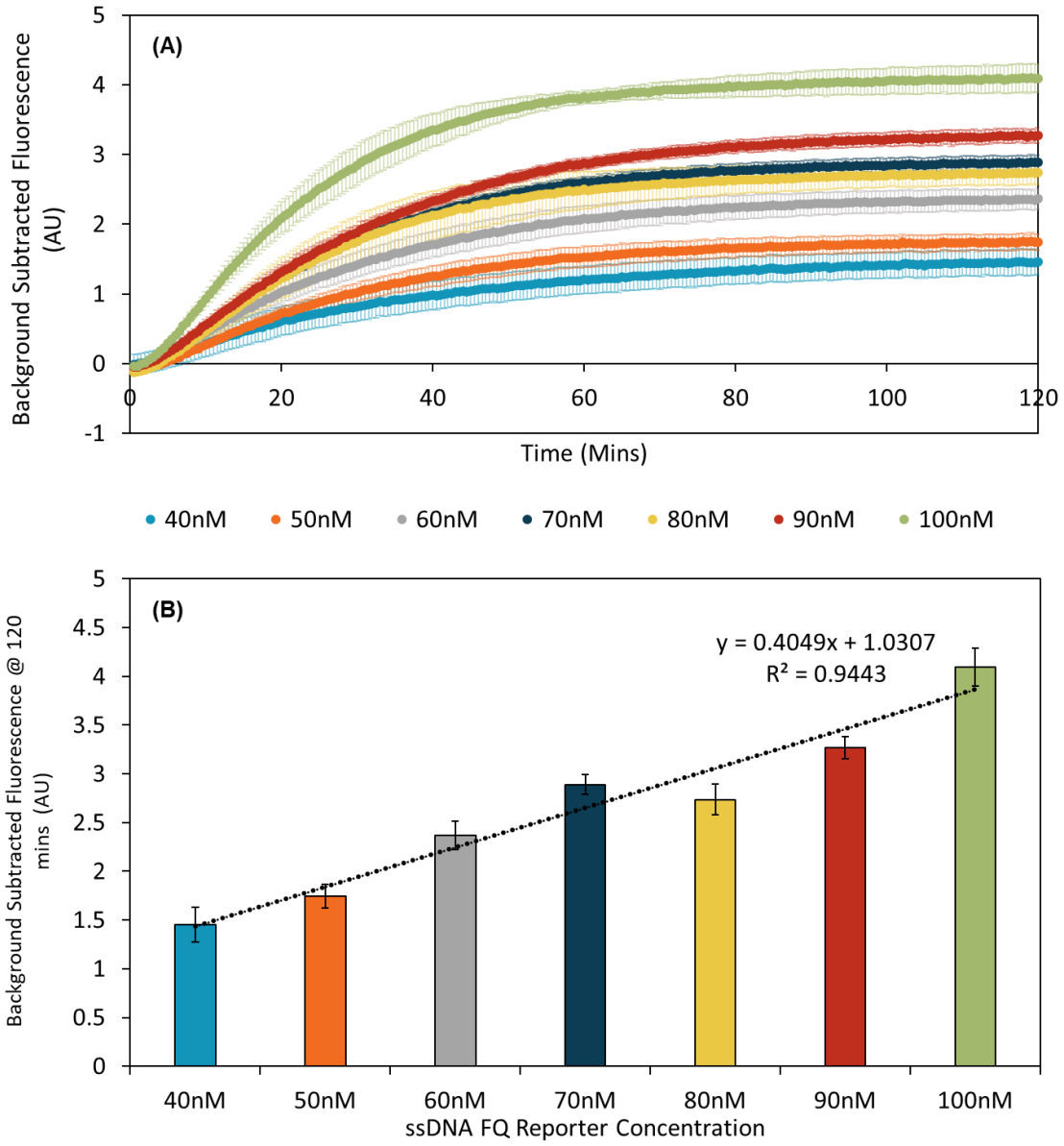

Figure 4.14 Optimisation of ssDNA-FQ reporter molecule concentration. Varying concentrations of ssDNA-FQ reporter, from 40 nM to 100 nM, were used for the CRISPR-Cas stage of the two-step RPA-CRISPR-Cas *S. salar* assay. RPA product using 0.5 ng/µL *S. salar* DNA isolated from tissue was used in all reactions. Error bars are mean ± standard deviation, where n = 3. (A) Fluorescence time course with measurements taken every 30 sec for 120 min at 37 °C (ƛex = 485 nm, ƛem = 535 nm). (B) Background subtracted fluorescence reported after 120 min incubation at 37 °C. Linear trend line shows a non-proportional response between ssDNA-FQ reporter concentration and background subtracted fluorescence. A concentration of 100 nM was selected as optimal.

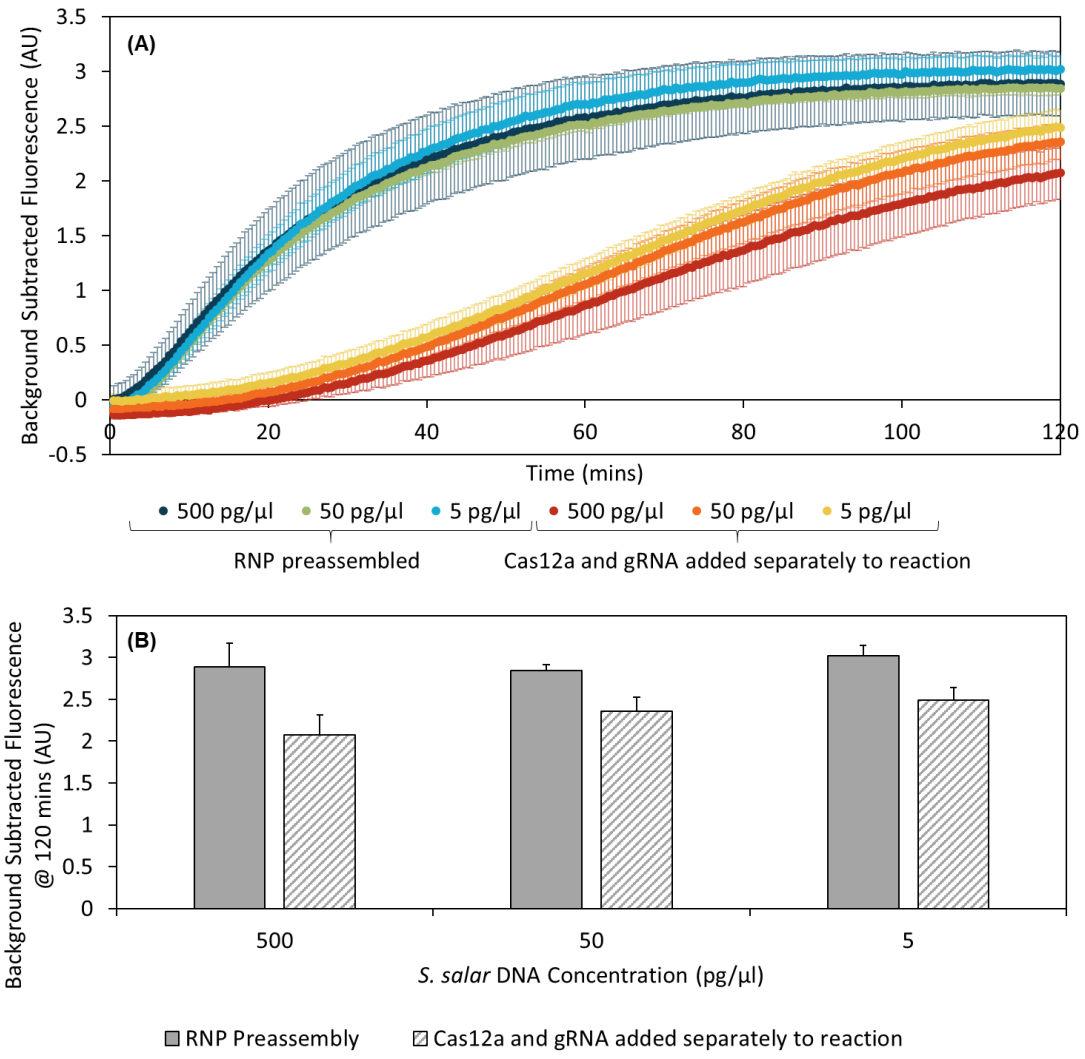

Figure 4.15 Necessity of RNP preassembly in the CRISPR-Cas step of the two-step RPA-CRISPR-Cas reaction. A final concentration of 50:62.5 nM Cas12a:gRNA was used in all reactions. This was either preassembled as an RNP via a 20 min incubation in PBS, or added directly into the reaction mix. RPA product using 500, 50 and 5 pg/µL *S. salar* DNA isolated from tissue was used. Error bars are mean ± standard deviation, where n = 3. (A) Time course of background subtracted fluorescence, with measurements taken every 30 sec for 120 min at 37 °C (λex = 485 nm, λem = 535 nm). (B) Background subtracted fluorescence reported after 120 min incubation at 37 °C. Although there is little difference in end-point fluorescence following 120 min incubation, preassembling the RNP speeds up fluorescence acquisition, with a fluorescent plateau reached sooner than when the Cas12a and gRNA are added separately to the reaction.

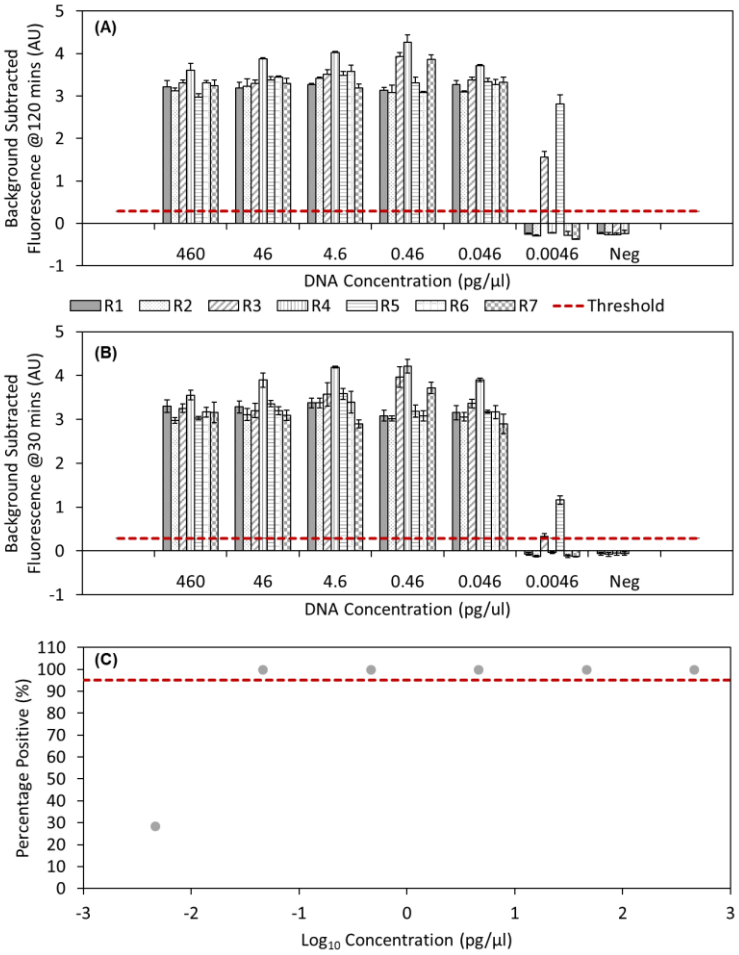

Figure 4.16 Sensitivity of *S. salar* specific RPA-CRISPR-Cas12a version 2 detection assay. RPA amplified *S. salar* DNA ranging from 460 – 0.0046 pg/µL was incubated for 120 min at 37 °C, with fluorescence measurements taken every 30 sec (λex = 485 nm, λem = 535 nm). Error bars are mean fluorescence ± standard deviation, where n = 3. Threshold value is 10 x standard deviation of background fluorescence (samples with no DNA template added). Neg refers to negative control whereby no DNA template was added to RPA reaction. (A) End-point background subtracted fluorescence reported after 120 min incubation. (B) End-point background subtracted fluorescence reported following 30 min incubation. (C) Percentage of positive samples (where n = 7) against log DNA concentration of sample. Percentage positive refers to successful detection of target DNA whereby background subtracted fluorescence is greater than the threshold value. LOD is defined as the concentration that produces at least 95% positive replicates. The red dotted line in (C) indicates this 95% cut off. *S. salar* specific RPA-CRISPR-Cas LOD estimated as 0.046 pg/µL.

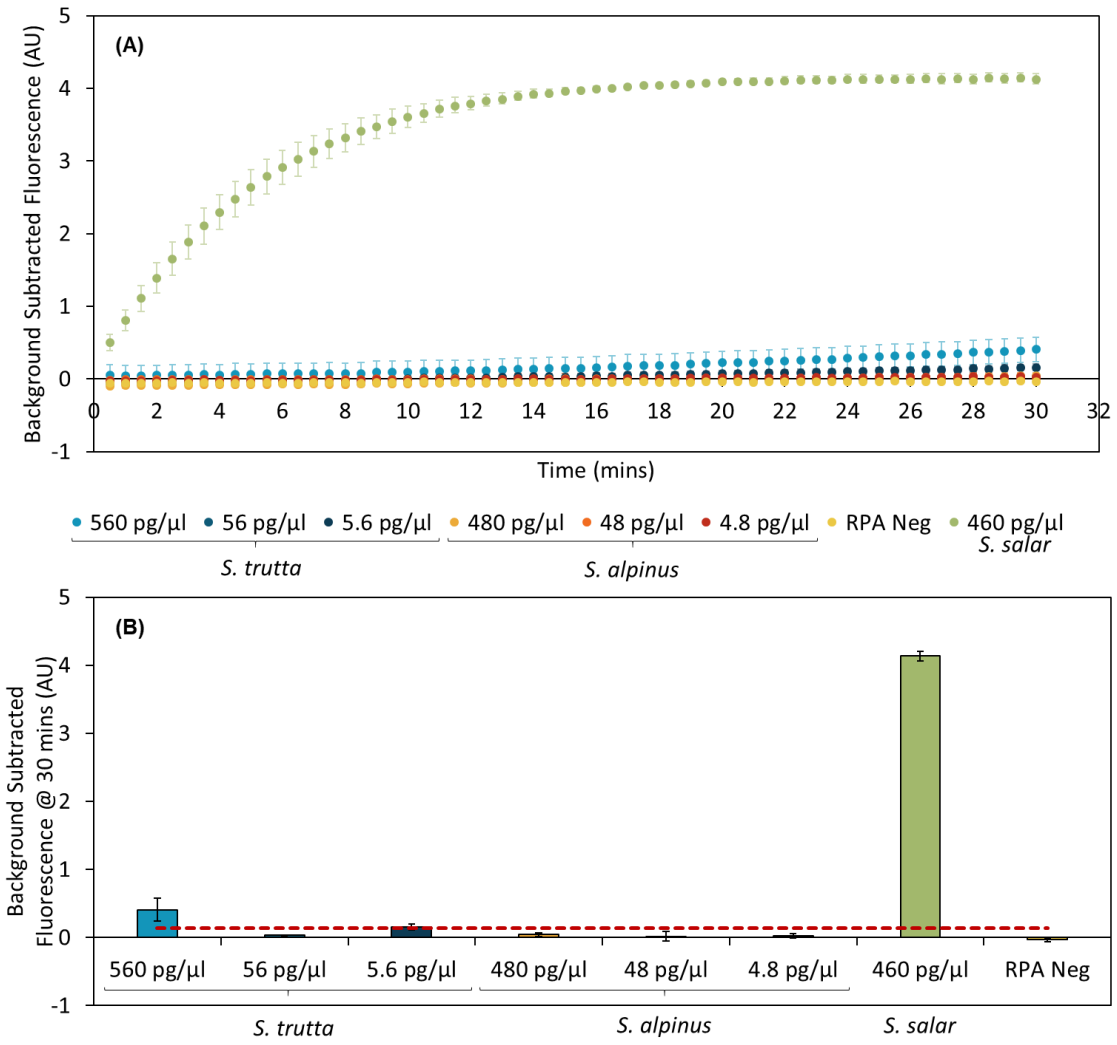

Figure 4.17 Specificity of *S. salar* RPA-CRISPR-Cas12a version 2 detection assay. (A) Time course of background subtracted fluorescence with measurements taken every 30 sec for 30 min at 37 °C (λex = 485 nm, λem = 535 nm). (B) Background subtracted fluorescence reported after 30 min incubation at 37 °C. Error bars are mean ± standard deviation, where n = 3. Threshold value is 10 x standard deviation of background fluorescence (samples with no DNA template added). RPA Neg refers to negative control whereby no DNA template was added to RPA reaction. Non-target detection seen above the threshold with 560 pg/µL of *S. trutta* DNA.

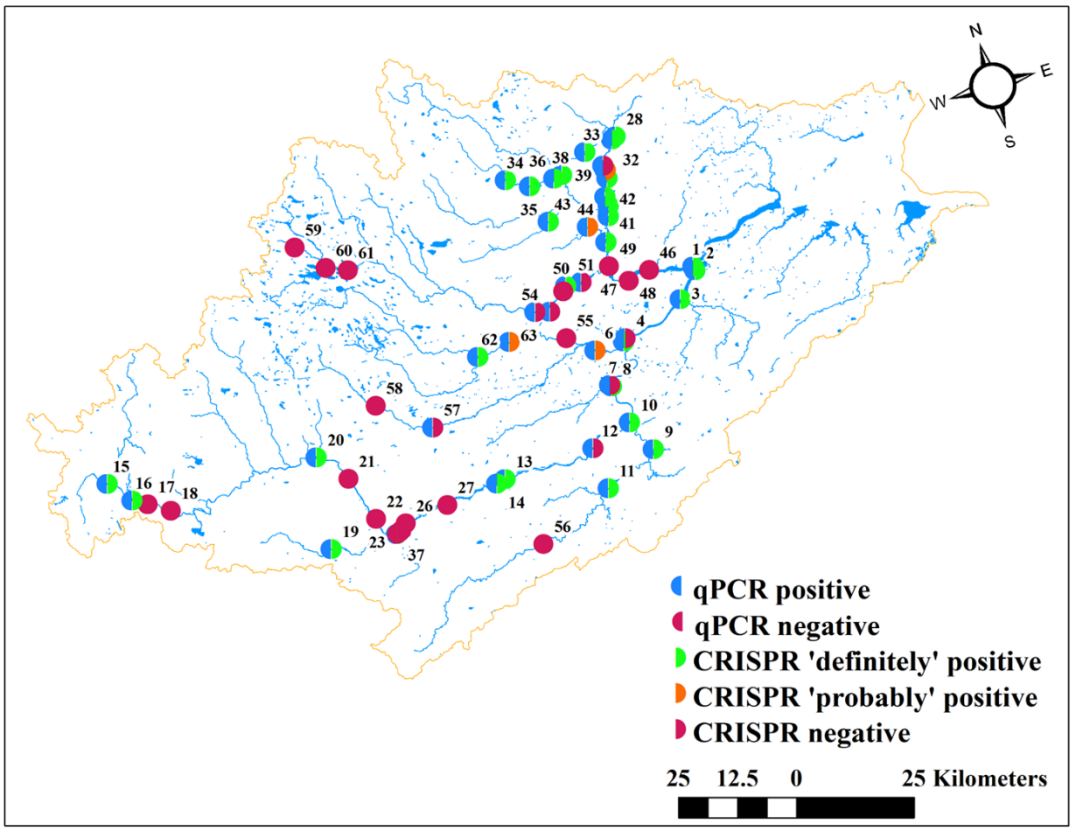

Figure 4.18 *S. salar* detection using RPA-CRISPR-Cas12a and qPCR in the Miramichi Watershed. Dots represent the sampling sites. Magenta shading is negative detection, blue shading is positive qPCR detection, green shading is positive CRISPR detection above the stringent criteria whereby at least 2 out of 3 replicates were positive and orange shading is positive CRISPR detection above the relaxed criteria whereby 1 out of 3 replicates were positive.

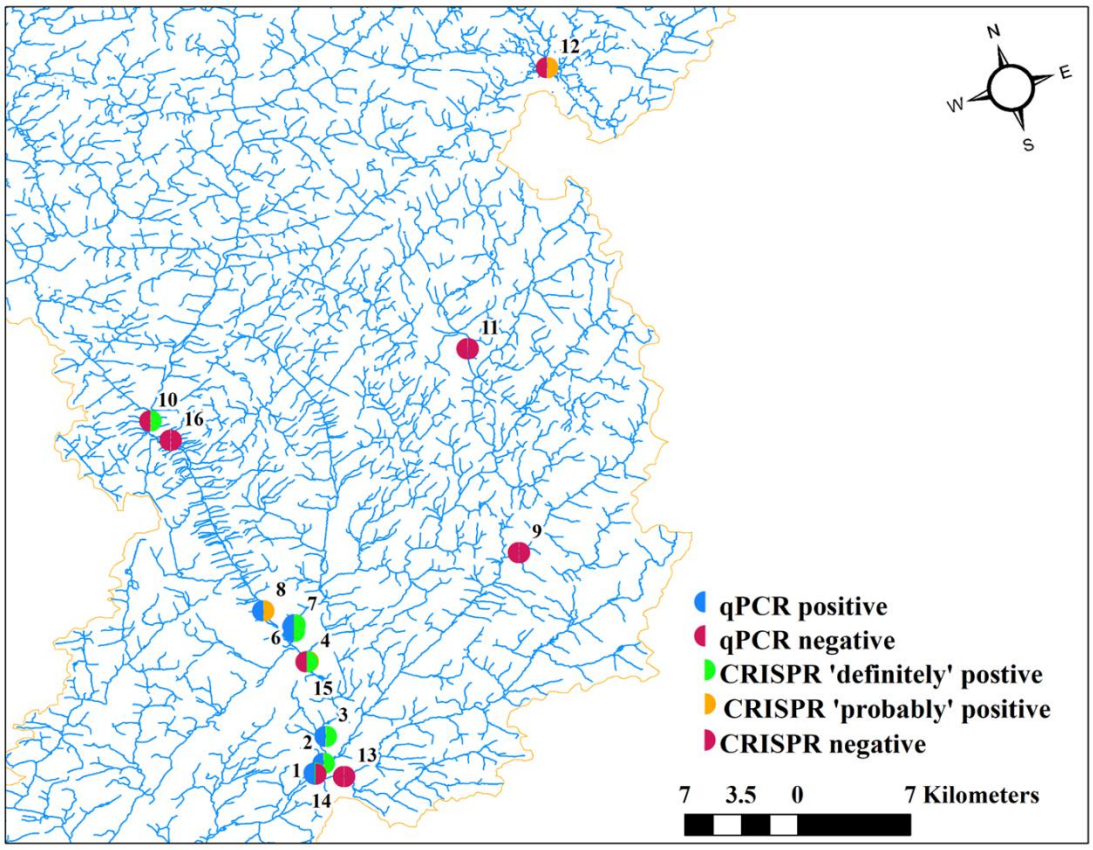

Figure 4.19 *S. salar* detection using RPA-CRISPR-Cas12a and qPCR in the Jacques-Cartier Watershed. Dots represent the sampling sites. Magenta shading is negative detection, blue shading is positive qPCR detection, green shading is positive CRISPR detection above the stringent criteria whereby at least 2 out of 3 replicates were positive and orange shading is positive CRISPR detection above the relaxed criteria whereby 1 out of 3 replicates were positive.

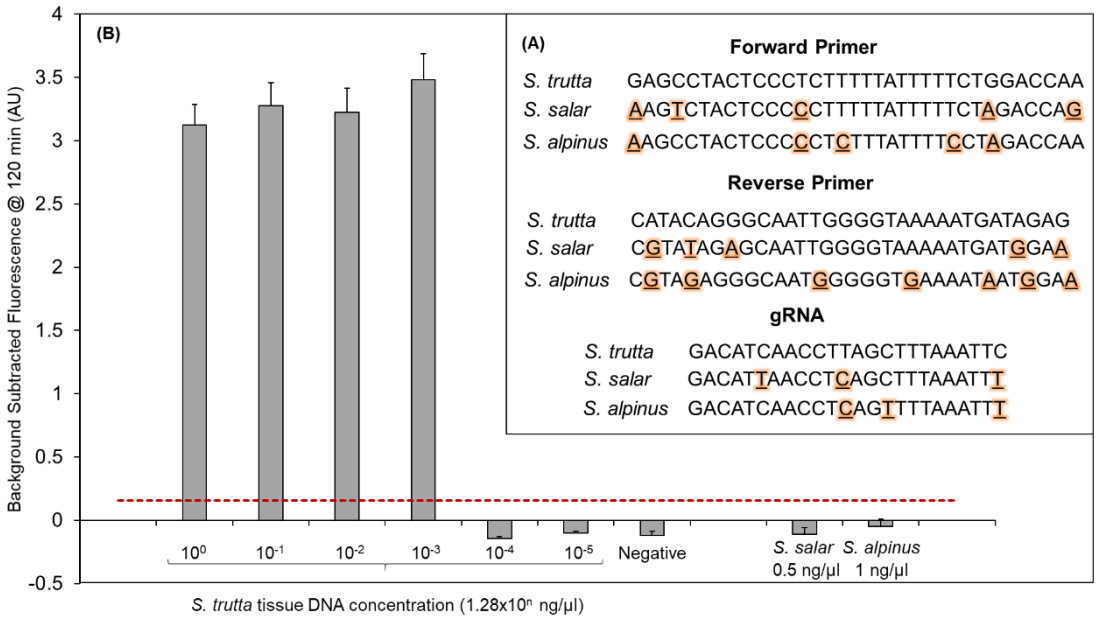

Figure 4.20 Sensitivity and specificity of *S. trutta* targeting RPA-CRISPR-Cas12a assay in whole genomic context. (A) Alignment of gRNA and primer binding sites in *S. trutta, S. salar* and *S. alpinus,* showing base pair differences. (B) Dilution series of DNA extracted from *S. trutta* tissue (1.28 – 1.28 x 10^{-5} ng/µL) and DNA extracted from *S. salar* tissue (0.5 ng/µL) and *S. alpinus* tissue (1 ng/µL). Background subtracted fluorescence reported after 120 min incubation at 37 °C (λex = 485 nm, λem = 535 nm). Error bars are mean ± standard deviation, where n = 3. Threshold value is 3 x standard deviation of background fluorescence (samples with no DNA template added). *S. trutta* was detected down to a concentration of 1.28 pg/µL and importantly showed no detection of the other salmonid species.

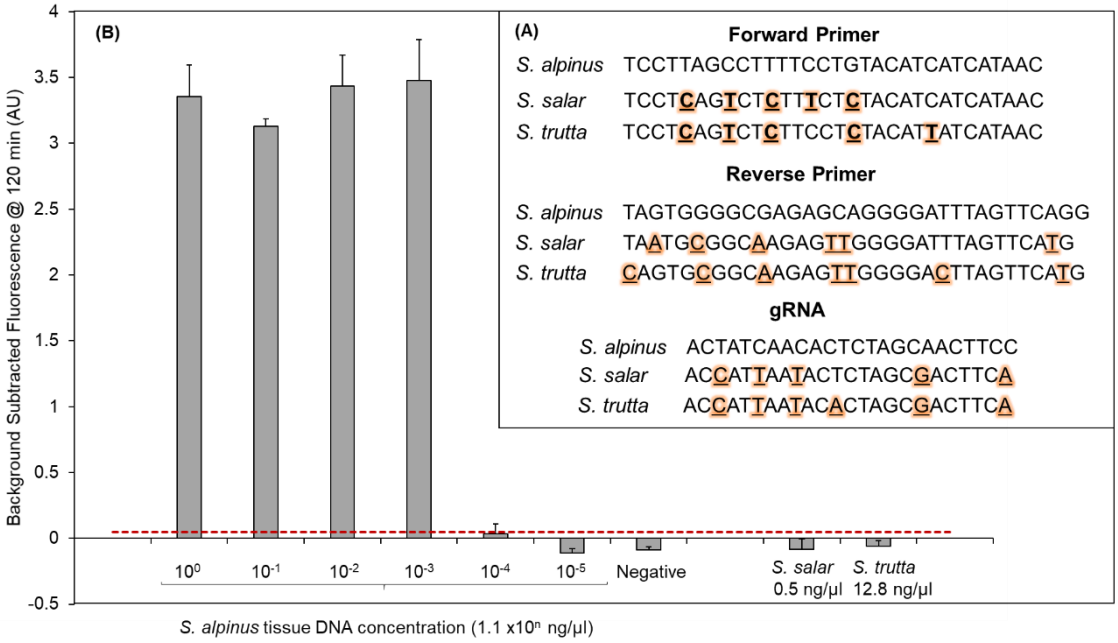

Figure 4.21 Sensitivity and specificity of *S. alpinus* targeting RPA-CRISPR-Cas12a assay in whole genomic context. (A) Alignment of gRNA and primer binding sites in *S. alpinus, S. salar* and *S. trutta,* showing base pair differences. (B) Dilution series of DNA extracted from *S. alpinus* tissue (1.1 – 1.1 x 10^{-5} ng/µL) and DNA extracted from *S. salar* tissue (0.5 ng/µL) and *S. trutta* tissue (12.8 ng/µL). Background subtracted fluorescence reported after 120 min incubation at 37 °C (ƛex = 485 nm, ƛem = 535 nm). Error bars are mean ± standard deviation, where n = 3. Threshold value is 3 x standard deviation of background fluorescence (samples with no DNA template added). *S. alpinus* detected down to a concentration of 1.1 pg/µL and importantly showed no detection of the other salmonid species.

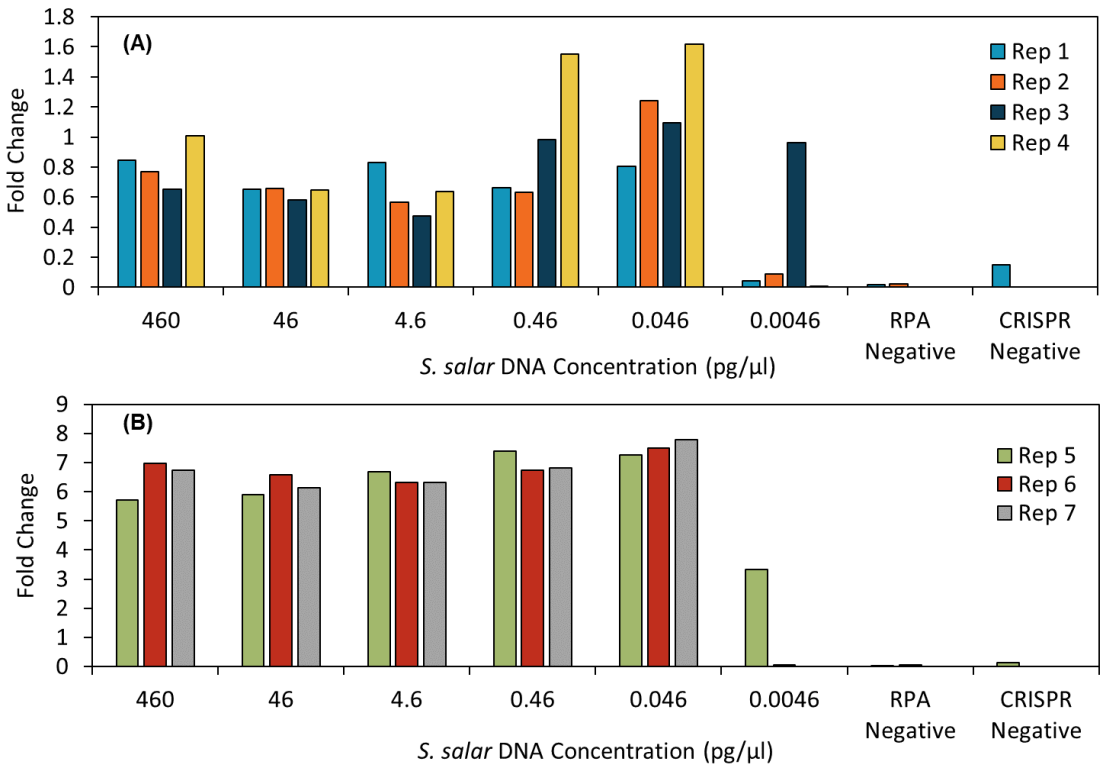

Figure 4.22 Sensitivity of *S. salar* specific RPA-CRISPR-Cas12a version 2 detection assay reanalysed using fold-change as an alternative data analysis method. Fold-change fluorescence of RPA amplified *S. salar* DNA ranging from 460 – 0.0046 pg/µL. Samples were incubated for 30 min at 37 °C. Fold-change values were calculated using fluorescence values (ƛex = 485 nm, ƛem = 535 nm) measured at 30 sec and 30 min. RPA Negative refers to no template being added to the RPA stage of the method, whilst CRISPR Negative contained molecular grade water instead of RPA product at the CRISPR detection stage of the protocol. (A) RPA replicates 1-4 run on one 96-well plate with delayed start. (B) RPA replicates 5-7 run on a 96-well plate with immediate start. Successful detection of *S. salar* seen down to a concentration of 0.046 pg/µL in all replicates.

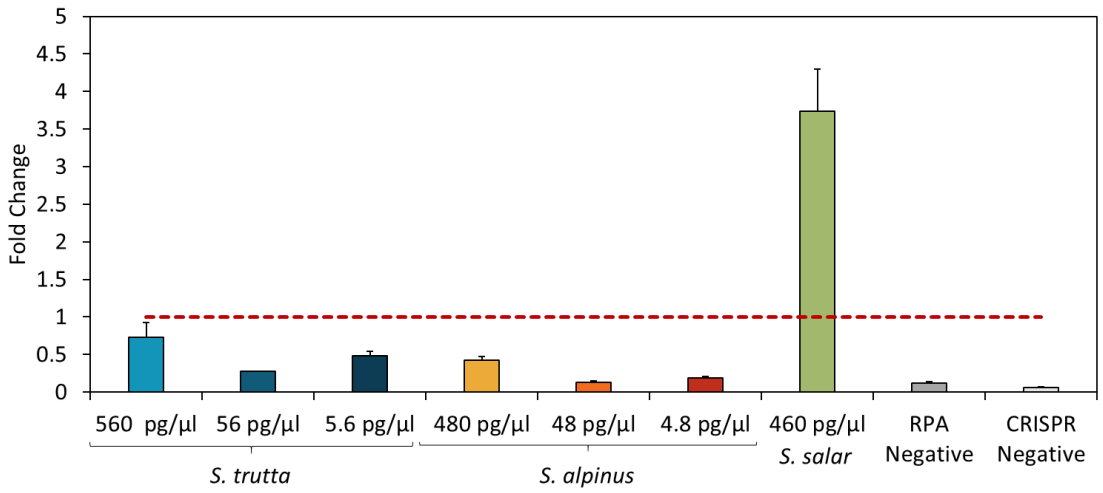

Figure 4.23 Specificity of *S. salar* targeting RPA-CRISPR-Cas12a detection assay reanalysed using fold-change as an alternative data analysis method. Samples were incubated for 30 min at 37 °C. Fold-change values were calculated using fluorescence values (λex = 485 nm, λem = 535 nm) measured at 30 sec and 30 min. Error bars are mean fold-change ± fold-change standard deviation, where n = 3. RPA Negative refers to no template being added to the RPA stage of the method, whilst CRISPR Negative contained molecular grade water instead of RPA product at the CRISPR detection stage of the protocol. A fold-change threshold of 1 was used, with only values above this considered positive. Detection above the threshold is only seen for *S. salar,* with no detection above the threshold for *S. trutta* and *S. alpinus.*

Chapter 5. Moving from the lab into the field: Fluorescence and lateral flow approaches to RPA-CRISPR-Cas12a detection of *Salmo salar.*

5.1. Introduction

5.1.1. Overview

The development of a portable biosensor device would enable rapid, on-site monitoring of species of interest using environmental DNA. As stated in Chapter 1.4, the vision for such a sensor involves developing a system that can be used at multiple sampling sites. This specification relies on minimal sampling handling whilst maintaining the high levels of sensitivity and target specificity seen with laboratory-based instrumentation. Ideally, the device should have the minimum number of steps required, operate at low temperatures and use an optical transducer. The RPA-CRISPR-Cas method adapted for *S. salar* detection (Chapter 4) is highly amenable to this development and has been used in the medical field to improve POC devices for rapid disease diagnostics (van Dongen *et al.*, 2020). In this chapter, several steps are made towards this vision. Firstly, the simplification from a two-step assay to a single reaction is assessed in order to reduce the current amount of sample handling. Secondly, two existing sensing platforms, fluorescence (ColiSense) and colorimetric (lateral flow) are adapted for *S. salar* detection. Both platforms display great potential for environmental DNA applications and progress the field towards on-site monitoring.

5.1.2. CRISPR-Cas POC devices

The CRISPR-Cas revolution has resulted in new nucleic acid detection methodologies, which combine the sensitivity and specificity of established methods with the speed and cost effectiveness of isothermal methods (as discussed in Chapter 4.1). Several papers have reviewed the applicability of CRISPR-Cas for nucleic acid sensing (Zhou *et al.*, 2018; Li *et al.*, 2019; Aman *et al.*, 2020) and its potential use in multiple applications such as the detection of pathogens from humans, animals and plants (Aman *et al.*, 2020). It is of no surprise that this includes advances in POC diagnostics (discussed in Chapter 1.4.2.1), applying CRISPR-Cas methodologies to on-site detection of pathogens and disease, as reviewed thoroughly in van Dongen *et al.,* (2020).

Developed devices have utilised type V (Cas12a) and type VI (Cas13a) CRISPR systems (van Dongen *et al.*, 2020) as the biological "sensing" element of the biosensor coupled to different read-out methods, primarily fluorescence and colorimetric (Table 5.1). As discussed in Chapter 4.1.3, these CRISPR systems display collateral cleavage activity of single stranded nucleotides upon target recognition (Gootenberg *et al.*, 2017; Chen *et al.*, 2018), enabling their use in nucleic acid sensing. Although still in the early stages of research, these systems highlight the potential of Point-of-care Testing (POCT) using CRISPR-Cas diagnostics (Figure 5.1).

5.1.2.1. Fluorescence based CRISPR-Cas devices

The original CRISPR-Cas sensing systems, such as SHERLOCK (Gootenberg *et al.*, 2017) and DETECTR (Chen *et al.*, 2018), utilised fluorescence signal amplification due to collateral cleavage of single stranded DNA fluorophore-quencher (ssDNA-FQ) reporters by an RNP upon target recognition. The miniaturisation of fluorometers allows these methods to be readily adapted to point-of-use detection, but with several drawbacks which prevent them being fully effective as POC devices. These include the numerous manual pipetting steps, the necessity of nucleotide amplification and the associated cost and storage of large reagent volumes. These limitations, although manageable in a laboratory-based setting, hinder the user-friendliness and cost effectiveness desired for POCT.

To address these concerns, Katzmeier *et al.,* (2019) developed a low cost, pocked sized fluorescence detector with assays conducted on filter paper. Synthetic RNA was used as the substrate for a CRISPR-Cas13a assay showing a rapid increased in fluorescence signal upon target recognition. Although promising, the developed device took longer to reach maximum fluorescence and had higher LOD when compared to an in-solution assay measured on a commercial plate reader (Katzmeier *et al.*, 2019). This is common in POC devices, which require a delicate trade-off between cost and sensitivity of detection.

He *et al.*, (2020) developed a Cas12a based fluorometer that enabled detection of the DNA-based virus African swine fever virus (ASFV). Within 120 min, a detection limit of 1 pM of pre-treated DNA is reported, which improved to 100 fM after a 24-hour incubation. This amplification-free system required incubation in a water-bath prior to sample addition onto an 80-well disposable cartridge, enabling high-throughput processing. This system shows huge potential for rapid detection of ASFV, nonetheless it still involves pre-treatment of sample to purify target DNA and requires trained personnel to add reagents to the cartridge.

Ideally, POC devices for pathogen detection should allow analysis directly from the unprocessed sample, in many cases from blood. Qian *et al.*, (2020) developed a platform that enables rapid detection of ASFV directly from pig's blood with visualisation by the naked eye. Their system used a target specific LAMP assay to amplify ASFV directly from an unprocessed blood sample. This was coupled to a dehydrated CRISPR-Cas assay, whereby CRISPR reagents were stabilised with 2% trehalose and 10% pullulan and dehydrated into a small film sheet (Qian *et al.*, 2020). This film was placed in the lid of a PCR tube and once dissolved, enabled reagent addition into the LAMP amplified product. Promisingly, the assay showed successful detection of ASFV directly from blood; however, at low concentrations the difference between negative and positive results could be misinterpreted (Qian *et al.*, 2020).

5.1.2.2. Colorimetric based CRISPR-Cas devices

Colorimetric devices are also optical sensors. They measure a colour change in the presence of target analytes and are common in POC diagnostics due to their ease of use and relatively low cost (van Dongen *et al.*, 2020). Simple, one-pot CRISPR-Cas reactions with colorimetric visualisation have shown suitability for plasmid template detection. Wang *et al.*, (2019) developed Cas12aVDet, a method consisting of spatially separated RPA reaction and CRISPR-Cas detection. Centrifugation was used to incorporate the Cas12a nuclease after a 15 min incubation of the RPA reaction, reporter and gRNA molecules. Bright green fluorescence signals, indicative of target presence, were

observed with a blue light imager. Using this method, they report successful detection down to a target DNA concentration of 10^1 aM, a sensitivity comparable to the DETECTR method (Wang *et al.*, 2019).

5.1.2.2.1. Nanoparticles

Colorimetric detection devices may also use nanoparticles to allow by eye visualisation. The use of gold nanoparticles (AuNPs) is a well-described method established by Elghanian *et al.*, (1997). It is a relatively simple and inexpensive detection format that relies on a change in optical properties based on aggregation and dispersion of AuNPs (Elghanian *et al.*, 1997). When aggregation occurs, there is a shift in absorption peak, causing a colour change from red to purple. For sequence specific gene detection, DNA probes can be attached to the AuNPs allowing capture, subsequent aggregation of AuNPs and thus detection of target sequence (Deng *et al.*, 2012). However, although a proven effective method of detection, using AuNp-DNA probes has several limitations. DNA probes are not universal. They must be redesigned and conjugated to new AuNPs for every assay, increasing the cost and time associated with assay optimisation. In addition, assays commonly rely on a red to purple colour change, which may be very subtle if the DNA target concentration is low resulting in a low signal to noise ratio (van Dongen *et al.*, 2020).

The CRISPR-Cas assay developed by Yuan *et al.*, (2020), circumvents some of these issues by using an RNP complex for target recognition and AuNPs for signal amplification. In this platform, universal AuNP-DNA probes were designed to hybridise to linker ssDNA or ssRNA molecules, which in turn cause aggregation of AuNPs and a visible colour change (Yuan *et al.*, 2020). These linker molecules also act as the *trans*-cleavage substrates for Cas12a and Cas13a nucleases. In the absence of the nucleic acid target, the linker sequences remain intact, enabling AuNP aggregation. However, upon detection of target sequence, Cas12a or Cas13a RNP complexes present in the reaction, will collaterally cleave the linker sequences. This prevents the AuNP-DNA probes from hybridising resulting in dispersal and no colour change (Figure 5.2). Unlike a typical

AuNP-DNA probe colorimetric assay, nucleic acid linker sequences and AuNP-DNA probes are universal, remaining the same regardless of the target sequence (Yuan *et al.*, 2020).

Platinum nanoparticles (PtNPs) have also been used to develop CRISPR-Cas colorimetric assays. The volumetric bar chart chip (MAV-chip) developed by Shao *et al.*, (2019) uses PtNPs tethered to a magnetic bead by a single stranded DNA molecule. Upon target recognition by a Cas12a RNP, this ssDNA tether is cleaved, releasing the PtNPs that move to a secondary chamber and catalyse the reaction of hydrogen peroxide to oxygen. This reaction creates a build-up of pressure in the secondary chamber, forcing a detection ink into the readout channel and allowing visualisation of positive detection. The advancements of the detection ink, resulting from the generated oxygen gas, indicate the amount of DNA target in the initial reaction. If no target is present, the PtNPs stay tethered to the magnetic beads in the first channel and no readout is seen (Shao *et al.*, 2019). This system has the potential for multiplexing by increasing the number of parallel chambers, however is limited in that it requires skilled personnel to load reagents and operate the device.

5.1.2.2.2. Lateral flow assays

By far the most popular colorimetric systems for CRISPR-Cas based POC diagnostics are lateral flow assays (LFAs). These assays, known for their wide applicability in protein and antibody sensing, have been readily adapted to nucleic acid analysis and gene identification (Mao *et al.*, 2009). LFAs have major advantages for POCT due to their easy read-out with the naked eye, leading to an increase in their development despite drawbacks including lack of efficiency and accuracy (Kasetsirikul *et al.*, 2020). LFAs for gene identification have previously involved using tagged primers, which enable capture of the amplicon of interest between the membrane and AuNPs. However, these systems make distinguishing between primer-dimers, incorrect amplification products and the true amplicon of interest, difficult resulting in false positive results (Li *et al.*, 2017).

Coupling Type V and VI CRISRP-Cas assays to lateral flow platforms relies on detecting the collateral cleavage activity resulting from target recognition, rather than detecting the actual amplicon itself. This eliminates the difficulties that occur when using tagged primers. Moreover, CRISPR-Cas sensing allows detection of dsDNA, ssDNA and ssRNA depending on the Cas effector used; Cas12a, Cas14 or Cas13a, respectively (Ford, 2019)

The majority of published CRISPR-Cas-LFAs are based on Nucleic Acid Lateral Flow ImmunoAssays (NALFIAs) using the commercially available HybriDetect-Universal Lateral Flow Assay Kit (Bai *et al.*, 2019; Sullivan *et al.*, 2019; Broughton *et al.*, 2020; van Dongen *et al.*, 2020). These lateral flow strips consist of a streptavidin control line and an antibody test line, which captures anti-FAM coated AuNPs (Breitbach, 2020). Dual labelling of a nucleic acid reporter molecule with FAM and Biotin enables detection of collateral cleavage activity by Type V and VI Cas effectors upon target recognition (Figure 5.3). Adaptation of this system, coupled with isothermal amplification has enabled detection of several pathogens from pre-treated samples including African Swine Fever Virus (Bai *et al.*, 2019) and Sars-Cov-2 (Broughton *et al.*, 2020). To reduce the number of pipetting steps involved in the assay, Bai *et al.*, (2019) lyophilised their Cas12a-based On-site and Rapid Detection System, termed CORDS, and achieved the same LOD after long term storage as the original assay. This shows promise for using a lyophilised CRISPR-Cas-LFA in settings with limited resources. Nevertheless, no study to date has combined a CRISPR-Cas assay with a biosensor device for environmental monitoring.

5.1.3. Aims and Objectives

The main aim of this chapter is to adapt the *S. salar* specific RPA-CRISPR-Cas assay (as developed in Chapter 4) to a biosensor platform. To achieve this aim, a number of objectives were proposed that involved modification of a portable fluorometer for fluorescence detection and use of lateral flow test strips for colorimetric readout. These objectives include:

1) Assessment of a one-pot RPA-CRISPR-Cas12a assay as a route to minimise sample handling.
2) Alteration and optimisation of the ColiSense system to enable RPA-CRISPR-Cas visualisation on a portable system.
3) Development of a *S. salar* specific RPA-CRISPR-Cas lateral flow assay to simplify results interpretation.

5.2. Methods

5.2.1. Development of a one-pot RPA-CRISPR-Cas12a assay

5.2.1.1. Buffer optimisation

A selection of buffers: binding buffer, NEBuffer 2.1 and the RPA rehydration buffer were used to assess the effect on the CRISPR-Cas detection step, using a two-step RPA-CRISPR-Cas set up. Reactions (total volume 20 µL) were composed of 50 nM:62.5 nM Cas12a:gRNA, 100 nM ssDNA-FQ Reporter, 1x buffer and RPA product made from 0.5 ng/µL and 5 pg/µL *S. salar* tissue. Reactions were incubated in a LightCycler 480 (Roche) for 90 min at 37°C with fluorescence measurements taken every 30 sec (λex = 485 nm, λem = 535 nm). Samples containing molecular grade water were run in triplicate and used for background-subtracted fluorescence.

The effect of buffer inhibition on amplification was assessed using reactions made up as follows (final volume of 50 µL): 0.48 µM forward and reverse primers, 1x buffer (NEBuffer 2.1, CRISPR binding buffer), 100 nM ssDNA-FQ Reporter, 1x RPA rehydration buffer, one RPA reaction pellet and 0.5 ng/µL or 5 pg/µL *S. salar* DNA. RPA reactions as normal (see Chapter 4.2.3.1) were set up alongside all in one reactions, acting as a control.

5.2.1.2. Delayed RNP integration

Reactions (50 µl final volume) contained: 1x rehydration buffer, 1x NEBuffer 2.1, 0. 48 µM forward and reverse primers, 100 nM ssDNA-FQ reporter, 14 mM MgOAc, 460 pg/µl or 4.6 pg/µl *S. salar* DNA extract and one RPA reaction pellet. The final RNP concentration in all reactions was 50 nM: 62.5 nM Cas12a:gRNA, with the pre-assembled RNP either added directly to the reaction or suspended in the lid and incorporated via centrifugation following a 15 min pre-incubation. All reactions were incubated for 15 min at 37 °C prior to being incubated in a LightCycler 96 (Roche) for 120 min at 37 °C with fluorescence acquisition every 30 sec (λex = 485 nm, λem = 535 nm).

5.2.1.3. One-pot assay sensitivity using tissue extracts

The sensitivity of the one-pot RPA-CRISPR-Cas assay was assessed using optimised conditions. Reactions (50 µl final volume) consisted of: 1x rehydration buffer, 1x NEBuffer 2.1, 0.48 µM forward and reverse primers, 100 nM ssDNA-FQ reporter, 14 mM MgOAc, 460 – 0.0046 pg/µl *S. salar* DNA extract, one RPA reaction pellet, 50 nM: 62.5 nM Cas12a:gRNA (preassembled as an RNP and added following 15 min incubation at 37 °C) and molecular grade water. Following RNP addition, reactions were incubated in a LightCycler 96 (Roche) for 120 min at 37 °C with fluorescence acquisition every 30 sec (λex = 485 nm, λem = 535 nm).

5.2.2. Adaptation of a portable fluorescence visualisation platform - the ColiSense system

The ColiSense system, developed at DCU Water Institute and published by Heery *et al.*, (2016) is an optical biosensor which utilises the enzymatic activity of *E. coli* to quantitatively monitor levels in bathing waters. This system is a field portable incubating fluorometer with triplicate sample chambers. It was specifically designed to measure β-d-Glucuronidase (GUS) activity of *E. coli* based on the hydrolysis of 6-Chloro-4-Methyl-

umbelliferyl-β-d-Glucuronide (6-CMUG) into glucuronic acid and a fluorescent molecule, 6-Chloro-4-Methyl-umbelliferyl (6-CMU). The ColiSense features three sample chambers to allow for triplicate detection, with each chamber set to incubate at 44 °C (Heery *et al.*, 2016). The fluorescence detection system consists of an LED for excitation at 362 nm and a photodiode to measure the emitted wavelength at 445 nm. When incorporated with a sample pre-concentration and lysing procedure, the ColiSense successfully detected *E. coli* in freshwater and seawater, providing results in 75 min from sample collection (Briciu-Burghina *et al.*, 2019).

5.2.2.1. ColiSense re-design - SensEDNA

To enable DNA detection using the RPA-CRISPR-Cas methodology, the ColiSense system was modified by Sean Power and Dr. Ciprian Briciu-Burghina. The modified system, renamed SensEDNA, (Figure 5.4) features three sample detection cells for triplicate analysis. Each cell simultaneously incubates at 37 °C (control within 0.5 °C) and measures fluorescent signals at 10 sec intervals.

Note: Modifications to the ColiSense system were carried out by Sean Power and Ciprian Briciu-Burghina in collaboration with Molly Ann Williams.

5.2.2.1.1. Engineering components

LEDs (LC503FBL1-15Q-A3-00001) with peak emission wavelength at 480 nm were obtained from Farnell, Ireland. Photodiodes (BPW21R), operational amplifiers (MCP601), voltage regulators (LM317), Darlington transistor array (ULN2803), digital temperature sensor (DS18b20) and silicone matt heater (1.25 W, 50 mm x 25 mm) were obtained from Radionics Ireland. Optical filters (35-852 - short pass, 12.5 mm square, ulra-thin, flexible; and 62-976 – long pass, 12.5 mm diameter) were obtained from Edmund Optics, UK. A Wixel micro-controller board was obtained from Cool-Components, UK. The instrument enclosure (Diatec S White) was obtained from OKW, UK. Glass sample vials (9301-1387) were obtained from Agilent. The heating block (anodised aluminium) was designed in-house and machined by Inmasoll Ltd.

5.2.2.1.2. Optical and mechanical design

Normalised absorption and emission spectra of 6-carboxyfluorescein are shown in Figure 5.4a, with $\lambda_{ex\ max}$= 485 nm and $\lambda_{em\ max}$= 535 nm. A 5 mm round LED lamp with peak emission at 480 nm was selected to excite the 6-carboxyfluorescein fluorophore close to its max, while a photodiode (PD) with enhanced sensitivity in the green region was selected as the photodetector (Figure 5.4a). Due to the low stoke shift of 6-carboxyfluorescein, two optical filters are used. A high-pass optical filter with a 500 nm cut-off was selected to reduce any interference from the LED and block the excitation light from the detector. To further reduce light source leaching into the detector a short-pass flexible cut-off filter was used on the LED side. This filter proved successful at removing the LED emission tail (Figure 5.4a), and further reducing the signal to noise ratio. Glass sample vials (100 µl) were used as cuvettes due to their disposable nature and low cost. To incubate the samples to 37 °C, an anodised aluminium block was designed and machined with 3 detection chambers and optoelectronic components integrated (Figure 5.4c). A self-adhesive silicone foil heater was attached to this and cork insulation (6 mm) was applied to exposed surfaces of the heating block to increase thermal efficiency. A digital temperature sensor was inserted in the block and fixed in place with thermally conductive epoxy. The components of the fluorescence detection system were incorporated into the heating block as shown in the schematic in Figure 5.4b. The fluorescent signal is measured at a 90 ° angle, with LEDs and short pass filters mounted at the bottom while the PDs and long pass filters are mounted at the side. The heating block, fluorescence detection system and boards mounted electronics were integrated into the instrument enclosure shown (Figure 5.4d).

5.2.2.1.3. Electronics

The electronic control system was designed around a Texas instruments CC2511F32 based micro-controller board called Wixel. The board offers a 3.3 V regulator, USB, low power radio and 12-bit differential Analog to Digital Converter (ADC). It has a small form factor and is highly versatile. Programming of the board was carried out as previously described in Heery *et al.*, (2016).

An LED light source was chosen for the device as it offers low power consumption, small size, low weight, high robustness and high monochromaticity. The emission spectrum is shown in Figure 5.4a. To maximise measurement sensitivity, the LED was powered at its maximum continuous rating (20 mA) and the sample rate was set to 0.1 Hz with a sample illumination duty cycle of 0.5%. A photodiode was chosen as the optical detector for the device as it offers low power consumption, small size, low weight and high robustness. The acceptance spectrum of the chosen photodiode is shown in Figure 5.4a, Further PD set-up information is provided in Heery *et al.*, (2016).

A silicone foil heater was selected as the heat source. This delivered 5 W of heat while powered with 24 V and drawing 200 mA. Temperature control was performed using a Dallas 1-wire digital temperature sensor (DS18B20) allowing control to within 0.5 °C. Detailed testing of power and temperature output is provided in Heery *et al.*, (2016) and the system was powered by a 24 V switch mode plug top supply for laboratory use and by a 24 V battery for field use. Communication to the PC was via USB.

5.2.2.1.4. Software

Function prototypes were created to control each of the system components. Raw data from each sample cell and the temperature are transmitted to the PC and displayed on ExtraPutty terminal while simultaneously being recorded in a log file. The log-files were subsequently imported into Microsoft Excel for analysis.

5.2.2.2. Fluorescence reporter optimisation

The optical capacity of the SensEDNA system was studied using a dilution series of a FAM-Biotin (FB) dual labelled ssDNA reporter, with concentrations ranging from 10,000 nM to 125 nM. The FAM fluorophore in these reporters is unquenched and thus can be detected without reporter cleavage. Standards were made up in NEBuffer 2.1 and 50 µl was added to 100 µl glass vials for measurement. Analysis was carried out in triplicate

with vials placed in channel A, B and C of the SensEDNA instrument, incubated at 37 °C and fluorescence response recorded.

The background fluorescence from ssDNA-FQ reporters was analysed using a dilution series with concentrations ranging from 10,000 nM to 125 nM. As above, standards were prepared in NEBuffer 2.1 and measured in triplicate in 100 µL glass vials. Comparing fluorescence output from the FQ- and FB- reporters allowed selection of the ssDNA-FQ reporter concentration for RPA-CRISPR-Cas detection.

5.2.2.3. SensEDNA performance using tissue extracts

The sensitivity of SensEDNA detection was assessed using a dilution series of RPA products from a *S. salar* tissue extract (as in Chapter 4.2.4.4). Reactions (final volume 50 µl) consisted of: 50 nM: 62.5 nM Cas12a:gRNA, 2 µM ssDNA-FQ reporter, 1x NEBuffer 2.1, 5 µl RPA product and molecular grade water. At each DNA concentration, triplicate analysis was performed with each replicate placed in one of the three SensEDNA chambers. Reactions were added to 100 µl glass vials and incubated in the SensEDNA for 30 min with fluorescence measurements made every 10 sec. Background subtraction was performed using a negative control, containing no template DNA, analysed in the respective chamber. Fold-change analysis was also performed, using the following equation:

$$\frac{(Fluorescence\ @\ 30\ min) - (Fluorescence\ @\ 10\ sec)}{(Fluorescence\ @\ 10\ sec)} \quad (3)$$

5.2.3. Adaptation to a lateral flow assay

Lateral flow assays were conducted using an ssDNA-FB reporter (5'-/56-FAM/TTATT/3Bio/-3') with commercially available lateral flow strips (Milenia HybriDetect 1, TwistDx). Two-step reactions consisted of RPA amplification (as described in Chapter 4.2.3.1) of target DNA followed by CRISPR-Cas12a cleavage of FB-reporters with a lateral flow visual readout.

5.2.3.1. Optimisation of FB-reporter and RNP concentration

The design of the Milenia HybriDetect lateral flow (LF) test strips (Figure 5.3) necessitates optimisation of the FB-reporter for test line elimination. A 1 in 2 dilution series of ssDNA-FB reporter was prepared in NEBuffer 2.1 with concentrations ranging from 1000 nM to 31.25 nM. A blank was also included which consisted of NEBuffer 2.1 only. The effect of varying reporter concentrations was assessed as follows; 10 µL of each reporter stock was added directly to the conjugate release pad (CRP) of the test strip. This was then placed in 80 µL of HybriDetect assay buffer and incubated for 2 min at RT prior to visualisation.

Additionally, the concentration of Cas12a and gRNA in the RNP were tested for the effect on test line density. The concentrations used were based on Bai et al., (2019); 250 nM:500 nM and 50 nM:62.5 nM of Cas12a:gRNA, respectively. The final reaction (20 µL total volume) consisted of varying concentrations of RNP, 250 nM FB-reporter, NEBuffer 2.1, 2 µL of RPA product from 0.46 ng/µL *S. salar* DNA extract and water. The reaction was incubated at 37 °C for 30 min, followed by 10 µL of the reaction being added directly to the test strip CRP then placed in 80 µL HybridDetect assay buffer and incubated for 2 min at RT prior to visualisation.

5.2.3.2. Lateral flow sensitivity using tissue extracts

The sensitivity of CRISPR-Cas detection with lateral flow visualisation was assessed using a dilution series of RPA products from a *S. salar* tissue extract (as in Chapter 4.2.4.4). The RNP was preassembled and diluted to a final concentration of 50 nM:62.5 nM Cas12a:gRNA in a solution containing 1x NEBuffer 2.1, 250 nM FB-reporter, 2 µL RPA product and water. The reaction was incubated at 37 °C for 30 min, 10 µL was then added directly to the test strip CRP, placed in 80 µL HybriDetect assay buffer and incubated at RT for 2 min prior to visualisation.

5.2.3.3. Lateral flow test band intensity

Assessment of lateral flow test band intensity was carried out using GelQuant.Net V1.7.8 software provided by biochemlabsolutions.com.

5.3. Results

The adaptation of a molecular assay to a biosensor device requires careful optimisation of reagents to account for any reduction in sensitivity that may arise when moving from a benchtop laboratory-based instrument to a small portable device. In CRISPR-Cas diagnostic assays, there is no consensus concentration for reagents used including the concentration of Cas nuclease and gRNA in the RNP and the reporter molecule (Gootenberg *et al.*, 2017; Bai *et al.*, 2019; Nguyen *et al.*, 2020). This is likely due to the study specific nature of these reagents and the need for different sensitivities depending on sample type. Ideally, the assay should also be as simple as possible to adhere to the WHO ASSURED guidelines for POC devices (as described in Chapter 1.3.2). For this reason, a one-pot assay would be preferable to the two-step assay described in previous chapters (Figure 5.5). To optimise the developed eDNA RPA-CRISPR-Cas assays for adaptation to a device, version 2 of the *S. salar* specific assay (4.2.1.1.2) was used.

5.3.1. Development of a one-pot RPA-CRISPR-Cas12a assay

5.3.1.1. NEBuffer 2.1 is optimal for both stages of the RPA-CRISPR-Cas12a assay and thus most suited for a one-pot assay.

Integration of the RPA reaction with the CRISPR-Cas detection assay into a one-pot reaction is required to prevent the addition of amplified product to the CRISPR-Cas reaction and thus reduce the risk of contamination. Previous studies have shown this requires careful buffer selection and the late addition of the Cas12a enzyme (Wang *et al.*, 2019) to ensure amplification can occur prior to Cas12a cleavage of the dsDNA target.

Binding buffer, NEBuffer 2.1 and RPA rehydration buffer all work effectively in the CRISPR-Cas stage of a two-step RPA-CRISPR-Cas detection assay for *S. salar* (Figure 5.6). The 90 min fluorescence time-course suggests NEBuffer 2.1 is the most suitable buffer for CRISPR-Cas detection, with a fluorescence plateau reached in under 30 min for both concentrations of RPA amplified *S. salar* product. The binding buffer (as used previously) shows the lowest value of fluorescence and largest error bars out of the three buffers.

The same buffers were used in RPA reactions at two concentrations of *S. salar* DNA and visualised on a 2% (w/v) agarose gel (Figure 5.7). The binding buffer appears to inhibit amplification, particularly at lower concentrations of target DNA (5 pg/µL) whereby no product is seen. For both DNA concentrations tested, the NEBuffer 2.1 and RPA rehydration buffer work efficiently in the reaction. Of note, rehydration buffer was included in all the reactions as recommended in the manufacturer's instructions for RPA.

It was found that the binding buffer is therefore unsuitable for incorporation into a one-pot assay due to its inhibition of RPA. It was decided that the NEBuffer 2.1 should be used for the one-pot assay due to its efficacy in both the RPA and CRISPR-Cas steps of the reaction. The NEBuffer 2.1 also shows applicability for the two-step reaction, enabling a reduced CRISPR-Cas incubation time from 120 min to 30 min.

5.3.1.2. Delayed RNP integration improves detection of *S. salar* tissue extract at low DNA concentrations

The importance of delayed RNP integration for successful detection was determined through comparison of direct addition of the RNP to the one-pot reaction and delayed integration of the RNP. Delayed RNP integration improves detection at low concentrations of *S. salar* DNA (Figure 5.8). Incorporation of the RNP directly into the reaction does not interfere with detection at 460 pg/µL of target DNA; however, at lower concentrations (4.6 pg/µL) it was found that fluorescence output is reduced

compared to delayed integration. Direct incorporation also results in greater variation of fluorescence, regardless of the DNA concentration – as shown by the larger error bars in these samples (Figure 5.8). It was thus decided that a delayed integration approach would be taken for the one-pot assay.

5.3.1.3. The one-pot RPA-CRISPR-Cas methodology is less sensitive than the two-step approach for *S. salar* detection

The one-pot RPA-CRISPR-Cas approach lacks sensitivity compared to the two-step approach (Figure 5.9). Using a 1 in 10 dilution series of *S. salar* tissue extract, showed that the one-pot approach allows detection down to a concentration of 4.6 pg/µL following a 120 min incubation period (Figure 5.9a). When the incubation time is shortened to 30 min, the sensitivity is reduced with detection only seen down to 46 pg/µL (Figure 5.9a). This sensitivity is two magnitudes higher than the two-step approach after 120 min incubation (Figure 5.9b) and three magnitudes higher after 30 min incubation (Figure 5.9c). Exact fluorescence values are arbitrary and based on the different LightCycler instrument used for each methodology.

5.3.2. Adaptation to a portable fluorescence visualisation platform - the SensEDNA system

5.3.2.1. The optimal fluorescence reporter concentration for SensEDNA visualisation is 2 µM.

The modified SensEDNA System was found to have an optimal detection range of ssDNA-FB reporter concentration between 500 nM and 4000 nM. Above and below these concentrations of FB reporter, fluorescence output plateaus in both the high and low channels (Figure 5.10). A concentration of 2000 nM ssDNA-FQ reporter was selected for SensEDNA visualisation of RPA-CRISPR-Cas detection. This concentration showed significant difference between the unquenched (FB reporter) and quenched (FQ

reporter) FAM molecules and peak fluorescence remains below the upper optical cut-off of the instrument (Figure 5.10).

5.3.2.2. SensEDNA detection of *S. salar* tissue extracts achieves the same sensitivity as detection on the LightCycler 480.

The sensitivity of the SensEDNA system was assessed using a dilution series of RPA products from a *S. salar* tissue extract (as in Chapter 4.2.4.4), with concentrations ranging from 460 pg/µl to 0.0046 pg/µl. Successful detection was observed down to 0.046 pg/µl in all three chambers and at both high/low fluorescence output values (Figure 5.11). This sensitivity is comparable to RPA-CRISPR-Cas with fluorescence visualisation using a benchtop LightCycler480 (Figure 4.16). Fluorescence saturation is seen in high output values, particularly chamber A, with a sudden fluorescence cut off reached (Figure 5.11). This is also clear when using fold-change analysis, as the overall fold-change in these samples is reduced in the high output value compared to the low output value (Figure 5.12). Ergo, even though the same sensitivity is reached, the low value output should be used when analysing environmental samples to reduce early saturation of the fluorescence signal.

5.3.3. Adaptation to lateral flow visualisation

5.3.3.1. Optimal test-line elimination of lateral flow strips requires a ssDNA-FB reporter concentration of 250 nM whilst optimal RNP concentration remains unchanged.

CRISPR-Cas applications, using the Milenia HybriDetect lateral flow strips, require optimisation of ssDNA-FB reporter concentration in order to eliminate presence of the test line. When there is no reporter present, only NEBuffer 2.1, a strong test line band is seen but no control line is observed (Figure 5.13). Using a 1 in 2 dilution of FB-reporter, the test line is never fully eliminated however, based on by eye visualisation (Figure

5.13a) and densitometry of band intensity (Figure 5.13b), a concentration of 250 nM has the faintest test line and is thus most suitable for analysis of environmental samples.

Optimisation of the RNP concentration, showed negligible difference in test line density when visualised by eye between 250 nM:500 nM and 50 nM: 62.5 nM Cas12a:gRNA, respectively (Figure 5.14a). However, densitometry analysis showed 50 nM:62.5 nM Cas12a:gRNA results in a more intense test line and a greater difference between positive and negative samples (Figure 5.14b). This concentration was therefore selected for future work.

5.3.3.2. Colorimetric visualisation of *S. salar* tissue extracts via lateral flow achieves the same sensitivity as fluorescence visualisation.

The sensitivity of lateral flow visualisation was assessed using a dilution series of RPA products generated from DNA isolated from *S. salar* tissue (as in Chapter 4.2.4.4), with concentrations ranging from 460 pg/µl to 0.0046 pg/µl. By eye visualisation and densitometry analysis (Figure 5.15) suggests possible detection down to 0.046 pg/µl, a sensitivity comparable with fluorescence visualisation using a benchtop LightCycler (Figure 5.15c) and the SensEDNA system (Figure 5.11 and 5.12).

5.4. Discussion

The WHO ASSURED guidelines (Affordable, Sensitive, Specific, User-friendly, Robust and rapid, Equipment-free, Deliverable to all people who need the test) (Kosack *et al.*, 2017) are designed to aid the development of POC devices but can also be applied to in-field environmental monitoring, with the aim to move away from highly trained personnel and towards citizen science (McConnell *et al.*, 2020). The results of this chapter demonstrate the utility of an RPA-CRISPR-Cas12a detection methodology as a biosensing element on a portable device. The potential of these two sensing systems, handheld fluorescence detection and colorimetric lateral flow, for environmental

monitoring is explored with LOD for the target organism, comparable between a benchtop instrument (Chapter 4) and the sensor systems.

Based on the ASSURED guidelines, and the vision for an eDNA sensor, a one-pot molecular reaction is preferable to the currently developed two-step approach as it removes the number of sample handling steps required for target detection. In addition, transferring of RPA amplicons in a two-step assay, increases the risk of carry-over contamination and prevents accurate quantification of target nucleic acids due to separate target amplification (Yin *et al.*, 2020). It is thus desired to reduce these limitations by combining the assay into a single reaction. Several optimisation steps are required to enable a one-pot assay. The choice of buffer should be selected based on reaction performance in both stages of the assay. Whilst previous methodology (Chapter 4) used a CRISPR binding buffer, this was found to inhibit the RPA reaction (Figure 5.7). In addition, this buffer was less efficient than NEBuffer 2.1 during the fluorescence acquisition stage of the reaction (Figure 5.6). For this reason, the binding buffer was no longer used and all assays going forward, both one-pot and two-step, used NEBuffer 2.1. Moreover, biocompatibility of the RPA and CRISPR enzymes needs to be assessed. At high concentrations of target DNA, introducing the Cas12a nuclease directly into the reaction results in a greater fluorescence signal than when delaying integration. However, at low DNA concentrations, delaying the integration of the Cas12a nuclease increased the resulting fluorescence signal (Figure 5.8). This suggests that at low target concentrations, the RPA enzymes and Cas12a nuclease have poor biocompatibility and are competing for the dsDNA substrate. Consequently, exponential amplification of the target is prevented and the overall collateral cleavage activity is reduced. Wang *et al.*, (2019) found similar results; when using a fully integrated RPA-CRISPR-Cas12a reaction, fluorescence values were below those that could be visualised if target DNA concentrations were low. They hypothesised that the Cas12a nuclease was digesting the DNA target prior to amplification. Ergo, the sensitivity would reflect that of CRISPR-Cas12a used without pre-amplification (as in Chapter 4.3.2).

To circumvent this, a delayed Cas12a integration approach was used enabling successful detection down to a concentration of 10^{-4} ng of target plasmid DNA (Wang *et al.*, 2019). However, even with delayed Cas12a integration, optimised buffer selection and optimised RNP concentration, the one-pot RPA-CRISPR-Cas12a method for *S. salar* monitoring shows a large reduction in sensitivity compared to the two-step method (Figure 5.9). Several studies have used different approaches to overcome these difficulties with adaptation to a one-pot reaction.

Yin *et al.*, (2020) developed a one-pot reaction for HPV16/18 diagnosis by utilising spatially separated but connected aqueous phases, the dynamic aqueous multiphase reaction (DAMR) system. This system takes advantage of the density difference with sucrose concentration to separate the RPA reaction (in the high-density bottom phase) and CRISPR-Cas12a fluorescence detection (in the low-density upper phase). Not only were fluorescence values much greater than in a one phase system, but a linear relationship was seen between threshold time and starting DNA concentration, implying its potential use as a quantitative detection system (Yin *et al.*, 2020). Li *et al.*, (2019) also created a one-pot reaction but combined a LAMP pre-amplification step with Cas12b detection. As with Cas12a, Cas12b exhibits *cis*-cleavage of target dsDNA and *trans*-cleavage of ssDNA (Li *et al.*, 2019), making it suitable for a CRISPR-Cas diagnostic assay. Their one-pot assay, HOLMESv2, showed potential for quantitative detection with higher DNA concentrations leading to more rapid signal generation and a greater end-point fluorescence intensity. This resulted in a linear relationship between target concentration and fluorescence at 120 min.

Another route to a one-pot assay is to use a Cas13a nuclease instead of Cas12a. This nuclease recognises an RNA target, therefore a transcription step is required if the intended target is DNA (Gootenberg *et al.*, 2017). To allow this, the SHERLOCK assay included a T7 promoter in the RPA primers enabling amplicon transcription via a T7 RNA polymerase (Gootenberg *et al.*, 2017). This step is performed in the same tube as the subsequent RPA and CRISPR-Cas13a reactions (Gootenberg *et al.*, 2017). Once

transcribed to RNA, the Cas13a nuclease exhibits target cleavage and subsequent collateral cleavage leading to fluorescence signal generation (Gootenberg *et al.*, 2017). Due to the differing substrates of the RPA reaction (DNA) and the Cas13a nuclease (RNA), these methods are biocompatible and can be easily combined into a single reaction (Gootenberg *et al.*, 2018). However, adaption to this SHERLOCK method would require a complete redesign of the existing *S. salar* assay and so was not suitable for this project. It was hence decided that a two-step approach would be used for development of both SensEDNA and lateral flow visualisation as the one-pot methodology presented in this chapter had insufficient sensitivity for environmental monitoring.

Nonetheless, the adapted SensEDNA system still progresses the field of eDNA monitoring towards on-site detection by using a simple, hand-held instrument instead of the costly, benchtop equipment previously used. The modified SensEDNA device successfully enabled triplicate detection down to a target DNA concentration of 0.046 pg/µL (Figure 5.11). This sensitivity is comparable to the benchtop RPA-CRISPR-Cas assay (presented in Chapter 4.3.3.4) suggesting its applicability for *S. salar* monitoring in freshwater samples. Both the background subtracted fluorescence and fold-change methods of analysis show the same sensitivity (Figures 5.11 and 5.12), however due to the variations in starting fluorescence (despite the same concentration of reporter) it is suggested that a fold-change method is preferable (as discussed in Chapter 4.4.4). In doing this, samples are only compared to themselves rather than an individually taken "blank" sample, which may have a different level of background fluorescent noise to the sample being analysed.

In addition, samples are currently analysed as three single replicates due to variation across chambers when analysing the entire RPA-CRISPR-Cas12a reaction (Figure 5.11). However, this might reflect pipetting errors as no such variation is seen when measuring the ssDNA reporters alone (Figure 5.10). Overall, the SensEDNA system is comparable to the benchtop approach when measuring *S. salar* DNA extracted from tissue and shows potential for eDNA monitoring.

Furthermore, lateral flow visualisation also shows promise for simple, rapid monitoring of *S. salar.* As with the benchtop and SensEDNA system, lateral flow visualisation enabled detection of *S. salar* DNA extract down to a concentration of 0.046 pg/µL (Figure 5.15). This implies that the visualisation stage of the assay has little effect on sensitivity when using control DNA, which aligns with the vision to maintain the specificity and sensitivity of a laboratory-based approach. Nevertheless, use of the commercial HybriDetect LF strips has some clear limitations, primarily that the test line is never fully eliminated.

The HybriDetect strips are universal lateral flow strips meaning they can be used for detection of amplicons, proteins, ribosomal RNAs or even whole cells (Dostatni, 2021). However, this means the strips have not been optimised for CRISPR-Cas applications and tweaking is needed to ensure intuitive interpretation of results. The main concern for interpretation is the faint presence of the test line in the negative controls. This artefact of the strips occurs due to two main reasons. Firstly, anti-FAM-AuNps present on the CRP may remain unbound by the reporter and thus travel to and bind the anti-rabbit capture antibodies present on the test line, producing a signal (Dostatni, 2021). This occurs if no or too little FB-reporter is used (Figure 5.13). On the other hand, too much reporter results in a phenomenon called dose hook effect whereby the number of labels exceeds the number of available binding sites on the control line and thus un-cleaved anti-FAM-AuNP bound reporters may not be halted at the control line. This results in a decreasing control line and increasing test line intensity (Dostatni, 2021). To overcome these effects, it is recommended that the concentration of reporter loaded onto the CRP is optimised, however even with such optimisation the test line was still not completely eliminated (Figure 5.13).

Further modifications are suggested by the manufacturer such as adjusting the HybriDetect running buffer to include polyethyleneglycol, which slows down lateral flow speed and can allow better accumulation of reporter at the control line (MileniaBiotec, 2020). It is also suggested that less sample is used or non-cleaved reporter is spiked into

the running buffer (Dostatni, 2021). Unfortunately, this crucial optimisation step is not mentioned in the literature of studies using a lateral flow CRISPR-Cas approach (Bai *et al.*, 2019; Broughton *et al.*, 2020; Patchsung *et al.*, 2020). Despite this concern for intuitive interpretation, the lateral flow approach shows promise for eDNA monitoring with sensitivity levels comparable to the alternative methods presented in this thesis.

To conclude, both the SensEDNA and lateral flow approaches developed in this chapter progress the field towards on-site environmental DNA monitoring. Whilst further optimisation is required to enhance these systems, they fulfil multiple requirements of the WHO ASSURED guidelines and the initial sensing vision; specificity and sensitivity are maintained, visualisation is optical and the whole method uses low isothermal temperatures. The main limitation still to be overcome is the number of sample handling steps required for both these biosensors, however as has been presented in this discussion, alternative approaches have since been published and could provide a route towards an in-field one-pot reaction for single species monitoring.

Table 5.1 Overview of major characteristics of some CRISPR-Cas POC devices.

Method Name	Sensor Type	Nuclease	Amplification	LOD[a]	Readout	Time	Sample Type	Target Type	Disease/Pathogen	Reference
MAV-chip	Platinum nanoreporter	Cas12a	-	10 pM	Colorimetric	60 min	Pre-treated	DNA	Liver Cancer	(Shao *et al.*, 2019)
-	Gold nanoparticle colorimetric	Cas12a/Cas13a	RPA/PCR	200 copies	Colorimetric	>20 min	Pre-treated	RNA/DNA	Various pathogenic bacteria	(Yuan *et al.*, 2020)
-	Fluorescence with paper fluidics	Cas13a	-	3.7 nM	Fluorescence	20 min	Synthetic	RNA	-	(Katzmeier *et al.*, 2019)
-	One pot reaction	Cas12a	LAMP	1 fM	Fluorescence	<60 min	Raw	DNA	African Swine Fever Virus	(Qian *et al.*, 2020)
-	Portable microplate reader	Cas12a	-	1 pM/0.2 nM	Fluorescence	60 min	Pre-treated	DNA	African Swine Fever Virus	(He *et al.*, 2020)
-	LFA	Cas13a	RPA	10 copies	Colorimetric	60 min	Pre-treated	RNA/DNA	White Spot Syndrome Virus	(Sullivan *et al.*, 2019)
CORDS	LFA	Cas12a	RAA	10 fM	Colorimetric	60 min	Pre-treated	DNA	African Swine Fever Virus	(Bai *et al.*, 2019)
DETECTR	LFA	Cas12a	RT-LAMP	20 aM	Colorimetric	<60 min	Pre-treated	RNA	SARS-CoV-2	(Broughton *et al.*, 2020)

LFA: Lateral flow assay. RPA: Recombinase polymerase amplification. PCR: Polymerase chain reaction. LAMP: Loop mediated isothermal amplification. RAA: Recombinase aided amplification. RT-LAMP: Reverse transcriptase loop mediated isothermal amplification. LOD: Limit of detection.

[a]As reported in original publications.

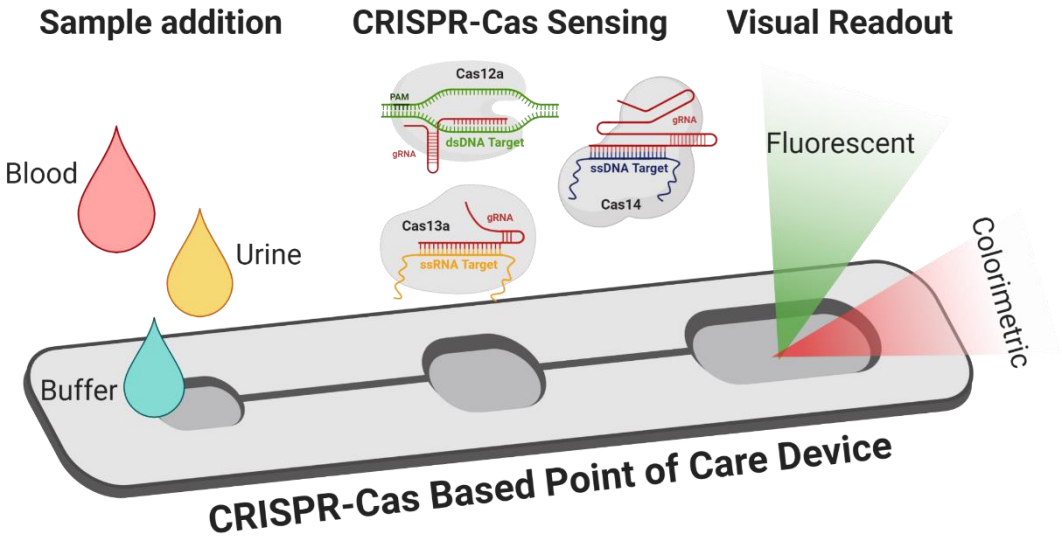

Figure 5.1 Schematic illustration of Point-of-Care Testing (POCT) using CRISPR-Cas diagnostics. Synthetic, pre-treated or raw samples are added to the device. CRISPR-Cas molecules act as the bio-sensing element and a visual readout is provided by fluorescent or colorimetric means. Figure adapted from van Dongen *et al.*, (2020).

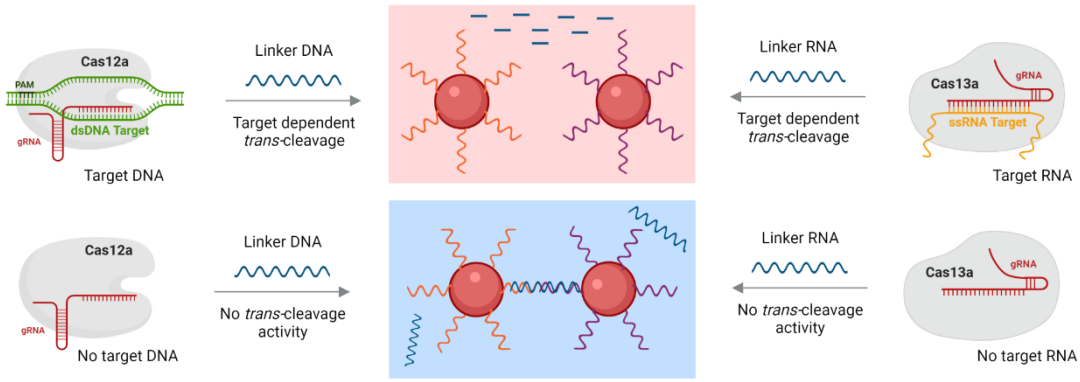

Figure 5.2 Schematic diagram of CRISPR-Cas detection using AuNP-DNA probes. Cas12a- and Cas13a- gRNA complexes are able to collaterally cleave ssDNA and ssRNA linker sequences. This degradation, prevents aggregation of AuNP-DNA probes, meaning in the presence of target DNA, AuNPs are dispersed and no colour change is seen. However, when no target is present these linker molecules remain intact and AuNP aggregation can occur, resulting in a visible colour change. Adapted from Yuan *et al.*, (2020).

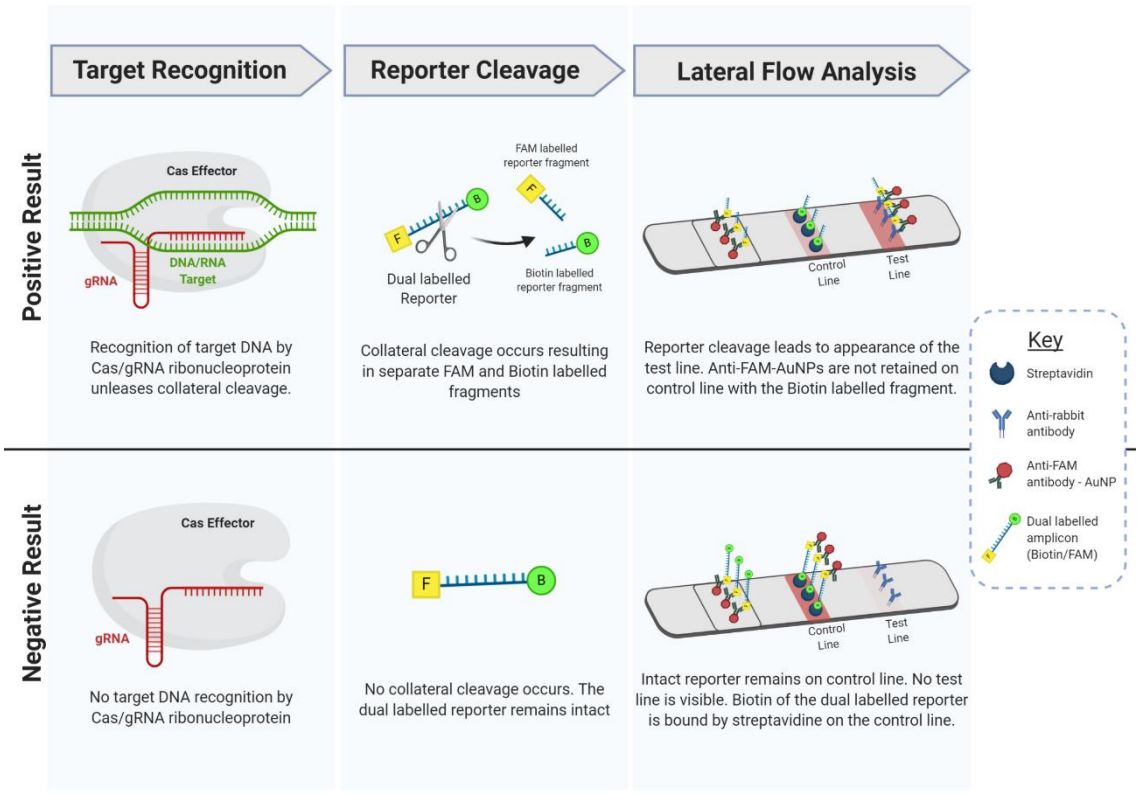

Figure 5.3 CRISPR-Cas based lateral flow assay using HybriDetect Universal Lateral Flow Assay Kit. Target recognition by the Cas/gRNA RNP results in collateral cleavage of a dual labelled FAM-Biotin reporter. The 5'-FAM is bound by anti-FAM-AuNP antibodies on the CRP and migrates to the test line where it is bound by an anti-rabbit antibody, a positive result. The 3'-biotin binds streptavidin on the control line, confirming successful lateral flow. If no target is present, the dual labelled reporter remains intact. This prevents migration of the anti-FAM-AuNP antibodies as the whole reporter binds streptavidin on the control line, resulting in visualisation of this band only, a negative result.

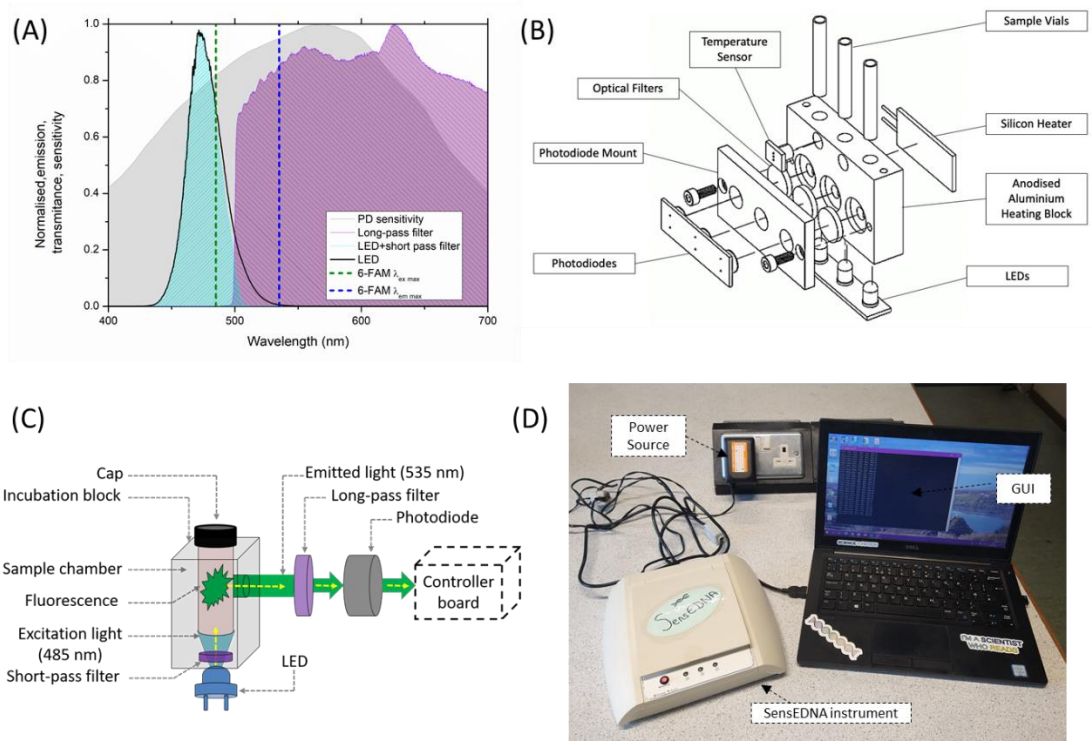

Figure 5.4 SensEDNA design and construction as modified for RPA-CRISPR-Cas diagnostics. (A) Normalised spectra of chemical components of the assay and optical components of the fluorescence detection system. (B) Schematic of the incubation and fluorescence detection system. (C) Physical realisation of key system components. (D) SensEDNA instrument with power source and Graphical user interface (GUI).

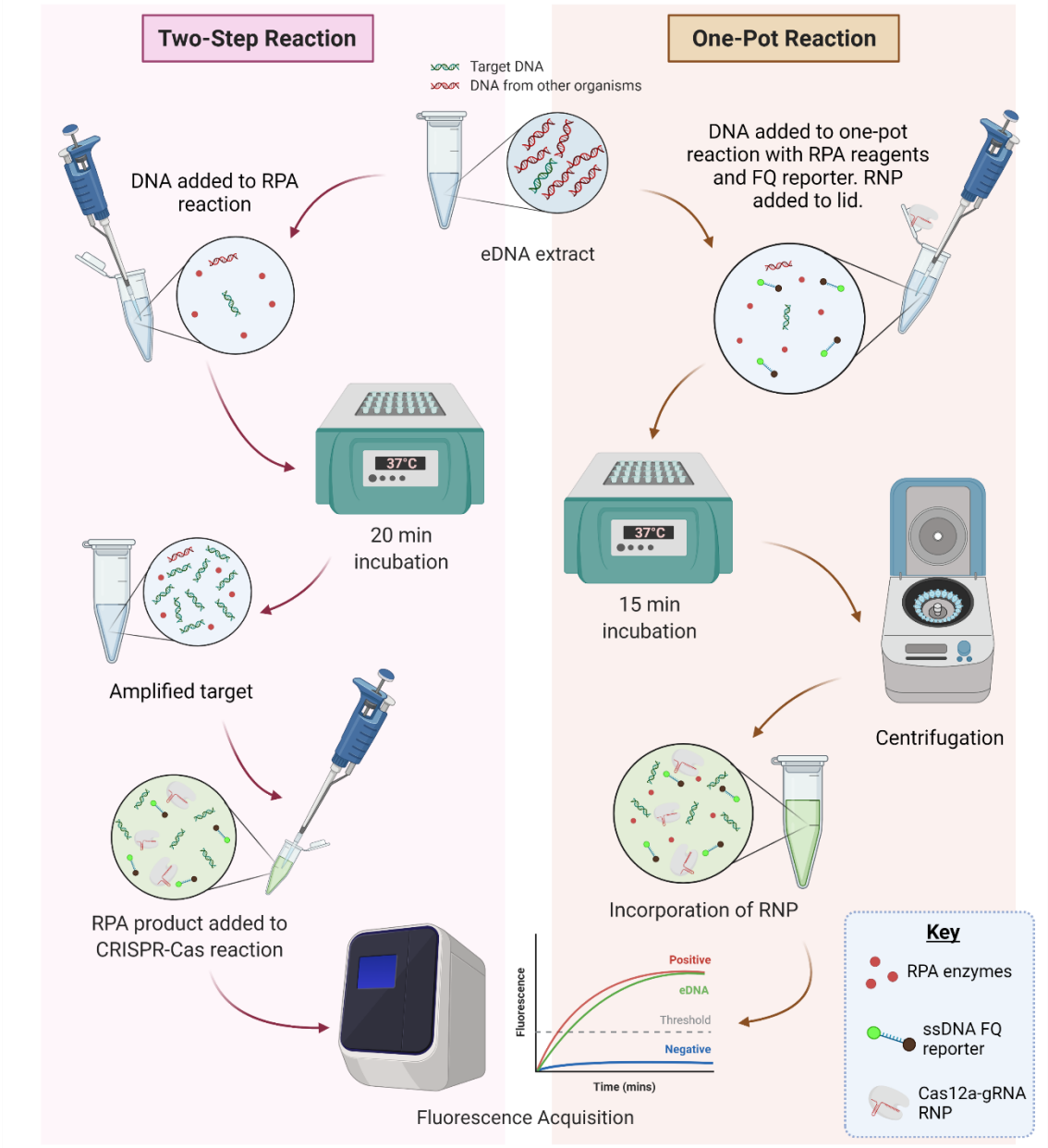

Figure 5.5 Schematic illustration of two-step and one-pot RPA-CRISPR-Cas workflow with fluorescence visualisation. The two-step approach is as described in Chapter 4. The one-pot approach is based on Wang *et al.*, (2019) with the Cas12a-gRNA RNP added to the lid and centrifuged into the reaction after 15 min incubation at 37 °C. RPA, Recombinase Polymerase Amplification; FQ, Fluorophore Quencher; RNP, Ribonucleoprotein.

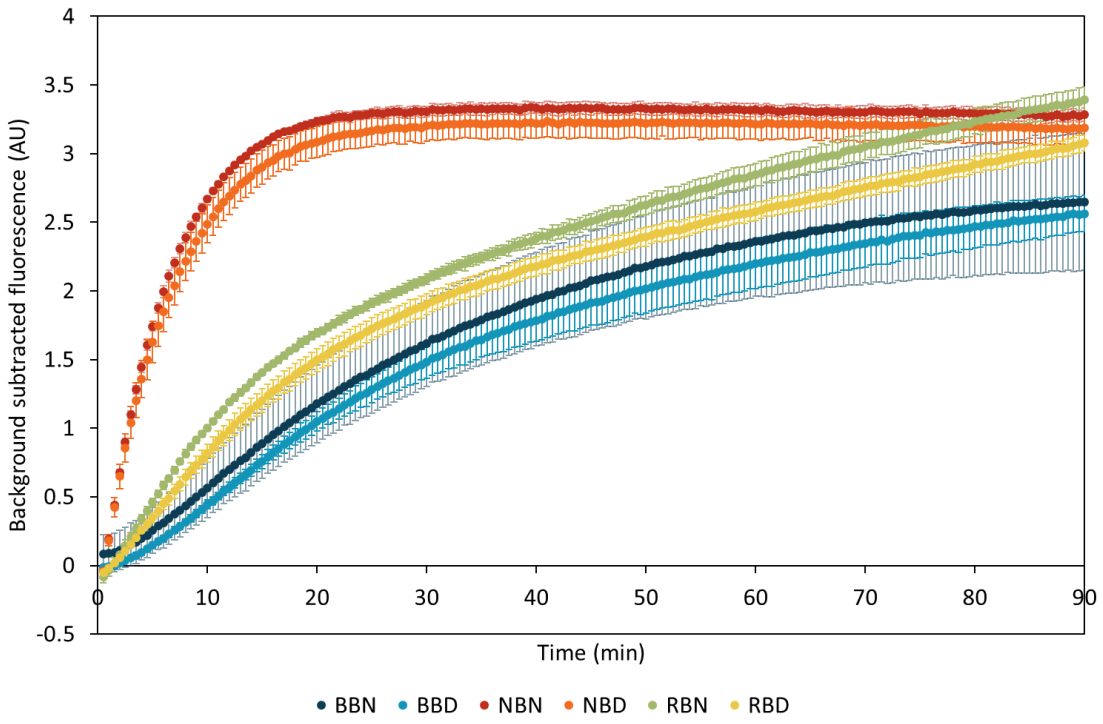

Figure 5.6 The effect of different buffers on CRISPR-Cas detection of RPA amplified *S. salar*. Time course of background subtracted fluorescence, with measurements taken every 30 sec for 90 min at 37 °C (λex = 485 nm, λem = 535 nm) on a LightCycler480. Error bars are mean ± standard deviation, where n = 3. BB, Binding Buffer (as used in Chapter 4); NB, NEBuffer 2.1 (as recommended by Wang *et al.*, (2019)); RB, Rehydration Buffer (as provided with the TwistDx RPA Basic Kit). N = 0.5 ng/µL *S. salar* DNA used in RPA reaction. D = 5 pg/µL *S. salar* DNA used in RPA reaction. NEBuffer 2.1 shows optimal performance with the fluorescence plateaux reached in under 30 min incubation.

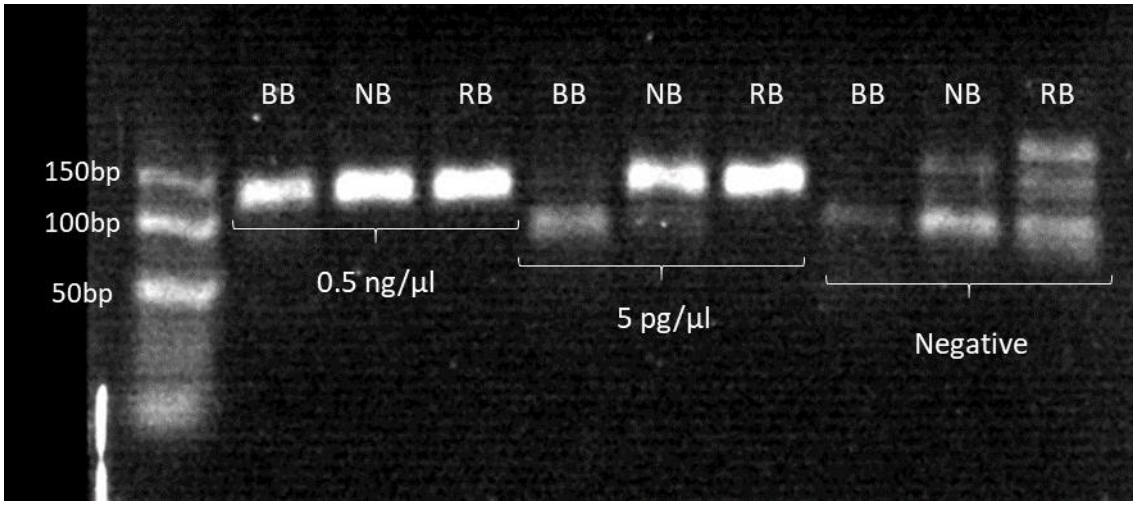

Figure 5.7 The effect of different buffers on RPA of two concentrations of *S. salar* DNA. Prior to visualisation on a 2% (w/v) agarose gel, reactions were incubated at 37 °C for 20 min (with manual mixing at 4 min) and cleaned up by heating to 65 °C for 10 min. BB, Binding Buffer (as used in Chapter 4); NB, NEBuffer 2.1 (as recommended by Wang *et al.*, (2019)); RB, Rehydration Buffer (as provided with the TwistDx RPA Basic Kit). The desired band of 120 bp was seen with all buffers at the higher concentration of DNA. At the lower concentration of 5 pg/µL, the CRISPR binding buffer appears to inhibit RPA. Note: bands seen in the negative controls are the result of primer dimers and artefacts of the RPA heat clean-up as also seen in Londoño *et al.*, (2016).

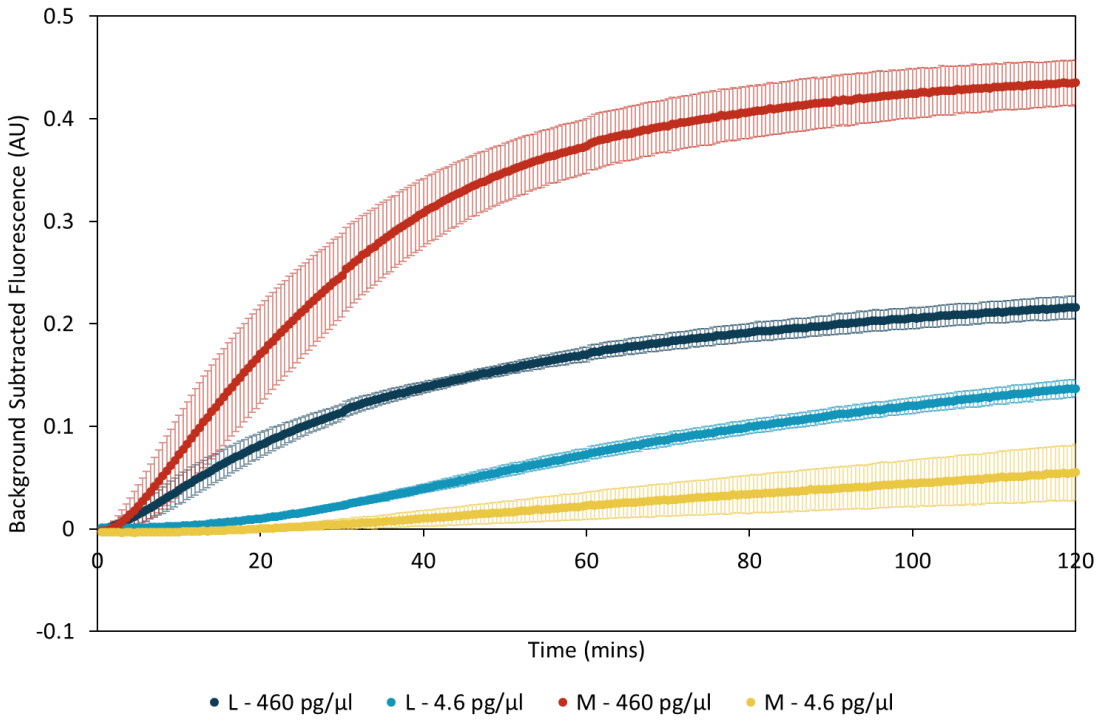

Figure 5.8 Delayed integration of a preassembled RNP into the one-pot RPA-CRISPR-Cas *S. salar* assay. The importance of delayed RNP integration was assessed at two *S. salar* concentrations (460 pg/µL and 4.6 pg/µL). L – Preassembled RNP added to the lid of the 0.2 mL RPA tube and incorporated following 15 min incubation at 37 °C. M – Preassembled RNP added directly into the one-pot reaction and incubated for 15 min at 37 °C. All reactions were then incubated in a LightCycler 96 (Roche) for 120 min at 37 °C with fluorescence acquisition every 30 sec (ƛex = 485 nm, ƛem = 535 nm). Error bars are mean ± standard deviation, where n = 3. Direct addition of the RNP into the one-pot reaction causes increased variation in fluorescence and at low DNA concentrations results in reduced fluorescence output.

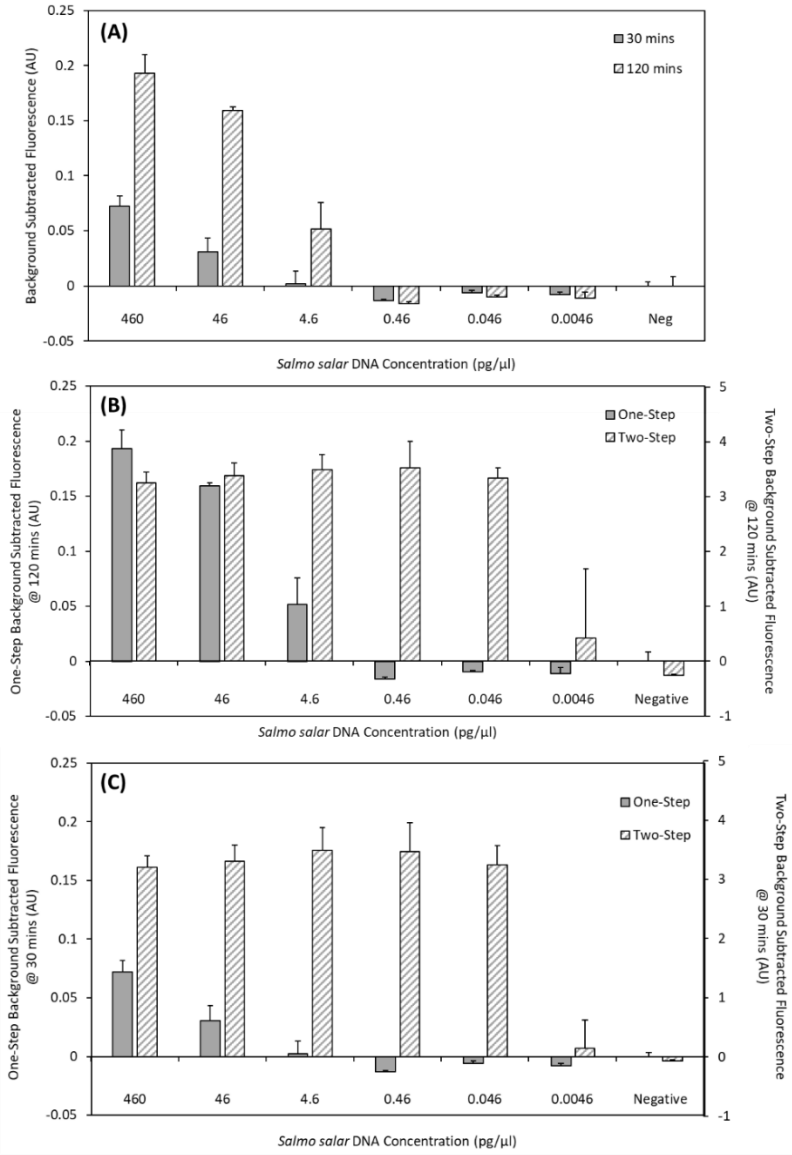

Figure 5.9 Sensitivity of the one-pot RPA-CRISPR-Cas assay for *S. salar* detection. A six-point 1:10 dilution series of *S. salar* DNA measured every 30 sec for 120 min (ƛex = 485 nm, ƛem = 535 nm). (A) One-pot assay with end-point fluorescence values reported after 30 min and 120 min incubation (where n = 3). (B) Comparison of a one-pot and two-step assay, with end-point fluorescence values reported after 120 min incubation (where n = 3 and n = 7, respectively). (C) Comparison of a one-pot and two-step assay, with end-point fluorescence values reported after 30 min incubation (where n = 3 and n = 7, respectively). Error bars are mean ± standard deviation. The one-pot assay shows reduced sensitivity compared to the two-step approach with a detection limit three magnitudes higher after a 30 min incubation.

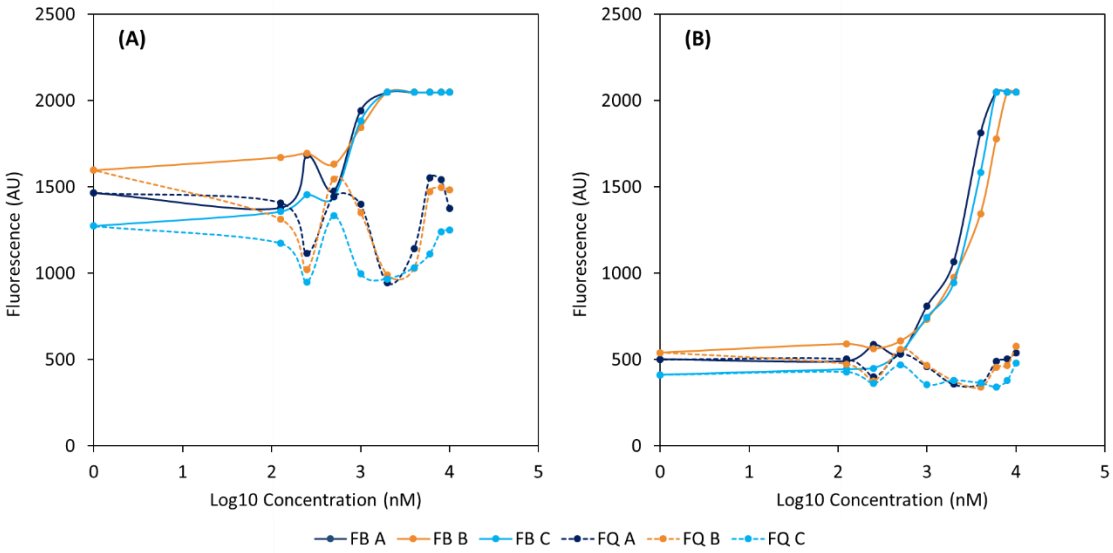

Figure 5.10 Fluorescence reporter optimisation using the SensEDNA system. Fluorescence measurements (λex = 485 nm, λem = 535 nm) from dilution series of a dual labelled FAM-Biotin (FB) reporter and a FAM fluorophore quencher (FQ) reporter, ranging from 10,000 nM to 125 nM. Each chamber of the SensEDNA (A, B or C) provides a (A) high and (B) low output value. A concentration of 2000 nM was considered optimal.

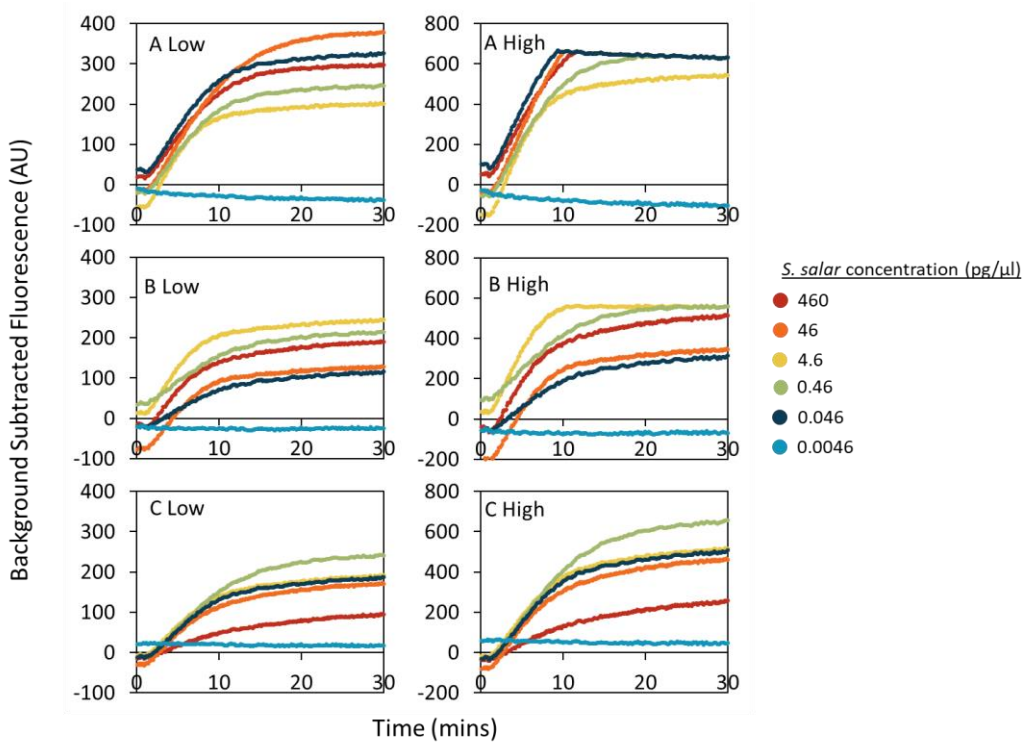

Figure 5.11 Background subtracted fluorescence of a 1 in 10 *S. salar* dilution series detected using the SensEDNA system. Time course of background subtracted fluorescence of RPA amplified *S. salar* DNA ranging from 460 – 0.0046 pg/µL with fluorescence measurements taken every 10 sec for 30 min at 37 °C (λex = 485 nm, λem = 535 nm). Background subtraction was performed using samples containing no template DNA. Each chamber of the SensEDNA (A, B or C) provides a low and high output value. The SensEDNA system successfully detects *S. salar* DNA down to 0.046 pg/µL in all three detection chambers at both the high and low output values.

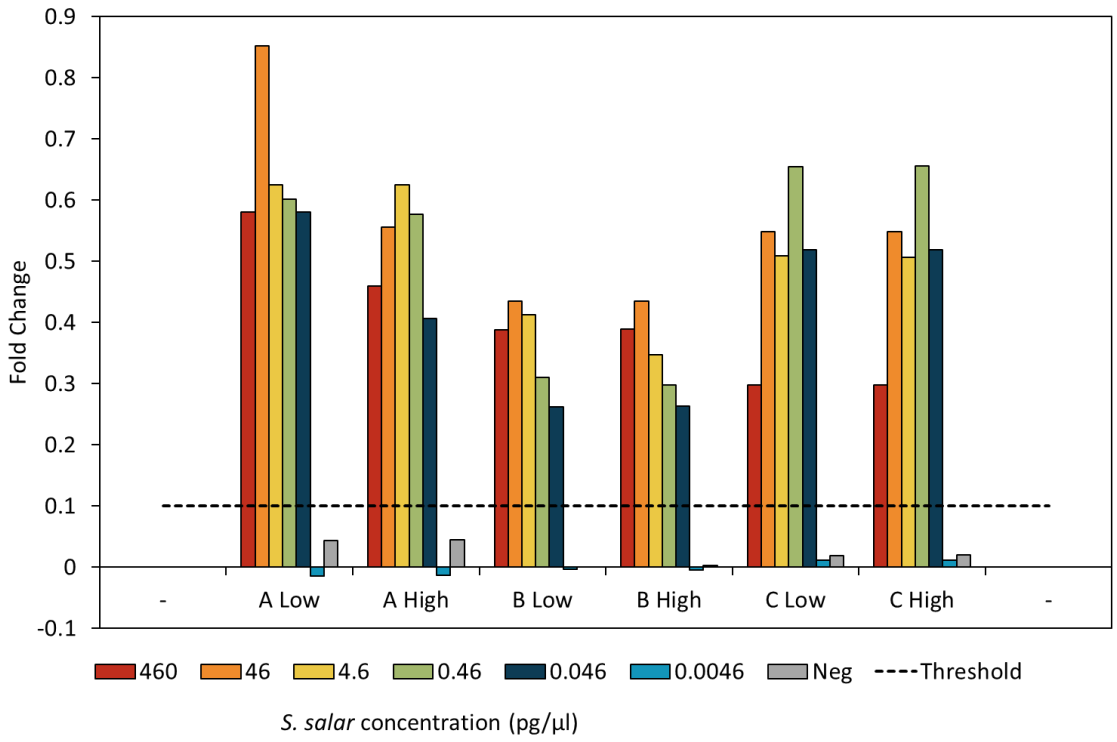

Figure 5.12 Fold-change of a 1 in 10 *S. salar* dilution series detected using the SensEDNA system. Fluorescence measurements of RPA amplified *S. salar* DNA ranging from 460 – 0.0046 pg/µL were taken every 10 sec for 30 min at 37 °C (λex = 485 nm, λem = 535 nm). Each chamber of the SensEDNA (A, B or C) provides a low and high output value. Fold-change was calculated based on fluorescence measurements at 10 sec and 30 min. Fold-change can be halted due to fluorescence saturation in the high output values as can be seen at 46 pg/µL measured in the A chamber, with a much greater fold-change seen in the low output value compared to the high output. A threshold value of 0.1 fold-change was used. Values above this threshold are considered positive for *S. salar.* Successful detection of *S. salar* DNA was seen down to 0.046 pg/µL in all three detection chambers at both the high and low output values.

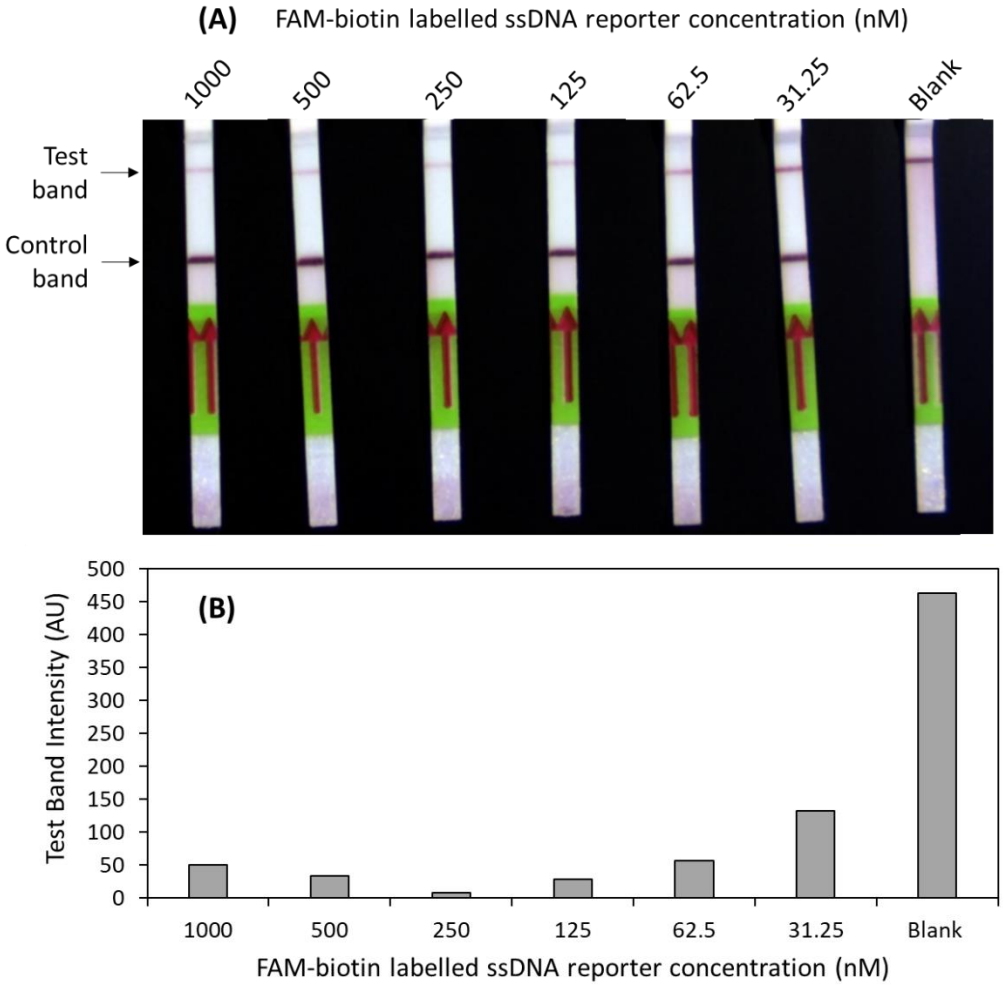

Figure 5.13 Optimisation of a dual labelled FAM-Biotin ssDNA reporter for test band elimination of HybriDetect lateral flow strips. A 1 in 2 dilution series, ranging from 1000 nM to 31.25 nM, of a FAM-Biotin ssDNA reporter was added directly to the lateral flow strips and incubated at RT for 2 min prior to visualisation. The Blank consisted of running buffer only. (A) Strips visualised by eye. (B) Test line band intensity measured using GelQuant.Net. A concentration of 250 nM was considered optimal due to having the lowest test band intensity.

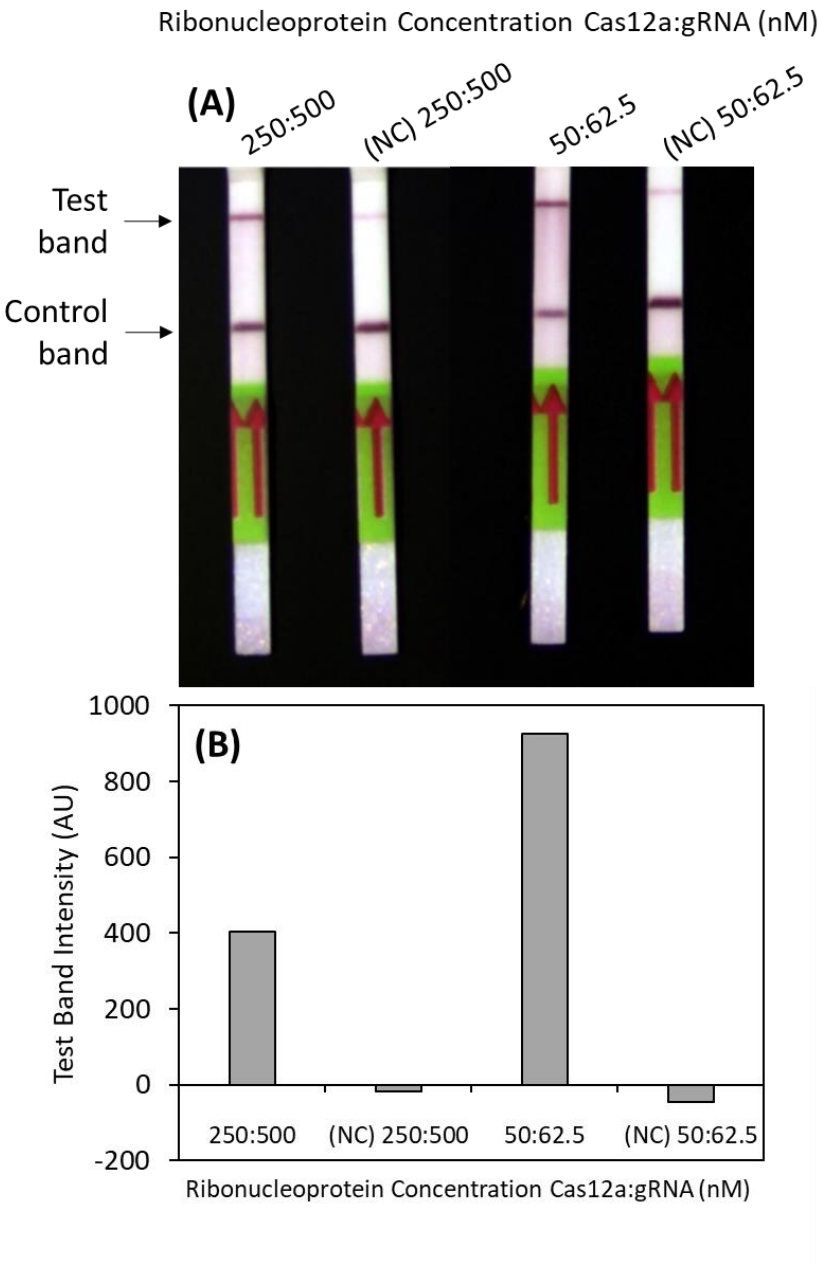

Figure 5.14 Optimisation of Cas12a and gRNA concentration in RNP for lateral flow visualisation. Two concentrations of Cas12a:gRNA were used (250:500 nM and 50:62.5 nM). RPA product made from 0.46 ng/µL *S. salar* DNA extract was used for both concentrations. Samples were incubated for 30 min at 37 °C prior to lateral flow visualisation. (NC) = Negative Control with no DNA template added. (A) Strips visualised by eye. (B) Test line band intensity measured using GelQuant.Net. A concentration of 50:62.5 nM Cas12a:gRNA was considered optimal.

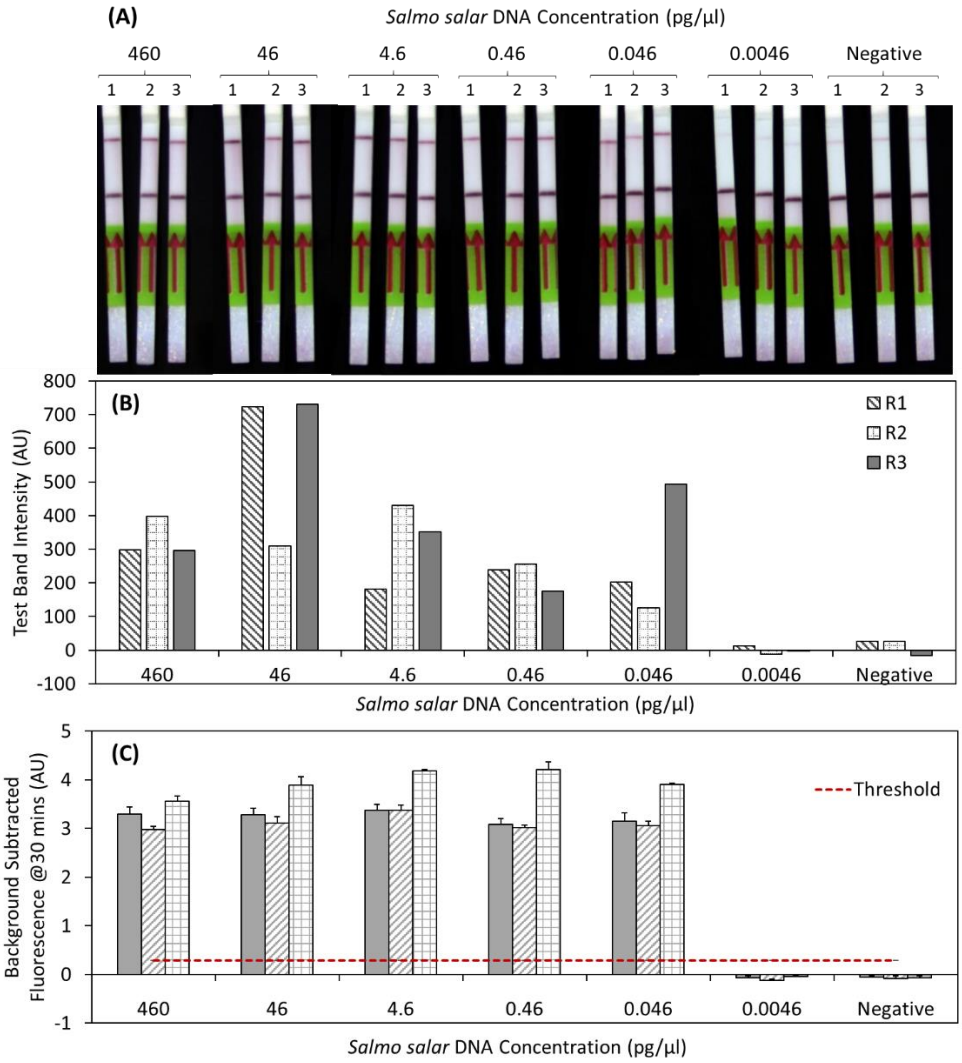

Figure 5.15 Detection of a 1 in 10 *S. salar* dilution series using RPA-CRISPR-Cas with visualisation on HybriDetect lateral flow strips. RPA amplified *S. salar* DNA ranging from 460 – 0.0046 pg/µL was used with a RNP concentration of 50:62.5 nM Cas12a:gRNA and a ssDNA FB-reporter concentration of 250 nM. Samples were incubated for 30 min at 37 °C prior to lateral flow visualisation. Negative = no template DNA added to RPA reaction. (A) Strips visualised by eye. (B) Test line band intensity measured using GelQuant.Net. (C) Background subtracted fluorescence data using an ssDNA-FQ reporter and measured on the LightCycler480 (adapted from Figure 4.16). Error bars are mean fluorescence ± standard deviation, where n = 3. Threshold value is 10 x standard deviation of background fluorescence (samples with no DNA template added). Successful detection of *S. salar* DNA was seen down to 0.046 pg/µL, which is comparable to that measured with benchtop fluorescence instrumentation.

Chapter 6. Salmonid monitoring in the Burrishoole Catchment: A comparison of detection methodologies

6.1. Introduction

6.1.1. Overview

The Burrishoole Catchment in Co. Mayo, Ireland is habitat to *S. salar, S. trutta* and *S. alpinus.* Since the development of a small research centre in the mid-1950s, the catchment has been invaluable for monitoring population sizes of diadromous salmonids, amongst other fish species. However, there is a deficit in knowledge prior to the development of this research centre. Sedimentary DNA (sedaDNA) from lake cores is a type of eDNA that is preserved for long periods (Kuwae *et al.*, 2020) and can thus act as a source of historical data enabling reconstruction of past species composition. This chapter aims to assess historical presence of *S. salar* in Lough Feeagh using sedaDNA and detection vs non-detection of *S. salar, S. trutta* and *S. alpinus* in freshwater from the Burrishoole Catchment using the methodology developed in this thesis (Figure 6.1). Due to the extensive knowledge of the catchment, it acts as the ideal test bed for newly developed technology.

6.1.2. The Burrishoole Catchment

The Burrishoole Catchment spans 100 km^2 of connected waterways in the Nephin Beg Mountains of Co. Mayo, Ireland. It lies in a north-south direction and drains into the northeast corner of Clew Bay (Figure 6.2). There are three main lakes in the Burrishoole Catchment: Bunaveela, Feeagh and Furnace (a brackish coastal lagoon). Like most other Irish lakes, these formed following ice retreat c. 11,000 years ago (de Eyto *et al.*, 2020). The lakes, drained by 45 km of rivers and streams, form a gradient from the oligotrophic, acid-neutral Lough Bunaveela and Lough Feeagh to the tidal transitional waters found in Lough Furnace. The mix of freshwater from upstream Lough Feeagh and tidal waters from Clew Bay result in the Lough Furnace water column being nearly always stratified (de Eyto *et al.*, 2020). Consequently, Lough Furnace has developed stagnant, deoxygenated conditions in the deep basin water with a water column mixing event only known to have occurred once (Cassina *et al.*, 2013). In this event, the upturn of the anoxic water caused a major fish kill that wiped out *S. trutta* and *S. alpinus* that were

caged in the lake at the time (Cassina *et al.*, 2013). The direct tidal connection of Lough Furnace to the Atlantic Ocean and subsequent channels to Lough Feeagh, the natural Salmon Leap and man-made Mill Race, make the Burrishoole perfect for diadromous fish populations. The Burrishoole rivers and lakes support stocks of *S. salar, S. trutta, Gasterosteus aculeatus* (three-spined stickleback), *S. alpinus* and *Anguilla anguilla* (European eel).

6.1.3. History of salmonid monitoring in Burrishoole

Although typical of many coastal humic catchments in the west of Ireland, the Burrishoole catchment is unique in terms of the long term monitoring of its diadromous fish populations such as *S. salar, S. trutta* and *A. anguilla* (Whelan *et al.*, 1998). As described in Chapter 1.1.2, these fish move between freshwater and marine habitats for parts of their life cycle (de Eyto *et al.*, 2020). Monitoring of such species began in the mid-1950s when the Guinness Company set up a small research station on the east side of Lough Feeagh (de Eyto *et al.*, 2020). The initial station was dedicated to understanding the dynamics of *S. salar* and *S. trutta* populations, with interest largely angling-based and a goal to improve the fishery of large *S. salar* "springers" returning to freshwater after more than one winter at sea (de Eyto *et al.*, 2020). In the 1970s, fish traps were constructed in the Salmon leap and Mill Race capturing the total migration of *S. salar* and *S. trutta* entering and exiting the catchment, as well as monitoring the *A. anguilla* returning to the Sargasso sea to spawn (de Eyto *et al.*, 2020). Since the original monitoring in the catchment, the western and upper parts now have Special Area of Conservation (SAC) status for the conservation of *S. salar* and *Lutra lutra* (Eurasian otter), with both species listed in Annex II of the European Habitats Directive (formally known as Council Directive 92/43/EEC on the Conservation of natural habitats and of wild fauna and flora).

However, although an excellent source of historic data, there is little known about salmonid populations prior to the establishment of the research centre. In recent years, eDNA technologies have been used to provide valuable insights into ancient

environments, using sedaDNA as a proxy to comprehend historic life (Kuwae *et al.*, 2020). sedaDNA extracted from sediment core samples has been used to understand livestock farming history (Giguet-Covex *et al.*, 2014), extinction events (Willerslev *et al.*, 2003; Haile *et al.*, 2009) and identification of native or alien species (Stager *et al.*, 2015). This approach is possible due to the concentration of DNA in lake sediments caused by a settling process (Turner *et al.*, 2015), which is then preserved due to slowed degradation under cold and unproductive conditions (Barnes *et al.*, 2014). The stratified deposition of eDNA in lake sediments, preserved for thousands of years, can thus provide details of historical species occupancy of both native and non-native aquatic populations (Stager *et al.*, 2015; Olajos *et al.*, 2018; Nelson-Chorney *et al.*, 2019). sedaDNA is yet to be explored in the Burrishoole Catchment, but could reveal information regarding the historic presence of salmonids prior to the founding of the research centre.

6.1.3.1. *Salmo salar*

Long-term fish census data of the Burrishoole catchment provides insights into population numbers of *S. salar*. In the 1970s, these numbers were high with over 16,000 migrating out of fresh water; however, in the late 1980s numbers plummeted to approximately 5,500 per annum (de Eyto *et al.*, 2020). Such declines in *S. salar* numbers have been linked to oceanic and atmospheric changes over this period in conjunction with anthropogenic pressures (Fealy *et al.*, 2007). Interestingly, there has also been a shift in the proportion of one sea winter (1SW) and two sea winter (2SW) fish. These terms define the amount of time spent in the marine part of the *S. salar* anadromous life cycle (Chaput, 2012). The spring component (2SW fish) of stock in the Burrishoole has not exceeded 100 fish per year since the early 60s, with the majority of fish returning after spending only one winter at sea (de Eyto *et al.*, 2020). A similar pattern has also been seen in Scottish returning *S. salar* (Bacon *et al.*, 2009), reflecting the threats to populations during the marine stage of the life cycle. The most likely reason for this decline in the Burrishoole spring stock is the result of overfishing, either by the commercial draft net fishery in Lough Furnace (ceased in 1965) or high sea fishery in

Greenland (ended in 2007) (de Eyto *et al.*, 2020). Whilst the cessation of such fishing should have increased the *S. salar* stocks, it is not the only source of ocean mortality and marine survival for *S. salar* continues to decline (Chaput, 2012).

Additionally, studies of the Burrishoole catchment have shown that there are substantial genetic differences between wild *S. salar* and ranched (captive-bred) strains (McGinnity *et al.,* 1997). The presence of ranched fish in spawning cohorts has a negative impact on the total production of wild smolts (McGinnity *et al.,* 2009) and there is a reduction in wild *S. salar* fitness due to interactions with farmed escapees (McGinnity *et al.,* 2003). This negative impact means that conservation focus should be on reducing exploitation and protecting crucial habitats for wild populations.

6.1.3.2. *Salmo trutta*

Monitoring in the Burrishoole catchment has also provided long-term census data for sea trout, the anadromous form of *S. trutta.* Smolt runs to the sea of two/three year old fish predominantly occur from March to June with downstream migrations of younger juveniles also occurring in autumn and early winter (de Eyto *et al.*, 2020). The time at sea is known to vary greatly (Jonsson and Jonsson, 2009) and unlike with *S. salar*, anadromous *S. trutta* migrate back to sea after the winter both as spawned kelts and fish that haven't spawned but may return to spawn in future years (de Eyto *et al.*, 2020). Unfortunately, in the late 1980s, stock of migratory *S. trutta* in the Burrishoole collapsed dropping from about 4,100 fish before 1990, to a current all-time low of less than 50 fish per annum (de Eyto *et al.*, 2020).

Anadromous forms of *S. trutta* are at a high risk of predation and infestation with pathogens and parasites during the marine stage of their life cycle (Jensen *et al.*, 2019). They also tend to reside in coastal areas during their migration meaning they are threatened by anthropogenic changes such as *S. salar* aquaculture, habitat alterations and fishing (Nevoux *et al.*, 2019). The negative impact of *S. salar* aquaculture is of

particular interest, primarily due to the abundance of *Lepeophtheirus salmonis* (sea lice) (Thorstad *et al.*, 2015) in open net pen farms which negatively affect wild salmonids in the area (Eldøy *et al.*, 2020). These infestations can cause increased mortality and also affect the growth of surviving individuals by reducing feeding activity and causing negative stress responses (Eldøy *et al.*, 2020). This has been seen in the Burrishoole catchment with high marine mortality of smolts paralleled by poor growth of surviving fish (de Eyto *et al.*, 2020). Although anadromous *S. trutta* populations are declining, resident *S. trutta* also occur throughout the catchment, with the Burrishoole lakes and rivers supporting good numbers. It is therefore likely that molecular assays will detect strong signals throughout the catchment coming from the resident populations rather than the migratory *S. trutta*.

6.1.3.3. *Salvelinus alpinus*

Compared to the other salmonid species in the catchment, much less is known about the *S. alpinus* population. A self-sustaining resident population that does not migrate is present in Lough Bunaveela. In the late 1960s, *S. alpinus* were stocked as fry into the Lough and some of these survived, however it is not known if the current population are related to this stocking or if they are descendents of the original native population (de Eyto *et al.*, 2020). As discussed in Chapter 1.1.2.3, *S. alpinus* populations are highly vulnerable to threats such as long term climate warming (Winfield *et al.*, 2010; Connor *et al.*, 2019). Conserving populations such as in the Burrishoole would maintain a source of biodiversity in the Bunaveela lake, which could in turn help stabilise ecosystem processes (Kelly *et al.*, 2020). It is therefore of interest to develop a molecular method to monitor this species in the catchment.

6.1.4. Threats to the Burrishoole Catchment

Freshwaters around the world face many challenges (WWF, 2020) and the rivers and lakes of Burrishoole, and their inhabitants, are no exception to this. The ubiquitous reality of climate change is affecting our freshwater environments, with warming water

temperatures, particularly in winter, already reported (Woolway *et al.*, 2019). Ectothermic species such as fish have critical temperature ranges in which incipient lethal levels define the tolerance zone within which the fish can survive for a considerable length of time (Jonsson and Jonsson, 2009). For salmonids, the lower incipient lethal temperature is 0 °C with upper limits ranging from 20-30 °C depending on the species (Jonsson and Jonsson, 2009). Whilst they may be able to survive for long periods within these limits, the exact temperature can impact animal performance such as spawning, growth and food consumption (Jonsson *et al.*, 2001; Larsson and Berglund, 2005; Forseth *et al.*, 2009).

In addition to the threat of climate change, the continued expansion of salmonid aquaculture needs careful management and regulation. Farmed *S. salar* now outnumber wild populations (de Eyto *et al.*, 2020) and as mentioned previously, not only do the farmed fish directly influence the fitness of wild *S. salar* (McGinnity *et al.,* 2003) but there are other challenges associated with the expansion of aquaculture such as the increased presence of parasites (Eldøy *et al.*, 2020). Ergo, it is vital that these systems are regulated to reduce the detrimental consequence of the interactions of wild salmonids with such farms.

Overall, the diadromous nature of native Irish *S. salar* and *S. trutta* means they are impacted in both their marine and freshwater environments. This presents a unique conservation challenge with measures needed at sea and in freshwater to help improve survival.

6.1.5. Aims and Objectives

The main aim of this chapter is to assess the efficacy of the methodology developed throughout this thesis for monitoring salmonid species in aquatic and historic sediment core samples from the Burrishoole catchment. To achieve this aim, a number of

objectives were proposed involving a freshwater sampling campaign coupled with analysis using the methods developed in the previous chapters:

1) Assessment of historical *S. salar* populations using both qPCR (developed in Chapter 3) and benchtop RPA-CRISPR-Cas (developed in Chapter 4) in sediment core samples.
2) Monitoring of *S. trutta* and *S. alpinus* in the Burrishoole catchment using species specific benchtop RPA-CRISPR-Cas assays (developed in Chapter 4).
3) Field validation of biosensor platforms, SensEDNA and lateral flow (developed in Chapter 5), via *S. salar* monitoring in the Burrishoole catchment.
4) Assessment of the effectiveness of traditional and molecular methodologies (qPCR, benchtop RPA-CRISPR-Cas, SensEDNA and lateral flow) for *S. salar* monitoring in the catchment.

6.2. Methods

6.2.1. Study sites

In August 2017, sediment core samples were taken from Lough Feeagh in the Burrishoole Catchment, Co. Mayo, Ireland (as described in Chapter 2.3.6). In April 2021, thirteen aquatic sites were sampled in duplicate in the Burrishoole Catchment (Figure 6.2). Field sampling and eDNA extraction was as described in Chapter 2.3.5.4.

6.2.2. Detection methodology

The methodology developed throughout this thesis were used to assess detection/non-detection of *S. salar, S. trutta* and *S. alpinus* from water and sediment samples (Figure 6.1). Although assay development has been described previously in the thesis, for ease, a summary of the methodology is defined below.

6.2.2.1. *S. salar* qPCR assay

The *S. salar* targeting qPCR assay developed in Chapter 3 was applied to eDNA extracts from both freshwater and sediment samples. Briefly, reactions (96-well, 20 µl) contained: 1x LightCycler 480 Probes Master, 0.5 µM forward and reverse primers, 0.1 µM hydrolysis probe, 5 µl eDNA sample and molecular grade water. A standard curve ranging from 2.5 ng/µl to 0.025 pg/µl of *S. salar* tissue extract, a non-template control, field and extraction blanks were included on each plate. All samples were run in triplicate on a LightCycler 480 (Roche).

Individual replicates were deemed positive if the C_T value was above the C_T cut-off threshold of 37, based on the assay LOD (Chapter 3.3.3). As for the eastern Canada samples (Chapter 4.2.7), only 1 positive replicate was required to deem a field sample positive for *S. salar* presence.

6.2.2.2. RPA of *S. salar, S. trutta* and *S. alpinus.*

RPA was carried out using the *S. salar* specific assay (Chapter 4.2.1.1.2) on both freshwater and sediment samples. Freshwater samples were also analysed using the *S. trutta* (Chapter 4.2.1.2) and *S. alpinus* (Chapter 4.2.1.3) specific assays. Briefly, reactions (50 µl) consisted of: 1x rehydration buffer, 0.48 µM forward and reverse primers, 14 mM MgOAc, one RPA reaction pellet, 5 µl eDNA template and molecular grade water. For each assay, field blanks, an extraction blank, an RPA blank and a positive control (consisting of 1 ng/µl of the respective tissue extract) were analysed. All samples and controls were amplified in triplicate.

RPA products were used for CRISPR-Cas analysis. Of note, the same *S. salar* RPA products were used across the three-visualisation platforms.

6.2.2.3. Benchtop CRISPR-Cas with fluorescence visualisation of *S. salar, S. trutta* and *S. alpinus.*

Benchtop CRISPR-Cas detection with fluorescence visualisation on the LightCycler 480 was carried out using the *S. salar* specific assay (Chapter 4.2.1.1.2) on both freshwater and sediment samples. Freshwater samples were also analysed using the *S. trutta* (Chapter 4.2.1.2) and *S. alpinus* (Chapter 4.2.1.3) specific assays. Briefly, the species specific RNP was preassembled at RT for 20 min and then diluted to 50 nM:62.5 nM Cas12a:gRNA in a 20 µl reaction containing 100 nM FQ-Reporter, 1x NEBuffer 2.1, 2 µl RPA product and molecular grade water. Reactions were incubated in a LightCycler 480 (Roche) for 30 min at 37°C with fluorescence measurements taken every 30 sec (λex = 485 nm, λem = 535 nm). A CRISPR-Cas negative control, consisting of molecular grade water instead of RPA product, was included at this step. All samples and controls were detected in triplicate.

Fluorescence values from CRISPR-Cas triplicates were required to have a standard deviation <0.5 to be accepted. Replicates with a standard deviation >0.5, are highlighted in the resulting graphs, but not considered as positive replicates. Fold-change analysis was used to show a change in fluorescence between the original output value (measured at 30 sec) and final value (measured at 30 min) following incubation. This was performed as previously (equation (2), Chapter 4.2.9).

A fold-change threshold value of one was used, indicating a doubling of fluorescence over time. For each RPA replicate, only fold-change values greater than this threshold were considered as positive detection of target. As previously, two criteria were used to assess species presence in a field sample: the stringent criterion required at least 2 out of 3 RPA replicates to show positive detection of target, whereas the relaxed criterion assumed 1 out of 3 positive RPA replicates infers species presence in the field replicate.

6.2.2.4. *S. salar* CRISPR-Cas with SensEDNA fluorescence visualisation

The SensEDNA system (Chapter 5.2.2.3) was used to analyse the Burrishoole freshwater samples using the *S. salar* specific assay only. Briefly, the *S. salar* specific RNP was preassembled at RT for 20 min and then diluted to 50 nM:62.5 nM Cas12a:gRNA in a 50 µl reaction containing 2 µM FQ-Reporter, 1x NEBuffer 2.1, 5 µl RPA product and molecular grade water. Reactions were incubated in the SensEDNA device for 30 min at 37°C with fluorescence measurements taken every 10 sec (ƛex = 485 nm, ƛem = 535 nm). Unlike with benchtop CRISPR-Cas, RPA replicates were visualised as single replicates.

The fold-change in fluorescence was calculated as previously (equation (3), Chapter 5.2.2.3). Individual reactions were deemed positive for *S. salar* if the fold-change was greater than a threshold of 0.1. As with the benchtop methodology two criteria were used to infer species presence in a field replicate, the stringent criterion required at least 2 out of 3 RPA replicates to show positive detection of target, whereas the relaxed criterion assumed 1 out of 3 positive RPA replicates infers species presence.

6.2.2.5. *S. salar* CRISPR-Cas with lateral flow colorimetric visualisation

The colorimetric lateral flow visualisation methodology (Chapter 5.2.3.2) was used to analyse the Burrishoole freshwater samples using the *S. salar* specific assay only. Briefly, the *S. salar* specific RNP was preassembled at RT for 20 min and then diluted to 50 nM:62.5 nM Cas12a:gRNA in a 20 µl reaction containing 250 nM FB-Reporter, 1x NEBuffer 2.1, 2 µl RPA product and molecular grade water. The reaction was incubated at 37 °C for 30 min, 10 µL was then added directly to the CRP of the LF test strips, placed in 80 µL HybriDetect assay buffer and incubated at RT for 2 min prior to visualisation. Unlike with benchtop CRISPR-Cas, RPA replicates were visualised singularly.

Lateral flow band intensity was assessed by eye and using GelQuant.Net. Intensity analysis deemed a replicate as positive if the test-line band intensity was greater than the mean of the negative controls. Positive *S. salar* detection in a field replicate was based on two criteria, as previously described. The stringent criterion required at least 2 out of 3 RPA replicates to show positive detection of target, whereas the relaxed criterion assumed 1 out of 3 positive RPA replicates infers species presence in the field replicate.

6.3. Results

6.3.1. Lough Feeagh core samples

6.3.1.1. *S. salar* was not detected in sediment core samples using SsaCOI470 qPCR analysis.

No *S. salar* DNA was detected, above the C_T threshold, in the Lough Feeagh Core samples using the SsaCOI470 qPCR assay (Table 6.1), as developed in Chapter 3. The C_T range of the standard curve was between 20.76 and 37.3, with an R^2 value of 0.9987 (Appendix V). Late C_T calls were seen in two replicates at 500 cm depth (C_T = 40) and no amplification occurred in any of the other core samples nor the negative controls (no DNA template added) or extraction blanks.

6.3.1.2. *S. salar* was detected intermittently throughout the sediment core using RPA-CRISPR-Cas with benchtop fluorescence visualisation.

S. salar was successfully detected at several depths of the Lough Feeagh sediment core using the RPA-CRISPR-Cas methodology (Figure 6.3). Fold-change analysis, with a threshold of one, was used to determine whether a replicate was positive or negative for *S. salar.* Successful detection was seen at 10 of the 13 sample depths. Six of the depths were deemed positive using the stringent criteria of 2 out of 3 positive replicates,

whilst four depths had only one positive replicate (Figure 6.3). The other three depths showed no indication of *S. salar* presence. One replicate of Extraction Blank 1 (EB1) appeared positive, however the standard deviation of the raw fluorescence values was greater than 0.5. This replicate was therefore excluded from the analysis. The second extraction blank, RPA negative and CRISPR negative showed no detection of *S. salar* (Figure 6.3 and Appendix W).

6.3.2. Burrishoole freshwater samples

In general, *S. salar* and *S. trutta* were detected throughout the Burrishoole Catchment using molecular methodologies, whilst *S. alpinus* was only detected at one site, Bunaveela south (Figure 6.4). This data is comparable to salmonid observation data from traditional monitoring using electrofishing, seine nets and traps (Figure 6.5 and Table 6.3). Additionally, all field, extraction, amplification and detection negative controls showed no positive detection (Appendix Y – AB) using either qPCR or RPA-CRISPR-Cas methodologies. This indicates the absence of contamination at any stage of the eDNA workflow and thus we can assume that positive detection of each salmonid species comes from the environmental sample.

6.3.2.1. *Salmo trutta* monitoring

6.3.2.1.1. S. trutta was positively detected in all but one site, Lough Furnace north, of the Burrishoole Catchment.

Duplicate samples were taken from thirteen sites throughout the Burrishoole Catchment with *S. trutta* successfully detected, above the fold-change threshold of one, in 12 of the 13 sites from the Burrishoole Catchment using the benchtop RPA-CRISPR-Cas methodology (Figure 6.6). No *S. trutta* was detected in either field replicate from site 13, Lough Furnace north. Two sites (Altahoney River and Black River) showed positive detection in one field replicate and this only met the relaxed criterion, with one positive RPA replicate. One site (Srahrevagh River bottom) met the relaxed criterion in

both field replicates and five sites (Bunaveela north, Bunaveela south, Goulaun River bottom, Maumaratta River and Lough Feeagh east) met the relaxed criterion in one field replicate and the stringent criterion of two or more positive RPA replicates in the second field replicate. The four other sites with successful *S. trutta* detection reached the stringent criterion in both field replicates (Appendix Z). Of note, two replicates were discarded from the presence/absence analysis due to the triplicate standard deviations of the raw fluorescence values being greater than 0.5 (Figure 6.6).

6.3.2.2. *Salvelinus alpinus* monitoring

6.3.2.2.1. *S. alpinus only positively detected in one site, Bunaveela south, of the Burrishoole Catchment*

S. alpinus was only successfully detected, above the fold-change threshold of one, in one of the 13 sites from the Burrishoole Catchment using the benchtop RPA-CRISPR-Cas methodology (Figure 6.7). At this site (Bunaveela south), only one RPA replicate showed positive amplification of *S. alpinus* meeting the relaxed criterion. All other sites showed no *S. alpinus* detection in either field replicate (Appendix AA).

6.3.2.3. *Salmo salar* monitoring

6.3.2.3.1. S. salar specific SsaCOI470 qPCR analysis successfully detected species presence at multiple sites in the Burrishoole catchment.

S. salar was positively detected at eleven sites using the SsaCOI470 qPCR assay (Table 6.2), as developed in Chapter 3. Two plates were analysed with field replicate 1 and 2 on separate plates. The C_T range of the standard curve for field replicate 1 was between 20.8 and 38.4 (Appendix X), and for field replicate 2 was between 20.7 and 37.5 (Appendix X). Both standard curves had R^2 values above 0.98. The lowest detected eDNA concentration within the range of the standard curves was 0.07 ng/L, at a C_T value of 36.9. In the two samples with this concentration, only one of three replicates was

deemed positive (Table 6.2). Interestingly, of the eleven positive sites, seven were deemed positive in both field replicates and four were only deemed positive in one. Sites one and three had only one positive technical replicate out of a possible six (across the two sites). The highest eDNA concentration detected was 17.55 ng/L (C_T value of 30.25 ± 0.05) in-field replicate 2 of site thirteen, Lough Furnace.

No *S. salar* was detected in site 8, which is located upstream of a *S. salar* migration barrier in the Srahrevagh River. There was also no *S. salar* detected in either field replicate of site 4, the top of the Goulaun River (Table 6.2).

6.3.2.3.2. S. salar positively detected in all but one site, Srahrevagh River top, of the Burrishoole Catchment using the benchtop RPA-CRISPR-Cas methodology

S. salar was successfully detected, above the fold-change threshold of one, in 12 of the 13 sites from the Burrishoole Catchment using the benchtop RPA-CRISPR-Cas methodology (Figure 6.8). Two of the sites (Goulaun Top and Mill Race) showed positive detection in only one field replicate, whilst the other ten sites showed *S. salar* presence in both field replicates. Both sites, and both field replicates, from the Bunaveela Lake met the relaxed criterion of only one out of three positive RPA replicates. The Lough Feeagh east sample met the relaxed criterion in one field replicate and the stringent criterion of two or more positive RPA replicates in the second field replicate. All other sites with successful *S. salar* detection reached the stringent criterion in both field replicates (Appendix Y). Of note, four replicates were discarded from the presence/absence analysis due to the triplicate standard deviations of the raw fluorescence values being greater than 0.5 (Figure 6.8). Importantly, no *S. salar* was detected in site 8, which is located upstream of a *S. salar* migration barrier in the Srahrevagh River.

6.3.2.3.3. S. salar is detected in fewer sites using the SensEDNA platform compared to the benchtop approach.

S. salar was positively detected, with fold-change values greater than the threshold in at least one of the field replicates, at eight of the 13 sites sampled. (Figure 6.9). Four of these sites (Altahoney River, Maumaratta River, Srahrevagh River bottom and Lough Feeagh east) only had positive detection in one of the field replicates. Three positive sites (Fiddaunveela River, Goulaun River bottom and Lough Furnace north) met the stringent criterion in both field replicates, whilst the other positive site (Black River), met the relaxed criterion in one field replicate and the stringent criterion in the other. No *S. salar* was detected in five of the 13 sites, including the top of the Srahrevagh River as expected (Figure 6.9).

6.3.2.3.4. S. salar is detected in fewer sites using lateral flow colorimetric visualisation compared to a benchtop and SensEDNA approach.

S. salar was only detected in five of the 13 sites in the Burrishoole Catchment using RPA-CRISPR-Cas with lateral flow visualisation (Figure 6.10). The threshold was calculated based on band intensity analysis of the RPA negative test line. The value was set at the mean intensity for the replicates, with only band intensities greater than this considered positive for *S. salar.* By eye visualisation was insufficient to interpret results accurately (Appendix AC). Only one site (Lough Furnace north), showed detection above the threshold in all three RPA replicates of both field replicates. The other four positive sites (Bunaveela south, Maumaratta River, Srahrevagh Bottom and Black River), only met the relaxed criteria in one of the field replicates. All other sites, had test line band intensities lower than this threshold in all field and RPA replicates (Figure 6.10).

6.3.2.4. Comparison of molecular detection to traditional methods for salmonid monitoring in the Burrishoole Catchment.

Traditional monitoring techniques showed that *S. salar* is present throughout the catchment with no detection seen in the Maumaratta River and the Srahrevagh River top (Figure 6.5). *S. trutta* has been detected in all sites in the catchment, whilst *S. alpinus* is isolated in the Bunaveela Lake (Figure 6.5).

Overall, the benchtop CRISPR-Cas methodology was the most similar to traditional monitoring, with the only major discrepancies being *S. salar* presence in the Maumaratta River and no *S. trutta* detection in Lough Furnace north (Table 6.3). The lateral flow approach showed the highest number of inconsistencies with the other monitoring methods, with the SensEDNA methodology also differing from traditional approaches at multiple sites in the catchment. *S. salar* analysis using qPCR also aligned with the traditional monitoring data with only two discrepancies: *S. salar* was detected in the Maumaratta River but not detected at the top of the Goulaun River (Table 6.3). Interestingly, site 13 (Lough Furnace north) had the highest concentration of *S. salar* eDNA in both field replicates compared to the other positive sites (Table 6.2). This site was the only site where *S. salar* was positively detected in all replicates using lateral flow visualisation (Figure 6.10) and showed the highest fold-change using both benchtop (Figure 6.8) and SensEDNA (Figure 6.9) visualisation methods.

6.4. Discussion

Monitoring of aquatic life, including salmonid species, is crucial to conserve the ever-declining populations of such freshwater organisms. Whilst traditional surveys such as electrofishing have served this purpose in the Burrishoole Catchment since the 1950s, the introduction of non-invasive methods is needed to decrease the potential harm to the target organisms and reduce habitat destruction. Ideally, this monitoring should be performed in the field as laboratory processing times can take days or weeks during which researchers do not know whether the target species' DNA is present or not

(Thomas *et al.*, 2019). Although this delay may not be as detrimental for conservation purposes, it limits the range of eDNA applications and could prevent its use in rapid management responses such as that of invasive species (Egan *et al.*, 2015) or parasites (Nguyen *et al.*, 2018). The results of this chapter further progress the eDNA field towards this desired on-site monitoring. The effectiveness of RPA-CRISPR-Cas detection for non-invasive monitoring of *S. salar, S. trutta* and *S. alpinus* in the Burrishoole catchment is shown, as well as for evaluating historic presence in the Lough Feeagh sediment core. In addition, two sensing platforms, SensEDNA and lateral flow visualisation, are assessed for their applicability to rapid eDNA detection. The results suggest that with further developments these platforms may be of use in the field.

6.4.1. Historical detection of *S. salar* from sediment samples

Sedimentary DNA extracted from lake cores can be used to reconstruct historic species composition (Giguet-Covex *et al.*, 2014). This ancient DNA preserved in sediment layers (Nelson-Chorney *et al.*, 2019) may be of low abundance and highly degraded (Olajos *et al.*, 2018), making detection difficult. The historical presence of *S. salar* is of cultural importance in Ireland featuring in Irish myths and legends such as the tale of Fionn and the Salmon of Knowledge (Lucey, 2020). In this study investigating the presence of *S. salar* in a Lough Feeagh sediment core, no *S. salar* was detected in any of the thirteen samples, above the C_T threshold, using qPCR detection methodology (Table 6.1). Similar results were found by collaborators in UCD (not published), suggesting the presence of PCR inhibitors in the extracted DNA. In order to remove these inhibitors, additional steps during the extraction process may be performed, for example, including extra humic acid wash steps (Matisoo-Smith *et al.*, 2008).

Unlike qPCR, the RPA-CRISPR-Cas12a methodology successfully detected *S. salar* throughout the sediment core (Figure 6.3), with six depths meeting the stringent criteria of 2 out of 3 positive replicates. Whilst the method is not quantitative (as discussed in Chapter 4.4.4), an increased fluorescence signal may be indicative of higher concentrations of *S. salar* DNA. Using this semi-quantitative approach would suggest

that a higher concentration of DNA was present at the lower depths of the core, with the greatest signal seen at 500 cm (Figure 6.3). This would also align with the late C_T detection seen in two of the qPCR technical replicates at this depth (Table 6.1). Detection was seen despite this sample having an initial total eDNA concentration less than 0.6 ng/µL (Appendix U). It is worth noting that for future studies the amount of eDNA added to the RPA reaction should be standardised by total eDNA concentration rather than volume. This would allow a more thorough comparison between signal intensities, despite not knowing the proportion of target DNA in the total eDNA. Moreover, future sedaDNA studies would benefit from having known negative samples included in the analysis. Such samples would account for false positive detection due to reporter degradation caused by the sedaDNA matrix.

Radiocarbon dating of the core was used to estimate the age of subsamples from six depths. These dates were then converted to calibrated YBP using the default calibration curve of IntCal20 and OxCal (ver 4.4) (Ramsey, 2009; Reimer *et al.*, 2020). This work provided by Ryan Smazal, estimates 438 cm to be around 4420 YBP and 538 cm to be 6190 YBP (Figure 6.3). This data therefore suggests that *S. salar* may have been present in Lough Feeagh in the Mesolithic period (around 4000 BC). Such presence would align with archaeological evidence suggesting that Riverside camps were present throughout Ireland and used when trapping *S. salar* (and *A. anguilla*) during the migratory seasons (Lucey, 2020).

Overall, these results support that RPA-CRISPR-Cas detection is less susceptible to environmental inhibitors than qPCR (as discussed in Chapter 4). Additionally, they indicate the relative robustness of the assays, with RPA-CRISPR-Cas potentially less susceptible to sequence degradation from processes such as base deamination, as is common in ancient DNA samples (Dabney *et al.*, 2013). The results also highlight the potential value of using RPA-CRISPR-Cas12a to analyse lake sedaDNA records as a way to address previously unanswerable questions regarding historical distribution of aquatic species (Stager *et al.*, 2015; Nelson-Chorney *et al.*, 2019).

6.4.2. Salmonid presence in the Burrishoole Catchment

Monitoring of current salmonid presence in the Burrishoole catchment further validates RPA-CRISPR-Cas as an additional method in the eDNA toolbox. *S. salar* and *S. trutta* were detected throughout the Burrishoole catchment using benchtop RPA-CRISPR-Cas approaches, whilst *S. alpinus* was only detected in Bunaveela (Figure 6.4). These results are comparable with salmonid presence data from traditional surveys (Table 6.3). Importantly, neither qPCR nor RPA-CRISPR-Cas showed detection of *S. salar* in the Srahrevagh Top sample, which is known to be above a migration barrier and thus inhabitable by this species. The only other site with no *S. salar* presence indicated by traditional surveys was Site 7, the Maumaratta River, however, both qPCR and RPA-CRISPR-Cas successfully detected *S. salar* in both field replicates at this site (Table 6.3). The exact site sampled via electrofishing was upstream of the eDNA water sample and anecdotal evidence suggests that *S. salar* were detected with traditional surveys downstream from the eDNA sampling site. It is therefore possible that *S. salar* are present in the Maumaratta River just not as high up in the catchment as the initial electrofishing survey and were therefore detected using eDNA studies but not traditional methods.

Unlike *S. salar* and *S. trutta,* which are both present throughout the catchment, *S. alpinus* are known to be limited to Lough Bunaveela (de Eyto *et al.*, 2020). Using RPA-CRISPR-Cas, only one replicate (out of a possible six across the two field samples) showed positive detection in the Bunaveela South sample and all samples appeared negative in Bunaveela North and the two outflow rivers, Goulaun Top and Fiddaunveela (Figure 6.7). This limited detection in areas with known presence is likely due to the biology of *S. alpinus.* They are cold-water fish (Kelly *et al.*, 2020) with a preference for deep lentic environments (Mirimin *et al.*, 2020). Previous eDNA studies in Lake Windermere, UK, have shown that *S. alpinus* is mainly detected in deep waters outside the species' spawning season (Hänfling *et al.*, 2016; Handley *et al.*, 2019; Muri, 2020) which typically occurs in late autumn and winter (Low *et al.*, 2011). In shoreline samples, *S. alpinus* was only detected during the autumn months (Handley *et al.*, 2019) when

adult populations migrate to breeding grounds at shallow sites (Miller *et al.*, 2015). Although the exact time of spawning is unknown in Bunaveela, it is predicted to occur during December at depths shallower than 3 m (Kelly *et al.*, 2020). The limited shoreline sampling in April is thus likely to have hindered the detection of *S. alpinus,* which were most probably located at the deepest areas of the lake during this time.

6.4.3. Comparison of methodology for salmonid monitoring – technical considerations

Compared to the benchtop approaches, the SensEDNA and lateral flow visualisation methods had a higher number of false negative detections (Table 6.3). Given the same RPA products were used for all methodologies, this difference in detection rate is likely due to reduced sensitivity of the sensor detection platforms. Based on the LOD study for each method (Chapter 5), the lowest detectable DNA concentration was identical across all platforms. However, these LOD studies were performed using DNA extracted from tissue samples, which have a relatively simple sample matrix compared to eDNA samples. Analysis of the raw time course data, shows that even at the lowest concentration of control DNA, fluorescence acquisition occurs rapidly and a high end-point fluorescence is reached after 30 min incubation (Appendix T). On the other hand, analysis of raw time course data from environmental samples shows there is a delay in initial fluorescence acquisition and the end-point fluorescence is much lower than that of the control sample (Appendix AD). This means the sensor sensitivity has to be sufficient to detect a reduced amount of reporter cleavage compared to the control samples. This delay in fluorescence acquisition could be caused by inhibitors present in the environment or due to the volume of background DNA, from non-target organisms, present in the sample. Rohrman and Richards-Kortum, (2015) suggest that although RPA is known to be resistant to common PCR inhibitors (Kersting *et al.*, 2014), it can be completely inhibited by background DNA present in whole blood samples. Whilst the maximum amount of background DNA tolerated varies depending on the amount of target DNA (Rohrman and Richards-Kortum, 2015), this inhibition could reduce the

amount of target copies amplified during the RPA step of the RPA-CRISPR-Cas assay which could consequently lead to reduced reporter cleavage.

Interestingly, *S. salar* was successfully detected at eight of the 13 sites using the SensEDNA platform (Figure 6.9) and when compared to the quantitative qPCR data (Table 6.2) these sites had higher concentrations of *S. salar* DNA than the sites where *S. salar* was falsely deemed absent. This additionally suggests that reduced detection rates are due to the SensEDNA sensitivity, which could potentially be improved by increasing the sample volume size, increasing the starting concentration of reporter or extending the assay incubation time. These enhancements aim to increase the amount of fluorescence reaching the detector in order to increase overall sensitivity.

Lateral flow visualisation also lacked sensitivity for environmental samples, with *S. salar* only detected in more than one replicate in the Lough Furnace sample (Figure 6.10). In the fluorescence based assays, it appears that less fluorescence is released in eDNA samples compared to control DNA (Appendix AD) implying that less reporter cleavage is occurring. For LF visualisation, this would result in an increase in intact ssDNA-FB reporters that would consequently remain on the control line during lateral flow and insufficient cleaved reporters to allow enough aggregation of anti-FAM-AuNPs on the test line to cause a visible colour change. This is highly problematic for interpretation due to the presence of the test-line artefact (as discussed in Chapter 5). In order to enhance the applicability of LF strips for environmental samples, the LOD needs to be improved. Potential optimisation steps include: eliminating the test-line artefact by using different LF strips designed for use with CRISPR-Cas reactions, increasing the sample incubation time to allow for greater reporter cleavage or loading more RPA product into the CRISPR reaction.

Interestingly, across all species and all detection methodologies, there are discrepancies in detection between field replicates i.e. positive detection may be seen in one field

replicate but not the second (Table 6.3). This highlights the importance of eDNA sampling design for catchment monitoring studies with decisions required regarding sample volume, number of field replicates and number of technical replicates. Schultz and Lance, (2015) used simulation modelling to show the effect on the minimum number of target copies required for detection with increasing field replicates, sample volume and technical replicates. They suggest that sample volume has the most significant effect with greater volumes increasing the likelihood of detection at low target concentrations (Schultz and Lance, 2015). Unfortunately, this might not always be feasible due to logistical constraints or small filter pore sizes leading to clogging (Goldberg *et al.*, 2018). Additionally, Schultz and Lance, (2015) suggest that at low target concentrations, a large number of field samples may be needed to detect the target marker with a high level of confidence. For this study, only two field replicates of 250 mL each were taken (Chapter 2.3.5.4), meaning populations of low abundance may have been missed.

Overall, this chapter provides strong evidence that RPA-CRISPR-Cas is an effective tool for monitoring salmonid species in the Burrishoole catchment and that, with further developments such as the necessary improvements in sensitivity, the technology could be adapted to both a colorimetric and fluorescence based biosensor.

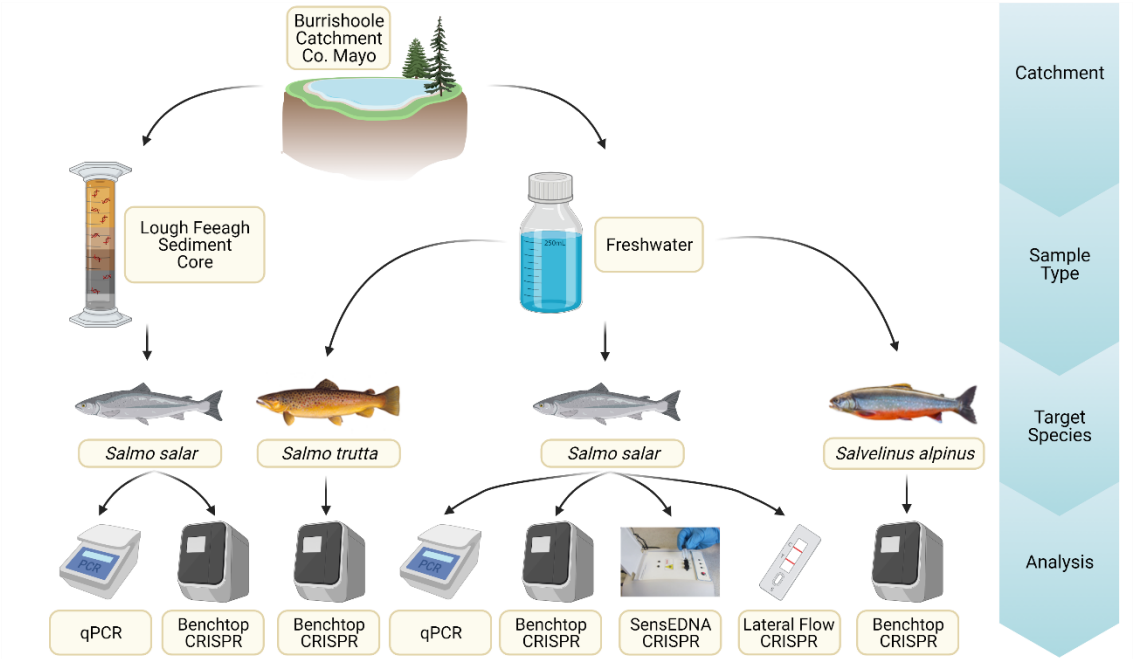

Figure 6.1 Burrishoole Catchment Monitoring Schematic. Sediment core samples taken from Lough Feeagh were analysed for *S. salar* presence using qPCR and benchtop CRISPR (fluorescence visualisation using LightCycler 480). Freshwater samples taken in duplicate from thirteen sites across the catchment were analysed for three species (*S. salar, S. trutta* and *S. alpinus*) using benchtop CRISPR and analysed for just *S. salar* using qPCR, CRISPR with SensEDNA visualisation and CRISPR with lateral flow visualisation.

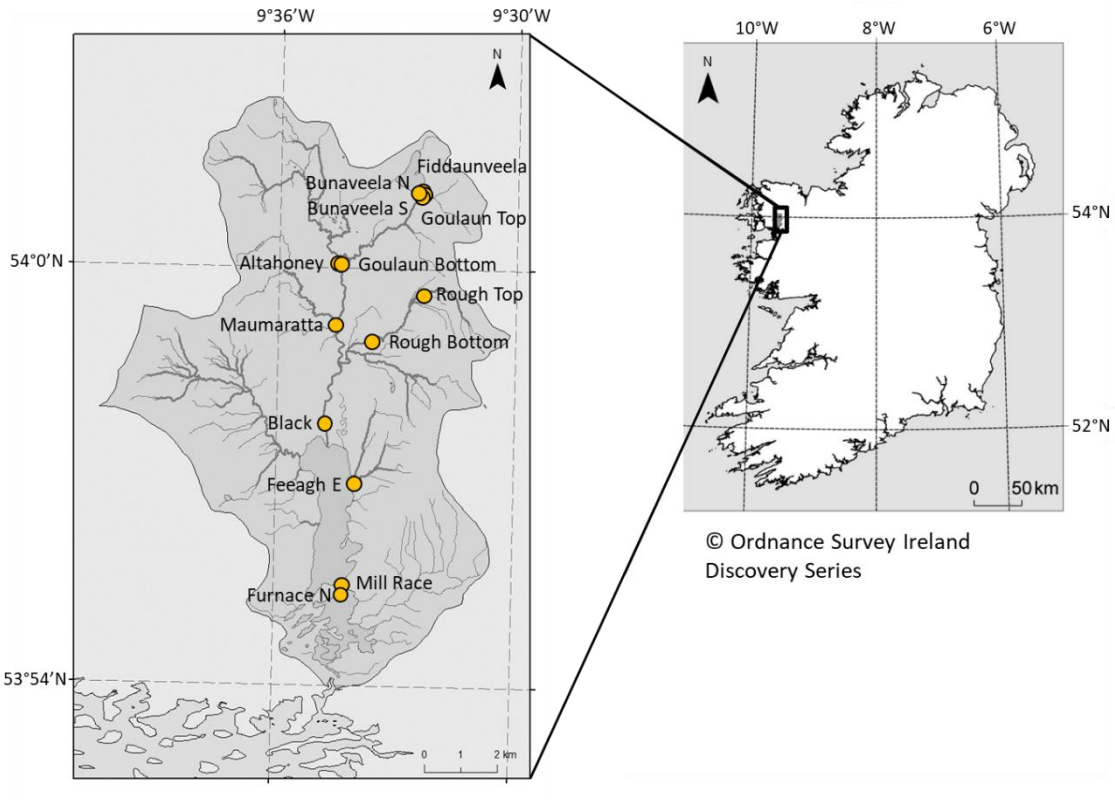

Figure 6.2 Location of sampling sites within the Burrishoole Catchment, Co. Mayo, Ireland. Thirteen sites were sampled across the catchment in April 2021.

Table 6.1 qPCR results from Lough Feeagh Core samples assessed using *S. salar* specific assay.

Sample Depth (cm)	*S. salar* present	Average C_T ± St.Dev (n=3)[‡]	No. of Positive Replicates (/3)
0	No	Undetermined[§]	0
5	No	Undetermined[§]	0
10	No	Undetermined[§]	0
15	No	Undetermined[§]	0
25	No	Undetermined[§]	0
50	No	Undetermined[§]	0
75	No	Undetermined[§]	0
100	No	Undetermined[§]	0
200	No	Undetermined[§]	0
305	No	Undetermined[§]	0
400	No	Undetermined[§]	0
500	No	40[†]	0
600	No	Undetermined[§]	0

[‡] The C_T values are indicative of the cycle number in which samples crossed the threshold into exponential amplification calculated using the second derivative maximum method. C_T values are reported as mean ± standard deviation for *S. salar* at each site.

[§] Undetermined used to describe samples with no *S. salar* detection

[†] C_T values greater than 37 and thus above the LOD threshold.

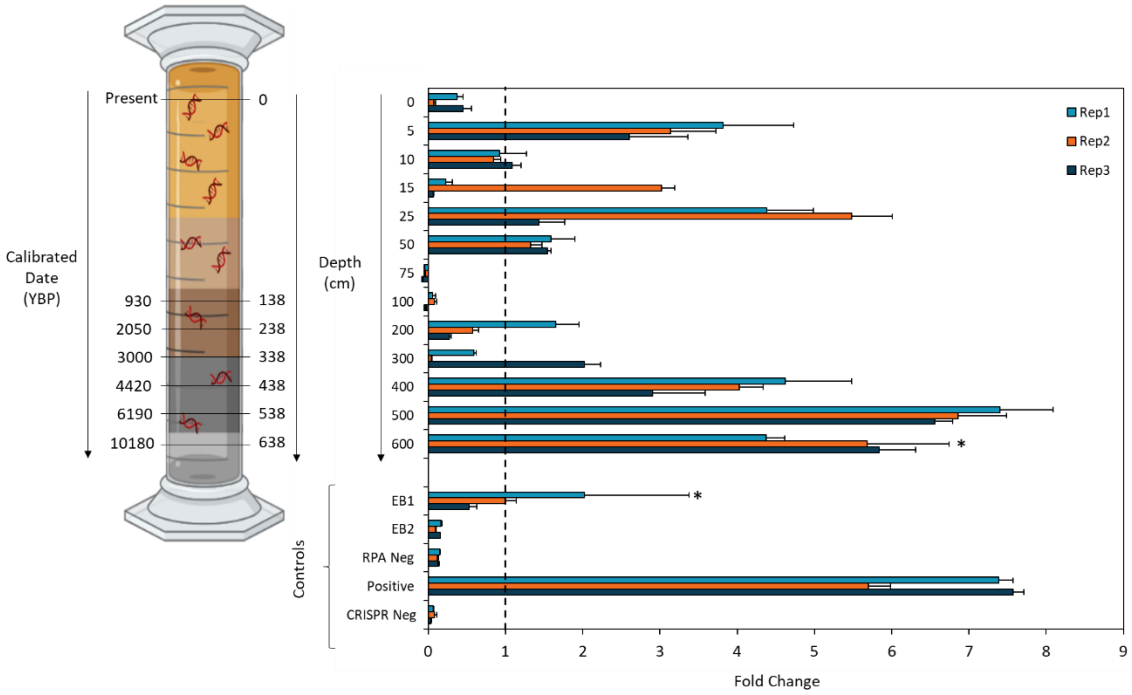

Figure 6.3 Detection of *S. salar* in Lough Feeagh sediment core samples using benchtop RPA-CRISPR-Cas analysis. Samples were incubated for 30 min at 37 °C. Fold-change values were calculated using fluorescence values (λex = 485 nm, λem = 535 nm) measured at 30 sec and 30 min. Error bars are mean fold-change ± fold-change standard deviation, where n = 3. The positive control consisted of 1 ng/µL *S. salar* DNA isolated from tissue. The RPA Neg refers to no template being added to the RPA stage of the method, whilst the CRISPR Neg contained molecular grade water instead of RPA product at the CRISPR detection stage of the protocol. EB, Extraction Blank. Rep 1, 2 & 3 refer to RPA replicates. * indicates replicates whereby the standard deviation of the raw fluorescence data is >0.5. These replicates were excluded from presence/absence analysis. Radiocarbon dating of the core was used to estimate the age of subsamples from six depths. These dates were converted to calibrated years before present (YBP) as represented in this figure.

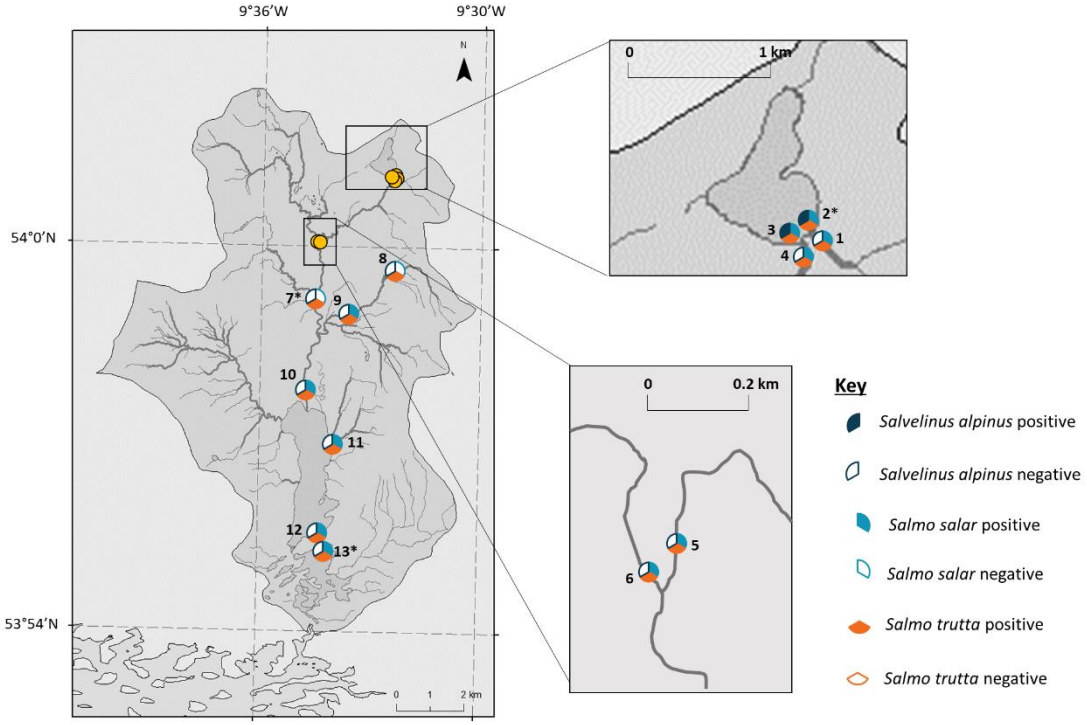

Figure 6.4 Monitoring of *S. alpinus, S. salar* and *S. trutta* in the Burrishoole Catchment using traditional methods. Filled in segments represent positive detection and empty segments represent negative detection. * Sites have differing results with RPA-CRISPR-Cas monitoring.

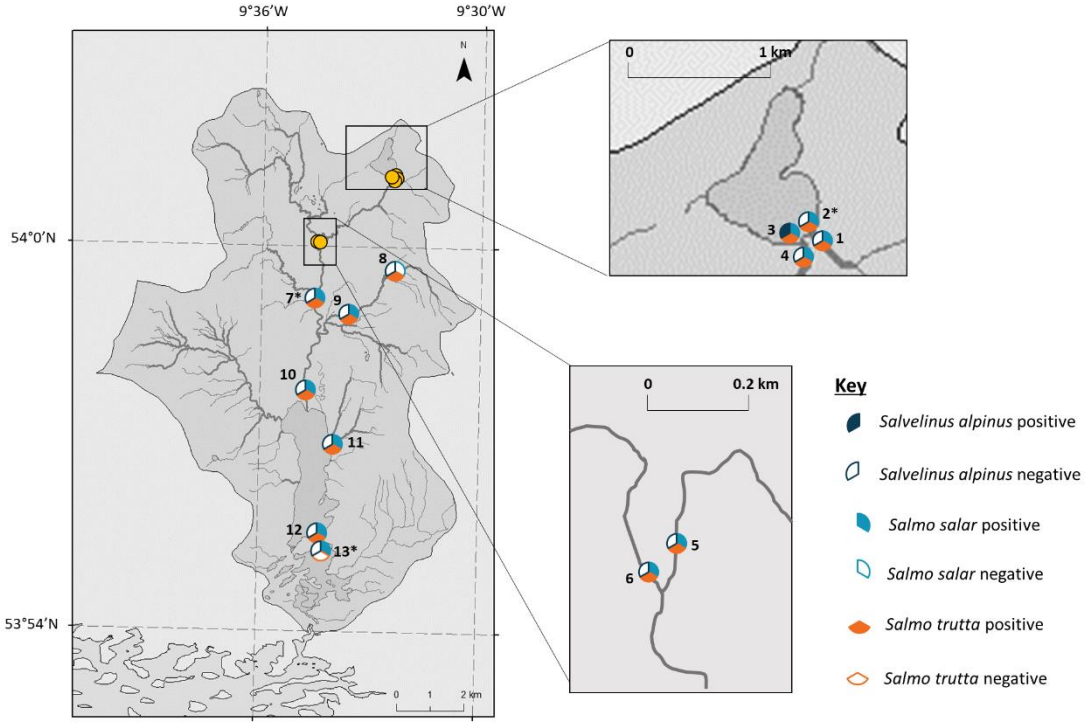

Figure 6.5 Salmonid monitoring of the Burrishoole Catchment using benchtop RPA-CRISPR-Cas. Filled in segments represent positive detection and empty segments represent negative detection. * Sites have differing results with traditional monitoring.

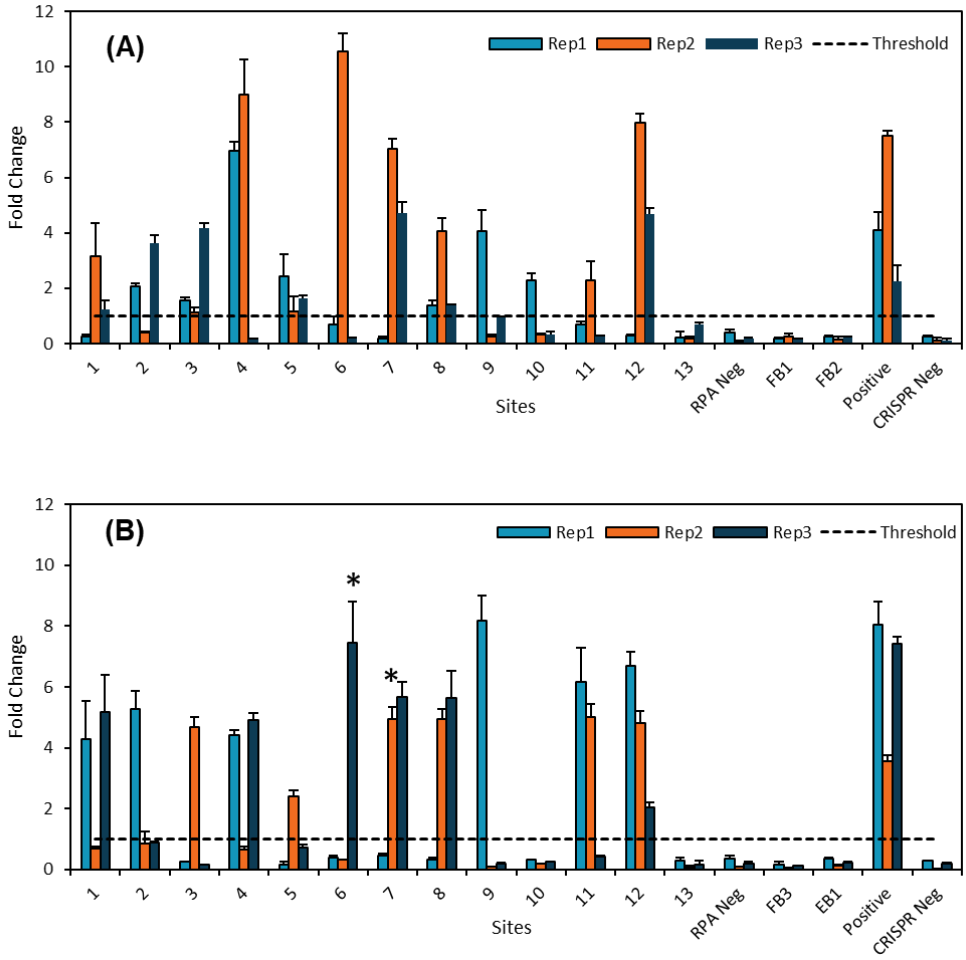

Figure 6.6 Detection of *S. trutta* in the Burrishoole Catchment using benchtop fluorescence RPA-CRISPR-Cas analysis. Samples were incubated for 30 min at 37 °C. Fold-change values were calculated using fluorescence values (λex = 485 nm, λem = 535 nm) measured at 30 sec and 30 min. Error bars are mean fold-change ± fold-change standard deviation, where n = 3. The positive control consisted of RPA product using 1 ng/µL *S. trutta* DNA isolated from tissue. The RPA Neg refers to no template being added to the RPA stage of the method, whilst the CRISPR Neg contained molecular grade water instead of RPA product at the CRISPR detection stage of the protocol. A fold-change threshold of 1 was used, with only values above this considered positive for *S. trutta.* EB, Extraction Blank. FB, Field Blank. Rep 1, 2 & 3 refer to RPA replicates. * indicates replicates whereby the standard deviation of the raw fluorescence data is >0.5. These replicates were excluded from presence/absence analysis. (A) Fold-change values from field replicate 1. (B) Fold-change values from field replicate 2.

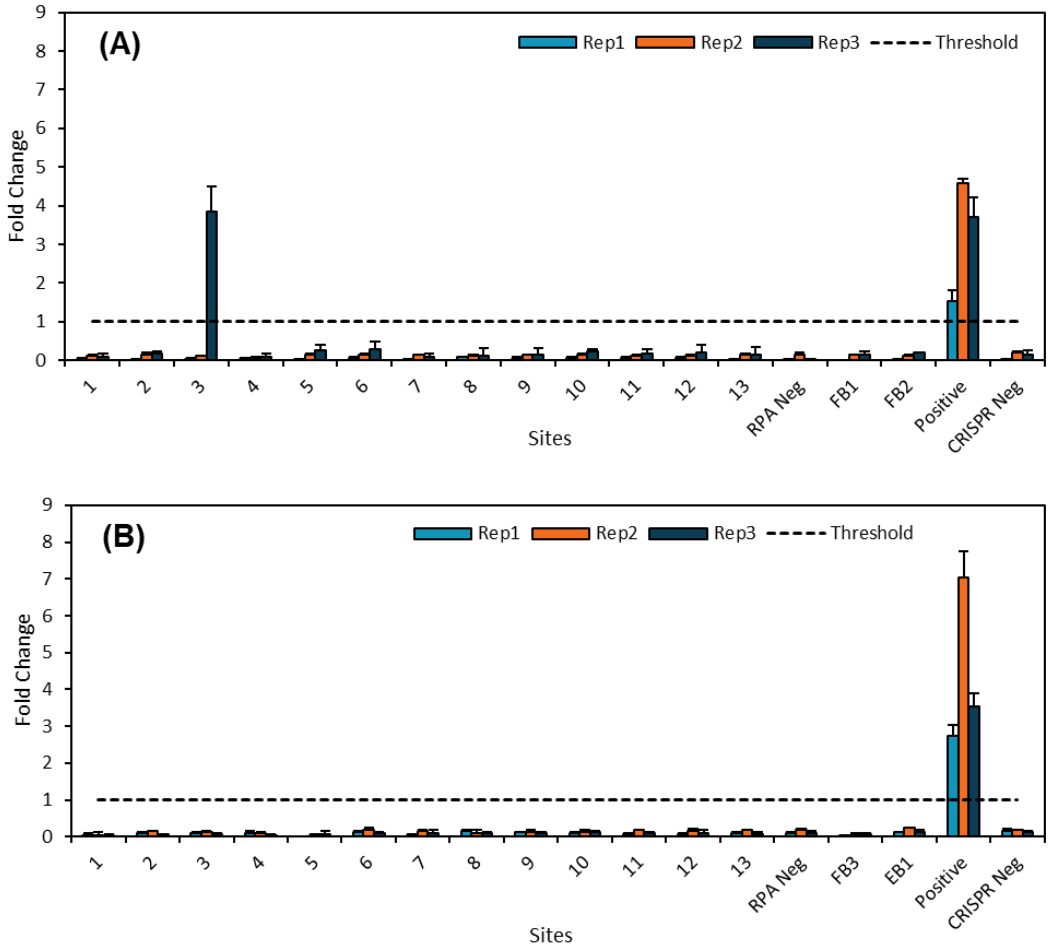

Figure 6.7 Detection of *S. alpinus* in the Burrishoole Catchment using benchtop fluorescence RPA-CRISPR-Cas analysis. Samples were incubated for 30 min at 37 °C. Fold-change values were calculated using fluorescence values (λex = 485 nm, λem = 535 nm) measured at 30 sec and 30 min. Error bars are mean fold-change ± fold-change standard deviation, where n = 3. The positive control consisted of RPA product using 1 ng/µL *S. alpinus* DNA isolated from tissue. The RPA Neg refers to no template being added to the RPA stage of the method, whilst the CRISPR Neg contained molecular grade water instead of RPA product at the CRISPR detection stage of the protocol. A fold-change threshold of 1 was used, with only values above this considered positive for *S. alpinus.* EB, Extraction Blank. FB, Field Blank. Rep 1, 2 & 3 refer to RPA replicates. (A) Fold-change values from field replicate 1. (B) Fold-change values from field replicate 2.

Table 6.2 C_T values and eDNA concentrations from Burrishoole Catchment Freshwater Samples.

Site		Field Rep	Average C_T ± St.Dev (n=3)[‡]	DNA Concentration (ng/L)[†]	No. of Positive Replicates (/3)
Fiddaunveela	1	1	34±0.03	0.76	3
		2	Undetermined[§]	Undetermined[§]	0
Bunaveela N	2	1	Undetermined[§]	Undetermined[§]	0
		2	36.9	0.07	1
Bunaveela S	3	1	36.47	0.16	1
		2	Undetermined[§]	Undetermined[§]	0
Goulaun Top	4	1	Undetermined[§]	Undetermined[§]	0
		2	Undetermined[§]	Undetermined[§]	0
Goulaun Bottom	5	1	33.85±0.22	0.84	3
		2	Undetermined[§]	Undetermined[§]	0
Altahoney	6	1	36.51±0.45	0.15	2
		2	33.76±0.05	1.31	3
Maumaratta	7	1	35.38±0.38	0.32	3
		2	34.32±0.59	0.89	3
Srahrevagh Top	8	1	Undetermined[§]	Undetermined[§]	0
		2	Undetermined[§]	Undetermined[§]	0
Srahrevagh Bottom	9	1	35.38±0.19	0.31	3
		2	34.73±0.33	0.58	3
Black	10	1	35.69±0.1	0.25	3
		2	35.31±0.56	0.36	3
Feeagh E	11	1	36.83±0.14	0.12	2
		2	35.82±0.26	0.21	3
Mill Race	12	1	36.04±0.387	0.21	3
		2	36.83	0.07	1
Furnace N	13	1	30.31±0.12	8.36	3
		2	30.25±0.05	17.55	3

[‡] The C_T values are indicative of the cycle number in which samples crossed the threshold into exponential amplification calculated using the second derivative maximum method. C_T values are reported as mean ± standard deviation for *S. salar* at each site.

[†]eDNA concentration in original field sample back-calculated from absolute DNA concentration from qPCR. Mean concentrations are given for each location.

[§] Undetermined used to describe samples with no *S. salar* detection or C_T values greater than 37 and thus above the LOD threshold.

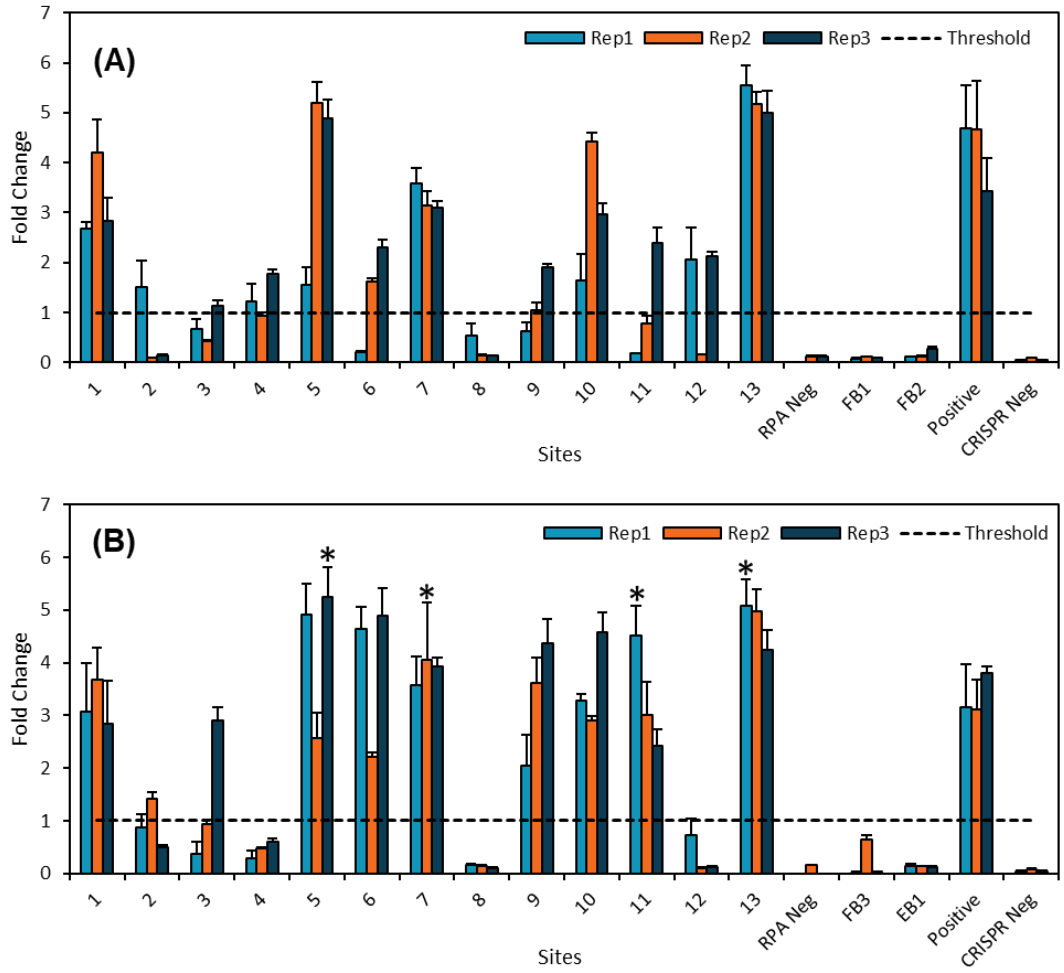

Figure 6.8 Detection of *S. salar* in the Burrishoole Catchment using benchtop fluorescence RPA-CRISPR-Cas analysis. Samples were incubated for 30 min at 37 °C. Fold-change values were calculated using fluorescence values (λex = 485 nm, λem = 535 nm) measured at 30 sec and 30 min. Error bars are mean fold-change ± fold-change standard deviation, where n = 3. The positive control consisted of RPA product using 1 ng/µL *S. salar* DNA isolated from tissue. The RPA Neg refers to no template being added to the RPA stage of the method, whilst the CRISPR Neg contained molecular grade water instead of RPA product at the CRISPR detection stage of the protocol. A fold-change threshold of 1 was used, with only values above this considered positive for *S. salar.* EB, Extraction Blank. FB, Field Blank. Rep 1, 2 & 3 refer to RPA replicates. * indicates replicates whereby the standard deviation of the raw fluorescence data is >0.5. These replicates were excluded from presence/absence analysis. (A) Fold-change values from field replicate 1. (B) Fold-change values from field replicate 2.

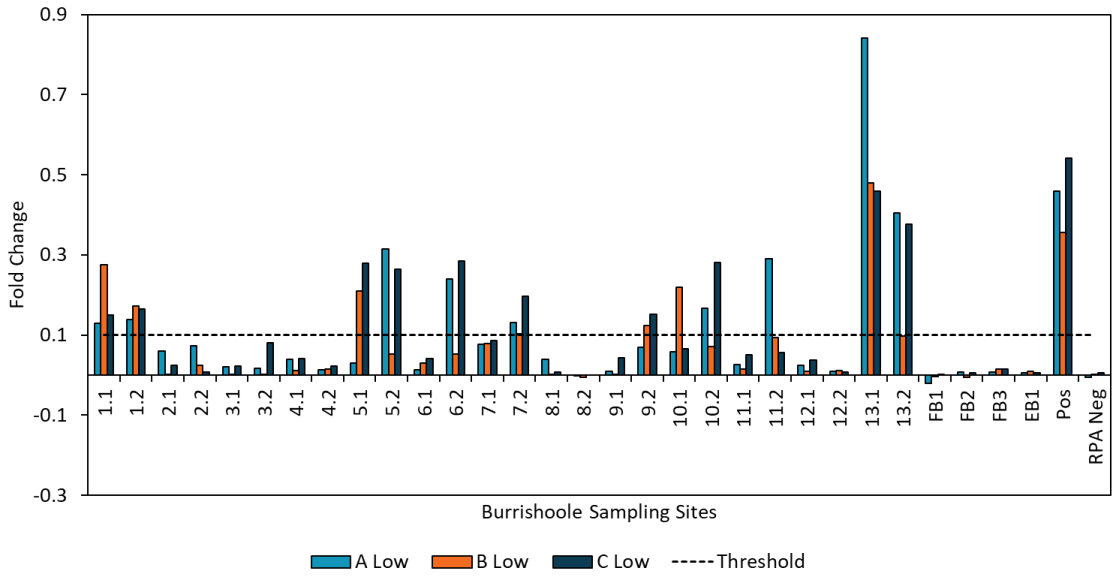

Figure 6.9 Detection of *S. salar* in the Burrishoole Catchment using RPA-CRISPR-Cas12a with fluorescence visualisation on the SensEDNA System. Samples were incubated for 30 min at 37 °C. Fold-change values were calculated using fluorescence values (λex = 485 nm, λem = 535 nm) measured at 10 sec and 30 min. The positive control consisted of RPA product using 1 ng/µL *S. salar* DNA isolated from tissue. The RPA Neg refers to no template being added to the RPA stage of the method. A fold-change threshold of 0.1 was used, with only values above this considered positive for *S. salar.* EB, Extraction Blank. FB, Field Blank. Each RPA replicate was visualised in a different chamber of the SensEDNA with the low fluorescence output reported (A low, B low and C low).

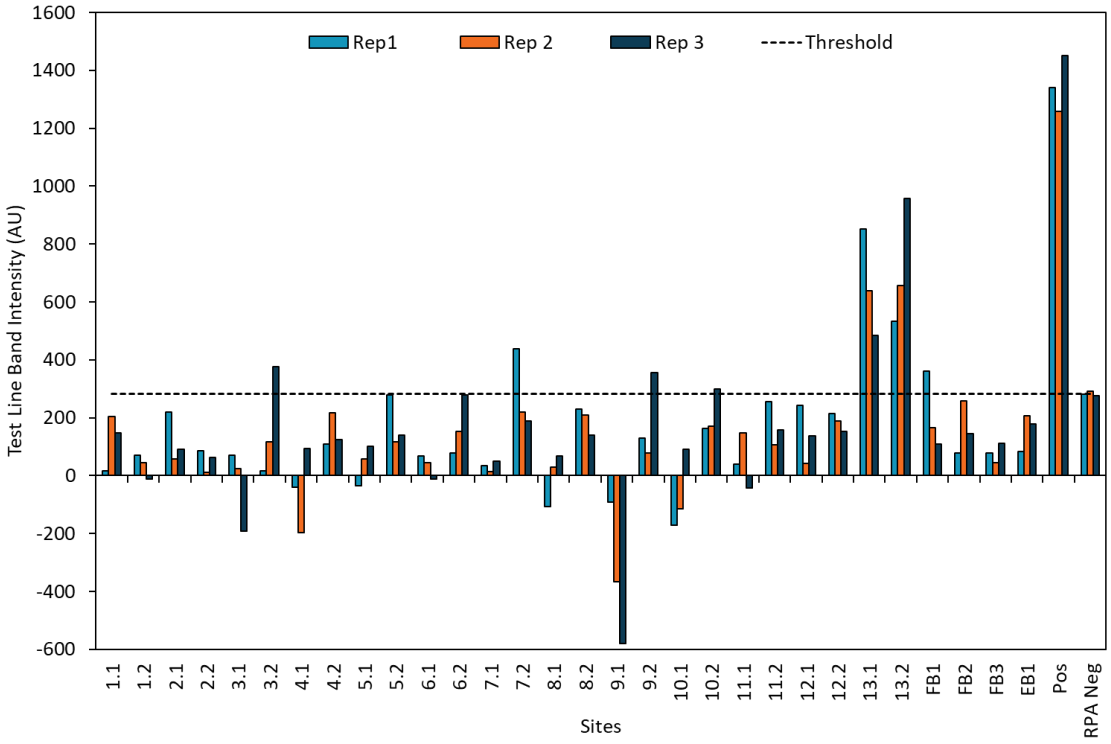

Figure 6.10 Detection of *S. salar* in the Burrishoole Catchment using RPA-CRISPR-Cas12a with lateral flow visualisation. Test band intensity reported based on analysis using GelQuant.Net. Samples were incubated for 30 min at 37 °C, prior to loading onto the lateral flow test strips. The positive control consisted of RPA product using 1 ng/µL *S. alpinus* DNA isolated from tissue. The RPA Neg refers to no template being added to the RPA stage of the method. The threshold was calculated based on band intensity analysis of the RPA negative test line. The value was set at the mean intensity for the replicates, with only band intensities greater than this considered positive for *S. salar.* EB, Extraction Blank. FB, Field Blank. Rep 1, 2 & 3 refer to RPA replicates.

Table 6.3 Comparison of all detection methodologies for *S. salar, S. trutta* and *S. alpinus* monitoring in the Burrishoole Catchment.

			Traditional Monitoring			qPCR	Benchtop CRISPR			SensEDNA	Lateral Flow
Site		**Field Rep**	**Salmon**	**Trout**	**Char**	**Salmon**	**Salmon**	**Trout**	**Char**	**Salmon**	**Salmon**
Fiddaunveela	1	1	Y	Y	N	3	3	2	0	3	0
		2				0	3	2	0	3	0
Bunaveela N	2	1	Y	Y	Y	0	1	2	0	0	0
		2				1	1	1	0	0	0
Bunaveela S	3	1	Y	Y	Y	1	1	3	1	0	0
		2				0	1	1	0	0	1
Goulaun Top	4	1	Y	Y	N	0	2	2	0	0	0
		2				0	0	2	0	0	0
Goulaun Bottom	5	1	Y	Y	N	3	3	3	0	2	0
		2				0	2	1	0	2	0
Altahoney	6	1	Y	Y	N	2	2	1	0	0	0
		2				3	3	0	0	2	0
Maumaratta	7	1	N	Y	N	3	3	2	0	0	0
		2				3	2	1	0	3	1
Srahrevagh Top	8	1	N	Y	N	0	0	3	0	0	0
		2				0	0	2	0	0	0
Srahrevagh Bottom	9	1	Y	Y	N	3	2	1	0	0	0
		2				3	3	1	0	2	1
Black	10	1	Y	Y	N	3	3	1	0	1	0
		2				3	3	0	0	2	1
Feeagh E	11	1	Y	Y	N	2	1	1	0	0	0
		2				3	2	2	0	1	0
Mill Race	12	1	Y	Y	N	3	2	2	0	0	0
		2				1	0	3	0	0	0
Furnace N	13	1	Y	Y	N	3	3	0	0	3	3
		2				3	2	0	0	2	3

Y/N refer to presence or absence of species monitored using traditional surveys. Detection with molecular methods (qPCR and RPA-CRISPR-Cas) is reported based on the number of positive replicates (/3).

Chapter 7. Conclusions

7.1. Conclusions

7.1.1. General

Rapid monitoring of aquatic organisms is essential for preserving the Earth's biodiversity, which is currently at risk due to the increasing threat of climate change (Revenga *et al.*, 2005; WWF, 2020). Management and conservation of aquatic species requires knowledge of distribution, traditionally gained through visual detection. However, such methodologies are expensive, labour intensive and can cause harm to the target organisms (Snyder, 2003). The use of environmental DNA (eDNA) offers a solution, using non-invasive molecular techniques to detect DNA shed into the environment (Thomsen and Willerslev, 2015). Despite this, current eDNA techniques, primarily using qPCR, are limited to the laboratory and require highly skilled individuals to perform experimentation. There is thus a drive to develop point-of-use systems which would enable rapid, on-site detection of species of interest.

This project aimed to develop a novel biosensor platform for the detection of single species using eDNA. The vision for the system involved a single sensor that can be used at multiple sites with minimal sample handling, whilst maintaining the high levels of sensitivity and target specificity seen with laboratory-based monitoring. The device should have the minimum number of steps required, run at low temperatures and ideally use an optical transducer. The project focused on the detection of salmonid species, *S. salar, S. trutta* and *S. alpinus,* within freshwater ecosystems, with a particular interest in monitoring of the Burrishoole Catchment, Co. Mayo, Ireland. These species are of ecological, economic and cultural importance, and are likely to be highly susceptible to the effects of climate change (de Eyto *et al.*, 2020). Consequently, it is vital that conservation efforts are made to prevent further vulnerability. As outlined in Chapter 1.5, the project had three main aims: the development of a biological assay for single species detection using eDNA, the adaptation of this assay to a biosensor device suitable for on-site monitoring and field validation of the developed methodology specifically for salmonid monitoring.

7.1.2. Chapter observations

Chapter 3 involved the development of a qPCR-based assay for *S. salar,* in line with the gold standard laboratory approach (Langlois *et al.*, 2020) and previously developed biosensors in other fields (Zhang and Xing, 2007). The development of a conventional eDNA detection method allowed verification of the eDNA workflow, including water sampling, contamination prevention, eDNA extraction and molecular detection, whilst simultaneously highlighting the utility of the eDNA approach for *S. salar.* The SsaCOI470 assay developed in Chapter 3, successfully detected *S. salar* eDNA from the Srahrevagh River demonstrating its applicability for environmental monitoring (Table 3.2). Despite this, limitations arose when considering the adaptability of qPCR as the bio-receptor of a sensor. Although commercial qPCR systems, such as Biomeme^{TM}, have been used in the field (Thomas *et al.*, 2019), they are limited in use due to their high expense, lower detection probabilities and greater influence from inhibitors than laboratory-based approaches (Sepulveda *et al.*, 2018). In addition, PCR-based methods require high temperatures and thermal cycling which make them difficult to adapt to a cheaper, custom-built sensor. For these reasons, an alternative molecular assay was sought with the goal to align more closely with the initial biosensor vision.

To meet this vision, chapter 4 involved the adaption of an isothermal method using RPA and CRISPR-Cas technology to eDNA monitoring. RPA is able to achieve exponential amplification of target DNA following a short incubation at 37-42 °C (Piepenburg *et al.*, 2006) and has successfully been used for detection of harmful algae (Toldrà *et al.*, 2019) and parasites from water and soil (Wu *et al.*, 2017). However, when used in isolation, RPA may lack specificity (Kaminski *et al.*, 2021) and thus is preferably coupled to specific detection, such as CRISPR-Cas technology. The CRISPR-Cas system, more commonly known for its role in genome editing, enables highly specific sequence recognition (Kaminski *et al.*, 2021); and by harnessing the collateral cleavage activity of the type V nuclease, Cas12a, is amenable to diagnostics (Chen *et al.*, 2018).

Chapter 4 presents the first use of CRISPR-Cas diagnostics for environmental monitoring. In this chapter, species specific assays are developed for *S. salar, S. trutta* and *S. alpinus,* with successful detection of *S. salar* seen in sites from Ireland and eastern Canada (Figures 4.11, 4.17, 4.18). These results highlight the utility of RPA-CRISPR-Cas in eDNA monitoring and suggest an alternative method to qPCR. As a field, CRISPR diagnostics is still in its infancy with the first paper, using a Cas nuclease with collateral cleavage activity, published by Gootenberg *et al.*, (2017). Since then, the number of studies has expanded, with 289 papers published in 2021 (based on a Scopus search for "CRISPR diagnostics").

Nevertheless, the infancy of this field means there are still lots of questions around the specific details of the method, such as cut-off thresholds (as discussed in Chapter 4.4), and the overall potential of this technology. For example, the method developed in this thesis is effectively end-point detection, whereby the target is fully amplified and then detected. Previously published DETECTR (Chen *et al.*, 2018), SHERLOCK (Gootenberg *et al.*, 2017) and HOLMES (Li *et al.*, 2018) assays are the same, meaning they are unable to quantify the amount of target DNA and are only qualitative. However, over time it is likely that a more quantitative aspect of CRISPR-Cas assays will develop as the enzyme kinetics of the various Cas nucleases are more fully explored (Cofsky *et al.*, 2020). To this extent, several more recent publications have alluded to quantification of target using isothermal amplification and CRISPR-Cas detection. In SHERLOCK v2 (Gootenberg *et al.*, 2018), quantitative accuracy is enhanced by lowering RPA primer concentrations to prevent saturation of the reaction. A concentration of 240 nM exhibited the greatest correlation between fluorescence signal and target input allowing for quantification as low as the attomolar range (Gootenberg *et al.*, 2018). HOLMES v2 (Li *et al.*, 2019) combined LAMP and Cas12b detection into a one-pot assay and measured fluorescence using a real-time plate reader. This enabled quantification of a plasmid target as low as 10^{-8} nM and generated a standard curve with R^2 value of 0.9934 (Li *et al.*, 2019). To further the accuracy of quantification, Wu *et al.*, (2021) developed WS-RADICA which involves combining a one-pot RT-LAMP and Cas12b detection assay with commercially available digital chips. The assay works similarly to ddPCR whereby the reaction is

divided into thousands of nanolitre reaction wells and the ratio of fluorescence-positive wells to all reaction wells is counted (Wu *et al.*, 2021). This enabled absolute quantification of SARS-CoV-2 in 60 min (Wu *et al.*, 2021). It is possible that such developments from the field of medical diagnostics could be applied to environmental monitoring to enable quantitative detection of eDNA.

Additionally, it is possible that CRISPR-Cas methods can be multiplexed to enable detection of multiple species in a single assay. Li *et al.*, (2019) discuss the potential of CRISRP-Cas multiplexed biosensing and suggest strategies such as Cas effector-based and separation-based multiplexing. Gootenberg *et al.*, (2018) achieved effector-based multiplexing of four targets by using four different nucleases (LwaCas13a, PsmCas13b, CcaCas13b and AsCas12a) with different nucleotide cutting preferences. This approach is limited by the elucidation of different Cas enzymes which may take a long time, however it could enable the incorporation of an internal positive control allowing detection of assay inhibition or early reporter cleavage. On the other hand, Shao *et al.*, (2019) used a physical separation strategy to enable multiplexed biosensing. Their platform involved separating Cas effectors and varying gRNA sequences into different microfluidic channels whereby each channel supports detection of a different target sequence (Shao *et al.*, 2019). This microfluidic approach is the most promising for multiplexed eDNA assays as it is not restricted by advancements in CRISPR biotechnology.

To facilitate the RPA-CRISPR-Cas assay as an on-site detection tool, Chapter 5 involved the development of two sensing platforms; a custom portable fluorometer and lateral flow. The previously developed ColiSense system (Heery *et al.*, 2016) was modified to enable DNA detection using the RPA-CRISPR-Cas methodology and renamed SensEDNA. In addition, the application of commercial lateral flow strips (HybriDetect) was explored due to their advantageous, by eye read out. Both systems maintained the sensitivity of the original benchtop assay when using genomic DNA, allowing detection of *S. salar* down to a concentration of 0.046 pg/µL. Nonetheless, a major limitation of these

platforms is the number of sample handling steps required. Investigation into a one-pot assay on a benchtop platform showed reduced sensitivity, with a low of 46 pg/µL *S. salar* DNA detected after 30 min incubation. Approaches, such as the DAMR system described by Yin *et al.*, (2020) and discussed in Chapter 5.4, may need to be investigated to overcome such challenges. Whilst further optimisation is required to enhance these systems (as discussed in Chapter 5.4), they fulfil multiple requirements of the WHO ASSURED guidelines and the initial sensing vision; specificity and sensitivity are maintained, visualisation is optical, low isothermal temperatures are used and readouts are simplified without complex instrumentation.

Chapter 6 involved field validation of the developed methodology specifically for salmonid monitoring in the Burrishoole Catchment. *S. trutta* and *S. alpinus* presence was monitored from freshwater using the RPA-CRISPR-Cas specific assays developed in Chapter 4, and showed comparable detection with traditional techniques (Table 6.3). Furthermore, historical presence of *S. salar* in the catchment was assessed by examining sediment core samples using qPCR and benchtop RPA-CRISPR-Cas. The qPCR assay was unsuccessful in detecting *S. salar* at any depth of the core. This result was unexpected as previous studies have shown the utility of a PCR-based approach to detect fish species from sedaDNA (Kuwae *et al.*, 2020) and suggests a lack of sensitivity with the developed SsaCOI470 assay leading to false negatives, as is common when working with ancient samples (Olajos *et al.*, 2018). On the other hand, RPA-CRISPR-Cas showed positive *S. salar* presence in at least 2 replicates at six depths of the core (Figure 6.3). This data suggests that RPA-CRISPR-Cas may be superior to qPCR when analysing sedaDNA and less susceptible to environmental inhibitors. Whilst further work is needed to investigate the effect of such inhibitors on this method (as discussed in Chapter 6.4), it offers great promise to be used when qPCR is unsuitable. Furthermore, the addition of known negative samples (sites or depths) would help elucidate the false positivity rate of RPA-CRISPR-Cas assays.

Chapter 6 additionally showed the applicability of the two sensing systems, developed in Chapter 5, for environmental monitoring. Compared to the benchtop approach, both SensEDNA and lateral flow had a higher number of false negative detections (Table 6.3). This indicates reduced sensitivity when investigating environmental samples whereby the sample matrix is complex and there is a high concentration of non-target DNA. A lack of sensitivity is particularly prevalent in the RPA-CRISPR-Cas lateral flow assay, with only one site showing positive *S. salar* presence in more than one replicate (Figure 6.10). This effect was not seen in the first lateral flow assay published for eDNA, which combined PCR with lateral flow and successfully detected *Acanthaster cf. solaris* from field samples (Doyle and Uthicke, 2021). However, the reliance of this method on PCR means that although the read-out may be simplified, the amplification of target DNA still requires complex instrumentation not suitable to in-field monitoring. To overcome the sensitivity limitations with RPA-CRISPR-Cas, it is possible that LF strips specific to CRISPR-Cas diagnostics are required or that sample incubation time needs to be increased to allow for greater reporter cleavage.

Furthermore, Chapter 6 showed that SensEDNA has great potential as a rapid eDNA sensing platform with *S. salar* successfully detected at eight of the twelve sites with known presence (Table 6.3). This platform removes the need for complex instrumentation and shows rapid detection on a simple device with incubating and fluorescence capabilities. Whilst SensEDNA progresses the field towards on-site monitoring, it is important to note a major limitation with portable eDNA detection, primarily the inability to extract eDNA in the field. Most existing eDNA assays require an initial 'clean up' step with extraction of DNA from a filter using a laboratory-based method such as phenol-chloroform extraction (Atkinson *et al.*, 2018) or a DNA extraction kit (Thomsen *et al.*, 2012). This current requirement limits the use of eDNA detection in the field and highlights the need for new methodology to be developed. One potential option is the direct amplification of DNA from filter paper as in screening tests of whole blood from Guthrie cards (Makowski *et al.*, 1997). This would enable water to be filtered on-site and added directly to the biosensor device enabling complete in-field assessment of eDNA. It has previously been shown that nucleic acids

can be amplified, using PCR, directly from a cellulose paper filter from plant, animal and microbe samples following a single wash step (Zou *et al.*, 2017), although there has been little investigation into the direct use of RPA from filters and the direct amplification of eDNA from filters. Exploration into such methodologies is required if in-field eDNA monitoring is to truly be a reality.

7.1.3. Contributions and concluding remarks

Overall, this thesis presents the first application of CRISPR-Cas diagnostics to eDNA monitoring and progresses the field towards an in-field sensor whilst expanding both the eDNA and CRISPR-Cas toolbox. Not only is the required instrumentation simplified compared to qPCR sensors (such as Biomeme^{TM}), but the molecular method may well be less susceptible to inhibitors (as discussed in Chapter 4.4 and suggested in Chapter 6.4). In addition, such a method could be applied to any species and may have use in early warning of invasive species, detection of harmful algae blooms (Durán-Vinet *et al.*, 2021) and detection of environmental pathogens (Liu and Li, 2020).

Bibliography

(OTA), O. of T.A. (1987) *Technologies to maintain biological diversity*. Washington, D.C.

Abudayyeh, O.O., Gootenberg, J.S., Konermann, S., Joung, J., Slaymaker, I.M., Cox, D.B.T., Shmakov, S., Makarova, K.S., Semenova, E., Minakhin, L., Severinov, K., Regev, A., Lander, E.S., Koonin, E. V. and Zhang, F. (2016) 'C2c2 is a single-component programmable RNA-guided RNA-targeting CRISPR effector', *Science*, 353(6299). doi:10.1126/science.aaf5573.

Adli, M. (2018) 'The CRISPR tool kit for genome editing and beyond', *Nature Communications*, 9(1), p. 1911. doi:10.1038/s41467-018-04252-2.

Alvarado-Quesada, I. and Weikard, H.-P. (2017) 'International Environmental Agreements for biodiversity conservation: a game-theoretic analysis', *International Environmental Agreements: Politics, Law and Economics 2017 17:5*, 17(5), pp. 731–754. doi:10.1007/S10784-017-9368-7.

Aman, R., Mahas, A. and Mahfouz, M. (2020) 'Nucleic Acid Detection Using CRISPR/Cas Biosensing Technologies', *ACS Synthetic Biology*, 9(6), pp. 1226–1233. doi:10.1021/acssynbio.9b00507.

Antognazza, C.M., Britton, J.R., Potter, C., Franklin, E., Hardouin, E.A., Gutmann Roberts, C., Aprahamian, M. and Andreou, D. (2019) 'Environmental DNA as a non-invasive sampling tool to detect the spawning distribution of European anadromous shads (Alosa spp.)', *Aquatic Conservation: Marine and Freshwater Ecosystems*, 29(1), pp. 148–152. doi:10.1002/aqc.3010.

Araki, H. and Schmid, C. (2010) 'Is hatchery stocking a help or harm?: Evidence, limitations and future directions in ecological and genetic surveys', *Aquaculture*, 308(SUPPL.1), pp. S2–S11. doi:10.1016/J.AQUACULTURE.2010.05.036.

Arismendi, I., Soto, D., Penaluna, B., Jara, C., Leal, C. and Leon-Munoz, J. (2009) 'Aquaculture, non-native salmonid invasions and associated declines of native fishes in Northern Patagonian lakes', *Freshwater Biology*, 54(5), pp. 1135–1147. doi:10.1111/J.1365-2427.2008.02157.X.

Arora, P., Sindhu, A., Dilbaghi, N. and Chaudhury, A. (2011) 'Biosensors as innovative tools for the detection of food borne pathogens', *Biosensors and Bioelectronics*, 28(1), pp. 1–12. doi:10.1016/J.BIOS.2011.06.002.

Asiello, P. and Baeumner, A. (2011) 'Miniaturised isothermal nucleic acid amplification, a review', *Lab on a Chip*, 11(8), p. 1420.

Atkinson, S., Carlsson, J.E.L., Ball, B., Egan, D., Kelly-Quinn, M., Whelan, K. and Carlsson, J. (2018) 'A quantitative PCR-based environmental DNA assay for detecting Atlantic salmon (*Salmo salar* L.)', *Aquatic Conservation: Marine and Freshwater Ecosystems*, 28(5), pp. 1238–1243.

doi:10.1002/aqc.2931.

Auroux, P.-A., Koc, Y., deMello, A., Manz, A. and Day, P.J.R. (2004) 'Miniaturised nucleic acid analysis', *Lab on a Chip*, 4(6), p. 534. doi:10.1039/b408850f.

Bacon, P.J., Palmer, S.C.F., MacLean, J.C., Smith, G.W., Whyte, B.D.M., Gurney, W.S.C. and Youngson, A.F. (2009) 'Empirical analyses of the length, weight, and condition of adult Atlantic salmon on return to the Scottish coast between 1963 and 2006', *ICES Journal of Marine Science*, 66(5), pp. 844–859. doi:10.1093/ICESJMS/FSP096.

Bai, J., Lin, H., Li, H., Zhou, Y., Liu, J., Zhong, G., Wu, L., Jiang, W., Du, H., Yang, J., Xie, Q. and Huang, L. (2019) 'Cas12a-Based On-Site and Rapid Nucleic Acid Detection of African Swine Fever', *Frontiers in Microbiology*, 10, p. 2830. doi:10.3389/fmicb.2019.02830.

Baker, C.S., Steel, D., Nieukirk, S. and Klinck, H. (2018) 'Environmental DNA (eDNA) From the Wake of the Whales: Droplet Digital PCR for Detection and Species Identification', *Frontiers in Marine Science*, 5, p. 133. doi:10.3389/fmars.2018.00133.

Baldigo, B.P., Sporn, L.A., George, S.D. and Ball, J.A. (2017) 'Efficacy of Environmental DNA to Detect and Quantify Brook Trout Populations in Headwater Streams of the Adirondack Mountains, New York', *Transactions of the American Fisheries Society*, 146(1), pp. 99–111. doi:10.1080/00028487.2016.1243578.

Barman, A., Deb, B. and Chakraborty, S. (2019) 'A glance at genome editing with CRISPR–Cas9 technology', *Current Genetics 2019 66:3*, 66(3), pp. 447–462. doi:10.1007/S00294-019-01040-3.

Barnes, M.A., Turner, C.R., Jerde, C.L., Renshaw, M.A., Chadderton, W.L. and Lodge, D.M. (2014) 'Environmental Conditions Influence eDNA Persistence in Aquatic Systems', *Environmental Science and Technology*, 48(3), pp. 1819–1827. doi:10.1021/ES404734P.

Barrangou, R. and Doudna, J.A. (2016) 'Applications of CRISPR technologies in research and beyond', *Nature Biotechnology*, 34(9), pp. 933–941. doi:10.1038/nbt.3659.

Bayley, H. (2015) 'Nanopore Sequencing: From Imagination to Reality', *Clinical Chemistry*, 61(1), pp. 25–31. doi:10.1373/CLINCHEM.2014.223016.

Beans, C. (2018) 'Core Concept: Environmental DNA helps researchers track pythons and other stealthy creatures.', *Proceedings of the National Academy of Sciences of the United States of America*, 115(36), pp. 8843–8845. doi:10.1073/pnas.1811906115.

Beng, K.C. and Corlett, R.T. (2020) 'Applications of environmental DNA (eDNA) in ecology and conservation: opportunities, challenges and prospects', *Biodiversity and Conservation*, 29, pp. 2089–2121. doi:10.1007/s10531-020-01980-0.

Biggs J, Ewald N, Valentini A, Gaboriaud C, Ra, G., Foster J, Wilkinson J, Arnett A, Williams P and Dunn F (2014) *Analytical and methodological development for improved surveillance of the Great Crested Newt. Appendix 5. Technical advice note for field and laboratory sampling of great crested newt (Triturus cristatus) environmental DNA.* Oxford.

Bodulev, O.L. and Sakharov, I.Y. (2020) 'Isothermal Nucleic Acid Amplification Techniques and Their Use in Bioanalysis', *Biochemistry. Biokhimiia*, 85(2), p. 147. doi:10.1134/S0006297920020030.

Boothroyd, M., Mandrak, N.E., Fox, M. and Wilson, C.C. (2016) 'Environmental DNA (eDNA) detection and habitat occupancy of threatened spotted gar (Lepisosteus oculatus)', *Aquatic Conservation: Marine and Freshwater Ecosystems*, 26(6), pp. 1107–1119. doi:10.1002/aqc.2617.

Bora, U., Bora, U., Sett, A. and Singh, D. (2013) 'Nucleic Acid Based Biosensors for Clinical Applications', *Biosensors Journal*, 02(01), pp. 1–8. doi:10.4172/2090-4967.1000104.

Breitbach, A. (2020) *Lateral Flow Readout for CRISPR/Cas-based detection strategies*. Available at: https://www.milenia-biotec.com/en/tips-lateral-flow-readouts-crispr-cas-strategies/ (Accessed: 12 January 2021).

Briciu-Burghina, C., Heery, B., Duffy, G., Brabazon, D. and Regan, F. (2019) 'Demonstration of an optical biosensor for the detection of faecal indicator bacteria in freshwater and coastal bathing areas', *Analytical and Bioanalytical Chemistry*, 411(29), pp. 7637–7643. doi:10.1007/s00216-019-02182-6.

Broadhurst, H.A., Gregory, L.M., Bleakley, E.K., Perkins, J.C., Lavin, J. V, Bolton, P., Browett, S.S., Howe, C. V, Tansley, D., Guimarães Sales, N. and McDevitt, A.D. (2021) 'Title: 1 Mapping differences in mammalian distributions and diversity using environmental 2 DNA from rivers 3 4 Authors', *bioRxiv*, p. 2021.04.27.441610. doi:10.1101/2021.04.27.441610.

Broughton, J.P., Deng, X., Yu, G., Fasching, C.L., Servellita, V., Singh, J., Miao, X., Streithorst, J.A., Granados, A., Sotomayor-Gonzalez, A., Zorn, K., Gopez, A., Hsu, E., Gu, W., Miller, S., Pan, C.Y., Guevara, H., Wadford, D.A., Chen, J.S. and Chiu, C.Y. (2020) 'CRISPR–Cas12-based detection of SARS-CoV-2', *Nature Biotechnology*, 38(7), pp. 870–874. doi:10.1038/s41587-020-0513-4.

Bunn, S.E. and Arthington, A.H. (2002) 'Basic Principles and Ecological Consequences of Altered

Flow Regimes for Aquatic Biodiversity', *Environmental Management 2002 30:4*, 30(4), pp. 492–507. doi:10.1007/S00267-002-2737-0.

Bustin, S.A., Benes, V., Garson, J.A., Hellemans, J., Huggett, J., Kubista, M., Mueller, R., Nolan, T., Pfaffl, M.W., Shipley, G.L., Vandesompele, J. and Wittwer, C.T. (2009) 'The MIQE Guidelines: Minimum Information for Publication of Quantitative Real-Time PCR Experiments', *Clinical Chemistry*, 55(4), pp. 611–622. doi:10.1373/CLINCHEM.2008.112797.

Bustin, S.A. and Mueller, R. (2005) 'Real-time reverse transcription PCR (qRT-PCR) and its potential use in clinical diagnosis', *Clinical Science*, pp. 365–379. doi:10.1042/CS20050086.

Butler, S.A., Khanlian, S.A. and Cole, L.A. (2001) 'Detection of Early Pregnancy Forms of Human Chorionic Gonadotropin by Home Pregnancy Test Devices', *Clinical Chemistry*, 47(12), pp. 2131–2136. doi:10.1093/CLINCHEM/47.12.2131.

Bylemans, J., Furlan, E.M., Hardy, C.M., McGuffie, P., Lintermans, M. and Gleeson, D.M. (2017) 'An environmental DNA-based method for monitoring spawning activity: a case study, using the endangered Macquarie perch (*Macquaria australasica*)', *Methods in Ecology and Evolution*. Edited by M. Gilbert, 8(5), pp. 646–655. doi:10.1111/2041-210X.12709.

Caesar, R.M., Sorensson, M. and Cognato, A.I. (2006) 'Integrating DNA data and traditional taxonomy to streamline biodiversity assessment: an example from edaphic beetles in the Klamath ecoregion, California, USA', *Diversity and Distributions*, 12(5), pp. 483–489. doi:10.1111/j.1366-9516.2006.00237.x.

Cai, W., Ma, Z., Yang, C., Wang, L., Wang, W., Zhao, G., Geng, Y. and Yu, D. (2017) 'Using eDNA to detect the distribution and density of invasive crayfish in the Honghe-Hani rice terrace World Heritage site', *PLoS ONE*, 12(5), p. e0177724.

Capo, E., Spong, G., Norman, S., Königsson, H., Bartels, P. and Byström, P. (2019) 'Droplet digital PCR assays for the quantification of brown trout (Salmo trutta) and Arctic char (Salvelinus alpinus) from environmental DNA collected in the water of mountain lakes', *PLOS ONE*. Edited by A. Palsson, 14(12), p. e0226638. doi:10.1371/journal.pone.0226638.

Caraguel, C.G.B., Stryhn, H., Gagné, N., Dohoo, I.R. and Hammell, K.L. (2011) 'Selection of a cutoff value for real-time polymerase chain reaction results to fit a diagnostic purpose: analytical and epidemiologic approaches.', *Journal of veterinary diagnostic investigation : official publication of the American Association of Veterinary Laboratory Diagnosticians, Inc*, 23(1), pp. 2–15. doi:10.1177/104063871102300102.

Carim, K.J., McKelvey, K.S., Young, M.K., Wilcox, T.M. and Schwartz, M.K. (2016) *A protocol for collecting environmental DNA samples from streams. General Technical Report RMRS-GTR-355*, *United States Department of Agriculture*. Available at: https://www.fs.fed.us/rm/pubs/rmrs_gtr355.pdf%255Cnhttps://www.treesearch.fs.fed.us/pubs/52466.

Carlsson, J.E.L., Egan, D., Collins, P.C., Farrell, E.D., Igoe, F. and Carlsson, J. (2017) 'A qPCR MGB probe based eDNA assay for European freshwater pearl mussel (*Margaritifera margaritifera* L.)', *Aquatic Conservation: Marine and Freshwater Ecosystems*, 27(6), pp. 1341–1344. doi:10.1002/aqc.2788.

Carvalho, S., Aylagas, E., Villalobos, R., Kattan, Y., Berumen, M. and Pearman, J.K. (2019) 'Beyond the visual: Using metabarcoding to characterize the hidden reef cryptobiome', *Proceedings of the Royal Society B: Biological Sciences*, 286(1896). doi:10.1098/rspb.2018.2697.

Cassedy, A., Parle-McDermott, A. and O'Kennedy, R. (2021) 'Virus Detection: A Review of the Current and Emerging Molecular and Immunological Methods', *Frontiers in Molecular Biosciences*, 0, p. 76. doi:10.3389/FMOLB.2021.637559.

Cassina, F., Dalton, C., Dillane, M., de Eyto, E., Poole, R. and Sparber, K. (2013) 'A multi-proxy palaeolimnological study to reconstruct the evolution of a coastal brackish lake (Lough Furnace, Ireland) during the late Holocene', *Palaeogeography, Palaeoclimatology, Palaeoecology*, 383–384, pp. 1–15. doi:10.1016/J.PALAEO.2013.04.016.

Chaput, G. (2012) 'Overview of the status of Atlantic salmon (Salmo salar) in the North Atlantic and trends in marine mortality', *ICES Journal of Marine Science*, 69(9), pp. 1538–1548. doi:10.1093/icesjms/fss013.

Chen, J.S., Ma, E., Harrington, L.B., Costa, M. Da, Tian, X., Palefsky, J.M. and Doudna, J.A. (2018) 'CRISPR-Cas12a target binding unleashes indiscriminate single-stranded DNase activity', *Science*, 360(6387), pp. 436–439. doi:10.1126/SCIENCE.AAR6245.

Chiba, S., Batten, S., Martin, C.S., Ivory, S., Miloslavich, P. and Weatherdon, L. V (2018) 'Zooplankton monitoring to contribute towards addressing global biodiversity conservation challenges', *Journal of Plankton Research*, 40(5), pp. 509–518. doi:10.1093/plankt/fby030.

Clark, L.C. and Lyons, C. (1962) 'Electrode systems for continuous monitoring in cardiovascular surgery', *Annals of the New York Academy of Sciences*, 102(1), pp. 29–45. doi:10.1111/j.1749-6632.1962.tb13623.x.

Cofsky, J.C., Karandur, D., Huang, C.J., Witte, I.P., Kuriyan, J. and Doudna, J.A. (2020) 'CRISPR-Cas12a exploits R-loop asymmetry to form double-strand breaks', *eLife*, 9, pp. 1–32. doi:10.7554/eLife.55143.

Collen, B., Whitton, F., Dyer, E.E., Baillie, J.E.M., Cumberlidge, N., Darwall, W.R.T., Pollock, C., Richman, N.I., Soulsby, A.-M. and Böhm, M. (2014) 'Global patterns of freshwater species diversity, threat and endemism', *Global Ecology and Biogeography*, 23(1), pp. 40–51. doi:10.1111/GEB.12096.

Collins, R.A., Wangensteen, O.S., O'Gorman, E.J., Mariani, S., Sims, D.W. and Genner, M.J. (2018) 'Persistence of environmental DNA in marine systems', *Communications Biology*, 1(1), p. 185. doi:10.1038/s42003-018-0192-6.

Connor, L., Shephard, S., Rocks, K. and Kelly, F.L. (2019) 'Potential climate change impacts on Arctic char Salvelinus alpinus L. in Ireland', *Fisheries Management and Ecology*, 26(6), pp. 527–539. doi:10.1111/FME.12327.

Cordier, T., Frontalini, F., Cermakova, K., Apothéloz-Perret-Gentil, L., Treglia, M., Scantamburlo, E., Bonamin, V. and Pawlowski, J. (2019) 'Multi-marker eDNA metabarcoding survey to assess the environmental impact of three offshore gas platforms in the North Adriatic Sea (Italy)', *Marine Environmental Research*, 146, pp. 24–34. doi:10.1016/j.marenvres.2018.12.009.

Creer, S., Deiner, K., Frey, S., Porazinska, D., Taberlet, P., Thomas, W.K., Potter, C. and Bik, H.M. (2016) 'The ecologist's field guide to sequence-based identification of biodiversity', *Methods in Ecology and Evolution*. Edited by R. Freckleton, 7(9), pp. 1008–1018. doi:10.1111/2041-210X.12574.

Dabney, J., Meyer, M. and Pääbo, S. (2013) 'Ancient DNA Damage', *Cold Spring Harbor Perspectives in Biology*, 5(7). doi:10.1101/CSHPERSPECT.A012567.

Daher, R.K., Stewart, G., Boissinot, M., Boudreau, D.K. and Bergeron, M.G. (2015) 'Influence of sequence mismatches on the specificity of recombinase polymerase amplification technology', *Molecular and Cellular Probes*, 29(2), pp. 116–121. doi:10.1016/j.mcp.2014.11.005.

Dalvin, S., Glover, K.A., Sørvik, A.G., Seliussen, B.B. and Taggart, J.B. (2010) 'Forensic identification of severely degraded Atlantic salmon (Salmo salar) and rainbow trout (Oncorhynchus mykiss) tissues', *Investigative Genetics*, 1(1), p. 12. doi:10.1186/2041-2223-1-12.

Damborský, P., Švitel, J. and Katrlík, J. (2016) 'Optical biosensors', *Essays in Biochemistry*, 60(1),

p. 91. doi:10.1042/EBC20150010.

Darling, J.A. and Mahon, A.R. (2011) 'From molecules to management: Adopting DNA-based methods for monitoring biological invasions in aquatic environments', *Environmental Research*, 111(7), pp. 978–988. doi:10.1016/J.ENVRES.2011.02.001.

Davidson, W.S., Koop, B.F., Jones, S.J., Iturra, P., Vidal, R., Maass, A., Jonassen, I., Lien, S. and Omholt, S.W. (2010) 'Sequencing the genome of the Atlantic salmon (Salmo salar)', *Genome Biology 2010 11:9*, 11(9), p. 403. doi:10.1186/gb-2010-11-9-403.

Davy, C.M., Kidd, A.G. and Wilson, C.C. (2015) 'Development and Validation of Environmental DNA (eDNA) Markers for Detection of Freshwater Turtles', *PLOS ONE*. Edited by A.R. Mahon, 10(7), p. e0130965. doi:10.1371/journal.pone.0130965.

Deiner, K. and Altermatt, F. (2014) 'Transport Distance of Invertebrate Environmental DNA in a Natural River', *PLoS ONE*. Edited by T. Gilbert, 9(2), p. e88786. doi:10.1371/journal.pone.0088786.

Deiner, K., Bik, H.M., Mächler, E., Seymour, M., Lacoursière-Roussel, A., Altermatt, F., Creer, S., Bista, I., Lodge, D.M., de Vere, N., Pfrender, M.E. and Bernatchez, L. (2017) 'Environmental DNA metabarcoding: Transforming how we survey animal and plant communities', *Molecular Ecology*, 26(21), pp. 5872–5895. doi:10.1111/mec.14350.

Dejean, T., Valentini, A., Duparc, A., Pellier-Cuit, S., Pompanon, F., Taberlet, P. and Miaud, C. (2011) 'Persistence of Environmental DNA in Freshwater Ecosystems', *PLoS ONE*. Edited by J.A. Gilbert, 6(8), p. e23398. doi:10.1371/journal.pone.0023398.

Dejean, T., Valentini, A., Miquel, C., Taberlet, P., Bellemain, E. and Miaud, C. (2012) 'Improved detection of alien invasive species through environmental DNA barcoding: the example of the American bullfrog Lithobates catesbeianus', *Journal of Applied Ecology*, 49(4), pp. 953–959.

DeLong, E.F. (2005) 'Microbial community genomics in the ocean', *Nature Reviews Microbiology*, 3(6), pp. 459–469. doi:10.1038/nrmicro1158.

Deng, H., Xu, Y., Liu, Y., Che, Z., Guo, H., Shan, S., Sun, Y., Liu, X., Huang, K., Ma, X., Wu, Y. and Liang, X.J. (2012) 'Gold nanoparticles with asymmetric polymerase chain reaction for colorimetric detection of DNA sequence', *Analytical Chemistry*, 84(3), pp. 1253–1258. doi:10.1021/ac201713t.

Dineva, M.A., Candotti, D., Fletcher-Brown, F., Allain, J.-P. and Lee, H. (2005) 'Simultaneous visual detection of multiple viral amplicons by dipstick assay.', *Journal of clinical microbiology*,

43(8), pp. 4015–21. doi:10.1128/JCM.43.8.4015-4021.2005.

Doi, H., Takahara, T., Minamoto, T., Matsuhashi, S., Uchii, K. and Yamanaka, H. (2015) 'Droplet Digital Polymerase Chain Reaction (PCR) Outperforms Real-Time PCR in the Detection of Environmental DNA from an Invasive Fish Species', *Environmental Science & Technology*, 49(9), pp. 5601–5608. doi:10.1021/acs.est.5b00253.

van Dongen, J.E., Berendsen, J.T.W., Steenbergen, R.D.M., Wolthuis, R.M.F., Eijkel, J.C.T. and Segerink, L.I. (2020) 'Point-of-care CRISPR/Cas nucleic acid detection: Recent advances, challenges and opportunities', *Biosensors and Bioelectronics*, 166, p. 112445. doi:10.1016/j.bios.2020.112445.

Doorenspleet, K., Jansen, L., Oosterbroek, S., Bos, O., Kamermans, P., Janse, M., Wurz, E., Murk, A. and Nijland, R. (2021) 'High resolution species detection: accurate long read eDNA metabarcoding of North Sea fish using Oxford Nanopore sequencing', *bioRxiv*, p. 2021.11.26.470087. doi:10.1101/2021.11.26.470087.

Dostatni, R. (2021) *Lateral Flow Readout » CRISPR/Cas-based detection strategies*. Available at: https://www.milenia-biotec.com/en/tips-lateral-flow-readouts-crispr-cas-strategies/ (Accessed: 19 August 2021).

Doyle, J. and Uthicke, S. (2021) 'Sensitive environmental DNA detection via lateral flow assay (dipstick)—A case study on corallivorous crown-of-thorns sea star (Acanthaster cf. solaris) detection', *Environmental DNA*, 3(2), pp. 323–342. doi:10.1002/EDN3.123.

Drummond, A.J., Newcomb, R.D., Buckley, T.R., Xie, D., Dopheide, A., Potter, B.C., Heled, J., Ross, H.A., Tooman, L., Grosser, S., Park, D., Demetras, N.J., Stevens, M.I., Russell, J.C., Anderson, S.H., Carter, A. and Nelson, N. (2015) 'Evaluating a multigene environmental DNA approach for biodiversity assessment', *GigaScience*, 4(1), p. 46. doi:10.1186/s13742-015-0086-1.

Dudgeon, D., Arthington, A.H., Gessner, M.O., Kawabata, Z.I., Knowler, D.J., Lévêque, C., Naiman, R.J., Prieur-Richard, A.H., Soto, D., Stiassny, M.L.J. and Sullivan, C.A. (2006) 'Freshwater biodiversity: Importance, threats, status and conservation challenges', *Biological Reviews of the Cambridge Philosophical Society*. Biol Rev Camb Philos Soc, pp. 163–182. doi:10.1017/S1464793105006950.

Durán-Vinet, B., Araya-Castro, K., Chao, T.C., Wood, S.A., Gallardo, V., Godoy, K. and Abanto, M. (2021) 'Potential applications of CRISPR/Cas for next-generation biomonitoring of harmful algae blooms: A review', *Harmful Algae*, 103, p. 102027. doi:10.1016/J.HAL.2021.102027.

Dysthe, J.C., Franklin, T.W., McKelvey, K.S., Young, M.K. and Schwartz, M.K. (2018) 'An improved environmental DNA assay for bull trout (Salvelinus confluentus) based on the ribosomal internal transcribed spacer I', *PLOS ONE*, 13(11), p. e0206851. doi:10.1371/JOURNAL.PONE.0206851.

Egan, S.P., Grey, E., Olds, B., Feder, J.L., Ruggiero, S.T., Tanner, C.E. and Lodge, D.M. (2015) 'Rapid Molecular Detection of Invasive Species in Ballast and Harbor Water by Integrating Environmental DNA and Light Transmission Spectroscopy', *Environmental Science and Technology*, 49(7), pp. 4113–4121. doi:10.1021/ES5058659.

Eichmiller, J.J., Bajer, P.G. and Sorensen, P.W. (2014) 'The Relationship between the Distribution of Common Carp and Their Environmental DNA in a Small Lake', *PLoS ONE*. Edited by A.C. Anil, 9(11), p. e112611. doi:10.1371/journal.pone.0112611.

El-Tholoth, M., Branavan, M., Naveenathayalan, A. and Balachandran, W. (2019) 'Recombinase polymerase amplification–nucleic acid lateral flow immunoassays for Newcastle disease virus and infectious bronchitis virus detection', *Molecular Biology Reports 2019 46:6*, 46(6), pp. 6391–6397. doi:10.1007/S11033-019-05085-Y.

Eldøy, S.H., Ryan, D., Roche, W.K., Thorstad, E.B., Næsje, T.F., Sjursen, A.D., Gargan, P.G. and Davidsen, J.G. (2020) 'Changes in growth and migration patterns of sea trout before and after the introduction of Atlantic salmon farming', *ICES Journal of Marine Science*, 77(7–8), pp. 2623–2634. doi:10.1093/ICESJMS/FSAA125.

Elfving, K., Andersson, M., Msellem, M.I., Welinder-Olsson, C., Petzold, M., Björkman, A., Trollfors, B., Mårtensson, A. and Lindh, M. (2014) 'Real-time PCR threshold cycle cutoffs help to identify agents causing acute childhood diarrhea in Zanzibar', *Journal of Clinical Microbiology*, 52(3), pp. 916–923. doi:10.1128/JCM.02697-13.

Elghanian, R., Storhoff, J.J., Mucic, R.C., Letsinger, R.L. and Mirkin, C.A. (1997) 'Selective colorimetric detection of polynucleotides based on the distance-dependent optical properties of gold nanoparticles', *Science*, 277(5329), pp. 1078–1081. doi:10.1126/science.277.5329.1078.

Ellison, S.L.R.R., English, C.A., Burns, M.J. and Keer, J.T. (2006) 'Routes to improving the reliability of low level DNA analysis using real-time PCR', *BMC biotechnology*, 6(1), p. 33. doi:10.1186/1472-6750-6-33.

Epp, L.S., Boessenkool, S., Bellemain, E.P., Haile, J., Esposito, A., Riaz, T., Erseus, C., Gusarov, V.I., Edwards, M.E., Johnsen, A., Stenoien, H.K., Hassel, K., Kauserud, H., Yoccoz, N.G., Brathen, K.A., Willerslev, E., Taberlet, P., Coissac, E. and Brochmann, C. (2012) 'New environmental

metabarcodes for analysing soil DNA: potential for studying past and present ecosystems', *Molecular Ecology*, 21(8), pp. 1821–1833. doi:10.1111/j.1365-294X.2012.05537.x.

Ercole, C., Del Gallo, M., Mosiello, L., Baccella, S. and Lepidi, A. (2003) 'Escherichia coli detection in vegetable food by a potentiometric biosensor', *Sensors and Actuators B: Chemical*, 91(1–3), pp. 163–168. doi:10.1016/S0925-4005(03)00083-2.

Erdem, A., Kerman, K., Meric, B., Akarca, U.S. and Ozsoz, M. (1999) 'DNA Electrochemical Biosensor for the Detection of Short DNA Sequences Related to the Hepatitis B Virus', *Electroanalysis*, 11(8), pp. 586–587. doi:10.1002/(SICI)1521-4109(199906)11:8<586::AID-ELAN586>3.0.CO;2-J.

Erickson, R.A., Rees, C.B., Coulter, A.A., Merkes, C.M., McCalla, S.G., Touzinsky, K.F., Walleser, L., Goforth, R.R. and Amberg, J.J. (2016) 'Detecting the movement and spawning activity of bigheaded carps with environmental DNA', *Molecular Ecology Resources*, 16(4), pp. 957–965. doi:10.1111/1755-0998.12533.

Erill, I., Campoy, S., Erill, N., Barbe, J. and Aguilo, J. (2003) 'Biochemical analysis and optimisation of inhibition and adsorption phenomena in glass-silicon PCR chips', *Sensors and Actuators B: Chemical*, 96(3), pp. 685–692.

de Eyto, E., Connolly, P., Cotter, D., Dalton, C., Jennings, E., McGinnity, P. and Poole, R. (2020) 'The Burrishoole Catchment', in Kelly-Quinn, M. and Reynolds, J.D. (eds) *Ireland's Rivers*. Dublin: University College Dublin Press, pp. 357–380.

Farmer, T.M., Marschall, E.A., Dabrowski, K. and Ludsin, S.A. (2015) 'Short winters threaten temperate fish populations', *Nature Communications 2015 6:1*, 6(1), pp. 1–10. doi:10.1038/ncomms8724.

Fealy, R., Allott, N., Broderick, C., De Eyto, E., Dillane, M., Erdil, R.M., Jennings, E., Mccrann, K., Murphy, C., O'toole, C., Poole, R., Rogan, G., Ryder, L., Taylor, D., Whelan, K. and White, J. (2007) 'RESCALE: Review and Simulate Climate and Catchment Responses at Burrishoole Climate and Catchment Environment'.

Ferguson, A., Reed, T.E., Cross, T.F., McGinnity, P. and Prodöhl, P.A. (2019) 'Anadromy, potamodromy and residency in brown trout Salmo trutta: the role of genes and the environment', *Journal of Fish Biology*, 95(3), pp. 692–718. doi:10.1111/JFB.14005.

Fernández-Vizarra, E., Enríquez, J.A., Pérez-Martos, A., Montoya, J. and Fernández-Silva, P. (2011) 'Tissue-specific differences in mitochondrial activity and biogenesis', *Mitochondrion*,

11(1), pp. 207–213. doi:10.1016/j.mito.2010.09.011.

Ficetola, G.F., Manenti, R. and Taberlet, P. (2019) 'Environmental DNA and metabarcoding for the study of amphibians and reptiles: species distribution, the microbiome, and much more', *Amphibia Reptilia*. Brill Academic Publishers, pp. 129–148. doi:10.1163/15685381-20191194.

Ficetola, G.F., Miaud, C., Pompanon, F. and Taberlet, P. (2008) 'Species detection using environmental DNA from water samples', *Biology Letters*, 4(4), pp. 423–425. doi:10.1098/rsbl.2008.0118.

Ficetola, G.F., Pansu, J., Bonin, A., Coissac, E., Giguet-Covex, C., De Barba, M., Gielly, L., Lopes, C.M., Boyer, F., Pompanon, F., Rayé, G. and Taberlet, P. (2015) 'Replication levels, false presences and the estimation of the presence/absence from eDNA metabarcoding data', *Molecular Ecology Resources*, 15(3), pp. 543–556. doi:10.1111/1755-0998.12338.

Fisher, A.C., Volpe, J.P. and Fisher, J.T. (2014) 'Occupancy dynamics of escaped farmed Atlantic salmon in Canadian Pacific coastal salmon streams: implications for sustained invasions', *Biological Invasions 2014 16:10*, 16(10), pp. 2137–2146. doi:10.1007/S10530-014-0653-X.

Fonfara, I., Richter, H., BratoviÄ, M., Le Rhun, A., Charpentier, E., Bratovič, M., Le Rhun, A. and Charpentier, E. (2016) 'The CRISPR-associated DNA-cleaving enzyme Cpf1 also processes precursor CRISPR RNA', *Nature*, 532(7600), pp. 517–521. doi:10.1038/nature17945.

Foran, D.R. (2006) 'Relative Degradation of Nuclear and Mitochondrial DNA: An Experimental Approach*', *Journal of Forensic Sciences*, 51(4), pp. 766–770. doi:10.1111/j.1556-4029.2006.00176.x.

Ford, T. (2019) *The Cas proteins behind CRISPR diagnostics - Mammoth Biosciences*. Available at: https://mammoth.bio/2019/06/10/the-cas-proteins-behind-crispr-diagnostics/ (Accessed: 10 September 2021).

Forootan, A., Sjöback, R., Björkman, J., Sjögreen, B., Linz, L. and Kubista, M. (2017) 'Methods to determine limit of detection and limit of quantification in quantitative real-time PCR (qPCR)', *Biomolecular Detection and Quantification*, 12, pp. 1–6. doi:10.1016/j.bdq.2017.04.001.

Forseth, T., Larsson, S., Jensen, A.J., Jonsson, B., Näslund, I. and Berglund, I. (2009) 'Thermal growth performance of juvenile brown trout Salmo trutta: no support for thermal adaptation hypotheses', *Journal of Fish Biology*, 74(1), pp. 133–149. doi:10.1111/J.1095-8649.2008.02119.X.

Franklin, T.W., McKelvey, K.S., Golding, J.D., Mason, D.H., Dysthe, J.C., Pilgrim, K.L., Squires, J.R.,

Aubry, K.B., Long, R.A., Greaves, S.E., Raley, C.M., Jackson, S., MacKay, P., Lisbon, J., Sauder, J.D., Pruss, M.T., Heffington, D. and Schwartz, M.K. (2019) 'Using environmental DNA methods to improve winter surveys for rare carnivores: DNA from snow and improved noninvasive techniques', *Biological Conservation*, 229, pp. 50–58. doi:10.1016/j.biocon.2018.11.006.

Friedland, K.D., MacLean, J.C., Hansen, L.P., Peyronnet, A.J., Karlsson, L., Reddin, D.G., O Maoileidigh, N. and McCarthy, J.L. (2008) 'The recruitment of Atlantic salmon in Europe', *ICES Journal of Marine Science*, 66(2), pp. 289–304. doi:10.1093/icesjms/fsn210.

Fukumoto, S., Ushimaru, A. and Minamoto, T. (2015) 'A basin-scale application of environmental DNA assessment for rare endemic species and closely related exotic species in rivers: A case study of giant salamanders in Japan', *Journal of Applied Ecology*. Edited by E. Crispo, 52(2), pp. 358–365. doi:10.1111/1365-2664.12392.

Furlan, E.M., Gleeson, D., Hardy, C.M. and Duncan, R.P. (2016) 'A framework for estimating the sensitivity of eDNA surveys', *Molecular Ecology Resources*, 16(3), pp. 641–654. doi:10.1111/1755-0998.12483.

Gargan, L.M., Morato, T., Pham, C.K., Finarelli, J.A., Carlsson, J.E.L. and Carlsson, J. (2017) 'Development of a sensitive detection method to survey pelagic biodiversity using eDNA and quantitative PCR: a case study of devil ray at seamounts', *Marine Biology*, 164(5), p. 112. doi:10.1007/s00227-017-3141-x.

Gargan, P., Fitzgerald, C., Kennedy, R., O'Maoileidigh, N., McLean, S. and Millane, M. (2020) 'The Status of Irish Salmon Stocks in 2019 with Catch Advice for 2020. Report of the Technical Expert Group on Salmon to the North-South Standing Scientific Committee for Inland Fisheries'.

Garneau, J.E., Dupuis, M.È., Villion, M., Romero, D.A., Barrangou, R., Boyaval, P., Fremaux, C., Horvath, P., Magadán, A.H. and Moineau, S. (2010) 'The CRISPR/cas bacterial immune system cleaves bacteriophage and plasmid DNA', *Nature*, 468(7320), pp. 67–71. doi:10.1038/nature09523.

Giguet-Covex, C., Pansu, J., Arnaud, F., Rey, P.-J., Griggo, C., Gielly, L., Domaizon, I., Coissac, E., David, F., Choler, P., Poulenard, J. and Taberlet, P. (2014) 'Long livestock farming history and human landscape shaping revealed by lake sediment DNA', *Nature Communications*, 5(1), pp. 1–7. doi:10.1038/ncomms4211.

Gill, P. and Ghaemi, A. (2008) 'Nucleic acid isothermal amplification technologies - a review', *Nucleosides, Nucleotides and Nucleic Acids*, 27(3), pp. 224–243.

Giuffrida, M. and Spoto, G. (2017) 'Integration of isothermal amplification methods in microfluidic devices: recent advances', *Biosensors and Bioelectronics*, 90, pp. 174–186.

Gleick, P.H. (1998) 'The human right to water', *Water Policy*, 1(5), pp. 487–503. doi:10.1016/S1366-7017(99)00008-2.

Goldberg, C.S., Pilliod, D.S., Arkle, R.S. and Waits, L.P. (2011) 'Molecular Detection of Vertebrates in Stream Water: A Demonstration Using Rocky Mountain Tailed Frogs and Idaho Giant Salamanders', *PLoS ONE*. Edited by B. Gratwicke, 6(7), p. e22746. doi:10.1371/journal.pone.0022746.

Goldberg, C.S., Sepulveda, A., Ray, A., Baumgardt, J. and Waits, L.P. (2013) 'Environmental DNA as a new method for early detection of New Zealand mudsnails (Potamopyrgus antipodarum)', *Freshwater Science*, 32(3), pp. 792–800. doi:10.1899/13-046.1.

Goldberg, C.S., Strickler, K.M. and Fremier, A.K. (2018) 'Degradation and dispersion limit environmental DNA detection of rare amphibians in wetlands: Increasing efficacy of sampling designs', *Science of The Total Environment*, 633, pp. 695–703. doi:10.1016/J.SCITOTENV.2018.02.295.

Goldberg, C.S., Strickler, K.M. and Pilliod, D.S. (2015) 'Moving environmental DNA methods from concept to practice for monitoring aquatic macroorganisms', *Biological Conservation*, 183, pp. 1–3. doi:10.1016/j.biocon.2014.11.040.

Goldberg, C.S., Turner, C.R., Deiner, K., Klymus, K.E., Thomsen, P.F., Murphy, M.A., Spear, S.F., McKee, A., Oyler-McCance, S.J., Cornman, R.S., Laramie, M.B., Mahon, A.R., Lance, R.F., Pilliod, D.S., Strickler, K.M., Waits, L.P., Fremier, A.K., Takahara, T., Herder, J.E. and Taberlet, P. (2016) 'Critical considerations for the application of environmental DNA methods to detect aquatic species', *Methods in Ecology and Evolution*. Edited by M. Gilbert, 7(11), pp. 1299–1307. doi:10.1111/2041-210X.12595.

Gonzales, F. and McDonough, S. (1998) 'Applications of Transcription-Mediated Amplification to Quantification of Gene Sequences', in Francois, F. (ed.) *Gene Amplification*. Boston: Birkhauser, pp. 189–204.

Goode, J.R., Buffington, J.M., Tonina, D., Isaak, D.J., Thurow, R.F., Wenger, S., Nagel, D., Luce, C., Tetzlaff, D. and Soulsby, C. (2013) 'Potential effects of climate change on streambed scour and risks to salmonid survival in snow-dominated mountain basins', *Hydrological Processes*, 27(5), pp. 750–765. doi:10.1002/HYP.9728.

Gootenberg, J.S., Abudayyeh, O.O., Kellner, M.J., Joung, J., Collins, J.J. and Zhang, F. (2018) 'Multiplexed and portable nucleic acid detection platform with Cas13, Cas12a, and Csm6', *Science*, 360(6387), pp. 439–444. doi:10.1126/science.aaq0179.

Gootenberg, J.S., Abudayyeh, O.O., Lee, J.W., Essletzbichler, P., Dy, A.J., Joung, J., Verdine, V., Donghia, N., Daringer, N.M., Freije, C.A., Myhrvold, C., Bhattacharyya, R.P., Livny, J., Regev, A., Koonin, E. V., Hung, D.T., Sabeti, P.C., Collins, J.J. and Zhang, F. (2017) 'Nucleic acid detection with CRISPR-Cas13a/C2c2', *Science*, 356(6336), pp. 438–442. doi:10.1126/science.aam9321.

Guisan, A., Tingley, R., Baumgartner, J.B., Naujokaitis-Lewis, I., Sutcliffe, P.R., Tulloch, A.I.T., Regan, T.J., Brotons, L., McDonald-Madden, E., Mantyka-Pringle, C., Martin, T.G., Rhodes, J.R., Maggini, R., Setterfield, S.A., Elith, J., Schwartz, M.W., Wintle, B.A., Broennimann, O., Austin, M., Ferrier, S., Kearney, M.R., Possingham, H.P. and Buckley, Y.M. (2013) 'Predicting species distributions for conservation decisions', *Ecology Letters*. Edited by H. Arita, 16(12), pp. 1424–1435. doi:10.1111/ele.12189.

Guo, L., Sun, X., Wang, X., Liang, C., Jiang, H., Gao, Q., Dai, M., Qu, B., Fang, S., Mao, Y., Chen, Y., Feng, G., Gu, Q., Wang, R.R., Zhou, Q. and Li, W. (2020) 'SARS-CoV-2 detection with CRISPR diagnostics', *Cell Discovery*. Springer Nature, pp. 1–4. doi:10.1038/s41421-020-0174-y.

Gurevitch, J. and Padilla, D.K. (2004) 'Are invasive species a major cause of extinctions?', *Trends in Ecology & Evolution*, 19(9), pp. 470–474. doi:10.1016/J.TREE.2004.07.005.

Haile, J., Froese, D.G., MacPhee, R.D.E., Roberts, R.G., Arnold, L.J., Reyes, A. V., Rasmussen, M., Nielsen, R., Brook, B.W., Robinson, S., Demuro, M., Gilbert, M.T.P., Munch, K., Austin, J.J., Cooper, A., Barnes, I., Möller, P. and Willerslev, E. (2009) 'Ancient DNA reveals late survival of mammoth and horse in interior Alaska', *Proceedings of the National Academy of Sciences*, 106(52), pp. 22352–22357. doi:10.1073/PNAS.0912510106.

Handley, L.L., Read, D.S., Winfield, I.J., Kimbell, H., Johnson, H., Li, J., Hahn, C., Blackman, R., Wilcox, R., Donnelly, R., Szitenberg, A. and Hänfling, B. (2019) 'Temporal and spatial variation in distribution of fish environmental DNA in England's largest lake', *Environmental DNA*, 1(1), pp. 26–39. doi:10.1002/EDN3.5.

Hänfling, B., Handley, L.L., Read, D.S., Hahn, C., Li, J., Nichols, P., Blackman, R.C., Oliver, A. and Winfield, I.J. (2016) 'Environmental DNA metabarcoding of lake fish communities reflects long-term data from established survey methods', *Molecular Ecology*, 25(13), pp. 3101–3119. doi:10.1111/MEC.13660.

Hansen, M.M. (2002) 'Estimating the long-term effects of stocking domesticated trout into wild brown trout (Salmo trutta) populations: an approach using microsatellite DNA analysis of historical and contemporary samples', *Molecular Ecology*, 11(6), pp. 1003–1015. doi:10.1046/J.1365-294X.2002.01495.X.

Harper, K.J., Anucha, P.N., Turnbull, J.F., Bean, C.W. and Leaver, M.J. (2018) 'Searching for a signal: Environmental DNA (eDNA) for the detection of invasive signal crayfish, Pacifastacus leniusculus (Dana, 1852)', *Management of Biological Invasions*, 9(2), pp. 137–148. doi:10.3391/mbi.2018.9.2.07.

Harper, L.R., Lawson Handley, L., Carpenter, A.I., Ghazali, M., Di Muri, C., Macgregor, C.J., Logan, T.W., Law, A., Breithaupt, T., Read, D.S., McDevitt, A.D. and Hänfling, B. (2019) 'Environmental DNA (eDNA) metabarcoding of pond water as a tool to survey conservation and management priority mammals', *Biological Conservation*, 238, p. 108225. doi:10.1016/j.biocon.2019.108225.

Harper, L.R., Lawson Handley, L., Hahn, C., Boonham, N., Rees, H.C., Gough, K.C., Lewis, E., Adams, I.P., Brotherton, P., Phillips, S. and Hänfling, B. (2018) 'Needle in a haystack? A comparison of eDNA metabarcoding and targeted qPCR for detection of the great crested newt (Triturus cristatus)', *Ecology and Evolution*, 8(12), pp. 6330–6341. doi:10.1002/ece3.4013.

Harrington, L.B., Burstein, D., Chen, J.S., Paez-Espino, D., Ma, E., Witte, I.P., Cofsky, J.C., Kyrpides, N.C., Banfield, J.F. and Doudna, J.A. (2018) 'Programmed DNA destruction by miniature CRISPR-Cas14 enzymes', *Science*, 362(6416), pp. 839–842. doi:10.1126/science.aav4294.

He, Q., Yu, D., Bao, M., Korensky, G., Chen, J., Shin, M., Kim, J., Park, M., Qin, P. and Du, K. (2020) 'High-throughput and all-solution phase African Swine Fever Virus (ASFV) detection using CRISPR-Cas12a and fluorescence based point-of-care system', *Biosensors and Bioelectronics*, 154, p. 112068. doi:10.1016/j.bios.2020.112068.

Hebert, P.D.N., Ratnasingham, S. and deWaard, J.R. (2003) 'Barcoding animal life: cytochrome c oxidase subunit 1 divergences among closely related species.', *Proceedings. Biological sciences*, 270 Suppl 1(Suppl 1), pp. S96-9. doi:10.1098/rsbl.2003.0025.

Heery, B., Briciu-Burghina, C., Zhang, D., Duffy, G., Brabazon, D., O'Connor, N. and Regan, F. (2016) 'ColiSense, today's sample today: A rapid on-site detection of β-d-Glucuronidase activity in surface water as a surrogate for E. coli', *Talanta*, 148, pp. 75–83. doi:10.1016/J.TALANTA.2015.10.035.

Hempel, C.A., Peinert, B., Beermann, A.J., Elbrecht, V., Macher, J.-N., Macher, T.-H., Jacobs, G.

and Leese, F. (2020) 'Using Environmental DNA to Monitor the Reintroduction Success of the Rhine Sculpin (Cottus rhenanus) in a Restored Stream', *Frontiers in Ecology and Evolution*, 8. doi:10.3389/fevo.2020.00081.

Hernandez, C.C., Bougas, B., Perreault-Payette, A., Simard, A., Côté, G., Bernatchez, L., Perreault, A., Simard, A., Cote, G. and Bernatchez, L. (2020) '60 specific eDNA qPCR assays to detect invasive, threatened and exploited freshwater vertebrates and invertebrates in Eastern Canada.', *Environmental DNA*, 2(3), pp. 373–386. doi:10.1002/edn3.89.

Herrero, B., Madriñán, M., Vieites, J.M. and Espiñeira, M. (2010) 'Authentication of Atlantic Cod (*Gadus morhua*) Using Real Time PCR', *Journal of Agricultural and Food Chemistry*, 58(8), pp. 4794–4799. doi:10.1021/jf904018h.

Hindson, C.M., Chevillet, J.R., Briggs, H.A., Gallichotte, E.N., Ruf, I.K., Hindson, B.J., Vessella, R.L. and Tewari, M. (2013) 'Absolute quantification by droplet digital PCR versus analog real-time PCR', *Nature Methods*, 10(10), pp. 1003–1005. doi:10.1038/nmeth.2633.

Holland, P.M., Abramson, R.D., Watson, R. and Gelfand, D.H. (1991) 'Detection of specific polymerase chain reaction product by utilizing the 5'----3' exonuclease activity of Thermus aquaticus DNA polymerase.', *Proceedings of the National Academy of Sciences of the United States of America*, 88(16), pp. 7276–80. doi:10.1073/pnas.88.16.7276.

Hórreo, J.L., Ayllón, F., Perez, J., Beall, E. and Garcia-Vazquez, E. (2011) 'Interspecific Hybridization, a Matter of Pioneering? Insights from Atlantic Salmon and Brown Trout', *Journal of Heredity*, 102(2), pp. 237–242. doi:10.1093/JHERED/ESQ130.

Horvath, P. and Barrangou, R. (2010) 'CRISPR/Cas, the immune system of Bacteria and Archaea', *Science*. doi:10.1126/science.1179555.

Hosgood, H.D., Liu, C.-S., Rothman, N., Weinstein, S.J., Bonner, M.R., Shen, M., Lim, U., Virtamo, J., Cheng, W., Albanes, D., Lan, Q. and Lan, Q. (2010) 'Mitochondrial DNA copy number and lung cancer risk in a prospective cohort study.', *Carcinogenesis*, 31(5), pp. 847–9. doi:10.1093/carcin/bgq045.

Hossain, S.M.Z. and Mansour, N. (2019) 'Biosensors for on-line water quality monitoring – a review', *https://doi.org/10.1080/25765299.2019.1691434*, 26(1), pp. 502–518. doi:10.1080/25765299.2019.1691434.

Hulley, E.N., Tharmalingam, S., Zarnke, A. and Boreham, D.R. (2019) 'Development and validation of probe-based multiplex real-time PCR assays for the rapid and accurate detection

of freshwater fish species.', *PloS one*, 14(1), p. e0210165. doi:10.1371/journal.pone.0210165.

Igoe, F., O'Grady, M., Byrne, C., Gargan, P., Roche, W. and O'Neill, J. (2001) 'Evidence for the recent extinction of two Arctic charr Salvelinus alpinus (L.) populations in the West of Ireland', *Aquatic Conservation: Marine and Freshwater Ecosystems*, 11(2), pp. 77–92. doi:10.1002/AQC.431.

Ikeda, K., Doi, H., Tanaka, K., Kawai, T. and Negishi, J.N. (2016) 'Using environmental DNA to detect an endangered crayfish Cambaroides japonicus in streams', *Conservation Genetics Resources*, 8(3), pp. 231–234. doi:10.1007/s12686-016-0541-z.

Inland Fisheries Ireland (2019) *Annual Report and Financial Statements*.

Iwasaki, W., Fukunaga, T., Isagozawa, R., Yamada, K., Maeda, Y., Satoh, T.P., Sado, T., Mabuchi, K., Takeshima, H., Miya, M. and Nishida, M. (2013) 'MitoFish and MitoAnnotator: A Mitochondrial Genome Database of Fish with an Accurate and Automatic Annotation Pipeline', *Molecular Biology and Evolution*, 30(11), pp. 2531–2540. doi:10.1093/molbev/mst141.

Jane, S.F., Wilcox, T.M., McKelvey, K.S., Young, M.K., Schwartz, M.K., Lowe, W.H., Letcher, B.H. and Whiteley, A.R. (2015) 'Distance, flow and PCR inhibition: eDNA dynamics in two headwater streams', *Molecular Ecology Resources*, 15(1), pp. 216–227. doi:10.1111/1755-0998.12285.

Janosik, A.M. and Johnston, C.E. (2015) 'Environmental DNA as an effective tool for detection of imperiled fishes', *Environmental Biology of Fishes*, 98(8), pp. 1889–1893. doi:10.1007/s10641-015-0405-5.

Jarvis, J.N., Percival, A., Bauman, S., Pelfrey, J., Meintjes, G., Williams, G.N., Longley, N., Harrison, T.S. and Kozel, T.R. (2011) 'Evaluation of a Novel Point-of-Care Cryptococcal Antigen Test on Serum, Plasma, and Urine From Patients With HIV-Associated Cryptococcal Meningitis', *Clinical Infectious Diseases*, 53(10), pp. 1019–1023. doi:10.1093/cid/cir613.

Jauset-Rubio, M., Svobodová, M., Mairal, T., McNeil, C., Keegan, N., Saeed, A., Abbas, M.N., El-Shahawi, M.S., Bashammakh, A.S., Alyoubi, A.O. and O´Sullivan, C.K. (2016) 'Ultrasensitive, rapid and inexpensive detection of DNA using paper based lateral flow assay', *Scientific Reports 2016 6:1*, 6(1), pp. 1–10. doi:10.1038/srep37732.

Javani, A., Javadi-Zarnaghi, F. and Rasaee, M.J. (2017) 'Development of a colorimetric nucleic acid-based lateral flow assay with non-biotinylated capture DNA', *Applied Biological Chemistry 2017 60:6*, 60(6), pp. 637–645. doi:10.1007/S13765-017-0321-9.

Jensen, A.J., Finstad, B. and Fiske, P. (2019) 'The cost of anadromy: marine and freshwater

mortality rates in anadromous Arctic char and brown trout in the Arctic region of Norway', *https://doi.org/10.1139/cjfas-2018-0428*, 76(12), pp. 2408–2417. doi:10.1139/CJFAS-2018-0428.

Jerde, C.L. (2019) 'Can we manage fisheries with the inherent uncertainty from eDNA?', *Journal of Fish Biology*, p. jfb.14218. doi:10.1111/jfb.14218.

Jerde, C.L., Mahon, A.R., Chadderton, W.L. and Lodge, D.M. (2011) '"Sight-unseen" detection of rare aquatic species using environmental DNA', *Conservation Letters*, 4(2), pp. 150–157. doi:10.1111/j.1755-263X.2010.00158.x.

Jinek, M., Chylinski, K., Fonfara, I., Hauer, M., Doudna, J.A. and Charpentier, E. (2012) 'A programmable dual-RNA-guided DNA endonuclease in adaptive bacterial immunity', *Science*, 337(6096), pp. 816–821. doi:10.1126/science.1225829.

Jolany vangah, S., Katalani, C., Boone, H.A., Hajizade, A., Sijercic, A. and Ahmadian, G. (2020) 'CRISPR-Based Diagnosis of Infectious and Noninfectious Diseases', *Biological Procedures Online 2020 22:1*, 22(1), pp. 1–14. doi:10.1186/S12575-020-00135-3.

Jonsson, B., Forseth, T., Jensen, A.J. and Næsje, T.F. (2001) 'Thermal performance of juvenile Atlantic Salmon, Salmo salar L.', *Functional Ecology*, 15(6), pp. 701–711. doi:10.1046/J.0269-8463.2001.00572.X.

Jonsson, B. and Jonsson, N. (2009) 'A review of the likely effects of climate change on anadromous Atlantic salmon Salmo salar and brown trout Salmo trutta, with particular reference to water temperature and flow', *Journal of Fish Biology*, 75(10), pp. 2381–2447. doi:10.1111/J.1095-8649.2009.02380.X.

Jonsson, B and Jonsson, N. (2009) 'Migratory timing, marine survival and growth of anadromous brown trout Salmo trutta in the River Imsa, Norway', *Journal of Fish Biology*, 74(3), pp. 621–638. doi:10.1111/j.1095-8649.2008.02152.x.

Jørgensen, K.M., Wennevik, V., Sørvik, A.G.E., Unneland, L., Prusov, S., Ayllon, F. and Glover, K.A. (2018) 'Investigating the frequency of triploid Atlantic salmon in wild Norwegian and Russian populations', *BMC Genetics*, 19(1). doi:10.1186/S12863-018-0676-X.

Joung, J., Ladha, A., Saito, M., Kim, N.-G., Woolley, A.E., Segel, M., Barretto, R.P.J., Ranu, A., Macrae, R.K., Faure, G., Ioannidi, E.I., Krajeski, R.N., Bruneau, R., Huang, M.-L.W., Yu, X.G., Li, J.Z., Walker, B.D., Hung, D.T., Greninger, A.L., Jerome, K.R., Gootenberg, J.S., Abudayyeh, O.O. and Zhang, F. (2020) 'Detection of SARS-CoV-2 with SHERLOCK One-Pot Testing', *New England*

Journal of Medicine, 383(15), pp. 1492–1494. doi:10.1056/nejmc2026172.

Justino, C.I.L., Duarte, A.C. and Rocha-Santos, T.A.P. (2017) 'Recent Progress in Biosensors for Environmental Monitoring: A Review', *Sensors (Basel, Switzerland)*, 17(12). doi:10.3390/S17122918.

Kaminski, M.M., Abudayyeh, O.O., Gootenberg, J.S., Zhang, F. and Collins, J.J. (2021) 'CRISPR-based diagnostics', *Nature Biomedical Engineering 2021 5:7*, 5(7), pp. 643–656. doi:10.1038/s41551-021-00760-7.

Kamoroff, C. and Goldberg, C.S. (2018) 'An issue of life or death: using eDNA to detect viable individuals in wilderness restoration', 37(3), pp. 685–696. doi:10.1086/699203.

Kasetsirikul, S., Shiddiky, M.J.A. and Nguyen, N.T. (2020) 'Challenges and perspectives in the development of paper-based lateral flow assays', *Microfluidics and Nanofluidics*. Springer, p. 17. doi:10.1007/s10404-020-2321-z.

Katchalski-Katzir, E. (1993) 'Immobilized enzymes — learning from past successes and failures', *Trends in Biotechnology*, 11(11), pp. 471–478. doi:10.1016/0167-7799(93)90080-S.

Katzmeier, F., Aufinger, L., Dupin, A., Quintero, J., Lenz, M., Bauer, L., Klumpe, S., Sherpa, D., Dürr, B., Honemann, M., Styazhkin, I., Simmel, F.C. and Heymann, M. (2019) 'A low-cost fluorescence reader for in vitro transcription and nucleic acid detection with Cas13a', *PLOS ONE*. Edited by M. Isalan, 14(12), p. e0220091. doi:10.1371/journal.pone.0220091.

Kelly, S., Moore, T.N., de Eyto, E., Dillane, M., Goulon, C., Guillard, J., Lasne, E., McGinnity, P., Poole, R., Winfield, I.J., Woolway, R.I. and Jennings, E. (2020) 'Warming winters threaten peripheral Arctic charr populations of Europe', *Climatic Change 2020 163:1*, 163(1), pp. 599–618. doi:10.1007/S10584-020-02887-Z.

Kersting, S., Rausch, V., Bier, F.F. and Von Nickisch-Rosenegk, M. (2014) 'Rapid detection of Plasmodium falciparum with isothermal recombinase polymerase amplification and lateral flow analysis', *Malaria Journal*, 13(1), p. 99. doi:10.1186/1475-2875-13-99.

Klymus, K.E., Merkes, C.M., Allison, M.J., Goldberg, C.S., Helbing, C.C., Hunter, M.E., Jackson, C.A., Lance, R.F., Mangan, A.M., Monroe, E.M., Piaggio, A.J., Stokdyk, J.P., Wilson, C.C. and Richter, C.A. (2020) 'Reporting the limits of detection and quantification for environmental DNA assays', *Environmental DNA*, 2(3), pp. 271–282. doi:10.1002/edn3.29.

Klymus, K.E., Richter, C.A., Chapman, D.C. and Paukert, C. (2015) 'Quantification of eDNA shedding rates from invasive bighead carp Hypophthalmichthys nobilis and silver carp

Hypophthalmichthys molitrix', *Biological Conservation*, 183, pp. 77–84. doi:10.1016/j.biocon.2014.11.020.

Koczula, K.M. and Gallotta, A. (2016) 'Lateral flow assays', *Essays in Biochemistry*, 60(1), p. 111. doi:10.1042/EBC20150012.

Kopp, M.U., Mello, A.J. de and Manz, A. (1998) 'Chemical Amplification: Continuous-Flow PCR on a Chip', *Science*, 280(5366), pp. 1046–1048. doi:10.1126/SCIENCE.280.5366.1046.

Kosack, C.S., Page, A.-L. and Klatser, P.R. (2017) 'A guide to aid the selection of diagnostic tests', *Bull World Health Organ* [Preprint]. doi:10.2471/BLT.16.187468.

Kozel, T.R. and Burnham-Marusich, A.R. (2017) 'Point-of-Care Testing for Infectious Diseases: Past, Present, and Future.', *Journal of clinical microbiology*, 55(8), pp. 2313–2320. doi:10.1128/JCM.00476-17.

Krkošek, M., Gottesfeld, A., Proctor, B., Rolston, D., Carr-Harris, C. and Lewis, M.A. (2007) 'Effects of host migration, diversity and aquaculture on sea lice threats to Pacific salmon populations', *Proceedings of the Royal Society B: Biological Sciences*, 274(1629), pp. 3141–3149. doi:10.1098/rspb.2007.1122.

Kubista, M., Andrade, J.M., Bengtsson, M., Forootan, A., Jonák, J., Lind, K., Sindelka, R., Sjöback, R., Sjögreen, B., Strömbom, L., Ståhlberg, A. and Zoric, N. (2006) 'The real-time polymerase chain reaction', *Molecular Aspects of Medicine*, 27(2–3), pp. 95–125. doi:10.1016/j.mam.2005.12.007.

Kutyavin, I. V., Afonina, I.A., Mills, A., Gorn, V. V, Lukhtanov, E.A., Belousov, E.S., Singer, M.J., Walburger, D.K., Lokhov, S.G., Gall, A.A., Dempcy, R., Reed, M.W., Meyer, R.B. and Hedgpeth, J. (2000) '3'-Minor groove binder-DNA probes increase sequence specificity at PCR extension temperatures', *Nucleic Acids Research*, 28(2), pp. 655–661. doi:10.1093/nar/28.2.655.

Kuwae, M., Tamai, H., Doi, H., Sakata, M.K., Minamoto, T. and Suzuki, Y. (2020) 'Sedimentary DNA tracks decadal-centennial changes in fish abundance', *Communications Biology 2020 3:1*, 3(1), pp. 1–12. doi:10.1038/s42003-020-01282-9.

Lacoursière-Roussel, A., Rosabal, M. and Bernatchez, L. (2016) 'Estimating fish abundance and biomass from eDNA concentrations: variability among capture methods and environmental conditions', *Molecular Ecology Resources*, 16(6), pp. 1401–1414. doi:10.1111/1755-0998.12522.

Lafferty, K.D., Benesh, K.C., Mahon, A.R., Jerde, C.L. and Lowe, C.G. (2018) 'Detecting Southern California's White Sharks With Environmental DNA', *Frontiers in Marine Science*, 5.

doi:10.3389/fmars.2018.00355.

Langlois, V.S., Allison, M.J., Bergman, L.C., To, T.A. and Helbing, C.C. (2020) 'The need for robust qPCR-based eDNA detection assays in environmental monitoring and species inventories', *Environmental DNA* [Preprint]. doi:10.1002/edn3.164.

Laramie, M.B., Pilliod, D.S. and Goldberg, C.S. (2015) 'Characterizing the distribution of an endangered salmonid using environmental DNA analysis', *Biological Conservation*, 183, pp. 29–37. doi:10.1016/J.BIOCON.2014.11.025.

Larsson, S. and Berglund, I. (2005) 'The effect of temperature on the energetic growth efficiency of Arctic charr (Salvelinus alpinus L.) from four Swedish populations', *Journal of Thermal Biology*, 30(1), pp. 29–36. doi:10.1016/J.JTHERBIO.2004.06.001.

Lawrence, D.J., Stewart-Koster, B., Olden, J.D., Ruesch, A.S., Torgersen, C.E., Lawler, J.J., Butcher, D.P. and Crown, J.K. (2014) 'The interactive effects of climate change, riparian management, and a nonnative predator on stream-rearing salmon', *Ecological Applications*, 24(4), pp. 895–912. doi:10.1890/13-0753.1.

Leduc, N., Lacoursière-Roussel, A., Howland, K.L., Archambault, P., Sevellec, M., Normandeau, E., Dispas, A., Winkler, G., McKindsey, C.W., Simard, N. and Bernatchez, L. (2019) 'Comparing eDNA metabarcoding and species collection for documenting Arctic metazoan biodiversity', *Environmental DNA*, 1(4), pp. 342–358. doi:10.1002/edn3.35.

Lee, H.H., Dineva, M.A., Chua, Y.L., Ritchie, A.V., Ushiro-Lumb, I. and Wisniewski, C.A. (2010) 'Simple Amplification-Based Assay: A Nucleic Acid–Based Point-of-Care Platform for HIV-1 Testing', *The Journal of Infectious Diseases*, 201(s1), pp. S65–S72. doi:10.1086/650385.

Lee, L., Nordman, E., Johnson, M. and Oldham, M. (2013) 'A Low-Cost, High-Performance System for Fluorescence Lateral Flow Assays', *Biosensors*, 3(4), pp. 360–373. doi:10.3390/bios3040360.

Leempoel, K., Hebert, T. and Hadly, E.A. (2020) 'A comparison of eDNA to camera trapping for assessment of terrestrial mammal diversity', *Proceedings of the Royal Society B: Biological Sciences*, 287(1918). doi:10.1098/rspb.2019.2353.

Li, C., Wen, A., Shen, B., Lu, J., Huang, Y. and Chang, Y. (2011) 'FastCloning: a highly simplified, purification-free, sequence- and ligation-independent PCR cloning method', *BMC Biotechnology*, 11(1), p. 92. doi:10.1186/1472-6750-11-92.

Li, J., Macdonald, J. and Von Stetten, F. (2019) 'Review: a comprehensive summary of a decade development of the recombinase polymerase amplification', *Analyst*. Royal Society of

Chemistry, pp. 31–67. doi:10.1039/c8an01621f.

Li, L., Li, S., Wu, N., Wu, J., Wang, G., Zhao, G. and Wang, J. (2019) 'HOLMESv2: A CRISPR-Cas12b-Assisted Platform for Nucleic Acid Detection and DNA Methylation Quantitation', *ACS Synthetic Biology*, 8(10), pp. 2228–2237. doi:10.1021/acssynbio.9b00209.

Li, S., Gu, Y., Lyu, Y., Jiang, Y. and Liu, P. (2017) 'Integrated Graphene Oxide Purification-Lateral Flow Test Strips (iGOP-LFTS) for Direct Detection of PCR Products with Enhanced Sensitivity and Specificity', *Analytical Chemistry*, 89(22), pp. 12137–12144. doi:10.1021/acs.analchem.7b02769.

Li, S.Y., Cheng, Q.X., Li, X.Y., Zhang, Z.L., Gao, S., Cao, R.B., Zhao, G.P., Wang, J.M. and Wang, J.M. (2018) 'CRISPR-Cas12a-assisted nucleic acid detection', *Cell Discovery*. Nature Publishing Groups, p. 20. doi:10.1038/s41421-018-0028-z.

Li, Y., Li, L., Fan, X., Zou, Y., Zhang, Y., Wang, Q., Sun, C., Pan, S., Wu, X. and Wang, Z. (2018) 'Development of real-time reverse transcription recombinase polymerase amplification (RPA) for rapid detection of peste des petits ruminants virus in clinical samples and its comparison with real-time PCR test', *Scientific Reports 2018 8:1*, 8(1), pp. 1–9. doi:10.1038/s41598-018-35636-5.

Li, Y., Li, S., Wang, J. and Liu, G. (2019) 'CRISPR/Cas Systems towards Next-Generation Biosensing', *Trends in Biotechnology*. Elsevier Ltd, pp. 730–743. doi:10.1016/j.tibtech.2018.12.005.

Li, Y., Liu, L. and Liu, G. (2019) 'CRISPR/Cas Multiplexed Biosensing: A Challenge or an Insurmountable Obstacle?', *Trends in Biotechnology*, 37(8), pp. 792–795. doi:10.1016/J.TIBTECH.2019.04.012.

Lien, S., Koop, B.F., Sandve, S.R., Miller, J.R., Kent, M.P., Nome, T., Hvidsten, T.R., Leong, J.S., Minkley, D.R., Zimin, A., Grammes, F., Grove, H., Gjuvsland, A., Walenz, B., Hermansen, R.A., von Schalburg, K., Rondeau, E.B., Di Genova, A., Samy, J.K.A., Olav Vik, J., Vigeland, M.D., Caler, L., Grimholt, U., Jentoft, S., Inge Våge, D., de Jong, P., Moen, T., Baranski, M., Palti, Y., Smith, D.R., Yorke, J.A., Nederbragt, A.J., Tooming-Klunderud, A., Jakobsen, K.S., Jiang, X., Fan, D., Hu, Y., Liberles, D.A., Vidal, R., Iturra, P., Jones, S.J.M., Jonassen, I., Maass, A., Omholt, S.W. and Davidson, W.S. (2016) 'The Atlantic salmon genome provides insights into rediploidization', *Nature*, 533(7602), pp. 200–205. doi:10.1038/nature17164.

Linders, T.E.W., Schaffner, U., Eschen, R., Abebe, A., Choge, S.K., Nigatu, L., Mbaabu, P.R.,

Shiferaw, H. and Allan, E. (2019) 'Direct and indirect effects of invasive species: Biodiversity loss is a major mechanism by which an invasive tree affects ecosystem functioning', *Journal of Ecology*, 107(6), pp. 2660–2672. doi:10.1111/1365-2745.13268.

Liu, D.-F. and Li, W.-W. (2020) 'Genome Editing Techniques Promise New Breakthroughs in Water Environmental Microbial Biotechnologies', *ACS ES&T Water*, 1(4), pp. 745–747. doi:10.1021/ACSESTWATER.0C00276.

Liu, M., Han, X., Yao, L., Zhang, W., Liu, B. and Chen, Z. (2018) 'Development and application of a simple recombinase polymerase amplification assay for rapid point-of-care detection of feline herpesvirus type 1', *Archives of Virology 2018 164:1*, 164(1), pp. 195–200. doi:10.1007/S00705-018-4064-7.

Lizardi, P.M., Huang, X., Zhu, Z., Bray-Ward, P., Thomas, D.C. and Ward, D.C. (1998) 'Mutation detection and single-molecule counting using isothermal rolling-circle amplification', *Nature Genetics*, 19(3), pp. 225–232. doi:10.1038/898.

Lobato, I.M. and O'Sullivan, C.K. (2018) 'Recombinase polymerase amplification: Basics, applications and recent advances', *TrAC Trends in Analytical Chemistry*, 98, pp. 19–35. doi:10.1016/J.TRAC.2017.10.015.

Londoño, M.A., Harmon, C.L. and Polston, J.E. (2016) 'Evaluation of recombinase polymerase amplification for detection of begomoviruses by plant diagnostic clinics', *Virology Journal*, 13(1), p. 48. doi:10.1186/s12985-016-0504-8.

Loughs Agency (2021) *Sea Trout Monitoring Projects*. Available at: https://www.loughs-agency.org/managing-our-loughs/conservation/freshwater-fisheries-monitoring-programme/sea-trout-monitoring-projects/ (Accessed: 8 July 2021).

Low, J.J., Igoe, F., Davenport, J. and Harrison, S.S.C. (2011) 'Littoral spawning habitats of three southern Arctic charr (Salvelinus alpinus L.) populations', *Ecology of Freshwater Fish*, 20(4), pp. 537–547. doi:10.1111/J.1600-0633.2011.00502.X.

Lowe, S., Browne, M., Boudjelas, S. and De Poorter, M. (2000) *100 of the World's Worst Invasive Alien Species. A Selection from the Global Invasive Species Database.*

Lucey, J. (2020) *Ireland's rivers: 10,000 years of use and abuse by humans*. Available at: https://www.irishtimes.com/culture/books/ireland-s-rivers-10-000-years-of-use-and-abuse-by-humans-1.4430914 (Accessed: 30 August 2021).

Lugg, W.H., Griffiths, J., Rooyen, A.R., Weeks, A.R. and Tingley, R. (2018) 'Optimal survey designs

for environmental DNA sampling', *Methods in Ecology and Evolution*. Edited by S. Jarman, 9(4), pp. 1049–1059. doi:10.1111/2041-210X.12951.

Macqueen, D.J., Primmer, C.R., Houston, R.D., Nowak, B.F., Bernatchez, L., Bergseth, S., Davidson, W.S., Gallardo-Escárate, C., Goldammer, T., Guiguen, Y., Iturra, P., Kijas, J.W., Koop, B.F., Lien, S., Maass, A., Martin, S.A.M., McGinnity, P., Montecino, M., Naish, K.A., Nichols, K.M., Ólafsson, K., Omholt, S.W., Palti, Y., Plastow, G.S., Rexroad, C.E., Rise, M.L., Ritchie, R.J., Sandve, S.R., Schulte, P.M., Tello, A., Vidal, R., Vik, J.O., Wargelius, A. and Yáñez, J.M. (2017) 'Functional Annotation of All Salmonid Genomes (FAASG): an international initiative supporting future salmonid research, conservation and aquaculture', *BMC Genomics*, 18(1), p. 484. doi:10.1186/s12864-017-3862-8.

Magnuson, J.J., Benson, B.J. and Mclain, A.S. (1994) 'Insights on species richness and turnover from long-term ecological research: Fishes in north temperate lakes', *Integrative and Comparative Biology*, 34(3), pp. 437–451. doi:10.1093/icb/34.3.437.

Maguire, I., Fitzgerald, J., Heery, B., Nwankire, C., O'Kennedy, R., Ducrée, J. and Regan, F. (2018) 'Novel Microfluidic Analytical Sensing Platform for the Simultaneous Detection of Three Algal Toxins in Water', *ACS Omega*, 3(6), pp. 6624–6634. doi:10.1021/acsomega.8b00240.

Maitland, P.S., Winfield, I.J., McCarthy, I.D. and Igoe, F. (2007) 'The status of Arctic charr Salvelinus alpinus in Britain and Ireland', *Ecology of Freshwater Fish*, 16(1), pp. 6–19. doi:10.1111/J.1600-0633.2006.00167.X.

Makarova, K.S., Haft, D.H., Barrangou, R., Brouns, S.J.J., Charpentier, E., Horvath, P., Moineau, S., Mojica, F.J.M., Wolf, Y.I., Yakunin, A.F., van der Oost, J. and Koonin, E. V. (2011) 'Evolution and classification of the CRISPR–Cas systems', *Nature Reviews Microbiology*, 9(6), pp. 467–477. doi:10.1038/nrmicro2577.

Makowski, G.S., Davis, E.L. and Hopfer, S.M. (1997) 'Amplification of Guthrie card DNA: Effect of quanidine thiocyanate on binding of natural whole blood PCR inhibitors', *Journal of Clinical Laboratory Analysis*, 11, pp. 87–93.

Malhotra, S., Verma, A., Tyagi, N. and Kumar, V. (2017) *Biosensors: Principle, types and applications*.

Mao, X., Ma, Y., Zhang, A., Zhang, L., Zeng, L. and Liu, G. (2009) 'Disposable nucleic acid biosensors based on gold nanoparticle probes and lateral flow strip', *Analytical Chemistry*, 81(4), pp. 1660–1668. doi:10.1021/ac8024653.

Marshall, N.T. and Stepien, C.A. (2019) 'Invasion genetics from eDNA and thousands of larvae: A targeted metabarcoding assay that distinguishes species and population variation of zebra and quagga mussels', *Ecology and Evolution*, 9(6), pp. 3515–3538. doi:10.1002/ece3.4985.

Martzy, R., Kolm, C., Brunner, K., Mach, R.L., Krska, R., Sinkovec, H., Sommer, R., Farnleitner, A.H. and Reischer, G.H. (2017) 'A loop-mediated isothermal amplification (LAMP) assay for the rapid detection of Enterococcus spp. in water', *Water Research*, 122, pp. 62–69.

Matisoo-Smith, E., Roberts, K., Welikala, N., Tannock, G., Chester, P., Feek, D. and Flenley, J. (2008) 'Recovery of DNA and pollen from New Zealand lake sediments', *Quaternary International*, 184(1), pp. 139–149. doi:10.1016/J.QUAINT.2007.09.013.

Mauvisseau, Q., Coignet, A., Delaunay, C., Pinet, F., Bouchon, D. and Souty-Grosset, C. (2018) 'Environmental DNA as an efficient tool for detecting invasive crayfishes in freshwater ponds', *Hydrobiologia*, 805(1), pp. 163–175. doi:10.1007/s10750-017-3288-y.

McConnell, E.M., Nguyen, J. and Li, Y. (2020) 'Aptamer-Based Biosensors for Environmental Monitoring', *Frontiers in Chemistry*, 0, p. 434. doi:10.3389/FCHEM.2020.00434.

McDowall, R.M. (2006) 'Crying wolf, crying foul, or crying shame: alien salmonids and a biodiversity crisis in the southern cool-temperate galaxioid fishes?', *Reviews in Fish Biology and Fisheries 2006 16:3*, 16(3), pp. 233–422. doi:10.1007/S11160-006-9017-7.

McGinnity, P., Jennings, E., deEyto, E., Allott, N., Samuelsson, P., Rogan, G., Whelan, K. and Cross, T. (2009) 'Impact of naturally spawning captive-bred Atlantic salmon on wild populations: depressed recruitment and increased risk of climate-mediated extinction', *Proceedings of the Royal Society B: Biological Sciences*, 276(1673), pp. 3601–3610. doi:10.1098/RSPB.2009.0799.

McGinnity, P., Prodöhl, P., Ferguson, A., Hynes, R., Maoiléidigh, N.O., Baker, N., Cotter, D., O'Hea, B., Cooke, D., Rogan, G., Taggart, J. and Cross, T. (2003) 'Fitness reduction and potential extinction of wild populations of Atlantic salmon, Salmo salar, as a result of interactions with escaped farm salmon.', *Proceedings of the Royal Society B: Biological Sciences*, 270(1532), p. 2443. doi:10.1098/RSPB.2003.2520.

McGinnity, P., Stone, C., Taggart, J.B., Cooke, D., Cotter, D., Hynes, R., McCamley, C., Cross, T. and Ferguson, A. (1997) 'Genetic impact of escaped farmed Atlantic salmon (Salmo salar L.) on native populations: use of DNA profiling to assess freshwater performance of wild, farmed, and hybrid progeny in a natural river environment', *ICES Journal of Marine Science*, 54(6), pp. 998–1008. doi:10.1016/S1054-3139(97)80004-5.

McKeague, M., McConnell, E.M., Cruz-Toledo, J., Bernard, E.D., Pach, A., Mastronardi, E., Zhang, X., Beking, M., Francis, T., Giamberardino, A., Cabecinha, A., Ruscito, A., Aranda-Rodriguez, R., Dumontier, M. and DeRosa, M.C. (2015) 'Analysis of In Vitro Aptamer Selection Parameters', *Journal of Molecular Evolution 2015 81:5*, 81(5), pp. 150–161. doi:10.1007/S00239-015-9708-6.

McKee, A.M., Spear, S.F. and Pierson, T.W. (2015) 'The effect of dilution and the use of a post-extraction nucleic acid purification column on the accuracy, precision, and inhibition of environmental DNA samples', *Biological Conservation*, 183, pp. 70–76. doi:10.1016/j.biocon.2014.11.031.

Merkes, C.M., McCalla, S.G., Jensen, N.R., Gaikowski, M.P. and Amberg, J.J. (2014) 'Persistence of DNA in Carcasses, Slime and Avian Feces May Affect Interpretation of Environmental DNA Data', *PLoS ONE*. Edited by R.C. Willson, 9(11), p. e113346. doi:10.1371/journal.pone.0113346.

MileniaBiotec (2020) 'A Short Guide for Improved Readout-Performance CRISPR/Cas-based Detection Methods and HybriDetect: Universal Test Strips-Individual Readout Lateral Flow-Detection Mechanism Lateral Flow-Interpretation'.

Miller, H., Winfield, I.J., Fletcher, J.M., James, J. Ben, Rijn, J. van, Bull, J.M. and Cotterill, C.J. (2015) 'Distribution, characteristics and condition of Arctic charr (Salvelinus alpinus) spawning grounds in a differentially eutrophicated twin-basin lake', *Ecology of Freshwater Fish*, 24(1), pp. 32–43. doi:10.1111/EFF.12122.

Minamoto, T., Uchii, K., Takahara, T., Kitayoshi, T., Tsuji, S., Yamanaka, H. and Doi, H. (2017) 'Nuclear internal transcribed spacer-1 as a sensitive genetic marker for environmental DNA studies in common carp Cyprinus carpio', *Molecular Ecology Resources*, 17(2), pp. 324–333. doi:10.1111/1755-0998.12586.

Minett, J.F., Leaniz, C.G. de, Brickle, P. and Consuegra, S. (2021) 'A new high-resolution melt curve eDNA assay to monitor the simultaneous presence of invasive brown trout (Salmo trutta) and endangered galaxiids', *Environmental DNA*, 3(3), pp. 561–572. doi:10.1002/EDN3.151.

Mirimin, L., Hickey, A., Barrett, D., DeFaoite, F., Boschetti, S., Venkatesh, S. and Graham, C.T. (2020) 'Environmental DNA detection of Arctic char (Salvelinus alpinus) in Irish lakes: Development and application of a species-specific molecular assay', *Environmental DNA*, 2(2), pp. 221–233. doi:10.1002/EDN3.60.

Miya, M., Sato, Y., Fukunaga, T., Sado, T., Poulsen, J.Y., Sato, K., Minamoto, T., Yamamoto, S., Yamanaka, H., Araki, H., Kondoh, M. and Iwasaki, W. (2015) 'MiFish, a set of universal PCR

primers for metabarcoding environmental DNA from fishes: detection of more than 230 subtropical marine species', *Royal Society Open Science*, 2(7). doi:10.1098/RSOS.150088.

Mohr, S., Zhang, Y., Macaskill, A., Day, P., Barber, R. and Goddard, N. (2007) 'Numerical and experimental study of a droplet-based PCR chip', *Microfluidics and Nanofluidics*, 3(5), pp. 611–621.

Molnar, J.L., Gamboa, R.L., Revenga, C. and Spalding, M.D. (2008) 'Assessing the global threat of invasive species to marine biodiversity', *Frontiers in Ecology and the Environment*, 6(9), pp. 485–492. doi:10.1016/j.jallcom.2015.08.157.

Mooney, H.A. and Cleland, E.E. (2001) 'The evolutionary impact of invasive species.', *Proceedings of the National Academy of Sciences of the United States of America*, 98(10), pp. 5446–51. doi:10.1073/pnas.091093398.

Mori, Y., Nagamine, K., Tomita, N. and Notomi, T. (2001) 'Detection of loop-mediated isothermal amplification reaction by turbidity derived from magnesium pyrophosphate formation', *Biochemical and Biophysical Research Communications*, 289(1), pp. 150–154. doi:10.1006/bbrc.2001.5921.

Muri, C. Di (2020) *Environmental DNA (eDNA) monitoring of priority conservation fish species in UK lentic ecosystems*. University of Hull.

Murugan, K., Seetharam, A.S., Severin, A.J. and Sashital, D.G. (2020) 'CRISPR-Cas12a has widespread off-target and dsDNA-nicking effects', *The Journal of Biological Chemistry*, 295(17), p. 5538. doi:10.1074/JBC.RA120.012933.

Mustafa, M.I. and Makhawi, A.M. (2021) 'SHERLOCK and DETECTR: CRISPR-cas systems as potential rapid diagnostic tools for emerging infectious diseases', *Journal of Clinical Microbiology*, 59(3). doi:10.1128/JCM.00745-20.

Nagel, B., Dellweg, H. and Gierasch, L. (1992) 'Glossary for chemists of terms used in biotechnology (IUPAC Recommendations 1992)', *Pure and Applied Chemistry*, 64(1), pp. 143–168.

Nathan, L.M., Simmons, M., Wegleitner, B.J., Jerde, C.L. and Mahon, A.R. (2014) 'Quantifying Environmental DNA Signals for Aquatic Invasive Species Across Multiple Detection Platforms', *Environmental Science & Technology*, 48(21), pp. 12800–12806. doi:10.1021/es5034052.

Nelson-Chorney, H.T., Davis, C.S., Poesch, M.S., Vinebrooke, R.D., Carli, C.M. and Taylor, M.K. (2019) 'Environmental DNA in lake sediment reveals biogeography of native genetic diversity',

Frontiers in Ecology and the Environment, 17(6), pp. 313–318. doi:10.1002/FEE.2073.

Nevoux, M., Finstad, B., Davidsen, J.G., Finlay, R., Josset, Q., Poole, R., Höjesjö, J., Aarestrup, K., Persson, L., Tolvanen, O. and Jonsson, B. (2019) 'Environmental influences on life history strategies in partially anadromous brown trout (Salmo trutta, Salmonidae)', *Fish and Fisheries*, 20(6), pp. 1051–1082. doi:10.1111/FAF.12396.

Newman, J.D. and Turner, A.P.F. (2005) 'Home blood glucose biosensors: a commercial perspective', *Biosensors and Bioelectronics*, 20(12), pp. 2435–2453. doi:10.1016/j.bios.2004.11.012.

Nguyen, H.H., Lee, S.H., Lee, U.J., Fermin, C.D. and Kim, M. (2019) 'Immobilized Enzymes in Biosensor Applications.', *Materials (Basel, Switzerland)*, 12(1). doi:10.3390/ma12010121.

Nguyen, L.T., Smith, B.M. and Jain, P.K. (2020) 'Enhancement of trans-cleavage activity of Cas12a with engineered crRNA enables amplified nucleic acid detection', *Nature Communications 2020 11:1*, 11(1), pp. 1–13. doi:10.1038/s41467-020-18615-1.

Nguyen, P.L., Sudheesh, P.S., Thomas, A.C., Sinnesael, M., Haman, K. and Cain, K.D. (2018) 'Rapid Detection and Monitoring of *Flavobacterium psychrophilum* in Water by Using a Handheld, Field-Portable Quantitative PCR System', *Journal of Aquatic Animal Health*, 30(4), pp. 302–311. doi:10.1002/aah.10046.

Nicholls, P.J. and Malcolm, A.D.B. (1989) 'Nucleic acid analysis by sandwich hybridization', *Journal of Clinical Laboratory Analysis*, 3(2), pp. 122–135. doi:10.1002/jcla.1860030210.

Niemz, A., Ferguson, T.M. and Boyle, D.S. (2011) 'Point-of-care nucleic acid testing for infectious diseases', *Trends in Biotechnology*, 29(5), pp. 240–250. doi:10.1016/j.tibtech.2011.01.007.

Njiru, Z.K., Mikosza, A.S.J., Armstrong, T., Enyaru, J.C., Ndung'u, J.M. and Thompson, A.R.C. (2008) 'Loop-mediated isothermal amplification (LAMP) method for rapid detection of Trypanosoma brucei rhodesiense', *PLoS Neglected Tropical Diseases*, 2(2). doi:10.1371/journal.pntd.0000147.

Northrup, M., Ching, M., White, R. and Watson, R. (1993) 'DNA amplification in a microfabricated reaction chamber', in *Proceedings of the 7th International Conference on Solid-State Sensors and Actuators (Transducers '93)*. Yokohama, Japan, pp. 924–926.

Notomi, T., Okayama, H., Masubuchi, H., Yonekawa, T., Watanabe, K., Amino, N. and Hase, T. (2000) 'Loop-mediated isothermal amplification of DNA', *Nucleic Acids Research*, 28(12), pp. 63e – 63.

O'Sullivan, A.M., Samways, K.M., Perreault, A., Hernandez, C., Gautreau, M.D., Curry, R.A. and Bernatchez, L. (2020) 'Space invaders: Searching for invasive Smallmouth Bass (Micropterus dolomieu) in a renowned Atlantic Salmon (Salmo salar) river', *Ecology and Evolution*, 10(5), pp. 2588–2596. doi:10.1002/ece3.6088.

Obande, G.A. and Singh, K.K.B. (2020) *Current and future perspectives on isothermal nucleic acid amplification technologies for diagnosing infections*, *Infection and Drug Resistance*. doi:10.2147/IDR.S217571.

OECD (2021) *Fisheries and Aquaculture in Ireland*.

Okumoto, S. (2012) 'Quantitative imaging using genetically encoded sensors for small molecules in plants', *The Plant Journal*, 70(1), pp. 108–117. doi:10.1111/j.1365-313X.2012.04910.x.

Olajos, F., Bokma, F., Bartels, P., Myrstener, E., Rydberg, J., Öhlund, G., Bindler, R., Wang, X.-R., Zale, R. and Englund, G. (2018) 'Estimating species colonization dates using DNA in lake sediment', *Methods in Ecology and Evolution*, 9(3), pp. 535–543. doi:10.1111/2041-210X.12890.

Olson, Z.H., Briggler, J.T. and Williams, R.N. (2012) 'An eDNA approach to detect eastern hellbenders (Cryptobranchus a. alleganiensis) using samples of water', *Wildlife Research*, 39, pp. 629–636.

Palchetti, I. and Mascini, M. (2008) 'Nucleic acid biosensors for environmental pollution monitoring', *The Analyst*, 133(7), p. 846. doi:10.1039/b802920m.

Palmer, M.A. and Menninger, H.L. (2013) 'Invertebrates, Freshwater, Overview', *Encyclopedia of Biodiversity: Second Edition*, pp. 369–378. doi:10.1016/B978-0-12-384719-5.00077-0.

Pardee, K., Green, A.A., Takahashi, M.K., Braff, D., Lambert, G., Lee, J.W., Ferrante, T., Ma, D., Donghia, N., Fan, M., Daringer, N.M., Bosch, I., Dudley, D.M., O'Connor, D.H., Gehrke, L. and Collins, J.J. (2016) 'Rapid, Low-Cost Detection of Zika Virus Using Programmable Biomolecular Components', *Cell*, 165(5), pp. 1255–1266. doi:10.1016/j.cell.2016.04.059.

Parsons, K.M., Everett, M., Dahlheim, M. and Park, L. (2018) 'Water, water everywhere: environmental DNA can unlock population structure in elusive marine species', *Royal Society Open Science*, 5(8), p. 180537. doi:10.1098/rsos.180537.

Patchsung, M., Jantarug, K., Pattama, A., Aphicho, K., Suraritdechachai, S., Meesawat, P., Sappakhaw, K., Leelahakorn, N., Ruenkam, T., Wongsatit, T., Athipanyasilp, N., Eiamthong, B., Lakkanasirorat, B., Phoodokmai, T., Niljianskul, N., Pakotiprapha, D., Chanarat, S., Homchan, A., Tinikul, R., Kamutira, P., Phiwkaow, K., Soithongcharoen, S., Kantiwiriyawanitch, C., Pongsupasa,

V., Trisrivirat, D., Jaroensuk, J., Wongnate, T., Maenpuen, S., Chaiyen, P., Kamnerdnakta, S., Swangsri, J., Chuthapisith, S., Sirivatanauksorn, Y., Chaimayo, C., Sutthent, R., Kantakamalakul, W., Joung, J., Ladha, A., Jin, X., Gootenberg, J.S., Abudayyeh, O.O., Zhang, F., Horthongkham, N. and Uttamapinant, C. (2020) 'Clinical validation of a Cas13-based assay for the detection of SARS-CoV-2 RNA', *Nature Biomedical Engineering 2020 4:12*, 4(12), pp. 1140–1149. doi:10.1038/s41551-020-00603-x.

Pecchia, S. and Da Lio, D. (2018) 'Development of a rapid PCR-Nucleic Acid Lateral Flow Immunoassay (PCR-NALFIA) based on rDNA IGS sequence analysis for the detection of Macrophomina phaseolina in soil', *Journal of Microbiological Methods*, 151, pp. 118–128. doi:10.1016/J.MIMET.2018.06.010.

Pejchar, L. and Mooney, H.A. (2009) 'Invasive species, ecosystem services and human well-being', *Trends in Ecology & Evolution*, 24(9), pp. 497–504. doi:10.1016/J.TREE.2009.03.016.

Piepenburg, O., Williams, C.H., Stemple, D.L. and Armes, N.A. (2006) 'DNA detection using recombination proteins.', *PLoS biology*, 4(7), p. e204. doi:10.1371/journal.pbio.0040204.

Piggott, M.P. (2016) 'Evaluating the effects of laboratory protocols on eDNA detection probability for an endangered freshwater fish', *Ecology and Evolution*, 6(9), pp. 2739–2750. doi:10.1002/ece3.2083.

Pilliod, D.S., Goldberg, C.S., Arkle, R.S. and Waits, L.P. (2013) 'Estimating occupancy and abundance of stream amphibians using environmental DNA from filtered water samples', *Canadian Journal of Fisheries and Aquatic Sciences*. Edited by J. Richardson, 70(8), pp. 1123–1130. doi:10.1139/cjfas-2013-0047.

Pilliod, D.S., Goldberg, C.S., Arkle, R.S. and Waits, L.P. (2014) 'Factors influencing detection of eDNA from a stream-dwelling amphibian', *Molecular Ecology Resources*, 14(1), pp. 109–116. doi:10.1111/1755-0998.12159.

Pochon, X., Zaiko, A., Fletcher, L.M., Laroche, O. and Wood, S.A. (2017) 'Wanted dead or alive? Using metabarcoding of environmental DNA and RNA to distinguish living assemblages for biosecurity applications', *PLOS ONE*, 12(11), p. e0187636. doi:10.1371/JOURNAL.PONE.0187636.

Pohanka, M. (2018) 'Overview of Piezoelectric Biosensors, Immunosensors and DNA Sensors and Their Applications.', *Materials (Basel, Switzerland)*, 11(3). doi:10.3390/ma11030448.

Prediger, E. (2013) *How to design primers and probes for PCR and qPCR | IDT*. Available at:

https://eu.idtdna.com/pages/education/decoded/article/designing-pcr-primers-and-probes (Accessed: 10 June 2019).

Qian, C., Wu, H., Shi, Y., Wu, J. and Chen, H. (2020) 'Dehydrated CRISPR-mediated DNA analysis for visualized animal-borne virus sensing in the unprocessed blood sample', *Sensors and Actuators, B: Chemical*, 305, p. 127440. doi:10.1016/j.snb.2019.127440.

Quilodrán, C.S., Currat, M. and Montoya-Burgos, J.I. (2014) 'A General Model of Distant Hybridization Reveals the Conditions for Extinction in Atlantic Salmon and Brown Trout', *PLOS ONE*, 9(7), p. e101736. doi:10.1371/JOURNAL.PONE.0101736.

Ramsey, C.B. (2009) 'Bayesian Analysis of Radiocarbon Dates', *Radiocarbon*, 51(1), pp. 337–360. doi:10.1017/S0033822200033865.

Rees, H.C., Maddison, B.C., Middleditch, D.J., Patmore, J.R.M. and Gough, K.C. (2014) 'REVIEW: The detection of aquatic animal species using environmental DNA - a review of eDNA as a survey tool in ecology', *Journal of Applied Ecology*. Edited by E. Crispo, 51(5), pp. 1450–1459. doi:10.1111/1365-2664.12306.

Reimer, P.J., Austin, W.E.N., Bard, E., Bayliss, A., Blackwell, P.G., Ramsey, C.B., Butzin, M., Cheng, H., Edwards, R.L., Friedrich, M., Grootes, P.M., Guilderson, T.P., Hajdas, I., Heaton, T.J., Hogg, A.G., Hughen, K.A., Kromer, B., Manning, S.W., Muscheler, R., Palmer, J.G., Pearson, C., Plicht, J. van der, Reimer, R.W., Richards, D.A., Scott, E.M., Southon, J.R., Turney, C.S.M., Wacker, L., Adolphi, F., Büntgen, U., Capano, M., Fahrni, S.M., Fogtmann-Schulz, A., Friedrich, R., Köhler, P., Kudsk, S., Miyake, F., Olsen, J., Reinig, F., Sakamoto, M., Sookdeo, A. and Talamo, S. (2020) 'The IntCal20 Northern Hemisphere Radiocarbon Age Calibration Curve (0–55 cal kBP)', *Radiocarbon*, 62(4), pp. 725–757. doi:10.1017/RDC.2020.41.

Reinhardt, T., van Schingen, M., Windisch, H.S., Nguyen, T.Q., Ziegler, T. and Fink, P. (2019) 'Monitoring a loss: Detection of the semi-aquatic crocodile lizard (Shinisaurus crocodilurus) in inaccessible habitats via environmental DNA', *Aquatic Conservation: Marine and Freshwater Ecosystems*, 29(3), pp. 353–360. doi:10.1002/aqc.3038.

Renshaw, M.A., Olds, B.P., Jerde, C.L., McVeigh, M.M. and Lodge, D.M. (2015) 'The room temperature preservation of filtered environmental DNA samples and assimilation into a phenol-chloroform-isoamyl alcohol DNA extraction', *Molecular Ecology Resources*, 15(1), pp. 168–176. doi:10.1111/1755-0998.12281.

Revenga, C., Campbell, I., Abell, R., Villiers, P. de and Bryer, M. (2005) 'Prospects for monitoring

freshwater ecosystems towards the 2010 targets', *Philosophical Transactions of the Royal Society B: Biological Sciences*, 360(1454), pp. 397–413. doi:10.1098/RSTB.2004.1595.

Robinson, C.V., Garcia de Leaniz, C., Rolla, M. and Consuegra, S. (2019) 'Monitoring the eradication of the highly invasive topmouth gudgeon (Pseudorasbora parva) using a novel eDNA assay', *Environmental DNA*, 1(1), pp. 74–85. doi:10.1002/edn3.12.

Roche.Diagnostics.GmbH (2008) *LightCycler ® 480 Instrument Operator's Manual V1.5*.

Rodgers, T.W. and Mock, K.E. (2015) 'Drinking water as a source of environmental DNA for the detection of terrestrial wildlife species', *Conservation Genetics Resources*, 7(3), pp. 693–696. doi:10.1007/s12686-015-0478-7.

Rohrman, B. and Richards-Kortum, R. (2015) 'Inhibition of Recombinase Polymerase Amplification by Background DNA: A Lateral Flow-Based Method for Enriching Target DNA', *Analytical Chemistry*, 87(3), pp. 1963–1967. doi:10.1021/AC504365V.

Rourke, M.L., Fowler, A.M., Hughes, J.M., Broadhurst, M.K., DiBattista, J.D., Fielder, S., Walburn, J.W. and Furlan, E.M. (2021) 'Environmental DNA (eDNA) as a tool for assessing fish biomass: A review of approaches and future considerations for resource surveys', *Environmental DNA*, 00, pp. 1–25. doi:10.1002/EDN3.185.

Royce, W.F. (1996) 'Food Chain and Resource Organisms', *Introduction to the Practice of Fishery Science*, pp. 92–134. doi:10.1016/B978-012600952-1/50007-4.

Ruppert, K.M., Kline, R.J. and Rahman, M.S. (2019) 'Past, present, and future perspectives of environmental DNA (eDNA) metabarcoding: A systematic review in methods, monitoring, and applications of global eDNA', *Global Ecology and Conservation*, 17, p. e00547. doi:10.1016/J.GECCO.2019.E00547.

Rusch, J.C., Hansen, H., Strand, D.A., Markussen, T., Hytterød, S. and Vrålstad, T. (2018) 'Catching the fish with the worm: a case study on eDNA detection of the monogenean parasite Gyrodactylus salaris and two of its hosts, Atlantic salmon (Salmo salar) and rainbow trout (Oncorhynchus mykiss)', *Parasites & Vectors*, 11(1), p. 333. doi:10.1186/s13071-018-2916-3.

Saint-Pé, K., Leitwein, M., Tissot, L., Poulet, N., Guinand, B., Berrebi, P., Marselli, G., Lascaux, J.-M., Gagnaire, P.-A. and Blanchet, S. (2019) 'Development of a large SNPs resource and a low-density SNP array for brown trout (Salmo trutta) population genetics', *BMC Genomics 2019 20:1*, 20(1), pp. 1–13. doi:10.1186/S12864-019-5958-9.

Sakata, M.K., Yamamoto, S., Gotoh, R.O., Miya, M., Yamanaka, H. and Minamoto, T. (2020)

'Sedimentary eDNA provides different information on timescale and fish species composition compared with aqueous eDNA', *Environmental DNA*, 2(4), pp. 505–518. doi:10.1002/edn3.75.

Sales, N.G., McKenzie, M.B., Drake, J., Harper, L.R., Browett, S.S., Coscia, I., Wangensteen, O.S., Baillie, C., Bryce, E., Dawson, D.A., Ochu, E., Hänfling, B., Lawson Handley, L., Mariani, S., Lambin, X., Sutherland, C. and McDevitt, A.D. (2020) 'Fishing for mammals: Landscape-level monitoring of terrestrial and semi-aquatic communities using eDNA from riverine systems', *Journal of Applied Ecology*, 57(4), pp. 707–716. doi:10.1111/1365-2664.13592.

Salter, I., Joensen, M., Kristiansen, R., Steingrund, P. and Vestergaard, P. (2019) 'Environmental DNA concentrations are correlated with regional biomass of Atlantic cod in oceanic waters', *Communications Biology 2019 2:1*, 2(1), pp. 1–9. doi:10.1038/s42003-019-0696-8.

Samy, J.K.A., Mulugeta, T.D., Nome, T., Sandve, S.R., Grammes, F., Kent, M.P., Lien, S. and Våge, D.I. (2017) 'SalmoBase: an integrated molecular data resource for Salmonid species', *BMC Genomics*, 18(1), p. 482. doi:10.1186/s12864-017-3877-1.

Sapsford, K.E., Charles, P.T., Patterson, C.H.J. and Ligler, F.S. (2002) 'Demonstration of Four Immunoassay Formats Using the Array Biosensor'. doi:10.1021/AC0157268.

Sawaya, N.A., Djurhuus, A., Closek, C.J., Hepner, M., Olesin, E., Visser, L., Kelble, C., Hubbard, K. and Breitbart, M. (2019) 'Assessing eukaryotic biodiversity in the Florida Keys National Marine Sanctuary through environmental DNA metabarcoding', *Ecology and Evolution*, 9(3), pp. 1029–1040. doi:10.1002/ece3.4742.

Schultz, M.T. and Lance, R.F. (2015) 'Modeling the Sensitivity of Field Surveys for Detection of Environmental DNA (eDNA)', *PLOS ONE*, 10(10), p. e0141503. doi:10.1371/JOURNAL.PONE.0141503.

Scognamiglio, V., Arduini, F., Palleschi, G. and Rea, G. (2014) 'Biosensing technology for sustainable food safety', *TrAC Trends in Analytical Chemistry*, 62, pp. 1–10. doi:10.1016/J.TRAC.2014.07.007.

Sepulveda, A.J., Hutchins, P.R., Massengill, R.L. and Dunker, K.J. (2018) 'Tradeoffs of a portable, field-based environmental DNA platform for detecting invasive northern pike (Esox lucius) in Alaska', *Management of Biological Invasions*, 9(3), pp. 253–258. doi:10.3391/mbi.2018.9.3.07.

Shao, N., Han, X., Song, Y., Zhang, P. and Qin, L. (2019) 'CRISPR-Cas12a Coupled with Platinum Nanoreporter for Visual Quantification of SNVs on a Volumetric Bar-Chart Chip', *Analytical Chemistry*, 91(19), pp. 12384–12391. doi:10.1021/acs.analchem.9b02925.

Sharber, N.G. and Carothers, S.W. (1988) 'Influence of Electrofishing Pulse Shape on Spinal Injuries in Adult Rainbow Trout', *North American Journal of Fisheries Management*, 8(1), pp. 117–122. doi:10.1577/1548-8675(1988)008<0117:IOEPSO>2.3.CO;2.

Sharma, S., Zapatero-Rodríguez, J., Estrela, P. and O'Kennedy, R. (2015) 'Point-of-Care Diagnostics in Low Resource Settings: Present Status and Future Role of Microfluidics', *Biosensors 2015, Vol. 5, Pages 577-601*, 5(3), pp. 577–601. doi:10.3390/BIOS5030577.

Shokralla, S., Spall, J.L., Gibson, J.F. and Hajibabaei, M. (2012) 'Next-generation sequencing technologies for environmental DNA research', *Molecular Ecology*, 21(8), pp. 1794–1805. doi:10.1111/j.1365-294X.2012.05538.x.

Sigsgaard, E.E., Carl, H., Møller, P.R. and Thomsen, P.F. (2015) 'Monitoring the near-extinct European weather loach in Denmark based on environmental DNA from water samples', *Biological Conservation*, 183, pp. 46–52. doi:10.1016/j.biocon.2014.11.023.

Skinner, M., Murdoch, M., Loeza-Quintana, T., Crookes, S. and Hanner, R. (2020) ' A mesocosm comparison of laboratory-based and on-site eDNA solutions for detection and quantification of striped bass (Morone saxatilis) in marine ecosystems ', *Environmental DNA* [Preprint]. doi:10.1002/edn3.61.

Smart, A.S., Weeks, A.R., van Rooyen, A.R., Moore, A., McCarthy, M.A. and Tingley, R. (2016) 'Assessing the cost-efficiency of environmental DNA sampling', *Methods in Ecology and Evolution*, 7(11), pp. 1291–1298. doi:10.1111/2041-210X.12598.

Snyder, D. (2003) 'Invite overview: conclusions from a review of electrofishing and its harmful effects on fish', *Reviews in Fish Biology and Fisheries*, 13, pp. 445–453.

Sontheimer, E.J. and Marraffini, L.A. (2010) 'Slicer for DNA', *Nature*, 468(7320). doi:10.1038/468045a.

Spencer, D.E., Molloy, K., Potito, A. and Jones, C. (2019) 'New insights into Late Bronze Age settlement and farming activity in the southern Burren, western Ireland', *Vegetation History and Archaeobotany 2019 29:3*, 29(3), pp. 339–356. doi:10.1007/S00334-019-00746-1.

Spens, J., Evans, A.R., Halfmaerten, D., Knudsen, S.W., Sengupta, M.E., Mak, S.S.T., Sigsgaard, E.E. and Hellström, M. (2017) 'Comparison of capture and storage methods for aqueous macrobial eDNA using an optimized extraction protocol: advantage of enclosed filter', *Methods in Ecology and Evolution*, 8(5), pp. 635–645. doi:10.1111/2041-210X.12683.

Stager, J.C., Sporn, L.A., Johnson, M. and Regalado, S. (2015) 'Of Paleo-Genes and Perch: What

if an “Alien” Is Actually a Native?’, *PLOS ONE*, 10(3), p. e0119071. doi:10.1371/JOURNAL.PONE.0119071.

Stewart, K.A. (2019) ‘Understanding the effects of biotic and abiotic factors on sources of aquatic environmental DNA’, *Biodiversity and Conservation*, 28(5), pp. 983–1001. doi:10.1007/s10531-019-01709-8.

Stewart, K.A. and Taylor, S.A. (2020) ‘Leveraging eDNA to expand the study of hybrid zones’, *Molecular Ecology*, 29(15), pp. 2768–2776. doi:10.1111/MEC.15514.

Stoeckle, M.Y., Das Mishu, M. and Charlop-Powers, Z. (2020) ‘Improved Environmental DNA Reference Library Detects Overlooked Marine Fishes in New Jersey, United States’, *Frontiers in Marine Science*, 7, p. 226. doi:10.3389/FMARS.2020.00226.

Strickler, K.M., Fremier, A.K. and Goldberg, C.S. (2015) ‘Quantifying effects of UV-B, temperature, and pH on eDNA degradation in aquatic microcosms’, *Biological Conservation*, 183, pp. 85–92. doi:10.1016/j.biocon.2014.11.038.

Sullivan, T.J., Dhar, A.K., Cruz-Flores, R. and Bodnar, A.G. (2019) ‘Rapid, CRISPR-Based, Field-Deployable Detection Of White Spot Syndrome Virus In Shrimp’, *Scientific Reports*, 9(1), pp. 1–7. doi:10.1038/s41598-019-56170-y.

Swarts, D.C., van der Oost, J. and Jinek, M. (2017) ‘Structural Basis for Guide RNA Processing and Seed-Dependent DNA Targeting by CRISPR-Cas12a’, *Molecular Cell*, 66(2), pp. 221-233.e4. doi:10.1016/j.molcel.2017.03.016.

Taberlet, P., Coissac, E., Hajibabaei, M. and Riesberg, L. (2012) ‘Environmental DNA’, *Molecular Ecology*, 21(8), pp. 1789–1793. doi:10.1111/j.1365-294X.2012.05542.x.

Taberlet, P., Coissac, E., Pompanon, F., Brochmann, C. and Willerslev, E. (2012) ‘Towards next-generation biodiversity assessment using DNA metabarcoding’, *Molecular Ecology*, 21(8), pp. 2045–2050. doi:10.1111/j.1365-294X.2012.05470.x.

Takahara, T., Minamoto, T., Yamanaka, H., Doi, H. and Kawabata, Z. (2012) ‘Estimation of Fish Biomass Using Environmental DNA’, *PLoS ONE*. Edited by J.A. Gilbert, 7(4), p. e35868. doi:10.1371/journal.pone.0035868.

Thomas, A.C., Tank, S., Nguyen, P.L., Ponce, J., Sinnesael, M. and Goldberg, C.S. (2019) ‘A system for rapid eDNA detection of aquatic invasive species’, *Environmental DNA* [Preprint]. doi:10.1002/edn3.25.

Thomsen, P.F., Kielgast, J., Iversen, Lars Lønsmann, Møller, P.R., Rasmussen, M. and Willerslev, E. (2012) 'Detection of a Diverse Marine Fish Fauna Using Environmental DNA from Seawater Samples', *PLoS ONE*. Edited by S. Lin, 7(8), p. e41732. doi:10.1371/journal.pone.0041732.

Thomsen, P.F., Kielgast, J., Iversen, Lars L., Wiuf, C., Rasmussen, M., Gilbert, M.T.P., Orlando, L. and Willerslev, E. (2012) 'Monitoring endangered freshwater biodiversity using environmental DNA', *Molecular Ecology*, 21(11), pp. 2565–2573. doi:10.1111/j.1365-294X.2011.05418.x.

Thomsen, P.F. and Willerslev, E. (2015) 'Environmental DNA – An emerging tool in conservation for monitoring past and present biodiversity', *Biological Conservation*, 183, pp. 4–18. doi:10.1016/J.BIOCON.2014.11.019.

Thorstad, E.B., Todd, C.D., Uglem, I., Bjørn, P.A., Gargan, P.G., Vollset, K.W., Halttunen, E., Kålås, S., Berg, M. and Finstad, B. (2015) 'Effects of salmon lice Lepeophtheirus salmonis on wild sea trout Salmo trutta—a literature review', *Aquaculture Environment Interactions*, 7(2), pp. 91–113. doi:10.3354/AEI00142.

Toldrà, A., Alcaraz, C., Andree, K.B., Fernández-Tejedor, M., Diogène, J., Katakis, I., O'Sullivan, C.K. and Campàs, M. (2019) 'Colorimetric DNA-based assay for the specific detection and quantification of Ostreopsis cf. ovata and Ostreopsis cf. siamensis in the marine environment', *Harmful Algae*, 84, pp. 27–35. doi:10.1016/j.hal.2019.02.003.

Tom, M.R. and Mina, M.J. (2020) 'To Interpret the SARS-CoV-2 Test, Consider the Cycle Threshold Value', *Clinical Infectious Diseases* [Preprint]. doi:10.1093/cid/ciaa619.

Truelove, N.K., Andruszkiewicz, E.A. and Block, B.A. (2019) 'A rapid environmental DNA method for detecting white sharks in the open ocean', *Methods in Ecology and Evolution*, 10(8), pp. 1128–1135. doi:10.1111/2041-210X.13201.

Tsuji, S., Iguchi, Y., Shibata, N., Teramura, I., Kitagawa, T. and Yamanaka, H. (2018) 'Real-time multiplex PCR for simultaneous detection of multiple species from environmental DNA: an application on two Japanese medaka species', *Scientific Reports*, 8(1), p. 9138. doi:10.1038/s41598-018-27434-w.

Turner, C.R., Barnes, M.A., Xu, C.C.Y., Jones, S.E., Jerde, C.L. and Lodge, D.M. (2014) 'Particle size distribution and optimal capture of aqueous macrobial eDNA', *Methods in Ecology and Evolution*. Edited by M. Gilbert, 5(7), pp. 676–684. doi:10.1111/2041-210X.12206.

Turner, C.R., Uy, K.L. and Everhart, R.C. (2015) 'Fish environmental DNA is more concentrated in aquatic sediments than surface water', *Biological Conservation*, 183, pp. 93–102.

doi:10.1016/J.BIOCON.2014.11.017.

Ushio, M., Fukuda, H., Inoue, T., Makoto, K., Kishida, O., Sato, K., Murata, K., Nikaido, M., Sado, T., Sato, Y., Takeshita, M., Iwasaki, W., Yamanaka, H., Kondoh, M. and Miya, M. (2017) 'Environmental DNA enables detection of terrestrial mammals from forest pond water', *Molecular Ecology Resources*, 17(6), pp. e63–e75. doi:10.1111/1755-0998.12690.

Uthicke, S., Lamare, M. and Doyle, J.R. (2018) 'eDNA detection of corallivorous seastar (Acanthaster cf. solaris) outbreaks on the Great Barrier Reef using digital droplet PCR', *Coral Reefs*. Edited by M. Gilbert, 37(4), pp. 1229–1239. doi:10.1007/s00338-018-1734-6.

Vashist, S.K. (2017) 'Point-of-Care Diagnostics: Recent Advances and Trends.', *Biosensors*, 7(4). doi:10.3390/bios7040062.

van der Velden, V.H.J., Cazzaniga, G., Schrauder, A., Hancock, J., Bader, P., Panzer-Grumayer, E.R., Flohr, T., Sutton, R., Cave, H., Madsen, H.O., Cayuela, J.M., Trka, J., Eckert, C., Foroni, L., zur Stadt, U., Beldjord, K., Raff, T., van der Schoot, C.E. and van Dongen, J.J.M. (2007) 'Analysis of minimal residual disease by Ig/TCR gene rearrangements: Guidelines for interpretation of real-time quantitative PCR data', *Leukemia*. Nature Publishing Group, pp. 604–611. doi:10.1038/sj.leu.2404586.

Walker, G.T., Fraiser, M.S., Schram, J.L., Little, M.C., Nadeau, J.G. and Malinowski, D.P. (1992) 'Strand displacement amplification--an isothermal, in vitro DNA amplification technique.', *Nucleic acids research*, 20(7), pp. 1691–6. doi:10.1093/nar/20.7.1691.

Wand, N., Bonney, L.C., Watson, R.J., Graham, V. and Hewson, R. (2018) 'Point-of-care diagnostic assay for the detection of zika virus using the recombinase polymerase amplification method', *Journal of General Virology*, 99(8), pp. 1012–1026. doi:10.1099/jgv.0.001083.

Wang, B., Wang, R., Wang, D., Wu, J., Li, J., Wang, J., Liu, H. and Wang, Y. (2019) 'Cas12aVDet: A CRISPR/Cas12a-Based Platform for Rapid and Visual Nucleic Acid Detection', *Analytical Chemistry*, 91(19), pp. 12156–12161. doi:10.1021/acs.analchem.9b01526.

Wang, J. (2002) 'Electrochemical nucleic acid biosensors', *Analytica Chimica Acta*, 469(1), pp. 63–71. doi:10.1016/S0003-2670(01)01399-X.

Ward, R.D., Zemlak, T.S., Innes, B.H., Last, P.R. and Hebert, P.D.. (2005) 'DNA barcoding Australia's fish species', *Philosophical Transactions of the Royal Society B: Biological Sciences*, 360(1462), pp. 1847–1857. doi:10.1098/rstb.2005.1716.

Wellcome Sanger Institute (2019) *Brown trout genome will help explain species' genetic*

superpowers. Available at: https://www.sanger.ac.uk/news_item/brown-trout-genome-will-help-explain-species-genetic-superpowers/ (Accessed: 12 July 2021).

Wellcome Sanger Institute (no date) *25 Genomes for 25 Years*. Available at: https://www.sanger.ac.uk/science/collaboration/25-genomes-25-years (Accessed: 14 May 2019).

Whelan, B., Aas, Ø., Uglem, I., Curtis, J. and Dervo, B. (2006) *Assessment of the socio-economic value of aquaculture and sport angling for wild salmonids in northwestern Europe. Implications for treatments for sea lice infestation. NINA Reporter no. 126.*

Whelan, K., Poole, W., McGinnity, P., Rogan, G. and Cotter, D. (1998) 'The Burrishoole System', in Moriarty, C. (ed.) *Studies of Irish Rivers and Lakes, Essays on the occasion of the XXVII Congress of Societas Internationalis Limnologiae*. Dublin, pp. 191–212.

Whiley, D.M. and Sloots, T.P. (2005) 'Sequence variation in primer targets affects the accuracy of viral quantitative PCR', *Journal of Clinical Virology*, 34(2), pp. 104–107. doi:10.1016/j.jcv.2005.02.010.

Wilcox, T.M., McKelvey, K.S., Young, M.K., Jane, S.F., Lowe, W.H., Whiteley, A.R. and Schwartz, M.K. (2013) 'Robust Detection of Rare Species Using Environmental DNA: The Importance of Primer Specificity', *PLoS ONE*. Edited by R.C. Willson, 8(3), p. e59520. doi:10.1371/journal.pone.0059520.

Wilcox, T.M., McKelvey, K.S., Young, M.K., Sepulveda, A.J., Shepard, B.B., Jane, S.F., Whiteley, A.R., Lowe, W.H. and Schwartz, M.K. (2016) 'Understanding environmental DNA detection probabilities: A case study using a stream-dwelling char Salvelinus fontinalis', *Biological Conservation*, 194, pp. 209–216. doi:10.1016/J.BIOCON.2015.12.023.

Willerslev, E., Cappellini, E., Boomsma, W., Nielsen, R., Hebsgaard, M.B., Brand, T.B., Hofreiter, M., Bunce, M., Poinar, H.N., Dahl-Jensen, D., Johnsen, S., Steffensen, J.P., Bennike, O., Schwenninger, J.-L., Nathan, R., Armitage, S., de Hoog, C.-J., Alfimov, V., Christl, M., Beer, J., Muscheler, R., Barker, J., Sharp, M., Penkman, K.E.H., Haile, J., Taberlet, P., Gilbert, M.T.P., Casoli, A., Campani, E. and Collins, M.J. (2007) 'Ancient biomolecules from deep ice cores reveal a forested southern Greenland.', *Science (New York, N.Y.)*, 317(5834), pp. 111–4. doi:10.1126/science.1141758.

Willerslev, E., Davison, J., Moora, M., Zobel, M., Coissac, E., Edwards, M.E., Lorenzen, E.D., Vestergård, M., Gussarova, G., Haile, J., Craine, J., Gielly, L., Boessenkool, S., Epp, L.S., Pearman,

P.B., Cheddadi, R., Murray, D., Bråthen, K.A., Yoccoz, N., Binney, H., Cruaud, C., Wincker, P., Goslar, T., Alsos, I.G., Bellemain, E., Brysting, A.K., Elven, R., Sønstebø, J.H., Murton, J., Sher, A., Rasmussen, M., Rønn, R., Mourier, T., Cooper, A., Austin, J., Möller, P., Froese, D., Zazula, G., Pompanon, F., Rioux, D., Niderkorn, V., Tikhonov, A., Savvinov, G., Roberts, R.G., Macphee, R.D.E., Gilbert, M.T.P., Kjær, K.H., Orlando, L., Brochmann, C. and Taberlet, P. (2014) 'Fifty thousand years of Arctic vegetation and megafaunal diet', *Nature*, 506(7486), pp. 47–51. doi:10.1038/nature12921.

Willerslev, E., Hansen, A.J., Binladen, J., Brand, T.B., Gilbert, M.T.P., Shapiro, B., Bunce, M., Wiuf, C., Gilichinsky, D.A. and Cooper, A. (2003) 'Diverse Plant and Animal Genetic Records from Holocene and Pleistocene Sediments', *Science*, 300(5620), pp. 791–795. doi:10.1126/SCIENCE.1084114.

Williams, J.E., Isaak, D.., Imhof, J., Hendrickson, D.. and McMillan, J.. (2015) 'Cold-Water Fishes and Climate Change in North America', *Reference Module in Earth Systems and Environmental Sciences* [Preprint]. doi:10.1016/B978-0-12-409548-9.09505-1.

Williams, K.E., Huyvaert, K.P. and Piaggio, A.J. (2017) 'Clearing muddied waters: Capture of environmental DNA from turbid waters', *PLOS ONE*. Edited by H. Doi, 12(7), p. e0179282. doi:10.1371/journal.pone.0179282.

Williams, M.-A., Hernandez, C., O'Sullivan, A.M., April, J., Regan, F., Bernatchez, L. and Parle-McDermott, A. (2021) 'Comparing CRISPR-Cas and qPCR eDNA assays for the detection of Atlantic salmon (Salmo salar L.)', *Environmental DNA*, 3(1), pp. 297–304. doi:10.1002/EDN3.174.

Williams, M.A., O'Grady, J., Ball, B., Carlsson, J., de Eyto, E., McGinnity, P., Jennings, E., Regan, F. and Parle-McDermott, A. (2019) 'The application of CRISPR-Cas for single species identification from environmental DNA', *Molecular Ecology Resources*, 19(5), pp. 1755–0998. doi:10.1111/1755-0998.13045.

Williams, M.R., Stedtfeld, R.D., Engle, C., Salach, P., Fakher, U., Stedtfeld, T., Dreelin, E., Stevenson, R.J., Latimore, J. and Hashsham, S.A. (2017) 'Isothermal amplification of environmental DNA (eDNA) for direct field-based monitoring and laboratory confirmation of Dreissena sp.', *PLOS ONE*. Edited by H. Doi, 12(10), p. e0186462. doi:10.1371/journal.pone.0186462.

Winfield, I.J., Hateley, J., Fletcher, J.M., James, J.B., Bean, C.W. and Clabburn, P. (2010) 'Population trends of Arctic charr (Salvelinus alpinus) in the UK: assessing the evidence for a widespread decline in response to climate change', *Hydrobiologia 2010 650:1*, 650(1), pp. 55–

65. doi:10.1007/S10750-009-0078-1.

Wood, Z.T., Erdman, B.F., York, G., Trial, J.G. and Kinnison, M.T. (2020) 'Experimental assessment of optimal lotic eDNA sampling and assay multiplexing for a critically endangered fish', *Environmental DNA*, 2(4), pp. 407–417. doi:10.1002/EDN3.64.

Woolway, R.I., Weyhenmeyer, G.A., Schmid, M., Dokulil, M.T., de Eyto, E., Maberly, S.C., May, L. and Merchant, C.J. (2019) 'Substantial increase in minimum lake surface temperatures under climate change', *Climatic Change 2019 155:1*, 155(1), pp. 81–94. doi:10.1007/S10584-019-02465-Y.

Wringe, B.F., Jeffery, N.W., Stanley, R.R.E., Hamilton, L.C., Anderson, E.C., Fleming, I.A., Grant, C., Dempson, J.B., Veinott, G., Duffy, S.J. and Bradbury, I.R. (2018) 'Extensive hybridization following a large escape of domesticated Atlantic salmon in the Northwest Atlantic', *Communications Biology 2018 1:1*, 1(1), pp. 1–9. doi:10.1038/s42003-018-0112-9.

Wu, X., Lee, Y.H., Lu, T.K. and Yu, H. (2021) 'A Warm-start Digital CRISPR-based Method for the Quantitative Detection of Nucleic Acids', *medRxiv*, p. 2021.06.10.21258725. doi:10.1101/2021.06.10.21258725.

Wu, Y.D., Xu, M.J., Wang, Q.Q., Zhou, C.X., Wang, M., Zhu, X.Q. and Zhou, D.H. (2017) 'Recombinase polymerase amplification (RPA) combined with lateral flow (LF) strip for detection of Toxoplasma gondii in the environment', *Veterinary Parasitology*, 243, pp. 199–203. doi:10.1016/j.vetpar.2017.06.026.

WWF (2020) *Living Planet Report 2020: Bending the Curve of Biodiversity Loss*. Edited by R. Almond, M. Grooten, and T. Petersen. Gland, Switzerland.

Xia, Z., Johansson, M.L., Gao, Y., Zhang, L., Haffner, G.D., MacIsaac, H.J. and Zhan, A. (2018) 'Conventional versus real-time quantitative PCR for rare species detection', *Ecology and Evolution*, 8(23), pp. 11799–11807. doi:10.1002/ece3.4636.

Xia, Z., Zhan, A., Gao, Y., Zhang, L., Haffner, G.D. and MacIsaac, H.J. (2018) 'Early detection of a highly invasive bivalve based on environmental DNA (eDNA)', *Biological Invasions*, 20(2), pp. 437–447. doi:10.1007/s10530-017-1545-7.

Yamano, T., Nishimasu, H., Zetsche, B., Hirano, H., Slaymaker, I.M., Li, Y., Fedorova, I., Nakane, T., Makarova, K.S., Koonin, E. V, Ishitani, R., Zhang, F. and Nureki, O. (2016) 'Crystal Structure of Cpf1 in Complex with Guide RNA and Target DNA.', *Cell*, 165(4), pp. 949–62. doi:10.1016/j.cell.2016.04.003.

Yamano, T., Zetsche, B., Ishitani, R., Zhang, F., Nishimasu, H. and Nureki, O. (2017) 'Structural Basis for the Canonical and Non-canonical PAM Recognition by CRISPR-Cpf1', *Molecular Cell*, 67(4), pp. 633-645.e3. doi:10.1016/j.molcel.2017.06.035.

Yang, R., Paparini, A., Monis, P. and Ryan, U. (2014) 'Comparison of next-generation droplet digital PCR (ddPCR) with quantitative PCR (qPCR) for enumeration of Cryptosporidium oocysts in faecal samples'. doi:10.1016/j.ijpara.2014.08.004.

Yang, S. and Rothman, R.E. (2004) 'PCR-based diagnostics for infectious diseases: uses, limitations, and future applications in acute-care settings', *The Lancet Infectious Diseases*, 4(6), pp. 337–348. doi:10.1016/S1473-3099(04)01044-8.

Yao, Y., Nellåker, C. and Karlsson, H. (2006) 'Evaluation of minor groove binding probe and Taqman probe PCR assays: Influence of mismatches and template complexity on quantification', *Molecular and Cellular Probes*, 20(5), pp. 311–316. doi:10.1016/j.mcp.2006.03.003.

Yin, K., Ding, X., Li, Z., Zhao, H., Cooper, K. and Liu, C. (2020) 'Dynamic Aqueous Multiphase Reaction System for One-Pot CRISPR-Cas12a-Based Ultrasensitive and Quantitative Molecular Diagnosis', *Analytical Chemistry*, 92(12), pp. 8561–8568. doi:10.1021/ACS.ANALCHEM.0C01459.

Yoo, E.-H. and Lee, S.-Y. (2010) 'Glucose Biosensors: An Overview of Use in Clinical Practice', *Sensors (Basel, Switzerland)*, 10(5), p. 4558. doi:10.3390/S100504558.

Yuan, C., Tian, T., Sun, J., Hu, M., Wang, Xusheng, Xiong, E., Cheng, M., Bao, Y., Lin, W., Jiang, J., Yang, C., Chen, Q., Zhang, H., Wang, H., Wang, Xiran, Deng, X., Liao, X., Liu, Y., Wang, Z., Zhang, G. and Zhou, X. (2020) 'Universal and Naked-Eye Gene Detection Platform Based on the Clustered Regularly Interspaced Short Palindromic Repeats/Cas12a/13a System', *Analytical Chemistry*, 92(5), pp. 4029–4037. doi:10.1021/acs.analchem.9b05597.

Zanoli, L.M. and Spoto, G. (2013) 'Isothermal amplification methods for the detection of nucleic acids in microfluidic devices.', *Biosensors*, 3(1), pp. 18–43. doi:10.3390/bios3010018.

Zetsche, B., Gootenberg, J.S., Abudayyeh, O.O., Slaymaker, I.M., Makarova, K.S., Essletzbichler, P., Volz, S.E., Joung, J., van der Oost, J., Regev, A., Koonin, E. V. and Zhang, F. (2015) 'Cpf1 Is a Single RNA-Guided Endonuclease of a Class 2 CRISPR-Cas System', *Cell*, 163(3), pp. 759–771. doi:10.1016/j.cell.2015.09.038.

Zhai, J., Cui, H. and Yang, R. (1997) 'DNA based biosensors.', *Biotechnology advances*, 15(1), pp. 43–58.

Zhang, C. and Xing, D. (2007) 'Miniaturized PCR chips for nucleic acid amplification and analysis:

latest advances and future trends.', *Nucleic acids research*, 35(13), pp. 4223–37. doi:10.1093/nar/gkm389.

Zhang, C., Xu, J., Ma, W. and Zheng, W. (2006) 'PCR microfluidic devices for DNA amplification', *Biotechnology Advances*, 24(3), pp. 243–284. doi:10.1016/J.BIOTECHADV.2005.10.002.

Zhang, W., Asiri, A.M., Liu, D., Du, D. and Lin, Y. (2014) 'Nanomaterial-based biosensors for environmental and biological monitoring of organophosphorus pesticides and nerve agents', *TrAC Trends in Analytical Chemistry*, 54, pp. 1–10. doi:10.1016/J.TRAC.2013.10.007.

Zhang, X., Ju, H., Wang, J., Fowler, J.M., Wong, D.K.Y., Halsall, H.B. and Heineman, W.R. (2008) 'Recent developments in electrochemical immunoassays and immunosensors', *Electrochemical Sensors, Biosensors and their Biomedical Applications*, pp. 115–143. doi:10.1016/B978-012373738-0.50007-6.

Zhao, C., Sun, F., Li, X., Lan, Y., Du, L., Zhou, T. and Zhou, Y. (2019) 'Reverse transcription-recombinase polymerase amplification combined with lateral flow strip for detection of rice black-streaked dwarf virus in plants', *Journal of Virological Methods*, 263, pp. 96–100. doi:10.1016/J.JVIROMET.2018.11.001.

Zhao, F., Maren, N.A., Kosentka, P.Z., Liao, Y.-Y., Lu, H., Duduit, J.R., Huang, D., Ashrafi, H., Zhao, T., Huerta, A.I., Ranney, T.G. and Liu, W. (2021) 'An optimized protocol for stepwise optimization of real-time RT-PCR analysis', *Horticulture Research 2021 8:1*, 8(1), pp. 1–21. doi:10.1038/s41438-021-00616-w.

Zheng, C., Wang, K., Zheng, W., Cheng, Y., Li, T., Cao, B., Jin, Q. and Cui, D. (2021) 'Rapid developments in lateral flow immunoassay for nucleic acid detection', *Analyst*, 146(5), pp. 1514–1528. doi:10.1039/D0AN02150D.

Zhou, L., Peng, R., Zhang, R. and Li, J. (2018) 'The applications of CRISPR/Cas system in molecular detection', *Journal of Cellular and Molecular Medicine*, 22(12), pp. 5807–5815. doi:10.1111/jcmm.13925.

Zou, Y., Mason, M.G., Wang, Y., Wee, E., Turni, C., Blackall, P.J., Trau, M. and Botella, J.R. (2017) 'Nucleic acid purification from plants, animals and microbes in under 30 seconds', *PLOS Biology*. Edited by T. Misteli, 15(11), p. e2003916. doi:10.1371/journal.pbio.2003916.

Appendices

Appendix A: Total eDNA concentrations of freshwater samples from the Burrishoole Catchment as determined using a Qubit Fluorometer.

Site		Field Rep	Total eDNA concentration (ng/µl)†
Fiddaunveela	1	1	1.04
		2	0.888
Bunaveela N	2	1	1.7
		2	2.44
Bunaveela S	3	1	2.31
		2	3.54
Goulaun Top	4	1	1.89
		2	1.77
Goulaun Bottom	5	1	0.707
		2	0.905
Altahoney	6	1	0.897
		2	1.03
Maumaratta	7	1	0.836
		2	1.15
Srahrevagh Top	8	1	0.32
		2	0.396
Srahrevagh Bottom	9	1	0.689
		2	0.661
Black	10	1	0.804
		2	1
Feeagh E	11	1	0.987
		2	1.11
Mill Race	12	1	1.71
		2	1.42
Furnace N	13	1	2.17
		2	2.94

†Values were quantified using the dsDNA high sensitivity assay kit.

Appendix B: Accession numbers of mitochondrial sequences for Burrishoole species used in multiple alignment during development of molecular eDNA assays.

Species	Accession Number
Salmo salar	U12143.1
Salmo trutta	JQ390057.1
Salvelinus alpinus	AF154851.1
Anguilla anguilla	AP007233.1
Gasterosteus aculeatus	AP002944.1
Sprattus sprattus	AP009234.1
Clupea harengus	AP009133.1
Dichentrachus labrax	KJ168065.1
Pollachius pollachius	FR751400.1
Chelon labrosus	JF911706.1

Sequences obtained from GenBank Release 229.0 (NCBI).

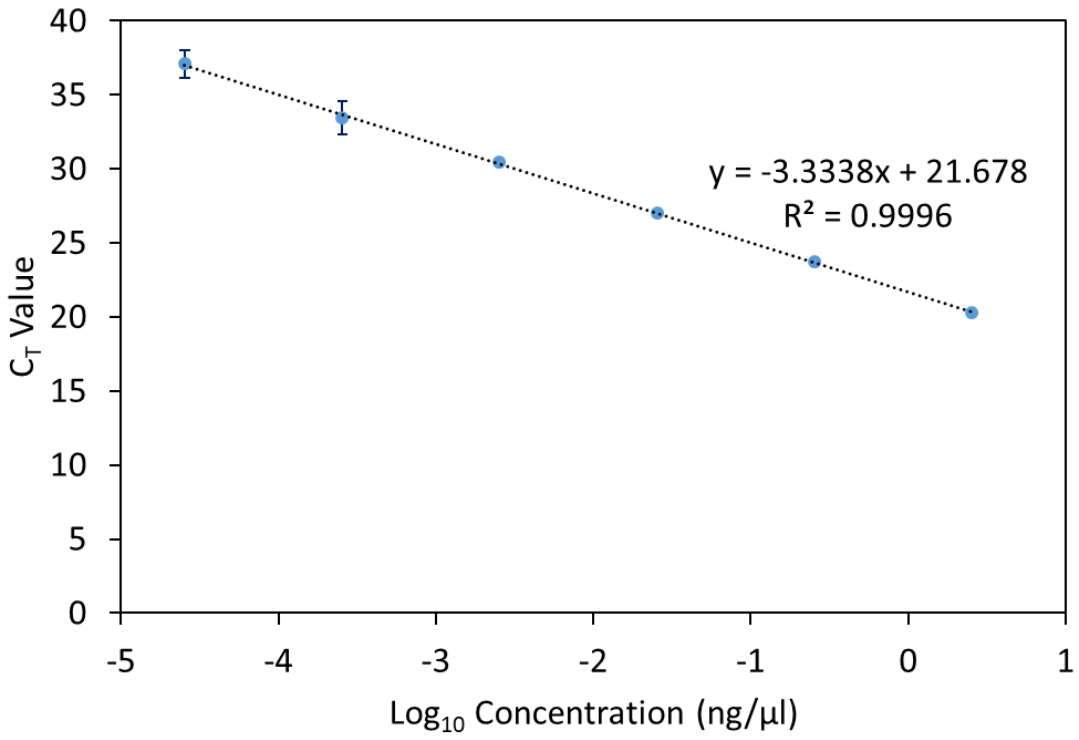

Appendix C: Standard curve for SsaCOI470 qPCR assay based on a 1:10 dilution series of *S. salar* tissue extract (n=3). Crossing point (C_T) values were calculated based on second derivation maximum method. Standard curve used to calculate absolute DNA concentration from eDNA samples.

Appendix D: Electrofishing data of *S. salar* and *S. trutta* for five Irish sampling sites used for eDNA analysis.

Age	Site	Latitude (DD)	Longitude (DD)	Waterfall[+]	Species	Presence/ absence	Estimated minimum number (m^2)
All	Burren	52.83388	-6.92822	Below	*S. salar*	Present	-
					S. trutta	Present	-
All	Delour	52.97957	-7.541	Below	*S. salar*	Present	-
					S. trutta	Present	-
All	Dalligan	52.11878	-7.51916	Above	*S. salar*	Absent	-
					S. trutta	Present	-
All	Srahrevagh	53.982842	-9.560707	Below	*S. salar*	Present	1.06±0.29
					S. trutta	Present	0.41±0.11
All	Srahrevagh	53.994119	-9.541121	Above	*S. salar*	Absent	0
					S. trutta	Present	0.25±0.08

[+] Waterfalls or other obstacles may prevent migration of *S. salar*. Waterfall refers to whether the sampling site was above or below these obstacles.

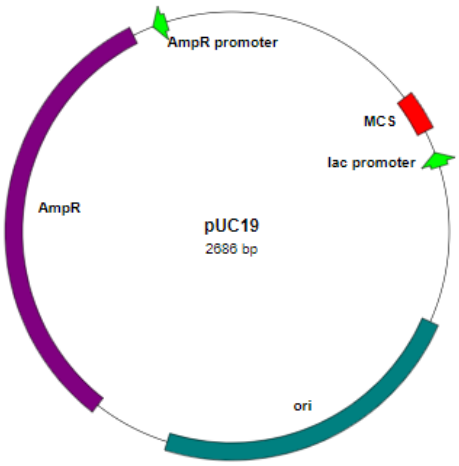

Appendix E: Vector map of empty pUC19. Vector contains ampicillin resistance (AmpR) selection marker and multiple cloning site (MCS). Map made using http://www.rf-cloning.org/savvy.php

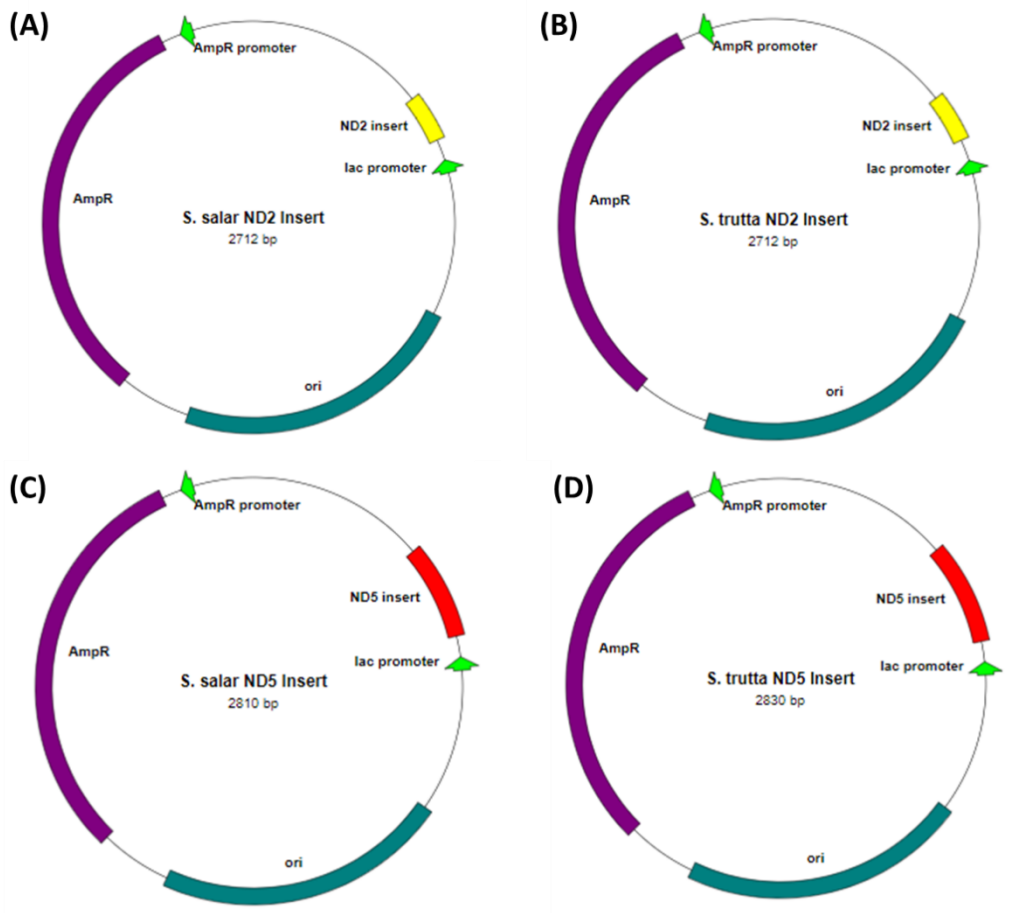

Appendix F: Vector map of recombinant clones. (A) *S. salar* ND2 insert. MCS of pUC19 vector was replaced with a 103 bp sequence from *S. salar* ND2 mitochondrial gene. (B) *S. trutta* ND2 insert. MCS of pUC19 vector was replaced with a 103 bp sequence from *S. trutta* ND2 mitochondrial gene. (C) *S. salar* ND5 insert. MCS of pUC19 vector was replaced with a 205 bp sequence from *S. salar* ND5 mitochondrial gene. (D) *S. trutta* ND5 insert. MCS of pUC19 vector was replaced with a 225 bp sequence from *S. salar* ND5 mitochondrial gene. Maps were made using http://www.rf-cloning.org/savvy.php

Appendix G: NADH dehydrogenase subunit 2 sequences inserted in pUC19 vector and primers used during fast cloning of insert.

S. salar ND2 insert	5'- CCCCCTGACGCCTCAACTTCACCCTCATTACCCTCCCTCTTTCGAT CATTACTATTTTAGCCCTAGGCTTGCTTCCCCTCACTCCAGCTGTG ACCACGTTACT-3'
S. trutta ND2 insert	5'- CCCCCTGACGCCTCAACTTCACCTTCATTACCCTCCCCCTTTCAAT CGTTACTATCTTGGCCCTAGGCCTGCTTCCCCTCACTCCGGCTGT AACCGCAATACT-3'
S. salar ND2 insert forward primer	5'- **ATCGTTACTATCTTGG**CCCTAGGCCTGCTTCCCCTCACTCCGGCT GTAACCGCAATACTAGCTGTTTCCTGTGTGAA-3'
S. salar ND2 insert reverse primer	5'- **CCAAGATAGTAACGAT**TGAAAGGGGGAGGGTAATGAAGGTGAAG TTGAGGCGTCAGGGGGGGCCGTCGTTTTACAACG-3'
S. trutta ND2 insert forward primer	5'- **GATCATTACTATTTTA**GCCCTAGGCTTGCTTCCCCTCACTCCAGCT GTGACCACGTTACTAGCTGTTTCCTGTGTGAA-3'
S. trutta ND2 insert reverse primer	5'- **TAAAATAGTAATGATC**GAAAGAGGGAGGGTAATGAGGGTGAAGTT GAGGCGTCAGGGGGGGCCGTGGTTTTACAAGG-3'

Primers are longer than usual PCR primers as they contain the sequence to be inserted into the vector.

Bold sequences overlap each other and underlined sequences anneal pUC19 vector.

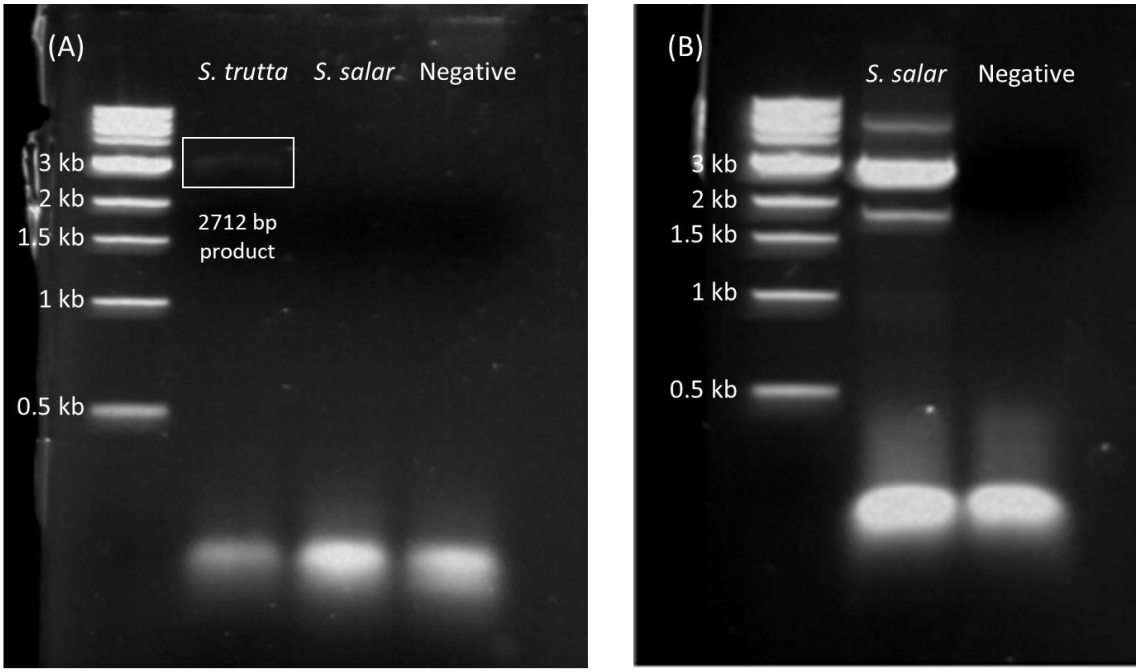

Appendix H: Confirmation of successful PCR amplification. (A) *S. trutta* insert confirmation using 1 pg/µL pUC19 DNA. (B) *S. salar* insert confirmation using 3.35 ng/µL pUC19 DNA.

Appendix I: NADH dehydrogenase subunit 5 sequences inserted into pUC19 vector and primers used for fast cloning of insert.

S. salar ND5 PCR product insert	5'-GCTTTACAGCTACAGCCCCTATTAATGAAAACAACCCCTCCGTTATTAATCCCATCAAACGACTAGCTTGAGGAAGCATTATTGCAGGACTTCTAATCACCTCAAACTTTCTACCCTCCAAAACCCCTATCATAACCATACCCCTCCCATTAAAATTAGCCGCCCTCCTAGTTACCATCTCAGGCCTTCTCATCGCACTAGAACT-3'
S. trutta ND5 PCR product insert	5'-ATAGCCTCCGAGTAGTCTTCTTCGTTTCAATAGGACACCCCCGCTTTACAGCTACAGCCCCTATTAATGAAAACAACCCCTCCGTTATTAACCCCATCAAACGACTAGCCTGAGGAAGCATTATTGCAGGACTTGTAATCACCTCAAACTTCCTCCCCTCCAAAACCCCCGTCATAACCATACCCCTCCCATTGAAGCTCGCCGCCCTCCTAGTTACCATCTCAG-3'
S. salar ND5 insert forward primer	5'-GACGTTGTAAAACGACGCTTTACAGCTACAGCCC-3'
S. salar ND5 insert reverse primer	5'-CACACAGGAAACAGCTAGTTCTAGTGCGATGAGAAG-3'
S. trutta ND5 insert forward primer	5'-GACGTTGTAAAACGACATAGCCTCCGAGTAGTCTTC-3'
S. trutta ND5 insert reverse primer	5'-CACACAGGAAACAGCTCTGAGATGGTAACTAGGAGG-3'
pUC19 plasmid forward primer	5'-AGCTGTTTCCTGTGTGAA-3'
pUC19 plasmid reverse primer	5'-GTCGTTTTACAACGTCGT-3'
FastCloneCheck_F primer	5'-GATTAAGTTGGGTAACGCCAGGG-3'

Underlined primer sequences overlap pUC19 vector.

FastCloneCheck_F was used for Sanger sequencing to ensure recombinant sequences were inserted correctly.

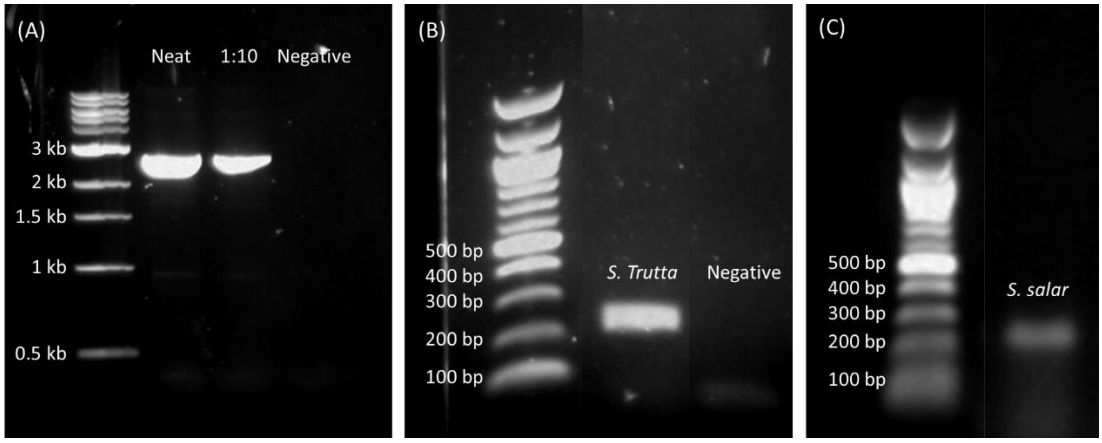

Appendix J: Confirmation of successful PCR amplification. (A) Linearised pUC19 plasmid (2605 bp) PCR amplified and visualised on a 1% (w/v) agarose gel. (B) *S. trutta* (225 bp) PCR amplified and visualised on a 2% (w/v) agarose gel. (C) *S. salar* (205 bp) PCR amplified and visualised on a 2% (w/v) agarose gel.

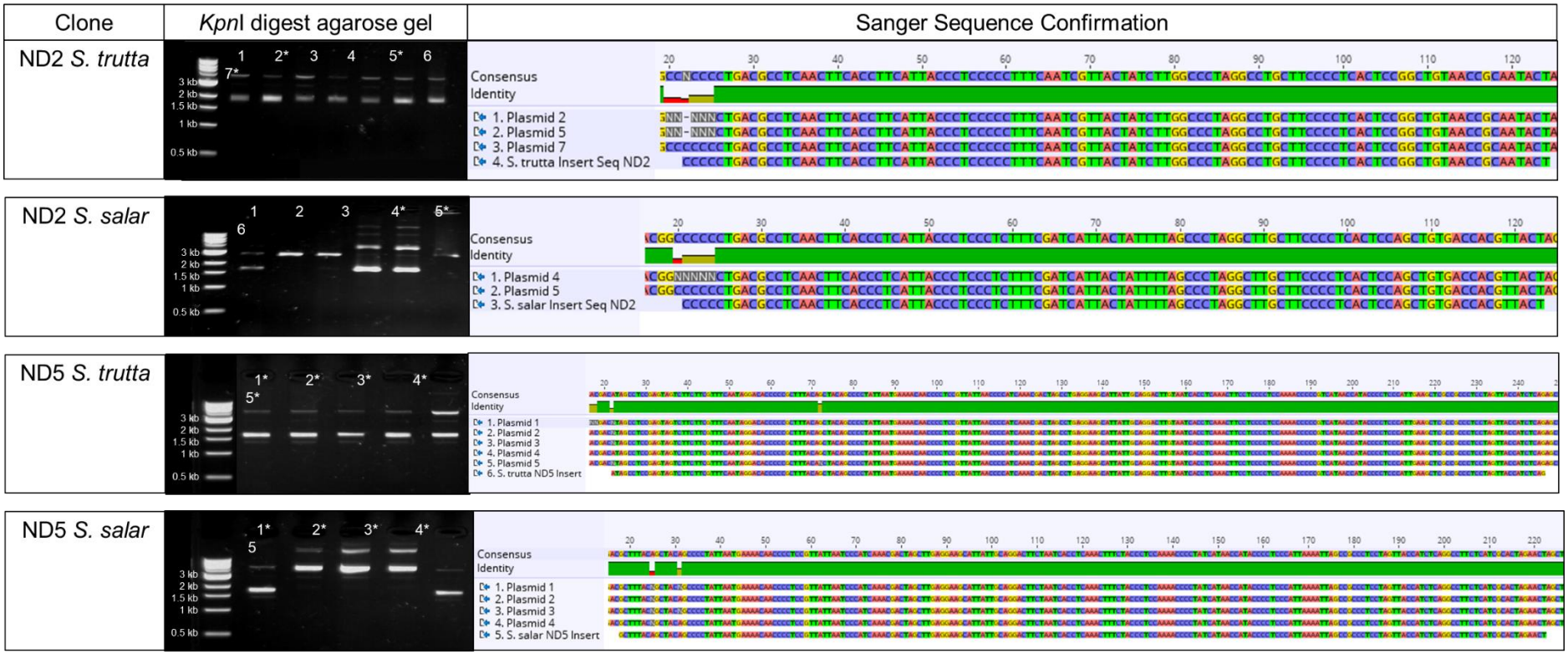

Appendix K: Selection of successful transformations. Purified plasmid DNA from transformed colonies was subject to a *Kpn*I digest and visualised on a 1% (w/v) agarose gel. Presumptive successful plasmids (indicated by an uncut plasmid) were confirmed by Sanger cycle sequencing (Source Biosciences) using a custom primer, FastCloneCheck_F. Sequences were aligned against the designed insert using Geneious V11.1.5.

Appendix L: Electrofishing data of *S. salar* and *S. trutta* for five Irish sampling sites used for eDNA analysis.

Age	Site	Latitude (DD)	Longitude (DD)	Waterfall[+]	Species	Presence/ absence	Estimated minimum number (m^2)
All	Burren	52.83388	-6.92822	Below	*S. salar*	Present	-
					S. trutta	Present	-
All	Delour	52.97957	-7.541	Below	*S. salar*	Present	-
					S. trutta	Present	-
All	Dalligan	52.11878	-7.51916	Above	*S. salar*	Absent	-
					S. trutta	Present	-
All	Srahrevagh	53.982842	-9.560707	Below	*S. salar*	Present	1.06±0.29
					S. trutta	Present	0.41±0.11
All	Srahrevagh	53.994119	-9.541121	Above	*S. salar*	Absent	0
					S. trutta	Present	0.25±0.08

[+] Waterfalls or other obstacles may prevent migration of *S. salar.* Waterfall refers to whether the sampling site was above or below these obstacles.

Appendix M: qPCR validation data for Burren and Dalligan sampling sites

River	Location[†]	*S. salar* present	Site Replicate	Average C_T[‡] (n=3 technical replicates)	DNA concentration (ng/L)[§]
Burren[¶]	Downstream	Yes	1	34.064	0.023
			2	33.464	0.035
			3	33.861	0.026
				33.796±0.31	**0.028±0.006**
Dalligan[¶]	Upstream	No	1	Undetermined	Undetermined
			2	Undetermined	Undetermined
			3	Undetermined	Undetermined

[†] Each of these rivers has an obstacle or barrier that has the potential to prevent migration of *S. salar.* Location refers to whether sampling was upstream or downstream of this obstacle.

[‡] Crossing point PCR cycle (Cp) value is the cycle at which fluorescence passes a threshold calculated using the second derivative maximum method. Cp values and eDNA concentrations (average over three technical replicates) for *S. salar* in each river.

[§]eDNA concentration in original field sample back-calculated from absolute DNA concentration from qPCR. Average concentrations (±SD) are given for each location.

[¶]Data as previously published in Atkinson *et al.*, (2018)

Appendix N: Geographical coordinates, qPCR and CRISPR-data for sampling sites in Miramichi Watershed.

			qPCR		CRISPR-Cas
Site	**LAT**	**LON**	**No. Positive**	**C_T values**	**No. Positive**
1	46.9645	-65.5954	6	33,23 ± 0,10	3
2	46.95729	-65.5903	6	36,24 ± 0,30	3
3	46.90173	-65.6318	6	34,61 ± 0,28	3
4	46.8279	-65.7865	6	31,95 ± 0,13	0
5	46.82185	-65.7901	6	32,78 ± 0,07	3
6	46.80551	-65.8706	6	34,42 ± 0,41	1
7	46.73843	-65.8301	6	31,46 ± 0,28	0
8	46.7359	-65.8256	6	32,60 ± 0,20	2
9	46.61444	-65.7107	6	33,52 ± 0,22	3
10	46.66648	-65.776	6	28,27 ± 0,04	2
11	46.54053	-65.8363	6	27,63 ± 0,05	3
12	46.61778	-65.8786	6	32,00 ± 0,10	0
13	46.55935	-66.1229	6	32,73 ± 0,17	3
14	46.5514	-66.1449	6	33,34 ± 0,27	3
15	46.54893	-67.2245	6	34,20 ± 0,25	3
16	46.51735	-67.1546	6	33,72 ± 0,22	3
17	46.51031	-67.1138	0	-	0
18	46.498	-67.049	0	-	0
19	46.42579	-66.6042	6	24,24 ± 0,08	3
20	46.60154	-66.6455	6	30,60 ± 0,06	3
21	46.56043	-66.5579	0	-	0
22	46.48389	-66.4815	0	-	0
23	46.45472	-66.4227	6	28,12 ± 0,11	3
24	46.45934	-66.4149	0	-	0
25	46.46191	-66.4112	0	-	0
26	46.47525	-66.3996	0	-	0
27	46.51016	-66.2846	0	-	0
28	47.21535	-65.8094	6	29,28 ± 0,14	3
29	47.13499	-65.8329	6	30,08 ± 0,09	3
30	47.15107	-65.8377	6	26,45 ± 0,10	3
31	47.15107	-65.8377	6	30,20 ± 0,11	1
32	47.20925	-65.8192	6	31,44 ± 0,08	3

33	47.18574	-65.8947	6	31,41 ± 0,16	3
34	47.13281	-66.1174	6	31,53 ± 0,30	3
35	47.12033	-66.0502	6	32,94 ± 0,13	3
36	47.13516	-65.9824	6	33,11 ± 0,29	3
37	46.45499	-66.4227	0	-	0
38	47.1417	-65.9597	6	32,44 ± 0,11	3
39	47.1592	-65.8444	6	29,08 ± 0,09	0
40	47.09972	-65.8389	6	34,24 ± 0,32	3
41	47.08213	-65.8303	6	31,28 ± 0,12	3
42	47.06208	-65.8306	6	31,67 ± 0,23	3
43	47.05247	-65.9981	6	32,32 ± 0,20	3
44	47.04216	-65.8886	3	37,83 ± 0,73	1
45	47.01286	-65.8374	6	32,84 ± 0,19	3
46	46.95884	-65.7195	0	-	0
47	46.93838	-65.7763	0	-	0
48	46.93838	-65.7763	0	-	0
49	46.96663	-65.8311	0	-	0
50	46.92926	-65.9508	6	31,47 ± 0,14	3
51	46.93606	-65.9082	6	34,02 ± 0,18	0
52	46.91887	-65.9593	0	-	0
53	46.87986	-65.9963	3	38,33 ± 0,53	0
54	46.8794	-66.0364	4	38,13 ± 0,50	0
55	46.8292	-65.9521	0	-	0
56[†]	46.43481	-66.0186	1	43,22	0
57[†]	46.65887	-66.3226	1	40,28	0
58	46.70103	-66.4826	0	-	0
59	47.0042	-66.7087	0	-	0
60	46.96498	-66.6219	0	-	0
61	46.96066	-66.5602	0	-	0
62	46.79444	-66.1971	6	35,99 ± 0,52	3
63	46.82234	-66.1091	6	33,97 ± 0,14	1

The number (No.) of positives from a total of 6 replicates for qPCR and total of 3 replicates for CRISPR-Cas. The C_T values are indicative of the cycle number in which samples crossed the threshold into exponential amplification and are reported as mean ± standard deviation.

[†] These sites were reported as negative for qPCR; C_T value exceeded 39, so positive detection deemed a PCR artefact.

Appendix O: Sanger sequencing results from positive Miramichi Watershed samples.

Sample ID	Concatenated Sequences	Chromatogram
9	TGACTTCTCCCTCCCTCCTTTCTTCTCCTCCTGGCCTCATCTGG AGTTGAAGCCGGCGCTGGCACCGGATGAACAGTCTACCCCCCT CTAGCAGGTAATCTTGCCCACGCAGGAGCTTCCGTTGACTTAAC TATTTTTTCCCTCCATTTGGCTGGTATTTC	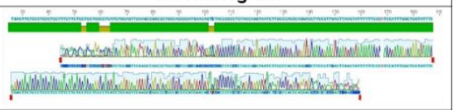
16	TGACTTCTCCCTCCCTCCTTTCTTCTCCTCCTGGCCTCATCTGG AGTTGAAGCCGGCGCTGGCACCGGATGAACAGTCTACCCCCCT CTAGCAGGTAATCTTGCCCACGCAGGAGCTTCCGTTGACTTAAC TATTTTTTCCCTCCATTTGGCTGGTATTTC	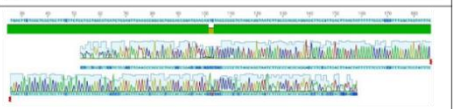
19	TGACTTCTCCCTCCCTCCTTTCTTCTCCTCCTGGCCTCATCTGG AGTTGAAGCCGGCGCTGGCACCGGATGAACAGTCTACCCCCCT CTAGCAGGTAATCTTGCCCACGCAGGAGCTTCCGTTGACTTAAC TATTTTTTCCCTCCATTTGGCTGGTATTTC	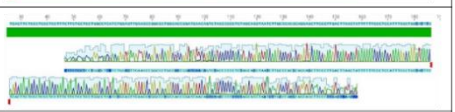
28	TGACTTCTCCCTCCCTCCTTTCTTCTCCTCCTGGCCTCATCTGG AGTTGAAGCCGGCGCTGGCACCGGATGAACAGTCTACCCCCCT CTAGCAGGTAATCTTGCCCACGCAGGAGCTTCCGTTGACTTAAC TATTTTTTCCCTCCATTTGGCTGGTATTTC	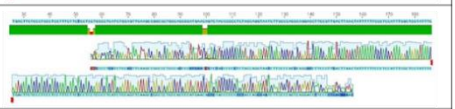
34	TGACTTCTCCCTCCCTCCTTTCTTCTCCTCCTGGCCTCATCTGG AGTTGAAGCCGGCGCTGGCACCGGATGAACAGTCTACCCCCCT CTAGCAGGTAATCTTGCCCACGCAGGAGCTTCCGTTGACTTAAC TATTTTTTCCCTCCATTTGGCTGGTATTTC	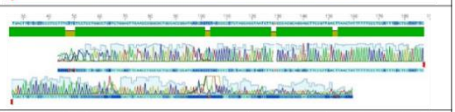
43	TGACTTCTCCCTCCCTCCTTTCTTCTCCTCCTGGCCTCATCTGG AGTTGAAGCCGGCGCTGGCACCGGATGAACAGTCTACCCCCCT CTAGCAGGTAATCTTGCCCACGCAGGAGCTTCCGTTGACTTAAC TATTTTTTCCCTCCATTTGGCTGGTATTTC	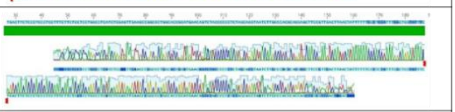
53	TGACTTCTCCCTCCCTCCTTTCTTCTCCTCCTGGCCTCATCTGG AGTTGAAGCCGGCGCTGGCACCGGATGAACAGTCTACCCCCCT CTAGCAGGTAATCTTGCCCACGCAGGAGCTTCCGTTGACTTAAC TATTTTTTCCCTCCATTTGGCTGGTATTTC	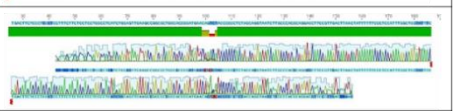
62	TGACTTCTCCCTCCCTCCTTTCTTCTCCTCCTGGCCTCATCTGG AGTTGAAGCCGGCGCTGGCACCGGATGAACAGTCTACCCCCCT CTAGCAGGTAATCTTGCCCACGCAGGAGCTTCCGTTGACTTAAC TATTTTTTCCCTCCATTTGGCTGGTATTTC	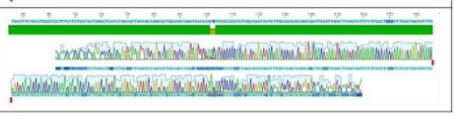

Amplicons were sequenced using forward and reverse primers. Sequences were aligned and primers were trimmed using Genious Prime (2020.2).

Appendix P: Fluorescence values of Miramichi Watershed samples using CRISPR-Cas detection.

Samples	Replicate 1		Replicate 2		Replicate 3		Overall (Y/N)
	Mean	StD	Mean	StD	Mean	StD	
1	1.630921	0.432598	1.781957	0.141938	1.723974	0.289634	Y
2	1.528643	0.016155	1.639127	0.113876	1.679861	0.122604	Y
3	1.595581	0.235247	1.71807	0.168978	1.824058	0.083424	Y
4	-0.07488	0.085765	-0.044899	0.048295	-0.03483	0.027301	N
5	1.57295	0.004475	1.388771	0.245689	1.460297	0.06227	Y
6	-0.1114	0.025931	0.004155	0.042048	1.097426	0.089512	Y (P)
7	-0.01534	0.068637	0.016636	0.031344	0.053996	0.066682	N
8	-0.0389	0.070377	1.327825	0.039471	1.589286	0.130599	Y
9	1.019848	0.128463	1.115083	0.029918	0.408911	0.038303	Y
10	1.719093	0.078793	STD >0.5	0.636452	1.68402	0.189206	Y
11	1.860332	0.129536	2.022178	0.137867	1.908883	0.174517	Y
12	-0.05747	0.061083	0.013651	0.065642	0.072427	0.137768	N
13	1.528925	0.169329	1.469789	0.077521	1.595782	0.102729	Y
14	1.57987	0.071572	1.485293	0.135117	1.62693	0.157268	Y
15	1.224718	0.066924	0.717317	0.053223	1.543205	0.147026	Y
16	1.820887	0.011211	1.766418	0.053941	1.880685	0.024656	Y
17	-0.10416	0.056091	-0.051989	0.116266	-0.05177	0.023239	N
18	-0.01358	0.159546	-0.013941	0.084236	0.069377	0.216482	N
19	1.668135	0.073105	1.561853	0.325453	0.96252	0.045422	Y
20	1.998719	0.04811	1.905482	0.079986	1.833829	0.203707	Y
21	-0.13867	0.043055	-0.011506	0.047821	-0.07752	0.046294	N
Pos‡	1.7	0.072092	1.7	0.056421	1.7	0.082239	-
Neg	0.139358	0.165889	0.103871	0.110075	0.163553	0.13006	-
Threshold†	0.406765		0.609327		0.306815		-
22	-0.07242	0.141308	0.070311	0.140021	-0.00665	0.089568	Y (P)
23	1.765406	0.094717	2.045641	0.200074	0.922121	0.199249	Y
24	-0.10005	0.033387	0.00324	0.103641	-0.03462	0.053519	N
25	-0.07745	0.02558	0.026394	0.003616	-0.02459	0.074272	N
26	-0.20646	0.017749	-0.085593	0.014843	-0.10925	0.003424	N
27	-0.12006	0.054484	-0.022203	0.009317	-0.02311	0.04986	N
28	1.852976	0.152087	2.628107	0.268803	1.829579	0.264502	Y
29	1.990576	0.069333	3.300555	0.417571	1.415272	0.334508	Y
30	1.557461	0.085022	1.656379	0.138347	0.973656	0.153226	Y
31	1.295245	0.181766	-0.016058	0.007567	-0.0105	0.009314	Y (P)
32	1.74465	0.123883	2.073952	0.207329	1.268697	0.246091	Y
33	1.951621	0.080663	2.232973	0.098733	1.266762	0.46502	Y
34	1.614966	0.165182	1.709529	0.055232	1.611284	0.059387	Y
35	1.01767	0.092589	1.494023	0.047463	0.492732	0.135171	Y
36	1.62591	0.152214	1.864999	0.0888	1.02846	0.185347	Y
37	-0.02434	0.057731	0.048314	0.026118	-0.00386	0.035994	N
38	1.587501	0.217396	1.611513	0.149658	1.657262	0.079282	Y
39	-0.07541	0.04554	0.051744	0.085761	-0.01425	0.088972	Y (P)
40	1.242619	0.123379	1.466098	0.065209	1.211651	0.1653	Y
41	1.908701	0.153708	2.284902	0.487017	1.459601	0.239499	Y
42	1.665712	0.072028	1.661497	0.128967	1.874282	0.10641	Y
Pos‡	1.7	0.094801	1.7	0.007669	1.7	0.138256	-
Neg	0.10488	0.094456	0.183765	0.124406	0.160247	0.181701	-
Threshold†	0.344403		0.171984		0.197398		-

43	1.692024	0.163031	1.832103	0.207506	1.766428	0.169951	Y
44	0.92923	0.128866	-0.082004	0.042438	-0.01577	0.025279	Y (P)
45	1.865849	0.135422	2.332154	0.132771	2.019896	0.220172	Y
46	0.01896	0.030365	0.032119	0.025932	0.04014	0.083794	N
47	-0.10833	0.013061	-0.173713	0.017517	-0.12967	0.025946	N
48	-0.03227	0.041167	-0.063528	0.014744	-0.03434	0.034986	N
49	0.02478	0.041068	0.099498	0.051392	-0.01795	0.058824	N
50	1.798549	0.268321	1.73615	0.097944	1.604197	0.173077	Y
51	-0.08416	0.051046	-0.141605	0.033879	-0.13461	0.022382	N
52	-0.00042	0.034635	-0.059268	0.044741	-0.04179	0.05056	N
53	0.045887	0.120973	0.070824	0.099909	0.046092	0.092294	Y (P)
54	0.027204	0.05529	0.202386	0.208165	0.120033	0.148769	Y
55	-0.09864	0.028384	-0.139649	0.031536	-0.09711	0.024178	N
56	0.066191	0.043172	-0.045601	0.025095	-0.06949	0.032364	Y (P)
57	0.008621	0.03925	0.000552	0.019521	-0.01722	0.03987	N
58	0.014913	0.01989	0.040276	0.061491	-0.00241	0.02464	N
59	-0.05516	0.054181	-0.078156	0.092106	-0.00457	0.092401	N
60	-0.00168	0.142616	-0.038721	0.117243	0.021807	0.110721	N
61	-0.00812	0.034355	-0.027737	0.024255	-0.0151	0.041258	N
62	1.427822	0.107498	1.969802	0.052178	1.194226	0.083683	Y
63	-0.06426	0.016263	1.410622	0.042445	-0.08734	0.027205	Y (P)
Pos‡	1.7	0.056346	1.7	0.090082	1.7	0.121387	-
Neg	0.197183	0.145455	0.209972	0.154292	0.172276	0.142397	-
Threshold†	0.116951		0.464828		0.18909		-

Values have undergone background subtraction and normalisation to the mean positive control value. The threshold value was calculated as ten times the standard deviation of the background. Only values greater than this threshold were considered positive for *S. salar.*

† Threshold value calculated per 96-well plate

‡ To account for inter-plate variation, fluorescence values were normalised against the mean fluorescence of the positive control. A value of 1.7 (AU)

Appendix Q: Geographical coordinates, qPCR and CRISPR-data for sampling sites in Jacques - Cartier Watershed.

			qPCR		CRISPR-Cas
Site	**LAT**	**LON**	**No. Positive**	**C_T values**	**No. Positive**
1	47.11308	-71.3659	3	37,48 ± 1,74	2
2	47.11849	-71.3608	5	37,5 ± 1,6	2
3	47.13366	-71.3596	6	37,33 ± 1,23	3
4	47.17548	-71.3698	1	37.93271255	1
5	47.19234	-71.3774	6	36,13 ± 0,6	2
6	47.19516	-71.3776	6	35,25 ± 0,78	2
7	47.19607	-71.3771	6	36,26 ± 1,36	2
8	47.20386	-71.3946	6	35,54 ± 0,68	1
9	47.23639	-71.2515	0	-	0
10	47.31002	-71.4576	0	-	2
11	47.35046	-71.2803	0	-	0
12	47.50777	-71.2358	0	-	1
13	47.11118	-71.3493	0	-	0
14	47.11242	-71.3654	3	37,76 ± 0,08	0
15	47.17541	-71.3702	0	-	2
16	47.29932	-71.4463	0	-	0

The number (No.) of positives from a total of 6 replicates for qPCR and total of 3 replicates for CRISPR-Cas. The C_T values are indicative of the cycle number in which samples crossed the threshold into exponential amplification. These are reported as mean ± standard deviation.

Appendix R: Sanger sequencing results from positive Jacques-Cartier Watershed samples.

Sample ID	Concatenated Sequences	Chromatogram
1	TGACTTCTCCCTCCCTCCTTTCTTCTCCTCCTGGCCTCATCTNGGAGT TGAAGCCGGCGCTGGCACCGGATGAACAGTCTACCCCCCCTCTAGCA GGTAATCTTGCCCACGCAGGAGCTTCCNTTGACTTAACTATTTTTTCC CTCCATTTGGCTGGTATTTC	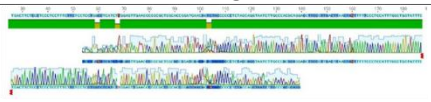
2	TGACTTCTCCCTCCCTCCTTTCTTCTCCTCCTGGCCTCATCTGGAGTT GAAGCCGGCGCTGGCACCGGATGAACAGTCTACCCCCCTCTAGCAG GTAATCTTGCCCACGCAGGAGCTTCCGTTGACTTAACTATTTTTTCCC TCCATTTGGCTGGTATTTC	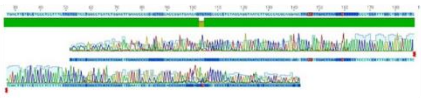
3	TGACTTCTCCCTCCCTCCTTTCTTCTCCTCCTGGCCTCATCTGGAGTT GAAGCCGGCGCTGGCACCGGATGAACAGTCTACCCCCCTCTAGCAG GTAATCTTGCCCACGCAGGAGCTTCCGTTGACTTAACTATTTTTTCCC TCCATTTGGCTGGTATTTC	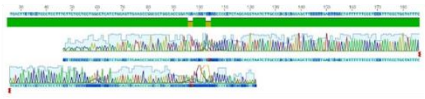
4	TGACTTCTCCCTCCCTCCTTTCTTCTCCTCCTGGCCTCATCTGGAGTT GAAGCCGGCGCTGGCACCGGATGAACAGTCTACCCCCCTCTAGCAG GTAATCTTGCCCACGCAGGAGCTTCCGTTGACTTAACTATTTTTTCCC TCCATTTGGCTGGTATTTC	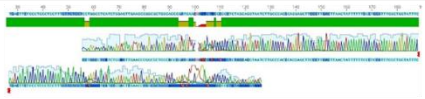
5	TGACTTCTCCCTCCCTCCTTTCTTCTCCTCCTGGCCTCATCTGGAGTT GAAGCCGGCGCTGGCACCGGATGAACAGTCTACCCCCCTCTAGCAG GTAATCTTGCCCACGCAGGAGCTTCCGTTGACTTAACTATTTTTTCCC TCCATTTGGCTGGTATTTC	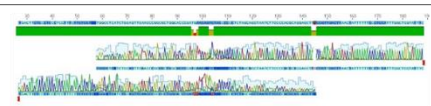
6	TGACTTCTCCCTCCCTCCTYTCTTCTMCTCCTGGCCTCATCTGGAGN TGAAGCCGGCGCGGCACCRGATGAACRRTCCACCSCCCKSYANCRS GTAATCTWGCCCACACANGAGCTTCCGTTGACNNNRCNATTWTTTCC CTCCATTTGGCTGGTATTTC	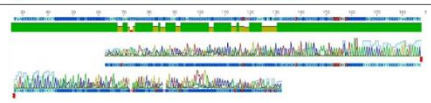
7	TGACTTCTCCCTCCCTCCTTTCTTCTCCTCCTGGCCTCATCTGGAGTT GAAGCCGGCGCTGGCACCGGATGAACAGTCTACCCCCCTCTAGCAG GTAATCTTGCCCACGCAGGAGCTTCCGTTGACTTAACTATTTTTTCCC TCCATTTGGCTGGTATTTC	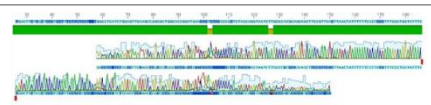
8	TGACTTCTCCCTCCCTCCTTTCTTCTCCTCCTGGCCTCATCTGGAGTT GAAGCCGGCGCTGGCACCGGATGAACAGTCTACCCCCCTCTAGCAG GTAATCTTGCCCACGCAGGAGCTTCCNTTGACTTAACTATTTTTTCCC TCCATTTGGCTGGTATTTC	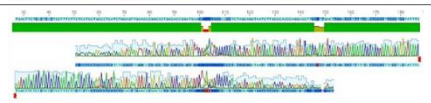
14	TGACTTCTCCCTCCCTCCTTTCTTCTCCTCCTGGCCTCATCTGGAGTT GAAGCCGGCGCTGGCACCGGATGAACAGTCTACCCCCCTCTAGCAG GTAATCTTGCCCACGCAGGAGCTTCCNTTGACTTAACTATTTTTTCCC TCCATTTGGCTGGTATTTC	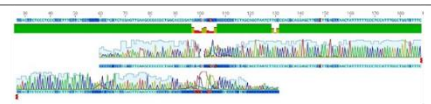

Amplicons were sequenced using forward and reverse primers. Sequences were aligned and primers were trimmed using Genious Prime (2020.2).

Appendix S: Fluorescence values of Jacques-Cartier Watershed samples using CRISPR-Cas detection.

Samples	Replicate 1		Replicate 2		Replicate 3		Overall (Y/N)
	Mean	StD	Mean	StD	Mean	StD	
1	-0.08847	0.123084	1.573427	0.139603	1.928517	0.071489	Y
2	-0.16285	0.05568	1.316996	0.090216	0.680411	0.039476	Y
3	2.882236	0.291596	0.604613	0.203067	1.749432	0.143861	Y
4	-0.10002	0.035326	-0.11636	0.055565	0.521256	0.033073	Y (P)
5	RPA Fail		1.624023	0.185165	1.725546	0.066627	Y
6	1.968768	0.269133	-0.11219	0.063192	1.870718	0.060206	Y
7	2.123408	0.263046	-0.07519	0.005811	0.433364	0.019622	Y
8	2.88359	0.253939	-0.18519	0.019719	-0.21686	0.02021	Y (P)
9	-0.12018	0.01809	-0.17625	0.012961	-0.30058	0.040968	N
10	2.31266	0.19594	-0.14136	0.023889	1.846979	0.268069	Y
11	-0.13363	0.059405	-0.12644	0.036255	-0.1287	0.116183	N
12	-0.07271	0.144472	-0.11867	0.057442	2.32193	0.110604	Y (P)
13	RPA Fail		-0.11816	0.011155	-0.29166	0.032187	N
14	StD >0.5	0.671171	-0.17988	0.018093	-0.24171	0.042219	N
15	0.903304	0.213357	-0.13856	0.01741	2.626176	0.197687	Y
16	-0.16368	0.007663	RPA Fail		-0.14172	0.057327	N
Pos[†]	1.7	0.033971	1.7	0.232869	1.7	0.061161	-
Neg	-0.03359	0.06395	-0.05378	0.111239	-0.11028	0.054454	-
Threshold	0.251499		0.269068		0.378373		-

Values have undergone background subtraction and normalisation to the mean positive control value. The threshold value was calculated as ten times the standard deviation of the background. Only values greater than this threshold were considered positive for *S. salar.*

[†]To account for inter-plate variation, fluorescence values were normalised against the mean fluorescence of the positive control. A value of 1.7 (AU)

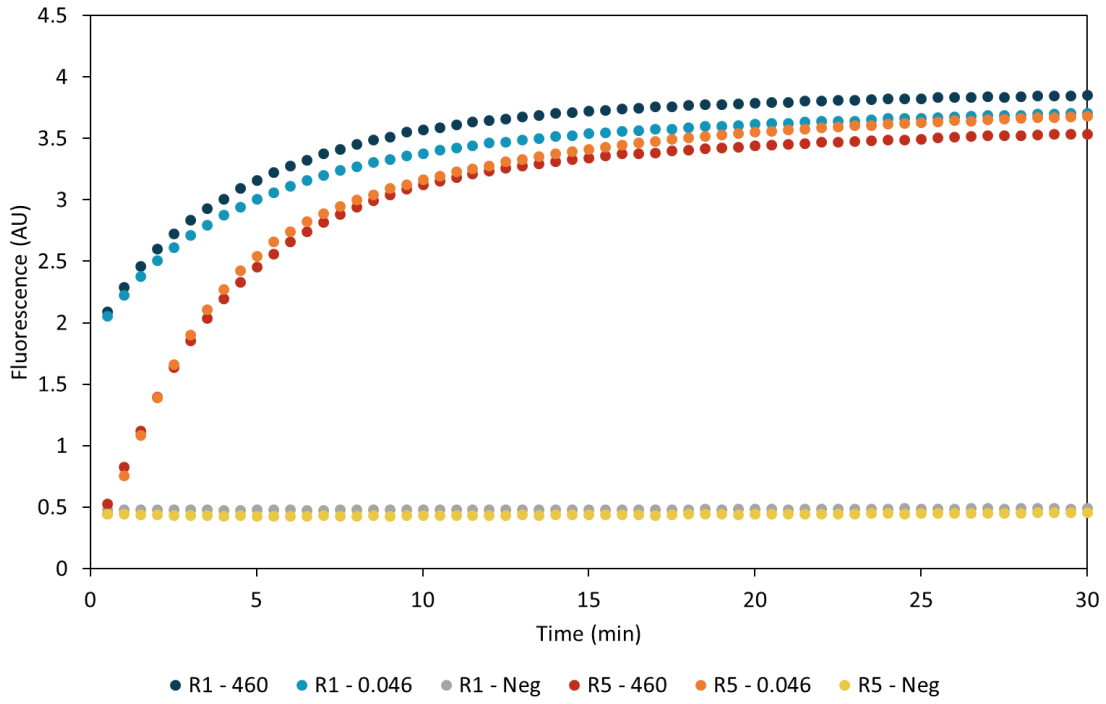

Appendix T: Raw fluorescence time course of *S. salar* RPA-CRISPR-Cas using 460 and 0.046 pg/µL of DNA extracted from *S. salar* tissue. Fluorescence measurements taken every 30 sec for 30 min at 37 °C (λex = 485 nm, λem = 535 nm). R1 = data from replicate 1 with delayed plate loading. R5 = data from replicate 5 with immediate plate loading.

Appendix U: Total eDNA concentration of sediment core samples as determined using a Qubit Fluorometer.

Sample Depth (cm)	Total eDNA concentration (ng/µl)
0 cm	12.6
5cm	0.913
10 cm	12.4
15 cm	1.9
25 cm	5.54
50 cm	8.87
75 cm	4.63
100 cm	5.34
200 cm	13.8
300 cm	0.053
400 cm	4.02
500 cm	0.527
600 cm	4.31

Values were quantified using the dsDNA high sensitivity assay kit.

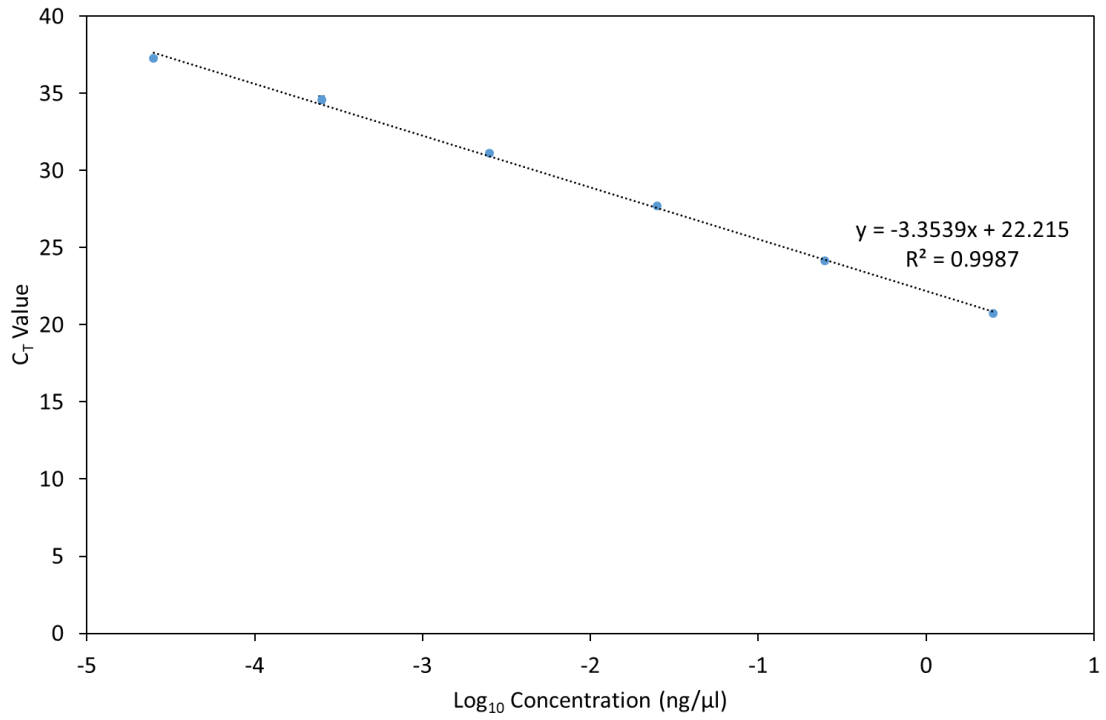

Appendix V: Standard Curve of a six-point 1:10 dilution series of *S. salar* (n=3). Standard curve used to calculate *S. salar* DNA concentrations of Lough Feeagh core samples. Crossing point (C_T) values were calculated based on second derivation maximum method.

Appendix W: Fold-change values of Lough Feeagh sediment core samples using CRISPR-Cas detection.

Samples Depth (cm)	RPA Replicate 1		RPA Replicate 2		RPA Replicate 3		Overall (Y/N)
	Mean‡	StD§	Mean‡	StD§	Mean‡	StD§	
0cm	0.377023	0.121462	0.072841	0.183234	0.449073	0.166974	N
5cm	3.816973	0.499093	3.140933	0.110932	2.601183	0.257217	Y
10cm	0.925103	0.126505	0.84441	0.027614	1.083045	0.03291	Y (P)
15cm	0.230092	0.047935	3.019927	0.033161	0.065609	0.034164	Y (P)
25cm	4.38183	0.079347	5.481124	0.314386	1.431656	0.149738	Y
50cm	1.588698	0.133261	1.324056	0.072859	1.539425	0.028421	Y
75cm	-0.04982	0.032633	-0.04795	0.015869	-0.07893	0.037839	N
100cm	0.059641	0.063156	0.083273	0.034467	-0.05426	0.020425	N
200cm	1.654395	0.155765	0.574871	0.023317	0.27312	0.066798	Y (P)
305cm	0.588163	0.028269	0.044559	0.011601	2.020118	0.079386	Y (P)
400cm	4.623098	0.032636	4.029901	0.401032	2.907519	0.149027	Y
500cm	7.398616	0.404779	6.861931	0.170923	6.558937	0.221213	Y
600cm	4.376572	0.301336	StD>0.5	0.525744	5.839488	0.073167	Y
Pos†	7.385481	0.122575	5.700356	0.038174	7.572909	0.14186	-
EB1¶	StD>0.5	0.520773	1.003739	0.099218	0.528827	0.014917	-
EB2¶	0.164901	0.037751	0.095411	0.030919	0.157657	0.025504	-
RPA Neg	0.151141	0.061811	0.116642	0.034274	0.126482	0.036336	-
CRISPR Neg	0.067156	0.021484	0.077899	0.010118	0.03609	0.010685	-

Green highlighted means indicate a value greater than 1. Red highlighted standard deviations indicate a value greater than 0.5, these samples were excluded from overall Y/N data.

† Positive control of 1 ng/µL *S. salar* DNA extract from tissue

‡ Mean fold-change of CRISPR triplicates

§Standard Deviation of triplicate raw fluorescence data. If >0.5 sample is excluded from data set

¶ Extraction blank included during Core Sediment eDNA extraction

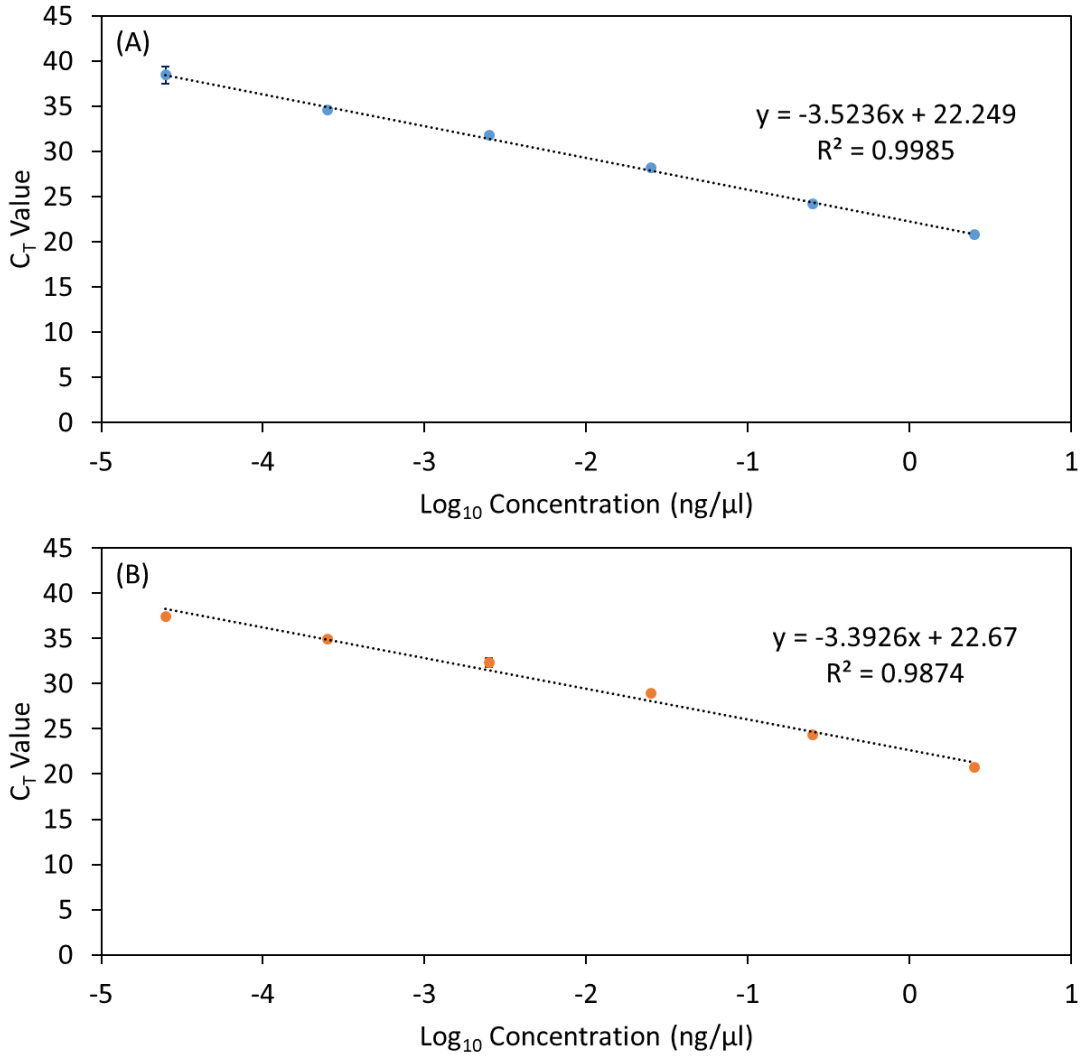

Appendix X: Standard Curve of a six-point 1:10 dilution series of *S. salar* (n=3). Standard curve used to calculate *S. salar* DNA concentrations of (a) Burrishoole Catchment Field Replicate 1 and (b) Burrishoole Field Replicate 2 water samples. Crossing point (C_T) values were calculated based on second derivation maximum method.

Appendix Y: *S. salar* RPA-CRISPR-Cas fluorescence fold-change values of samples taken from the Burrishoole Catchment.

Site		Field Rep	RPA Replicate 1		RPA Replicate 2		RPA Replicate 3		Overall (Y/N)
			Mean‡	StD§	Mean‡	StD§	Mean‡	StD§	
Fiddaunveela	1	1	2.673648	0.485901	4.204839	0.232975	2.838286	0.229445	Y
		2	3.072282	0.289831	3.683565	0.100344	2.84002	0.187564	Y
Bunaveela N	2	1	1.507618	0.176097	0.099517	0.026757	0.134478	0.01805	Y (P)
		2	0.868185	0.13765	1.427405	0.055364	0.493286	0.064994	Y (P)
Bunaveela S	3	1	0.665875	0.070592	0.422213	0.012063	1.136421	0.016408	Y (P)
		2	0.372261	0.09074	0.942644	0.004906	2.895094	0.155188	Y (P)
Goulaun Top	4	1	1.215544	0.196048	0.932662	0.062502	1.782562	0.021901	Y
		2	0.283494	0.079233	0.469017	0.03481	0.595365	0.022494	N
Goulaun Bottom	5	1	1.552361	0.165277	5.188797	0.279548	4.877264	0.04069	Y
		2	4.90459	0.336385	2.578471	0.096853	StD > 0.5	0.63574	Y
Altahoney	6	1	0.202546	0.017877	1.61149	0.047017	2.296301	0.097288	Y
		2	4.640399	0.345954	2.208406	0.053148	4.889982	0.425659	Y
Maumaratta	7	1	3.575111	0.430935	3.132994	0.072092	3.109217	0.178288	Y
		2	3.564963	0.496652	StD > 0.5	0.52962	3.92315	0.180608	Y
Srahrevagh Top	8	1	0.537419	0.131863	0.15077	0.028648	0.135232	0.013387	N
		2	0.152688	0.025629	0.141449	0.028233	0.109086	0.008419	N
Srahrevagh Bottom	9	1	0.636256	0.038516	1.038979	0.024242	1.912606	0.111391	Y
		2	2.037601	0.121222	3.618664	0.083777	4.368431	0.180941	Y
Black	10	1	1.645334	0.2331	4.413034	0.122735	2.976118	0.161026	Y
		2	3.283132	0.096297	2.900257	0.084374	4.576048	0.349583	Y
Feeagh East	11	1	0.176436	0.054107	0.792974	0.046557	2.396263	0.042764	Y (P)
		2	StD > 0.5	0.582362	3.015645	0.103305	2.423011	0.018521	Y
Mill Race	12	1	2.066319	0.339642	0.166308	0.011196	2.127564	0.036385	Y
		2	0.737649	0.145243	0.100506	0.003778	0.128634	0.012414	N
Furnace North	13	1	5.542063	0.276611	5.166078	0.236893	4.98886	0.406135	Y
		2	StD > 0.5	0.526126	4.971566	0.176442	4.251866	0.49174	Y
Field Blank 1			0.086695	0.040572	0.111057	0.025612	0.096783	0.034061	-
Field Blank 2			0.11092	0.012151	0.123662	0.025109	0.280302	0.016116	-
Field Blank 3			0.024473	0.037549	0.650171	0.051638	0.032125	0.031313	-
Extraction Blank			0.150018	0.016489	0.131363	0.012017	0.120591	0.009518	-
Positive Control†		1	4.680474	0.169734	4.657658	0.17648	3.437062	0.097552	-
		2	3.146627	0.119971	3.103934	0.187213	3.796869	0.294202	-
RPA Negative		1	N/A	N/A	0.122697	0.022405	0.124946	0.019613	-
		2	N/A	N/A	0.155435	0.022196	N/A	N/A	-
CRISPR Negative		1	0.045004	0.019618	0.097188	0.027112	0.045456	0.020356	-
		2	0.046896	0.022154	0.079993	0.019158	0.045656	0.022702	-

Green highlighted means indicate a value greater than 1. Red highlighted standard deviations indicate a value greater than 0.5, these samples were excluded from overall Y/N data.

† Positive control of 1 ng/µL *S. salar* DNA extract from tissue

‡ Mean fold-change of CRISPR triplicates

§Standard Deviation of triplicate raw fluorescence data. If >0.5 sample is excluded from data set

Appendix Z: *S. trutta* RPA-CRISPR-Cas fluorescence fold-change values of samples taken from the Burrishoole Catchment.

Site		Field Rep	RPA Replicate 1		RPA Replicate 2		RPA Replicate 3		Overall (Y/N)
			Mean‡	StD§	Mean‡	StD§	Mean‡	StD§	
Fiddaunveela	1	1	0.27074	0.110101	3.14696	0.14713	1.23804	0.157755	Y
		2	4.277996	0.258611	0.672316	0.145685	5.187617	0.274495	Y
Bunaveela N	2	1	2.054778	0.028913	0.39731	0.026373	3.630306	0.154563	Y
		2	5.264786	0.121939	0.86865	0.133616	0.901839	0.012323	Y (P)
Bunaveela S	3	1	1.562016	0.057132	1.133745	0.039179	4.158002	0.059229	Y
		2	0.256251	0.002929	4.695111	0.228531	0.163582	0.008348	Y (P)
Goulaun Top	4	1	6.960169	0.11231	9.001285	0.206951	0.172128	0.014879	Y
		2	4.421856	0.027345	0.655402	0.057512	4.901812	0.13908	Y
Goulaun Bottom	5	1	2.423159	0.070278	1.173618	0.073247	1.63127	0.015878	Y
		2	0.156742	0.020504	2.387782	0.042846	0.7157	0.04148	Y (P)
Altahoney	6	1	0.704499	0.023059	10.5594	0.185616	0.183633	0.001865	Y (P)
		2	0.376372	0.01327	0.30981	0.013048	StD > 0.5	0.516201	N
Maumaratta	7	1	0.1984	0.074167	7.053902	0.153987	4.706764	0.031265	Y
		2	0.463214	0.040992	StD > 0.5	0.576121	5.669134	0.385683	Y (P)
Srahrevagh Top	8	1	1.363006	0.047208	4.058561	0.107173	1.382329	0.032584	Y
		2	0.323691	0.0151	4.92984	0.275195	5.643049	0.436917	Y
Srahrevagh Bottom	9	1	4.061929	0.116219	0.250065	0.011482	0.94046	0.009432	Y (P)
		2	8.159748	0.257545	0.087887	0.014913	0.183452	0.014186	Y (P)
Black	10	1	2.268728	0.06601	0.339544	0.006063	0.333011	0.043536	Y (P)
		2	0.311382	0.022574	0.179428	0.011226	0.244857	0.032272	N
Feeagh East	11	1	0.683857	0.023473	2.300199	0.14303	0.253643	0.022486	Y (P)
		2	6.159268	0.208546	4.997104	0.16919	0.412241	0.055662	Y
Mill Race	12	1	0.276416	0.018021	7.970503	0.063814	4.675432	0.198458	Y
		2	6.690409	0.11385	4.815437	0.24649	2.050213	0.037875	Y
Furnace North	13	1	0.234821	0.015868	0.16912	0.017455	0.705857	0.033566	N
		2	0.284925	0.016029	0.078169	0.024476	0.174304	0.065971	N
Field Blank 1			0.178621	0.010119	0.241215	0.012153	0.173457	0.02792	-
Field Blank 2			0.270761	0.015191	0.133346	0.054784	0.24667	0.011863	-
Field Blank 3			0.157434	0.035381	0.037706	0.050375	0.112001	0.0134	-
Extraction Blank			0.364742	0.016316	0.141629	0.021085	0.241628	0.023022	-
Positive Control†		1	4.105779	0.186127	7.507879	0.071142	2.260117	0.238837	-
		2	8.052787	0.199804	3.554042	0.134607	7.416473	0.093886	-
RPA Negative		1	0.389636	0.003132	0.086233	0.023082	0.190281	0.001929	-
		2	0.358976	0.014283	0.081723	0.014596	0.198681	0.030896	-
CRISPR Negative		1	0.266685	0.029186	0.092431	0.097573	0.115451	0.212015	-
		2	0.294515	0.011167	0.025727	0.005394	0.200178	0.026614	-

Green highlighted means indicate a value greater than 1. Red highlighted standard deviations indicate a value greater than 0.5, these samples were excluded from overall Y/N data.

† Positive control of 1 ng/µL *S. trutta* DNA extract from tissue

‡ Mean fold-change of CRISPR triplicates

§Standard Deviation of triplicate raw fluorescence data. If >0.5 sample is excluded from data set

Appendix AA: *S. alpinus* RPA-CRISPR-Cas fluorescence fold-change values of samples taken from the Burrishoole Catchment.

Site		Field Rep	RPA Replicate 1		RPA Replicate 2		RPA Replicate 3		Overall (Y/N)
			Mean‡	StD§	Mean‡	StD§	Mean‡	StD§	
Fiddaunveela	1	1	0.031775	0.103912	0.113638	0.102245	0.093637	0.092472	N
		2	0.038805	0.094547	0.050206	0.079942	0.05038	0.084862	N
Bunaveela N	2	1	0.028664	0.019879	0.155243	0.012241	0.187745	0.025567	N
		2	0.086248	0.026686	0.146867	0.018216	0.061089	0.005343	N
Bunaveela S	3	1	0.02158	0.017442	0.107072	0.007667	3.841217	0.171329	Y (P)
		2	0.093226	0.014651	0.133908	0.003126	0.077657	0.013229	N
Goulaun Top	4	1	0.027229	0.0308	0.022994	0.018236	0.092126	0.011312	N
		2	0.10685	0.042746	0.107887	0.033602	0.047306	0.014387	N
Goulaun Bottom	5	1	0.025985	0.021261	0.146681	0.019183	0.266459	0.034716	N
		2	-0.02337	0.020298	0.013277	0.029994	0.059229	0.003481	N
Altahoney	6	1	0.062362	0.013124	0.161131	0.009193	0.280854	0.059485	N
		2	0.123783	0.012832	0.193248	0.004392	0.103895	0.003688	N
Maumaratta	7	1	0.013517	0.013093	0.134325	0.016802	0.080366	0.007181	N
		2	0.037791	0.039746	0.159888	0.034072	0.111811	0.036397	N
Srahrevagh Top	8	1	0.078822	0.051912	0.123914	0.00939	0.128469	0.03116	N
		2	0.165814	0.038282	0.109177	0.026288	0.097026	0.027386	N
Srahrevagh Bottom	9	1	0.04086	0.023384	0.142276	0.016951	0.141476	0.006592	N
		2	0.117223	0.012402	0.132114	0.008586	0.102401	0.032372	N
Black	10	1	0.057159	0.011551	0.147806	0.014373	0.232147	0.017244	N
		2	0.105283	0.009807	0.134869	0.011604	0.141164	0.021615	N
Feeagh East	11	1	0.052004	0.047638	0.120301	0.036109	0.167563	0.01321	N
		2	0.065001	0.040029	0.172874	0.028542	0.104836	0.038164	N
Mill Race	12	1	0.053142	0.01232	0.108893	0.006774	0.200549	0.026475	N
		2	0.055703	0.01095	0.144389	0.005869	0.099	0.011327	N
Furnace North	13	1	0.012694	0.030536	0.155685	0.019223	0.136114	0.031248	N
		2	0.092402	0.017477	0.17476	0.049069	0.077572	0.013481	N
Field Blank 1			-0.02189	0.020407	0.143488	0.013745	0.140497	0.015758	-
Field Blank 2			0.009125	0.005124	0.123921	0.015413	0.195889	0.019527	-
Field Blank 3			0.01457	0.008275	0.044655	0.017035	0.053756	0.019828	-
Extraction Blank			0.120114	0.009401	0.233532	0.017898	0.136589	0.019069	-
Positive Control†		1	1.52907	0.030657	4.589044	0.151614	3.709185	0.407526	-
		2	2.750967	0.053484	7.032713	0.44496	3.541484	0.107545	-
RPA Negative		1	0.010383	0.014116	0.149954	0.015194	0.028951	0.011119	-
		2	0.09161	0.017738	0.181835	0.022908	0.092336	0.012026	-
CRISPR Negative		1	0.001728	0.013795	0.20405	0.010915	0.149526	0.035415	-
		2	0.167806	0.011036	0.175829	0.019267	0.120808	0.006327	-

Green highlighted means indicate a value greater than 1.

† Positive control of 1 ng/µL *S. alpinus* DNA extract from tissue

‡ Mean fold-change of CRISPR triplicates

§Standard Deviation of triplicate raw fluorescence data. If >0.5 sample is excluded from data set

Appendix AB: Fold-change fluorescence values measured with the SensEDNA system.

Site		Field Rep	SensEDNA Chamber‡			Overall (Y/N)
			A Low	B Low	C Low	
Fiddaunveela	1	1	0.12848	0.275789	0.150649	Y
		2	0.137767	0.17207	0.164286	Y
Bunaveela N	2	1	0.060345	0.002119	0.023747	N
		2	0.072639	0.02439	0.007335	N
Bunaveela S	3	1	0.020202	0.002786	0.023196	N
		2	0.017429	0.00188	0.079625	N
Goulaun Top	4	1	0.039046	0.010724	0.040921	N
		2	0.0125	0.015385	0.021845	N
Goulaun Bottom	5	1	0.029106	0.210526	0.28	Y
		2	0.315011	0.053061	0.264423	Y
Altahoney	6	1	0.012438	0.030043	0.040921	N
		2	0.239737	0.053118	0.284314	Y
Maumaratta	7	1	0.077465	0.07947	0.085366	N
		2	0.131258	0.102459	0.197619	Y
Srahrevagh Top	8	1	0.038922	0.001992	0.007264	N
		2	-0.00229	-0.00624	0	N
Srahrevagh Bottom	9	1	0.010246	0.002525	0.04401	N
		2	0.069977	0.123596	0.150852	Y
Black	10	1	0.058411	0.218504	0.065854	Y (P)
		2	0.166329	0.070281	0.28125	Y
Feeagh East	11	1	0.026455	0.014881	0.050761	N
		2	0.28976	0.093525	0.05569	Y (P)
Mill Race	12	1	0.023454	0.009732	0.036585	N
		2	0.008811	0.01046	0.007299	N
Furnace North	13	1	0.841981	0.479212	0.458234	Y
		2	0.405594	0.098185	0.375959	Y
Field Blank 1			-0.01984	-0.00413	0.002381	-
Field Blank 2			0.006787	-0.00579	0.004706	-
Field Blank 3			0.006726	0.015424	0.014218	-
Extraction Blank			0.006527	0.008602	0.004717	-
Positive Control†			0.458515	0.355713	0.541667	-
RPA Negative			-0.00501	0.001505	0.004975	-

Green highlighted means indicate a value greater than 0.1.

† Positive control of 1 ng/µL *S. salar* DNA extract from tissue

‡ Fold-change of fluorescence values between 30 min and 10 sec

Appendix AC: Burrishoole Catchment lateral flow strips visualised by eye.

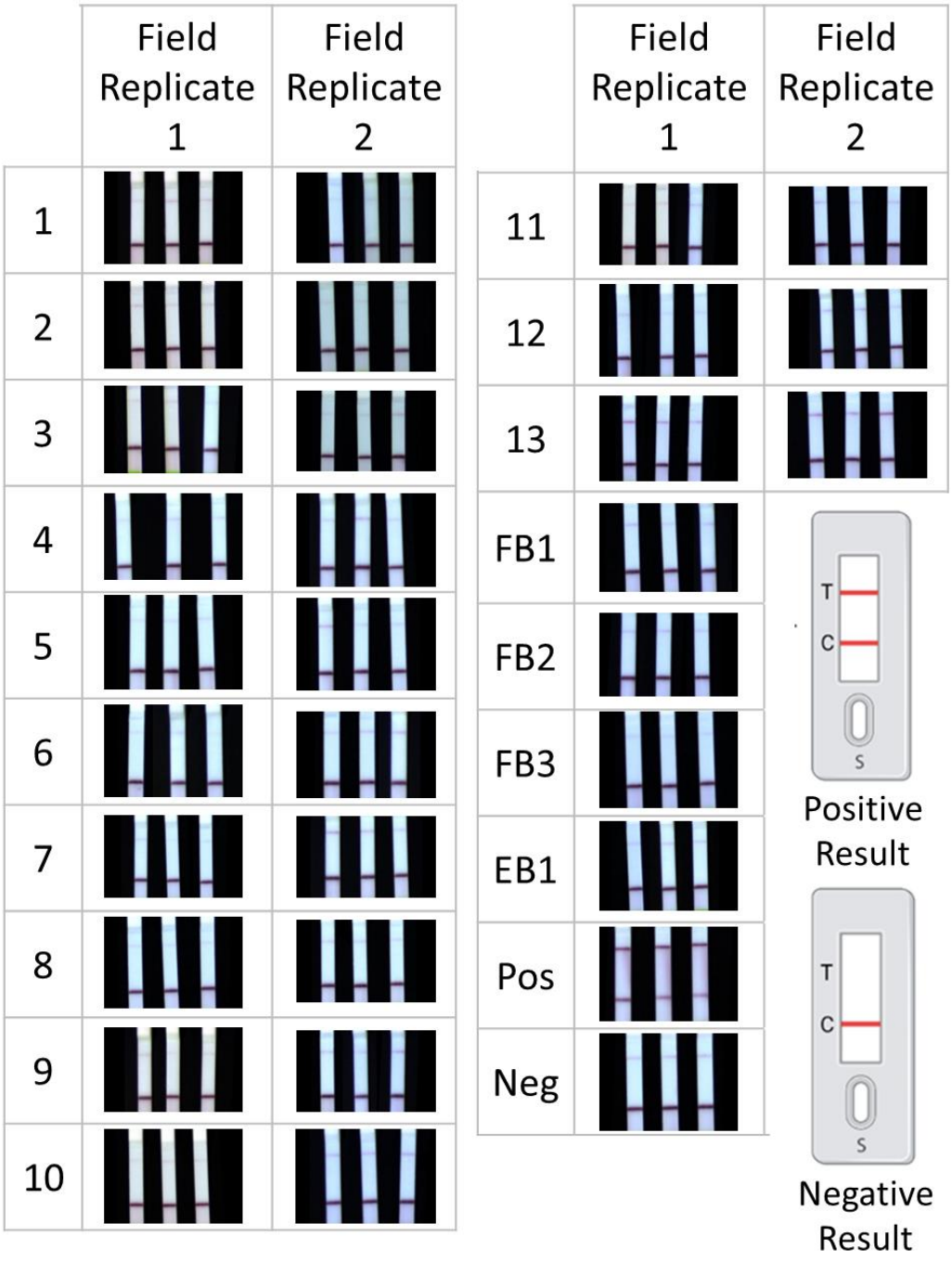

FB = field blank, EB = extraction blank. Pos = positive control consisting of 1 ng/µL *S. salar* DNA extracted from tissue. Neg = negative control with no template DNA added to the RPA reaction.

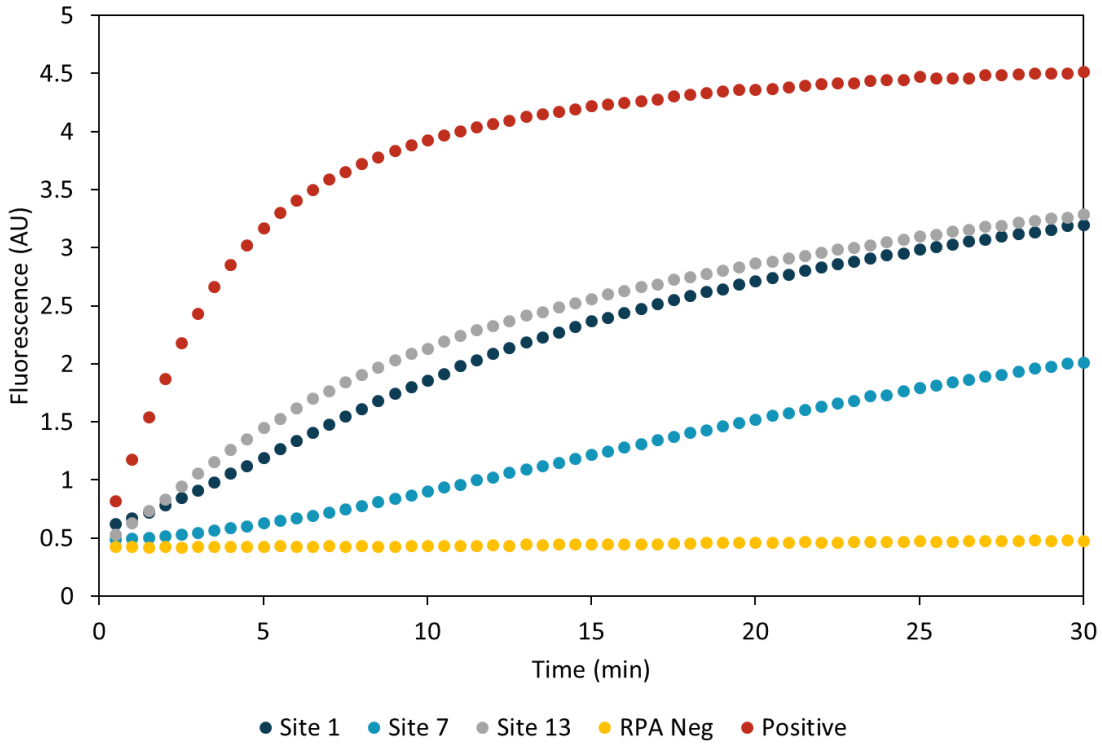

Appendix AD: Raw fluorescence data of *S. salar* benchtop RPA-CRISPR-Cas analysis of Burrishoole Catchment (Sites 1, 7 + 13). Fluorescence measurements taken every 30 sec for 30 min at 37 °C (ƛex = 485 nm, ƛem = 535 nm). Positive control of 1 ng/µL of DNA extracted from *S. salar* tissue. RPA Neg = negative control with no template DNA added to the RPA reaction.